ALMA MATER STUDIORUM – UNIVERSITÀ DI BOLOGNA

---

Dottorato di Ricerca in
**Biologia Cellulare e Molecolare**
Ciclo XVIII

Settore Concorsuale di afferenza**: 05/I1**
Settore Scientifico disciplinare: **BIO/18**

# Uncovering the relationship between endocytosis and Awd, the *Drosophila* homolog of Nme metastasis suppressor proteins

Presentata da:
**Marilena IGNESTI**

Coordinatore:
Prof. **Giovanni CAPRANICO**

Relatore:
Prof. **Giuseppe GARGIULO**

Esame finale anno 2017

# Acknowledgements

To get this PhD is an important milestone for me, and nevertheless I would not have achieved it without the support, help and love of many people, who I specifically want to thank.

First and foremost, of course, I desire to say thank you to Prof. Gargiulo and Prof. Cavaliere for having trusted in me since the first time and for having always sustained, encouraged and supported me. It was an honour to be part of your group and to learn from passionate drosophilists as you are. Thanks for our discussions on, around and outside of science: each of them has prompted me thinking and trying harder and better. Thank you for everything you have taught me and for having enriched my knowledge, skills and abilities to such a grade that I never believed I could reach. Thanks for our happy hours and for the good time spent together.

Special thanks go to my sister-in-adventure, Patri, for everything she has taught me and continues to teach and because she has been and still continues to be not only my mentor in the lab but also a dear friend out of there. Thanks also to the sweet sweet Giorgia: you, Patri and I were a wonderful trio at the fourth floor! Thanks for fun and support, girls!

Thanks to my partner-in-crime Ettore, I really adore you and I will never stop to say thank you for the complicity. Thanks to Beppe and Laura, it was so good working together.

Thanks to Manu, Simona and Simone: without you it would not have been the same to experience this PhD. Also thanks to Elisa, for being so gentle and patient.

I cannot forget to thank Daniela for the numerous scientific debates we had, and for having always spurred me to think beyond schemes. But, above all, at least here, allow me to thank you also for listening to me in difficult moments.

Thanks to Rob, for the time you spent in late evenings to support and teach me and for having trusted in me. Thanks for all your help and the scientific encouragement.

Thanks to Davide for the scientific help, for debates but also for our chats on the most diverse subjects.

Thanks to all the guys who, for various reasons, have spent time at the fourth floor because they brought a breath of freshness and novelty, that never hurts.

A super, special thanks to my friends Vale, Lisa, Diana. We are friends since long time, you are wonderful, I love you and I will always worship you. Many thanks for the good time we spent together, for our chats, dinners, laughs and for having always offered me your point of view. It is rare to find friends like you. Thanks for having been to my side, I hope you will continue to be there forever.

Thanks to my mate Giorgia (bella rossa!) for her infinite sweetness: I was super lucky to meet you and I'm honoured to have you as a friend.

Now I get to the most touching acknowledgements, those addressed to my family, to which I must say a huge thank you. Mom, thanks for having always encouraged me, despite your qualms. Thanks for our "serate-cinema" sitting two on a chair. Dad, thanks for having always held me on a pedestal and for having paid every day attention that I would not fall from there. My dear dear Ciuchino, thank you for having been always there, for having dissolved my rough edges, for having reminded me every day what is really important and how to find happiness. You're the most important person in my life. Thanks to my wonderful, wonderful grandma who I love with all my heart; without her, this PhD would have been much sadder.

Thanks to my nephew Sky, for his prr prrrr that melt your heart and warm you when you need it; I really love you.

Thanks to all Lorenzo's family members, especially Greta, Alex, Giusy and Beppe, Franca and Bruno, for welcoming me, loving me and for being all so immensely special. Thanks to Goku and Simba for your true love and for being so sweet.

Finally, a special thanks to the great love of my life, Lorenzo: without him, who knows where I would be today. My love, thanks for your infinite patience. Also, thanks for your love with which every day you coat me, making me so lucky and my life so wonderful.

# Abstract

The work presented in this PhD thesis focuses on the study of *awd* (*abnormal wing discs*) gene function during the development of *Drosophila melanogaster*. *awd* gene product is the ortholog of Nme1 and Nme2 (non-metastatic cell expression 1 and 2, respectively), which display metastasis suppressor abilities.

In the first part, the main purpose of my research plan is to investigate the requirement of *awd* gene function for the correct activation of Notch (N) signalling pathway. N signalling is a highly conserved cell-cell communication pathway that mediates critical cell fate decision events occurring both in insects and vertebrates. Results presented in this PhD thesis clearly show that *awd* loss of function impairs N receptor trafficking, resulting in defective N signal transduction.

In the second part, the issue of my work concern the investigation of Awd dynamics inside and outside cells. Nme1 is found in human body fluids and its protein level correlates with prognosis in cancer patients. This prompted me to gain further insights into the mechanisms through which intracellular and extracellular Awd amounts are controlled. Through molecular genetic approaches, I found that conditional block of Shi activity reduces Awd intracellular amount, indicating that Shi controls intracellular level of Awd.

Finally, in the third part, I direct my research towards the study of dVHL, a well-known Awd interactor. The haploinsuffcient *dVHL* (*von-Hippel Lindau*) gene is the *Drosophila* homolog of the human *VHL* tumour suppressor gene. By applying omics approaches, I found that reduced *dVHL* gene dosage alters the expression levels of genes involved in chromatin organisation and cell metabolism. Alteration in these cellular activities are recurrently found in cancer cells.

# Table of contents

**Acknowledgements** ........ **i**

**Abstract** ........ **iii**

**Table of contents** ........ **v**

**Chapter 1 Introduction** ........ **1**

1.1 The war on cancer ........ 1

1.2 Metastasis suppressor genes ........ 3

1.3 The *Nme* gene family ........ 5

1.4 *Drosophila* oogenesis ........ 10

1.4.1 Follicular epithelium morphogenesis and functions ........ 12

1.5 *Drosophila* embryogenesis ........ 15

1.6 *Drosophila* larval and pupal development ........ 16

1.6.1 Imaginal tissues ........ 16

1.6.2 Wing disc development: morphogenesis, structure and function ........ 17

1.6.3 *Drosophila* larval fat body: morphogenesis, structure and function ........ 20

1.7 N signalling pathway ........ 22

1.7.1 N signalling functions during *Drosophila* oogenesis ........ 26

1.7.2 N signalling functions during *Drosophila* wing disc development ........ 30

1.8 Cellular trafficking routes: endocytosis and exocytosis (secretion) ........ 31

1.8.1 Role of endocytosis on N signalling pathway ........ 35

1.9 The *Drosophila awd* gene ........ 36

**Chapter 2 Aims of the Thesis** ........ **43**

**Chapter 3 Materials and Methods** ........ **45**

3.1 Stocks and genotypes ........ 45

3.1.1 Fly food preparation ........ 45

3.1.2 Stocks used in this work ........ 45

3.2 Clonal analysis ........ 47

3.2.1 MARCM mosaic analysis technique ........ 47

3.2.2 Induction of MARCM clones ....................................................................49

3.2.3 The Flp-out/Gal4 technique ......................................................................50

3.2.4 Induction of Flp-out clones ........................................................................51

3.3 Antibodies ........................................................................................ 52

3.4 Immunofluorescent microscopy............................................................ 54

3.5 Statistics .......................................................................................... 55

**Chapter 4 Results ........................................................................... 57**

4.1 The loss of *awd* gene function arrests N signalling during the development of *Drosophila melanogaster*............................................. 58

4.1.1 *awd* function is required during oogenesis to activate N signalling in FCs...........58

4.1.2 *awd* function is required during wing disc development to activate N signalling at the DV boundary ...........................................................................................61

4.2 The loss of *awd* gene function affects the intracellular distribution of N receptor............................................................................................ 63

4.2.1 N receptor accumulates in endocytic vesicles in $awd^{J2A4}$ mutant FCs...................63

4.2.2 The N signalling defect in homozygous $awd^{J2A4}$ cells is not correlated to the loss of cell polarity ............................................................................................65

4.3 The loss of *awd* gene function arrests N proteolytic processing beyond the S2 metalloprotease-mediated cleavage ............................................ 67

4.3.1 Overexpression of the NEXT fragment in homozygous $awd^{J2A4}$ FCs doesn't restore N signalling .............................................................................................69

4.3.2 Overexpression of the NICD fragment in homozygous $awd^{J2A4}$ FCs restores N signalling..........................................................................................................69

4.3.3 Comparison of N receptor intracellular distribution and signalling outcome in endocytic mutants suggests an endocytic defect in early steps beyond internalisation in $awd^{J2A4}$ mutant FCs .....................................................71

4.4 Analysis of N receptor localisation in $awd^{J2A4}$ mutant cells .................... 73

4.4.1 N receptor accumulates in immature early endosomes in $awd^{J2A4}$ mutant FCs.....73

4.4.2 N receptor does not accumulate in Rab7-positive late endosomes in $awd^{J2A4}$ mutant FCs ..........................................................................................................76

4.4.3 Acidification of endosomal compartments is not affected in $awd^{J2A4}$ mutant FCs 77

4.4.4 N receptor does not accumulate in Rab11-positive recycling endosomes in $awd^{J2A4}$ mutant FCs .....................................................................................77

4.5 Genetic analysis of Awd and Rab5 interaction in N signalling activation ........................................................................................... 78

4.5.1 N receptor accumulates in enlarged Rab5$^{CA}$-positive vesicles in *awd*$^{J2A4}$ mutant FCs ........ 79

4.5.2 Overexpression of Rab5$^{CA}$ in *awd*$^{J2A4}$ mutant FCs recruits Hrs to the membrane of N-containing vesicles ........ 80

4.5.3 Overexpression of Rab5$^{CA}$ does not restore N signalling n *awd*$^{J2A4}$ mutant in *awd*$^{J2A4}$ mutant FCs ........ 81

4.6 Genetic analysis of Awd and Shi interaction in N signalling activation 83

4.6.1 Overexpression of a dominant negative form of Shi arrests N signalling ........ 83

4.6.2 Overexpression of an enhanced GFP-tagged form of Awd does not perturb N signalling ........ 84

4.6.3 Overexpression of Awd::eGFP in FCs devoid of Shi activity restores N signalling ........ 20

4.7 Shi controls shuttling of Awd protein between the intracellular and extracellular milieux ........ 88

4.7.1 Awd level is strongly reduced in FCs overexpressing the dominant negative form of Shi ........ 88

4.7.2 Awd level is strongly reduced in adipocytes overexpressing the dominant negative form of Shi ........ 88

4.7.3 Adipocytes with impaired Shi activity accumulate Rab7-positive vesicles ........ 90

4.7.4 Shi controls extracellular Awd protein level ........ 91

4.7.5 Role of Rab5 in regulating Awd intracellular level ........ 91

**Chapter 5 Discussion ........ 93**

**Chapter 6 Appendix ........ 99**

6.1 Introduction ........ 99

6.1.1 The human and the *Drosophila VHL* genes ........ 99

6.1.2 Development, structure and functions of *Drosophila* Malpighian tubules ........ 102

6.2 Objective of the research ........ 104

6.3 Materials and methods ........ 105

6.3.1 *Drosophila* Malpighian tubule RNA extraction ........ 105

6.3.2 cDNA generation, amplification and labelling ........ 106

6.3.3 FL004 hybridation ........ 107

6.3.4 Data acquisition and processing ........ 108

6.3.5 qRT-PCR ........ 108

6.4 Results ........................................................................................ 109

6.4.1 Overview of the microarray technology.............................................................109

6.4.2 Differentially expressed genes in *dVHL*$^{1.1}$/+ Malpighian tubules .......................110

6.4.3 GO analysis ..........................................................................................112

6.4.4 Validation..............................................................................................117

6.5 Discussion ........................................................................................ 118

**Chapter 7 Bibliography ........................................................................ 121**

# Chapter 1

# Introduction

## 1.1 The war on cancer

Nowadays, one of the first disease-related cause of death worldwide is cancer. Cancer accounts for 82 million death *per* year and 14 million of new cases are diagnosed each year (Stewart *et al.*, 2014).

Cancer is an umbrella term that encompasses more than 100 different types of diseases. Biology, biochemistry, medicine and all the life science disciplines gave in the past years great contributions towards the comprehension of tumour cell behaviour, thus opening the way to fight cancer. Indeed, the number of cancer survivors increases each year (DeSantis *et al.*, 2014). Despite this positive trend, the “war on cancer” is far from being won. The major causes of today’s failure are metastases. Metastases, indeed, are the leading cause of cancer morbidity and mortality, since they are responsible for ~90% of cancer deaths (Chaffer and Weinberg, 2011) and this grade of mortality hasn’t been seriously impaired by scientific progresses toward a cure (Faguet, 2005).

Metastases arise when cancer has spread from a primary site to distant organ(s), where cancerous cells proliferate giving rise to new tumour colonies. If cancer is diagnosed at an early stage, before it starts spreading, treatments through surgical resection and local irradiation are often successful; but if cancer is diagnosed when it has already metastasised, then the prognosis is more often poor. Metastasis represents the most challenging obstacle to successful cancer management and it could be considered the last frontier of cancer research (Bacac and Stamenkovic, 2008).

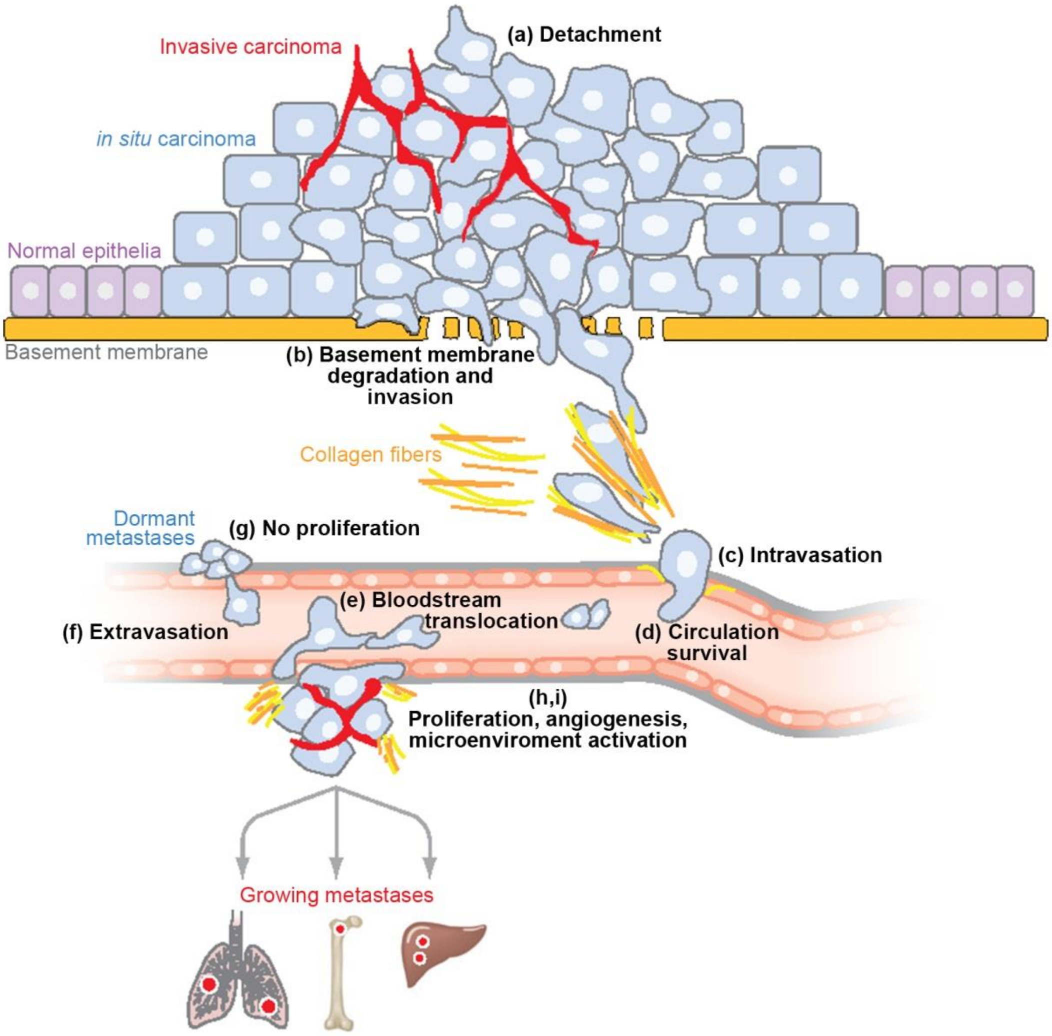
Invasive carcinoma
(a) Detachment
*in situ* carcinoma
Normal epithelia
Basement membrane
(b) Basement membrane degradation and invasion
Collagen fibers
Dormant metastases
(g) No proliferation
(c) Intravasation
(e) Bloodstream translocation
(f) Extravasation
(d) Circulation survival
(h,i) Proliferation, angiogenesis, microenviroment activation
Growing metastases

**Figure 1 Principal steps in the metastatic cascade.** *in situ* carcinoma arises from transformation of epithelial cells. The development of blood vessel supply and invasive traits are the hallmarks of the acquisition of a malignant attitude. When basement membrane gets broken, collagen fibers are degraded and cancer cells invade the surrounding stroma. Intravasation and subsequent extravasation allow cancer cells to get disseminated at secondary sites. Modified from Bacac and Stamenkovic, 2008.

Metastasisation is a complex and multistep process (Figure 1). A tumour cell that initiates the metastatic cascade must pass through the following steps: (a) it detaches from the primary tumour; (b) it degrades the basement membrane, gaining access to the surrounding stroma and invades it; (c) it enters the microvasculature of the lymph or blood systems (intravasation); (d) it must survive in the circulation, avoiding immune detection; (e) it translocates through the bloodstream in distant tissues; (f) it exits from the bloodstream (extravasation); (g) it must survive in the microenvironment of the distant tissues (micro-metastasis); (h) it adapts to the foreign microenvironment; (i) it possibly starts to proliferate to form a secondary tumour focus (metastatic colonisation with formation of macro-metastasis), eventually establishing new blood supplies (Bacac and Stamenkovic, 2008; Chaffer and Weinberg, 2011; Chambers *et al.*, 2002). The failure in completing one of these steps will cause the metastasis not to occur or develop. Unfortunately, the molecular mechanisms that drive each of these steps are complex and poorly understood. It was commonly (but erroneously) believed that the first steps, particularly those preceding the extravasation, were the most rate-limiting. This was supported by the consideration that it would take time to cells to gain all the genetic and epigenetic modifications required to become malignant. This belief addressed scientists to search for therapeutic treatments targeting the very first steps of the metastatic cascade. The research of the rate-limiting steps is justified by the necessity to let time to therapy to act, to be effective and successful. Anyway, several lines of evidence revealed that the initial steps of the metastatic cascade are not rate-limiting and that probably the most rate limiting events are those at the cascade termini. Indeed, clinical studies reported that:

- in patients with a still localised primary tumour the dissemination of cancer cells to secondary sites often has already occurred;
- however, not all patients with tumour cells at secondary sites do develop clinically significant metastatic lesions, even in the absence of therapy. This data, in particular, has a strong resonance, since it explains why most of the research in this field is focused on the study of cancer cell survival at the secondary sites and of metastatic colonisation. The basic idea is to let the dormancy period of micro-metastasis last all life long.

It should in any case be stated that any gene implicated in any phase of the metastatic cascade should potentially be a therapeutic target.

Metastatic process is described as highly inefficient (Weiss, 2000). Indeed, each metastasis is clonal: this means it derives from a single cancer cell. This shouldn’t fool: despite their clonal origin, metastases (as well as the primary tumour, it should be stated) are characterised by heterogeneous traits, because of the alteration of proliferation control mechanisms causing their inability to block cell division, stimulate DNA repair and if necessary induce apoptosis if mutations are discovered.

## 1.2 Metastasis suppressor genes

The metastatic potential of a primary tumour cell is directly linked to the level of aberrant expression of specific genes able to promote or to inhibit the metastatic dissemination. In tumour cells, the so-called tumour suppressor genes (TSGs) are typically inactivated through mutations, while the (proto-)oncogenes are aberrantly activated (Weinberg, 2007). This combination promotes tumour growth. Following this line of reasoning, in malignant cancer, metastasis suppressor genes (MSGs) are specifically downregulated (Yan *et al.*, 2013) while metastasis-promoting genes get upregulated to improve the metastatic abilities of cancer cells. MSGs are characterised by their ability to inhibit metastasis formation without affecting primary tumour growth. One important difference between TSGs and MSGs is that while TSGs are generally mutated to allow dysregulation of proliferation control machineries, MSGs are typically simply downregulated in most cases (Dong *et al.*, 1996; Fujimoto *et al.*, 1998; Kim *et al.*, 2001; Su *et al.*, 2002) through epigenetic mechanisms, such as alteration in the DNA methylation content at CpG promoter regions or through post-transcriptional or post-translational modification events (Kauffman *et al.*, 2003; Steeg *et al.*, 2003). This difference is crucial, since it allows the possibility of a therapeutic approach to be half-seen in which the expression of MSGs is simply restored to wild type levels (Iiizumi *et al.*, 2008).

To date, approximately thirty MSGs have been identified (Figure 2), and many others, such as members of the Tetraspanin superfamily (e.g. CD63) are currently under investigation for their potential role as MSGs (Zhijun *et al.*, 2007); some of them are not indicated as MSGs yet because of their uncertain role on tumour growth. It should be stated that, for most of the identified MSGs, the metastasis suppressor role is strictly “context dependent”: there are specific tumour cohorts in which these genes correspond exactly to the definition of a MSGs; in others, their role is still unclear and, finally, tumours in which it is possible to find a direct correlation between the expression levels of these genes and metastasis. Thus, the landscape is more complicated and intricate than it could appear at first sight and none MSGs could and should be considered as an independent prognostic or predictive factor for any cancer type. It appears that this is a new born and growing field destined to shed new light on metastasisation process, drawing the path to eventually find a cure. A closer look at Figure 2 reveals that some kind of “metastasis pathways” start to be delineated, principally related to MAPK signalling and other pathways involved in apoptosis, cell adhesion, differentiation and regulation of cell cycle, that have been already implicated in tumour progression (Shevde and Welch, 2003).

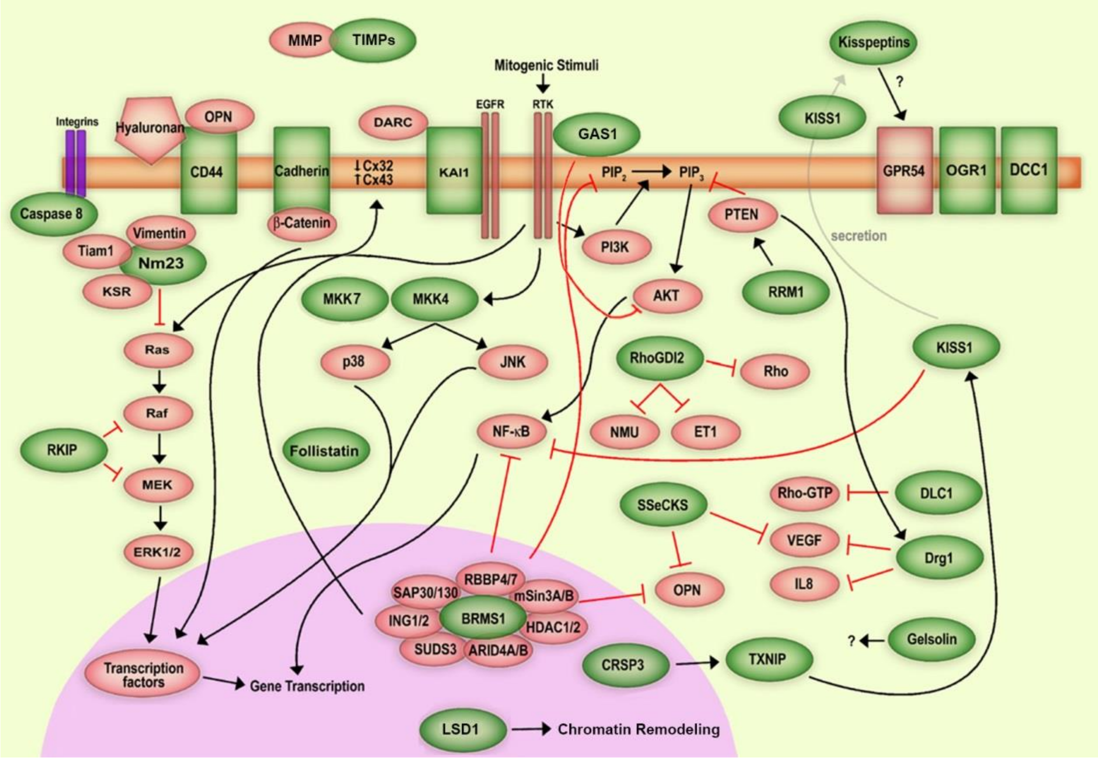
MMP
TIMPs
Mitogenic Stimuli
EGFR
RTK
Kisspeptins
?
Integrins
Hyaluronan
OPN
DARC
GAS1
KISS1
CD44
Cadherin
↓Cx32
↑Cx43
KAI1
PIP$_2$
PIP$_3$
GPR54
OGR1
DCC1
Caspase 8
β-Catenin
PTEN
secretion
Vimentin
Tiam1
Nm23
PI3K
KSR
AKT
RRM1
MKK7
MKK4
Ras
p38
JNK
RhoGDI2
Rho
KISS1
Raf
NF-κB
NMU
ET1
RKIP
Follistatin
MEK
SSeCKS
Rho-GTP
DLC1
VEGF
Drg1
ERK1/2
RBBP4/7
OPN
IL8
SAP30/130
mSin3A/B
ING1/2
BRMS1
HDAC1/2
SUDS3
ARID4A/B
?
Gelsolin
CRSP3
TXNIP
Transcription factors
Gene Transcription
LSD1
Chromatin Remodeling

**Figure 2 Involvement of known MSGs in cellular signalling pathways.** The MSGs are indicated in green. Modified from Stafford *et al.*, 2008 and updated.

## 1.3 The *Nme* gene family

The *Nme* gene family, name in accordance with the current official gene nomenclature, previously known as *Nm23* gene family (where Nm- stands for "non-metastatic cell expression"), consists of a huge and still growing up family of evolutionarily conserved proteins, that is present in all 3 domains of life: *Eubacteria*, *Archaea* and *Eukarya* (Bilitou *et al.*, 2009).

At least a single Nme protein is present in virtually all organisms, from unicellular organisms generally bearing just one member (e.g. *S. cerevisiae*) to humans, whose genome carries 10 *Nme* genes (Desvignes *et al.*, 2009). On the basis of gene organisation in introns/exons, of the functional domain(s) in the protein sequence and of phylogenetic analysis, *Nme* genes have been divided in two groups: group I, to which *Nme1-4* belong, and group II, to which *Nme5-10* belong. Proteins belonging to group I own a single nucleoside diphosphate kinase domain, share 58% to 88% identity and display NDPK activity (E.C. 2.7.4.6), that's the reason why Nme1-4 are also designed as NDPK A-D. Proteins of group II are more divergent, have one to three NDPK domains of different types and some of them are not complete or are truncated; moreover, other functional domains could be recognised in their sequences. Nme5-10 proteins share 22% to 44% identity and only for Nme6 it has been demonstrated a genuine NDPK activity as for Nme1-4 (Tsuiki *et al.*, 1999). A representation of the organisation of *Nme* proteins is shown in Figure 3.

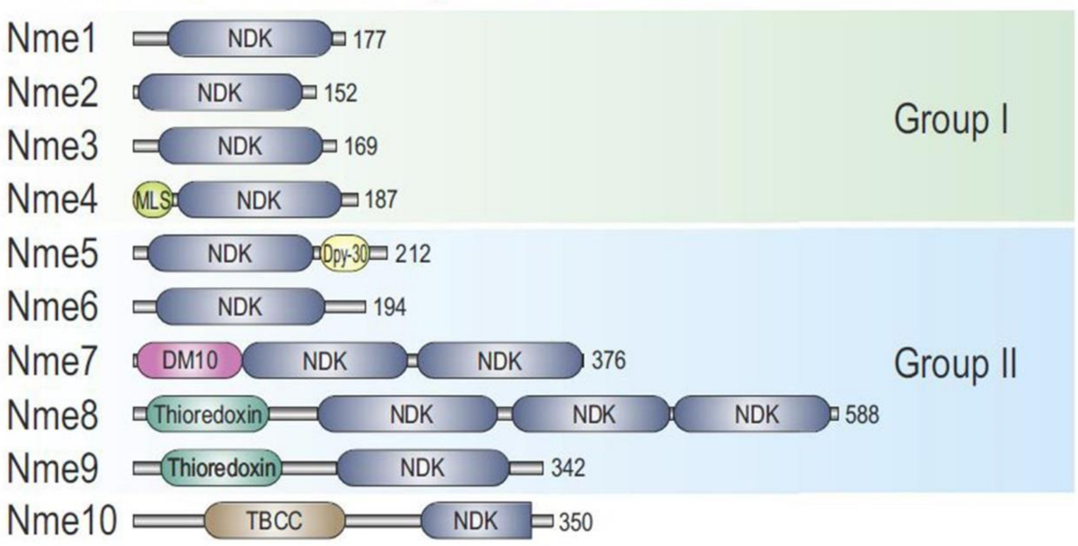

**Figure 3 Architecture of *Nme* proteins.** Members of the gene family are divided in two groups. Nme10 is set apart because of peculiar evolutive origin. The number at the end of each schematic representation of a protein indicates its length in amino acids. Different domains composing each protein are highlighted with a diverse coloured box. NDK=nucleoside diphosphate kinase domain; MLS=mitochondria localisation sequence; DM10=recognised domain with unknown function; Thioredoxin=thioredoxin domain; TBCC=tubulin-specific chaperone protein co-factor C domain. Adapted and modified from Cetkovic *et al.*, 2015.

NDPKs have an oligomeric quaternary structure: in particular, in *Dictyostelium*, *Drosophila* and vertebrates NDPKs are hexameric enzymes, while in bacteria they are tetrameric. Nme1 and Nme2 subunits are able to form fully functional heterohexameric enzymes, in all the possible combinations. During evolution, there has been an independent and progressive loss of group II members, especially in nematodes and insects (Bilitou *et al.*, 2009).

To be correct, the biochemical name of NDPK is NTP/NDP transphosphorylase since this enzyme catalyses the transfer of the γ-phosphate group from 5'-triphosphate to 5'-diphosphate nucleotides (or 2'-deoxynucleotides), by generating a high-energy intermediate, in which a histidine residue in the catalytic site of the enzyme receives the phosphate group from the NTP (auto-phosphorylation). The physiological role of NDPKs is to equilibrate the (d)NDP and (d)NTP cellular pools independently of the nature of the purine or pyrimidine bases (Lascu and Gonin, 2000).

The first member of the *Nme* gene family has been identified in 1988 by Patricia Steeg through a screening of differentially expressed genes in 7 murine melanoma cell lines of varying metastatic potential (Steeg *et al.*, 1988). All these cell lines were derived from the K-1735 murine melanoma line. The expression level of *Nme1* inversely correlates with the metastatic potential in K-1735 derived cell lines and in N-nitroso-N-methylurea-induced rat mammary carcinomas: the less metastatic cell lines showed the highest levels of *Nme* gene expression.

From this very first and pioneering work, the field of *Nme* research has exploded, and the other members of this family have been found. *Nme1* and *Nme2* are until now those studied most, for their implications in tumour progression and metastatic dissemination. Starting from the 90s, several other studies investigated the correlation between *Nme* expression and aggressiveness; indeed, *Nme1* (more than *Nme2*, even if a clear role as MSG has been established also for NDPK B, Thakur *et al.*, 2011) appears to be downregulated in highly metastatic breast, gastric, colon, ovarian, liver, cervical, hepatocellular carcinomas and melanoma cohorts, and this correlates with poor prognosis (Boissan and Lacombe, 2012; Palmieri *et al.*, 2006). On the other hand, in advanced neuroblastomas and in many haematological malignancies, *Nme* expression is increased and this is associated with an adverse outcome (Tee *et al.*, 2006). It is worth noting that, at least in hepatocellular carcinoma and colon cancers, a bimodal expression of Nme1 has been demonstrated: while its expression levels are enhanced in the main tumour mass, it appears strongly downregulated or totally absent at the invasive front, suggesting a possible role for Nme1 as a barrier against the conversion of *in situ* carcinoma into invasive carcinoma (Boissan *et al.*, 2010). This surprising finding makes the comprehension of Nme1 functions in metastasisation even more complicated.

Many progresses have been done toward the understanding of the metastasis suppressor function of Nme proteins, also to achieve their use as clinical markers of aggressiveness; indeed, many biochemical functions have been assigned to Nme proteins, particularly to Nme1 and Nme2, apart from their role as NDPK (Postel, 2003; Steeg *et al.*, 2011):

a) histidine-dependent protein phosphotransferase activity (Srivastava *et al.*, 2006; Wagner and Vu, 1995, 2000), with a similar mechanism to that in NDPK activity (reviewed in Attwood and Wieland, 2015);
b) DNA binding and DNA nuclease, with a role in transcription regulation and gene expression (Ma *et al.*, 2002; Postel *et al.*, 2000);
c) 3’-5’ exonuclease activity (Ma *et al.*, 2004), which appears necessary for its metastasis-suppressor function (Zhang *et al.*, 2011);
d) DNase activity with a role in Granzyme A-mediated death (Fan *et al.*, 2003).

Moreover, many interacting partners have been identified, with the aim to elucidate the molecular pathway in which Nme proteins are involved in order to shed light on the mechanisms underlying their role in metastasis progression. Among these physical interacting proteins there are cytoskeletal, endocytic and oncogenic proteins (e.g. VHL, Chapter 6 Appendix); importantly, many functional or physical associations with small GTPases such as Dynamin (Baillat *et al.*, 2002, Arf6 Palacios *et al.*, 2002, Rad Zhu *et al.*, 1999) and Rac1 (Otsuki *et al.*, 2001) have been found. G proteins are transducers of signalling from GPCRs (G protein-coupled receptors, also known as seven-transmembrane receptor, 7TM, for their typical structure); GPCRs are important receptors for a broad range of stimuli and regulate many cellular responses and adaptation, such as growth and differentiation. This panorama is one of the most attractive if one works with a MSG displaying a NDPK activity, since this allows to speculate a possible role as GTP supplier for G proteins (or a GEF-like function) involved in important signalling pathways. Indeed, for some GTPases such as Dynamin a role as GTP supplier has been demonstrated (Conery *et al.*, 2010).

By analysing all these functions, it appears that Nme is involved in diverse biological processes ranging from proliferation, differentiation, development, cell adhesion and migration, vesicular trafficking and endocytosis, ciliary functions (Boissan *et al.*, 2009). However, even if enormous efforts have been done in trying to get a comprehensive view of Nme activities, the molecular mechanisms of its metastatic suppression remain elusive.

Another perspective which could finally help unravel the puzzling results correlating *Nme* expression and tumour outcome in different tumour cohorts and in reconciling all the different biochemical activities assigned to Nme is to look at their subcellular localisation. Localisation was one of the hot-themes at the recent NDPK 2016 meeting (International Congress of the NDP Kinase/Nm23/Awd Family, Dubrovnik, Croatia, October 9-13, 2016) and already Bosnar and collaborators claimed for a deeper analysis of the subcellular distribution of Nme proteins in order to gain insights in their biological function (Bosnar *et al.*, 2009). On the basis of immunohistochemical data it was shown that Nme1 and 2 are predominantly cytoplasmic proteins. In some occasion they could be found at the cell membrane, where Nme1 interacts with Dynamin to support the pinching off of vesicles from the plasma membrane and in modulating intracellular trafficking routes, and in the nucleus, reinforcing the notion of their DNA-related biochemical activities. Nme3 was found at the outer membrane of mitochondria, but it lacks a proper localisation peptide (Figure 3). It was suggested that NDPK C at this location could interact with the Dynamin Drp1 in regulating mitochondrial fission. NDPK D, instead, has a typical MLS (mitochondria localisation sequence) and indeed it was found associated with cristae in the inner mitochondrial membrane where it interacts with the Dynamin-like OPA1, guiding mitochondrial fusion events (Boissan *et al.*, 2014). Most of the group II genes are essentially expressed in ciliated structures such as primary cilia and sperm flagella (refer to Desvignes *et al.*, 2009 review for a complete bibliography on that theme).

The theme of location of Nme proteins has become even more fascinating and intriguing since the discovery of the presence of these enzymes, in particular Nme1 and Nme2, in extracellular environments, such as the culture medium of cell lines (Okabe-Kado *et al.*, 1992) and human body fluids (Lilly *et al.*, 2015). More interestingly, increased Nme1 and Nme2 extracellular levels were associated with resistance to chemotherapy and with an overall poor prognosis in patients affected by different kinds of AML (acute myeloid leukaemia, Wakimoto *et al.*, 1998). The correlation is great to such an extent that serum level of Nme1 in AML and malignant lymphomas is used as prognostic marker (Niitsu *et al.*, 2000; Niitsu, 2001).

If the function of Nme proteins has been intensively studied in different tumoural cell lines or in pathological conditions, the physiological role of Nme proteins has been analysed to a less extent. Indeed, most of the researchers complain about the necessity of animal models to clarify in deeper details the role of *Nme* genes during development (Takacs-Vellai *et al.*, 2015). It should be mentioned, also, that many of the most important findings regarding Nme function with possible implication for human pathologies came in the past years from animal models.

*****

During my PhD, I have been involved in several projects, all focusing on the use of *Drosophila melanogaster* as a model system; among them, I have investigated the function of Awd (Abnormal Wing Discs), the only demonstrated *Nme* gene family member in *Drosophila* during fruit fly development. In addition, during the period I spent in Dr. Adryan lab, I also explored the role of VHL (Von Hippel-Lindau), a well-established partner of Awd, in Malpighian tubules. For genetic and developmental research *Drosophila* represents the most amenable model system: with a genome of 137 Mb, divided in 4 chromosome pairs, 3 autosomes and a sexual one, gene redundancy is infrequent. This allows to escape compensatory effects from other genes (not a secondary aspect for a gene family which accounts for 10 members, Arnaud-Dabernat *et al.*, 2003). Moreover, the availability of potent and powerful genetic analysis tools available in this tiny model system makes *Drosophila* incomparable for the fine-tuning molecular dissection of signalling pathways and developmental processes.

## 1.4 *Drosophila* oogenesis

A *Drosophila* female has got two ovaries, which are the largest organs of an adult fly. They are connected through a lateral oviduct to the common one. In the common oviduct, two spermathecae, two seminal receptacles and accessory glands open out, so that the egg gets fertilised while reaching the uterus and then exits the body (Figure 4, King, 1970).

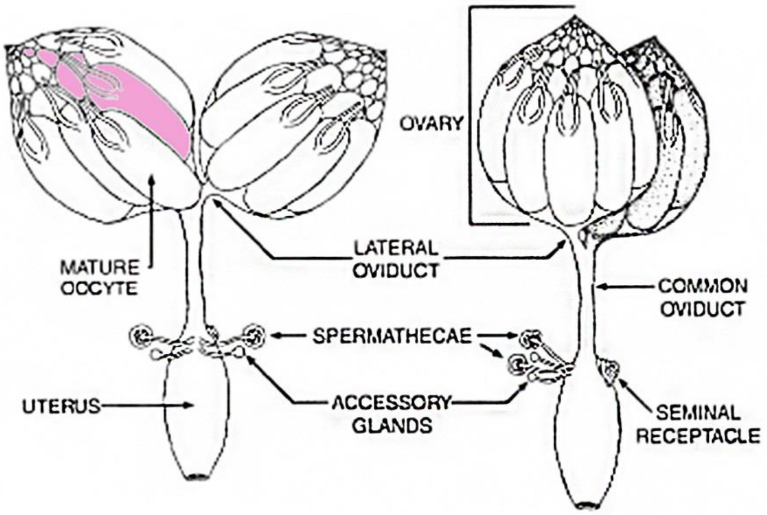

**Figure 4 Representation of an adult *Drosophila* female reproductive system shown from dorsal and lateral perspectives.** An ovariole inside an ovary is highlighted in pink. Modified from Bloch Qazi *et al.*, 2003.

Each ovary, covered by a peritoneal sheath (a network of anastomosing muscle fibers), is composed of 14-16 ovarioles. An ovariole represents an egg production line with chains of developing oocytes, generally 6-7 per string. Single oocyte development takes place into an egg chamber, which consists of a 16-germ cell cyst (1 oocyte and 15 nurse cells to support oocyte development) and a monolayer of epithelial cells of somatic (mesodermal) origin, the follicular epithelium composed of follicle cells (FCs). Oogenesis begins in the germarium, located in the most distal region of each ovariole. The germarium is a unique structure where somatic and germline stem cells harbour and egg chambers are assembled. In the vitellarium, the most proximal part of each ovariole, egg chambers complete their development, giving rise to an egg able to be fertilised (King, 1970; Spradling, 1993).

Ovarioles are surrounded by a *tunica propria* and an epithelial sheath (composed of two layers of epithelial tissue separated by a layer of circular muscles, with an important role in the movement of egg chambers toward the proximal region). Terminal filaments connect the germaria with the epithelial and ovariole sheaths.

The oogenic process is arbitrary divided into 14 stages; egg chambers of each stage can be recognised based on morphological criteria and relative dimensions of oocyte respect to nurse cells (Figure 5).

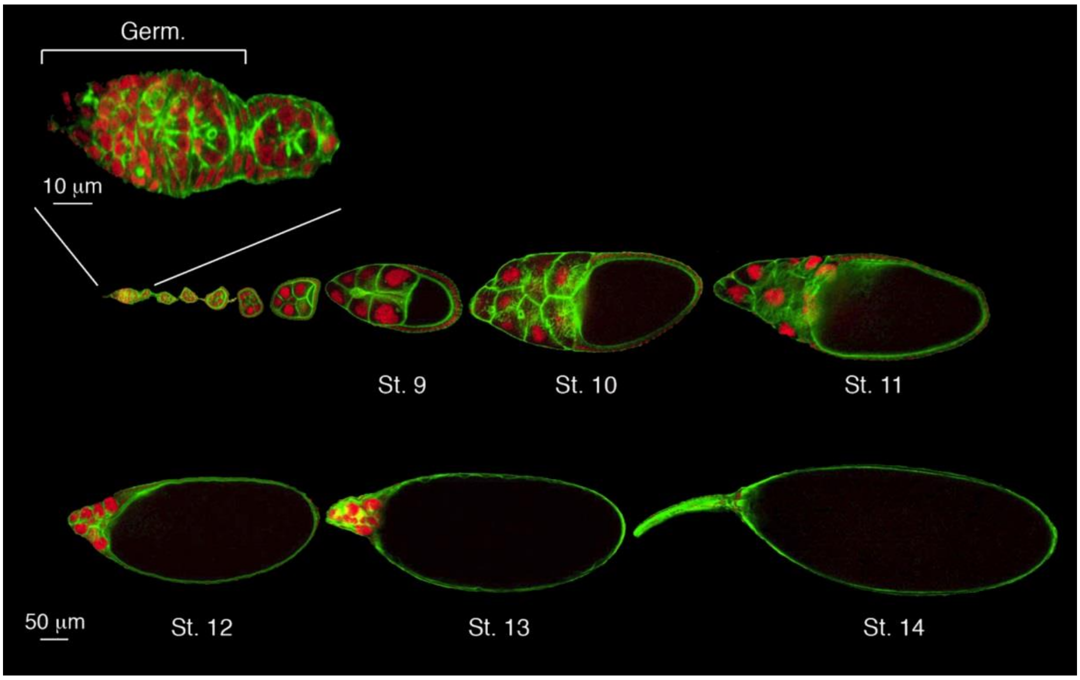

**Figure 5 *Drosophila* egg chamber development**. Confocal cross-sections of *Drosophila* wild type egg chambers stained with FITC-phalloidin (green) that reveals F-actin cytoskeleton and with the nuclear dye propidium iodide (red). A higher magnification of the germarium and of a stage-1 egg chamber are shown (top left).Oogenesis is generally broadly divided in early (stages 1-6), mid (stages 7-10) and late (11-14). As long as the egg chamber develops, oocyte dimensions increase. Germ=germarium. Modified from Cavaliere *et al.*, 2008.

New egg chambers are generated in the germarium, in which 4 regions (named 1, 2a, 2b and 3) have been distinguished, thanks to clonal analysis studies and microscopic observations (Schupbach, 1987; Wieschaus and Szabad, 1979). In region 1, 2-3 germline stem cells (GSCs) are present. Their maintenance is dependent on a GSC niche formed by terminal filaments and cap cells. Cap cells specifically physically contact GSCs through adherens junctions (Song *et al.*, 2002).

The formation of the germline cyst begins in region 1 of the germarium, where a GSC divides asymmetrically, giving rise to a daughter cell (self-renewing) and a cystoblast. Cystoblast is already a committed cell: it undergoes 4 mitotic cell divisions with incomplete cytokinesis, giving rise to the 16-germ cell cyst. In this syncytium, cells, called cystocytes, are interconnected through cytoplasmic bridges, named ring canals. One of the two cells with 4 ring canals will be specified as the oocyte and will migrate posteriorly in the cyst. The exact molecular mechanism regulating oocyte selection is unknown, but a central role has been assigned to fusome, an intracellular branched germline-specific organelle formed by membrane tubules and cytoskeleton proteins with properties similar to the ER, that connects all cystocytes but asymmetrically segregates during the cystocyte division (de Cuevas *et al.*, 1997). Posterior migration of the oocyte is mediated by homophilic adhesions (Godt and Tepass, 1998). While oocyte proceeds through the meiotic division, arresting at prophase I, nurse cells become polyploid; they will transport mRNA, proteins and organelles to the oocyte through ring canals during oogenesis (Lin and Spradling, 1993). At the crossroad between region 2a and 2b, 2 follicle cell stem cells (FCSCs) stand; the same niche of GSCs also maintains FCSCs through secreted signals. FCSC asymmetric division, which is coordinated with that of GSCs, gives rise to a daughter cell and a FC precursor, which divides few times. When germline cyst reaches this region of the germarium, it gets encapsulated by FC precursors that migrate among the different cysts, separating one from the others. Migration involves an EMT (epithelial-mesenchymal transition) of precursors of FCs; finally, these cells wrap the cysts, forming one single layer of epithelial cells Roth, 2001. Cyst encapsulation gives rise to the egg chamber. Indeed, in the region 3 of the germarium a stage 1 egg chamber is formed (Figure 6).

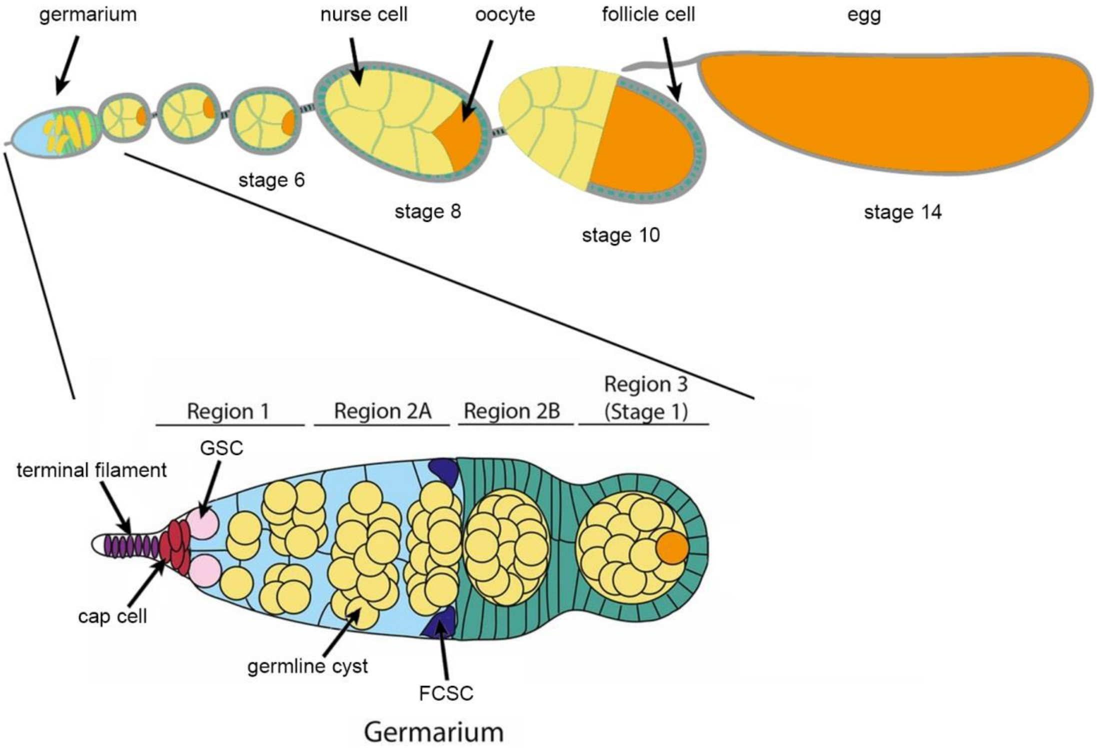

**Figure 6 *Drosophila* oogenesis.** In the upper panel a scheme of the oogenic process is reported. In the lower panel, a representation of the germarium highlights the principal cell population residing in each region. Modified from Silva and Jemc, 2015.

### 1.4.1 Follicular epithelium morphogenesis and functions

Follicular epithelium, a derivative of the mesodermal layer, has a primary role in oocyte development: interactions between FCs and oocyte define oocyte and embryonic orthogonal polar axes (antero-posterior and dorso-ventral axes) and eggshell deposition is due to active secretion of vitelline membrane and eggshell components by FCs.

In the follicular epithelium different subpopulations can be recognised that are specified during oogenesis through multiple signalling events. The first recognisable sign of FC differentiation coincides with the first contact between somatic and germ cells and it occurs in the germarium: 16 precursors of FCs stop dividing and migrate toward a cyst. Complex signalling pathway integrations and signal modulations allow the definition of 2 subpopulations: stalk cells and polar cells. While polar cells define the egg chamber tips, stalk cells are essential to separate cysts, avoiding cyst fusions (Wu *et al.*, 2008).

Notch (N) signalling pathway plays a key role in the specification of polar cells (Lopez-Schier and St Johnston, 2001). Anterior polar cells are specified first (Figure 7), thanks to Delta (Dl) exposure (the N ligand) on the membrane of germline cells when the cyst reaches the boundary between regions 2a and 2b of the germarium (Nystul and Spradling, 2010). N activation specifies 4-6 FCs as polar cells. The posterior polar cells are specified shortly after, in the region 2b, again thanks to the signalling mediated by Dl from the germline cysts. These newly induced polar cells release signals to activate the N and JAK/STAT signalling pathways in adjacent cells; these two pathways act together to specify stalk cells. The non-induced cells (which lie in lateral regions of the cyst) differentiate as epithelial cells.

During the first stages of oogenesis the polar cell number is restricted to two per tip by apoptosis of extranumerary polar cells (Khammari *et al.*, 2011).

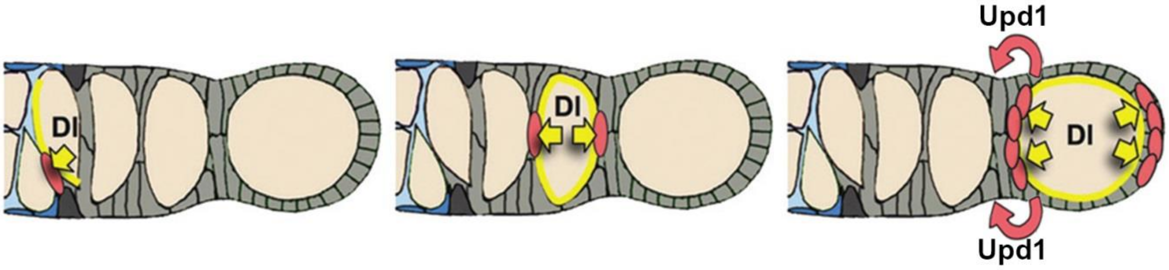

**Figure 7 Model showing the activation of N signalling in the germarium to specify polar and stalk cells.** A signal from cysts near the region 2a/2b border (left) induces FSC daughters to cross-migrate. A signal from the posterior region 2b cyst initiates the first round of polar cell specification (middle) and a later signal (right) maintains polar cell fate. Moreover, secreted Unpaired1 (Upd1), the ligand of JAK/STAT pathway, from polar cells subsequently determines specification of stalk cells. Modified from Nystul and Spradling, 2010.

A follicular epithelium of ~80 cells surrounds the germ cyst as it enters in the vitellarium. While polar and stalk cells do not divide anymore after their specification, epithelial FCs continue to divide and proliferate until stage 6, giving rise to a monolayered epithelium of 650-1000 cuboidal FCs. FCs proliferation occurs through 4 mitotic cycles and allow FCs to accommodate and coat the growing cyst; indeed, the cyst size increases dramatically throughout oogenesis. Proliferation of FCs ends at stage 6, when upregulation of germline Dl induces a second round of N activation in FCs (Lopez-Schier and St Johnston, 2001). This induces FCs to switch from mitotic cycle to endocycle, in which 3 rounds of DNA replication aren't followed by cytokinesis: in this way, FCs become polyploid and competent to respond to subsequent signals emanating from polar cells and oocyte for epithelium patterning.

Polyploidy is also essential for the final size of FCs. While egg chamber proceeds from stages 6 to 9, antero-posterior and dorso-ventral axes specification becomes obvious through spatial localisation of specific mRNAs and proteins (Riechmann and Ephrussi, 2001).

During mid-oogenesis, the uniform cuboidal epithelium starts to differentiate and many other subpopulations are determined. The first event takes place at stage 5, when polar cells induce 10-11 cells at each egg chamber termini to differentiate as terminal FCs; the remaining cells are named main body FCs. At stage 7, anterior polar cells induce 4-6 neighbouring cells to adopt border cell fate through secretion of Upd1 (Unpaired1) and subsequent activation in presumptive border cells of the JAK/STAT signalling pathway (Xi *et al.*, 2003). These cells are competent for an active migration through the germ cyst to reach the anterior surface of the oocyte. Delamination and subsequent migration of border cell cluster occurs at stage 9. The successful migration of this group of cells is crucial for development since border cells are responsible for the formation of the micropyle, the sperm’s entry point. While border cells invade the germ cyst reaching the oocyte, most of the main body FCs also migrate posteriorly to cover the entire oocyte. While this migration occurs, FCs undergo a morphological cell shape change, becoming columnar cells. About 50-80 FCs remain in the anterior half of the egg chamber to cover nurse cells. To do so they assume an extremely thin shape, hence the name of squamous cells (Horne-Badovinac and Bilder, 2005). Finally, at stage 10b, some columnar FCs named centripetal FCs migrate at the interface between oocyte and nurse cells to cover the entire anterior surface of the oocyte. At stage 10b, FCs undergo another change in the cell cycle, by performing selective amplification cycles of specific genomic loci encoding proteins with a primary role in the synthesis of egg coating layers. This is important since, at late oogenesis, FCs synthesise yolk proteins and components of the eggshell that will be secreted from their apical surface toward the oocyte (Cavaliere *et al.*, 2008).

After stage 10, an intense dumping of nurse cell cytoplasm toward oocyte can be observed, followed by oocyte cytoplasm streaming (Quinlan, 2016) and nurse cell apoptosis (Cavaliere *et al.*, 1998; Foley and Cooley, 1998). At late oogenesis also FCs undergo apoptosis (Nezis *et al.*, 2002) and a fully-developed egg emerges from the vitellarium.

As it clearly appears from this description, many morphogenetic events occur during oogenesis, requiring activation of many different signalling pathways and intense crosstalk between soma and germline. These features make *Drosophila* oogenesis an amenable model system for multiple purposes, from stem cell lineage studies to cell cycle control mechanisms and fate specification analyses; moreover, genetic tractability of *Drosophila* ovaries, easiness of access and dispensability for fly survival definitively elect oogenesis as a powerful model for genetic and developmental studies. It is worth noting that follicular epithelium and mammalian epithelia share many common features, including a pronounced apical-basal polarity. Loss of apical-basal cell polarity is one of the first signs of transformation in epithelial cells. Because carcinomas are the most recurrent form of human cancers, *Drosophila* follicular epithelium represents a tissue in which carcinogenesis can be approached through genetic manipulation.

## 1.5 *Drosophila* embryogenesis

*Drosophila* embryogenesis is an extremely rapid process, 23 hours at 25 °C, subdivided in 17 stages which culminate with the hatching of a first instar (L1) larva from a specialised structure in the eggshell called operculum. The egg is extremely huge, and filled up with nutrients and maternal signals to drive and support embryo development. The necessity of rapidity in completing embryogenesis is due to the fact that eggs aren't able to eat and their complete dependence on maternal supplies makes them attractive to predators. Because eggs also aren't able to defend themselves nor to move away from dangers, rapidity in carrying out this first phase of development probably appeared to evolution the most adaptive choice to guarantee species survival (Farrell and O'Farrell, 2014).

Once a *Drosophila* female mated, fertilisation, egg activation, and completion of oocyte meiosis take place. Neuroendocrine and endocrine signals, besides environmental and physiological cues, regulate egg laying (Bloch Qazi *et al.*, 2003). The very first phase of embryogenesis rely on maternal gene products specifically loaded into the egg in a spatially-specific manner, generating a highly polarised embryo. At the beginning of embryogenesis a rapid series of mitotic nuclear divisions occurs, not accompanied by cytokinesis, thus generating a syncytial blastoderm. During the first 9 synchronised mitotic divisions nuclei remain in the internal region of the embryo. Starting from the 10th cycle most of them migrate at the periphery. Pole nuclei, the precursors of germ cells, after nuclear cycle 8 reach the posterior pole, where a specialised cytoplasm (named pole plasm) has been deposited during oogenesis. Pole cell cellularisation occurs at nuclear cycle 9, while the other nuclei cellularise at the 14th cycle (Mazumdar and Mazumdar, 2002).

After the 14th cycle zygotic gene activation takes place, indicating that the maternal-to-zygotic transition has occurred. A rapid gastrulation follows, and cells get segregated into two cell lineages: larval cells and imaginal cells (Harbecke *et al.*, 1996). Larval cells stop dividing and differentiate in the larval organs during embryogenesis. During the subsequent larval life, these cells will grow by increasing their size becoming polyploid. Instead, the imaginal cells during larval life organise in small clusters, named imaginal discs, and remain diploid, continuing to divide by mitosis until metamorphosis.

## 1.6 *Drosophila* larval and pupal development

*Drosophila* larval development consists of 3 instars (L1, L2, L3) spaced out by two molts. Each instar is extremely rapid: 24, 24 and 48 hours respectively at 25 °C. At the end of the third instar, well-fed L3 larvae become wandering: they stop feeding and look for an appropriate (dry and safe) place where they can pupate. After puparium formation, metamorphosis occurs. Hormonal signals trigger both molts and pupation phases, at the end of which a completely different individual will emerge (Buszczak and Segraves, 2000). Indeed, metamorphosis in holometabolous insects like *Drosophila* implies dramatic changes in larval organisation to give rise to the imago; these changes include histolysis of most larval organs and their replacement with specific adult structures generated by morphogenesis, differentiation and eversion of imaginal tissues.

### 1.6.1 Imaginal tissues

*Drosophila* larvae host in their body as many as 10 imaginal disc pairs plus the genitalia disc. Imaginal discs are flattened sacs of undifferentiated epithelial cells which lie in stereotypical positions inside the larval body. During metamorphosis, they will give rise to the adult limbs (including legs, wings, antennae, mouth parts, etc.) and part of the body wall, accordingly to their name (Figure 8). With the exception of Malpighian tubules, which just undergo remodelling events during metamorphosis, most of the other larval organs are replaced thanks to imaginal cells organised in imaginal nests or rings. Abdomen derives from histoblasts, another type of imaginal cells nested into the larval integument.

As previously stated, imaginal cell segregation occurs during embryogenesis, when small clusters of 5-40 imaginal cells get set aside. During larval life, imaginal disc cells start to proliferate, initially quickly, then as development proceeds, the division rate diminishes. This intense proliferation activity allows to form folded, single layer, epithelial sacs of about 50,000-80,000 cells (Bryant and Schmidt, 1990). By the end of the third instar to the first day of pupal development, imaginal discs proliferation stops and differentiation takes place. During *Drosophila* metamorphosis, extensive remodelling of imaginal discs occurs. This process has been split into 2 stages: elongation and eversion (Fristrom and Fristrom, 1993).

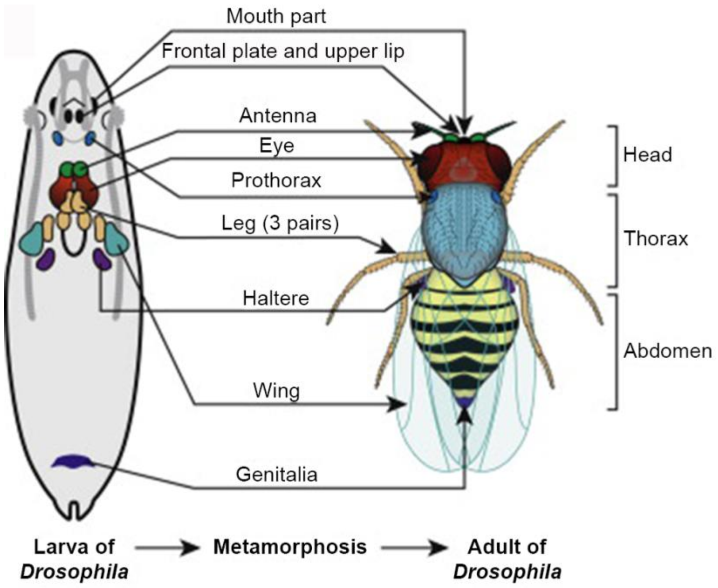

**Figure 8 Localisation and presumptive fate of *Drosophila* imaginal discs.** All the appendages and genitalia structures of an adult of *Drosophila* derive from appropriate imaginal discs that will undergo metamorphic processes during pupation. Modified from Aldaz and Escudero, 2010.

Imaginal discs are typically composed of two epithelia, a columnar layer, also called disc proper, and a squamous layer, the peripodial epithelium. The disc proper is a pseudolayered epithelium, since cell nuclei do not lie on a hypothetical straight line. The basal sides of all cells directly contact basement membrane; however, not all cells reach the apical surface of the epithelium. Although the imaginal discs are composed of undifferentiated epithelial cells, positional information map, as well as axes formation, become established during disc growth (Cohen, 1993).

### 1.6.2 Wing disc development: morphogenesis, structure and function

When a larva hatches, wing disc primordia are formed by 20-50 cells; proliferation onset occurs 15-17 hours after hatching, with a doubling time of 8.5-10.6 hours. By the end of the third larval stage wing discs will reach 50,000-75,000 cells. Cessation of proliferation occurs 21 hours after puparium formation.

Because of its epithelial origin and its high proliferation rate, wing discs have been long used as model systems to study cell proliferation, genetic control of tissue size, shape and patterning and its connection to tumorous behaviours.

In a L3 wing disc it is easy to distinguish a columnar layer and a peripodial epithelium separated by a lumen. The apical surfaces of both epithelia are oriented toward the lumen (Figure 9A, left panel). Growth of the wing disc is controlled by the activity of many signalling pathways acting on a short or long range to pattern the wing primordium. Indeed, during wing disc development, many territories get determined: the wing pouch will give rise to the wing blade, the notum will build up the body wall parts to which the wing is linked and the hinge will make the connection between the body cuticle and the appendage (Figure 9A,B). As could be inferred from Figure 9A representing the wing fate map, a concentric-ring pattern characterises the organisation of the wing disc along the proximo-distal axis. Antero-posterior and dorso-ventral axes, instead, are patterned in a more conventional way, in which the opposed compartments are separated by specific boundaries (Figure 9A, right panel; for more details, see below). The unusual proximo-distal pattern is linked to the 2D nature of wing disc, while the future adult structure requires a 3D organisation. The concentric-ring profile appears to be the cleverest way to pattern along 3 axes a 2D primordia. In the establishment of distalisation information required for the patterning of the wing disc along the proximo-distal axis, Wingless (Wg), Decapentaplegic (Dpp) and EGFR pathways play a key role (Cavodeassi *et al.*, 2002; Klein, 2001).

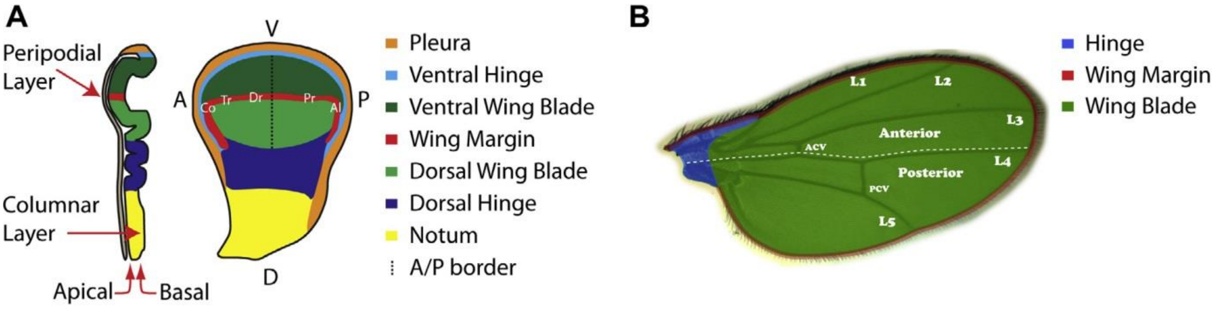

**Figure 9 Morphology and fate map of wing imaginal disc. (A,B)** The different coloured regions in the primordia of the wing disc (in A) will give rise in the adult wing to the same coloured structures. Cells of the wing pouch margin will differentiate into unique classes of bristles and hairs. In the adult wing, 5 longitudinal veins (L1-L5) can be recognised, L1-L3 in the anterior wing blade while L4, L5 in the posterior. 2 crossveins are present: the anterior crossvein (ACV) linking L3 and L4 and the posterior crossvein (PCV) linking L4 and L5. In A right panel A=anterior; P=posterior; D=dorsal; V=ventral. Modified from Hartl and Scott, 2014.

The subdivision of the wing disc into an anterior (A) and a posterior (P) compartments arises first and very soon during development: it is inherited from the embryo and further established during the early larval life. Indeed, during embryogenesis the genetic control of embryo segmentation involves a cascade of gene regulation: the expression of *gap* genes followed by *pair-rule*, *segment polarity* and *homeotic* ones, progressively define more and more accurately the polarisation and pattern of each segment, also providing positional clues that define each segment identity. The homeobox gene *engrailed* (*en*) belongs to the segment polarity gene class; its expression is restricted to the posterior compartment of each segment and it is also inherited as it is by the larva (Lawrence and Morata, 1976). In the anterior compartment, *cubitus interruptus* (*ci*) expression is upregulated, marking the anterior cells.

One important feature of *en* is that it acts as a selector gene: it determines the differentiation between anterior and posterior cells and it generates and maintains an AP border, which not only keeps separated the two compartments (a cell lineage restriction exists between cells of the 2 opposite compartments, Garcia-Bellido *et al.*, 1973) but also drives the formation of a boundary between *en*-expressing and non-*en*-expressing cells (Mann and Morata, 2000). Importantly, at this boundary a pattern organising centre get established and cells secrete Dpp, a long range acting morphogen that regulates cell proliferation (Martin-Castellanos and Edgar, 2002) and AP patterning, beside distalisation (Lawrence and Struhl, 1996).

The dorso-ventral compartmentalisation starts to be established at the beginning of the second larval instar. An early subdivision of the wing disc into the presumptive wing blade and notum is guaranteed by the antagonistic action of two signalling pathways, EGFR (epidermal growth factor receptor) and Wnt (Figure 10A). They are activated thanks to the secretion of Vein (Vn) and Wingless (Wg, a *Drosophila* Wnt-1 homolog) in the dorsal and ventral region respectively. *vn* expression in the ventral compartment is suppressed by Wg. Instead, Vn-stimulated activation of EGFR signalling represses *wg* expression in the dorsal compartment (Baonza *et al.*, 2000), upregulates the expression of *Iro-C* gene complex and especially of *apterus* (*ap*) gene (Wang *et al.*, 2000). *ap* acts as a selector gene: its expression subdivides the disc into two compartments, composed of *ap*-expressing and non-*ap*-expressing cells. Ap is a transcription factor that induces the expression of *fringe* (*fng)* and *serrate* (*Ser*) in the whole dorsal compartment (de Celis and Bray, 1997). In the non-*ap*-expressing cells, *Dl* expression is stimulated.

*fng* encodes a glycosyltransferase; it acts on N receptor in the Golgi apparatus. Fng-mediated post-translational glycosylation makes N receptor unable to respond to Ser and thus prevents the activation in the dorsal compartment of N signalling pathway. On the other hand, the glycosylated form of the receptor can trigger pathway activation as a consequence of Dl stimulation. In the ventral compartment, N receptor is not post-translationally modified by Fng activity, so also in this compartment N signalling activation doesn’t occur.

However, at the boundary, interaction between the N receptors and the appropriate ligands occurs and positive activation of the pathway takes place. Cells at this border stop proliferating, giving rise to a ZNC (zone of non-proliferating cells) and to a pattern organising centre (Herranz and Milan, 2008). N signalling positively regulates the expression of the morphogen Wg at the boundary (de Celis *et al.*, 1996). Wg acts as a morphogen that allows further patterning of the two compartments. Thus, it appears that Dpp and Wg are both morphogens (Cadigan, 2002), involved in the establishment of polarity in the wing imaginal disc, acting through the formation of gradients that allow the activation of specific target genes in a concentration-dependent manner (Figure 10B).

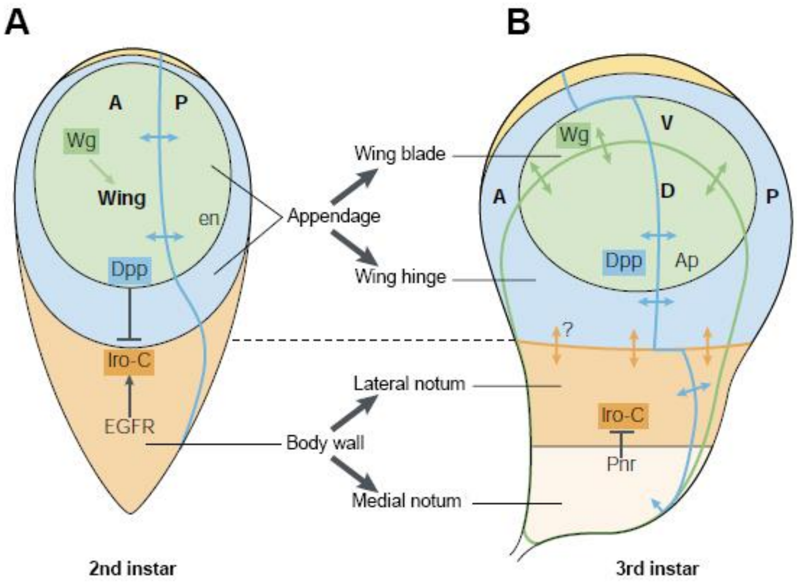

**Figure 10 Territorial subdivision of the imaginal wing disc. (A)** Drawing of an L2 wing imaginal disc with indication of the principal signalling pathways participating in its patterning. During the 2nd instar, 3 main regions of subdivision of the wing disc are established: the wing pouch (green), the hinge (light blue) and the notum (orange). The AP organising centre is indicated with a light blue line and arrows. **(B)** During the third instar, the disc grows and gets subdivided in smaller domains that ultimately will give rise to most of the structures of the mesothorax of the fly, including the wing. Complex signalling pathway participates in disc patterning along the three axes. The second patterning centre at the DV boundary is indicated with green line and arrows. A third organising centre at the boundary between the pouch and the notum is supposed to exist (orange line), but the putative signalling molecule and its pathway (orange arrows) are unknown. Modified from Gomez-Skarmeta *et al.*, 2003.

### 1.6.3 *Drosophila* larval fat body: morphogenesis, structure and function

*Drosophila* larval fat body is the largest larval organ; it is a multilobed tissue extending the whole length of the larval body. It lies between the gut and the body wall musculature. Two arms can be distinguished, a ventral and a dorsal ones, linked through a bridge. Fat body cells, also known as trophocytes or adipocytes, have a flat polygonal shape and appear tightly associated with one another. They arise in the embryo from a portion of the somatic mesoderm during stage 11-12 (Butterworth *et al.*, 1965). As the other larval organs, adipocyte proliferation occurs during embryogenesis to get a final cell number of 2000-2500 cells; instead, during larval life, particularly the second instar, they grow by increasing their size through polyploidy (their nuclei reach 256C in DNA content); indeed, during larval life, the overall fat body tissue mass increases of 250-fold (Andersen *et al.*, 2013). Larval gonads are embedded into the ventral fat body arm.

As the name suggests, fat body is the principal larval lipid storage: in well-fed larvae, adipocytes take up from the haemolymph (the unique *Drosophila* extracellular circulating fluid) circulating lipids (mostly diacylglycerol, transported as lipoproteins named lipophorins) and accumulate triglycerides (TAGs) into cytoplasmic lipid droplets (Canavoso *et al.*, 2001). Fat body cells also store sugars in the form of glycogen and proteins. Growth and storage of nutrients in fat body cells is promoted by activation of the *Drosophila* Insulin like receptor

(InR)/phosphoinositide-3-kinase (PI3K)/target of rapamycin (TOR) pathway. Moreover, the fat body is a major source of basal laminae components (Fessler and Fessler, 1989), such as Viking (a subunit of Collagen IV and a major component of basement membrane) and Cg25C (also known as Collagen type IV alpha 1) proteins. Because of these roles, fat body is considered as the equivalent of mammalian adipose tissue and liver (Arquier and Leopold, 2007). During fasting (e.g. during pupal stage), mobilisation of reserves requires the activation of an autophagy mechanism triggered by hormonal signals (Rusten *et al.*, 2004) and amino-acid sensing mediated by the TSC/TOR signalling pathway (Zhang *et al.*, 2000).

Moreover, fat body couples organismal growth (that is, it coordinates the growth of the different larval organs) in response to nutrient availability through humoral signal secretion (Colombani *et al.*, 2003; Mirth and Riddiford, 2007). One of them has been recently identified (Rajan and Perrimon, 2012): fat cells synthesise and secrete Unpaired2 (Upd2), which acts on a subpopulation of GABAergic neurons, able to stimulate the release of DILPs (*Drosophila* insulin-like peptides) by IPCs (insulin-producing cells). DILPs are potent activators of anabolism, thus regulate peripheral tissue growth (Brogiolo *et al.*, 2001). Upd2 is produced in response to high fat and high sugar levels. The humoral signal produced in response to high amino acid diet has remain unknown until recently (Koyama and Mirth, 2016). More and more signals are being discovered (Delanoue *et al.*, 2016), revealing the existence of an intense crosstalk of signalling pathways and inter-organ communication through secreted signals arranging the overall larval development (Figure 11 and Andersen *et al.*, 2013).

Besides this important role in coordination of larval growth, fat body exerts another important function during larval life: it has a primary role in *Drosophila* innate immune response, together with Malpighian tubules and haemocytes. Indeed fat body and haemocytes are the primary immune organs of insects (Lemaitre and Hoffmann, 2007) and they are able to synthesise and secrete anti-microbial peptides.

It is pretty much clear that the fat body unrolls an intense activity during larval life. To accomplish all these different functions of orchestrating larval growth while protecting it from infection, endo- and exo-cytic trafficking routes are deeply employed.

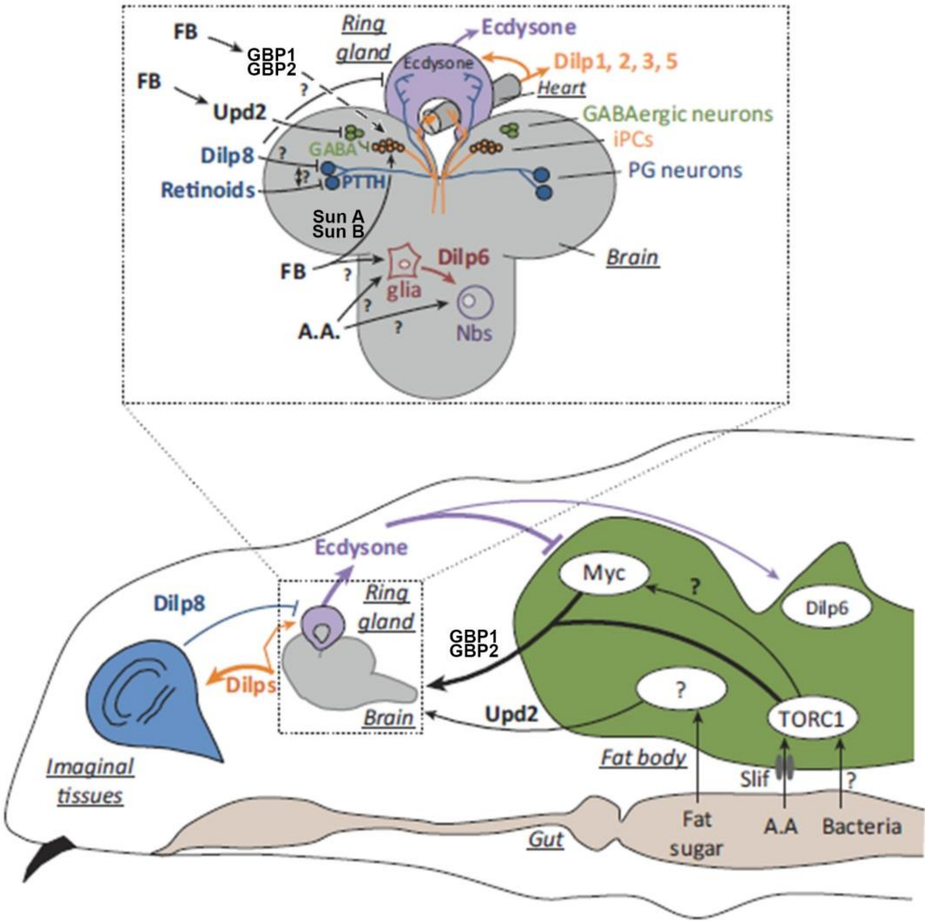
FB
GBP1
GBP2
Ring gland
Ecdysone
Ecdysone
Dilp1, 2, 3, 5
Heart
FB
Upd2
GABAergic neurons
IPCs
Dilp8
GABA
Retinoids
PTTH
PG neurons
Sun A
Sun B
FB
Dilp6
glia
Brain
A.A.
Nbs
Ecdysone
Myc
Dilp6
Dilp8
Ring gland
GBP1
GBP2
Dilps
Brain
Upd2
TORC1
Imaginal tissues
Fat body
Slif
Gut
Fat
sugar
A.A
Bacteria

**Figure 11 Physiological interplay between larval and imaginal tissues couples growth in response to nutrient availability.** Sensing of nutrient availability occurs in the fat body that adsorbs them directly from the gut. Activation of TOR signalling in adipocytes in response to nutrients, insulin (InR) signalling and PI3K activity promotes tissue growth, through positive regulation of dMyc, and inhibits autophagy. Moreover, fat body-derived humoral signals provide information on the nutrient availability and metabolic status of the larva that are received by specific brain subpopulations which, in turn, orchestrate the overall development. In particular, TOR activity in adipocytes allows the release of DILPs. DILPs released from the brain promote growth in peripheral tissues including the imaginal discs.
Larval moulting and pupation are regulated by the steroid hormone 20-hydroxyecdysone (20E). 20E synthesis occurs in the ring gland and is regulated by InR/PI3K signalling. Once synthesized, 20E is released in the haemolymph. During pupation, 20E induces alteration in the morphology and function of fat body cells: indeed, autophagy is stimulated through inhibition of InR/PI3K signalling. Moreover, 20E also inhibits growth by downregulating dMyc. Modified from Andersen *et al.*, 2013.

## 1.7 N signalling pathway

N signalling is probably the most widely employed short-range intercellular communication pathway, highly evolutionarily conserved among metazoans. The first *N* mutant in *Drosophila* was isolated about 100 years ago by Morgan. Since then, many other studies of genetics, biochemistry and cellular biology, contributed to the comprehension of this pleiotropic signalling at a great extent (Artavanis-Tsakonas and Muskavitch, 2010).

Typically, the N pathway enables short-range communication between adjacent/neighbouring cells. Indeed, successful transmission of N signals requires a physical interaction between the signal-sending and the signal-receiving cells. The final outcome of N signalling activation is strictly context dependent, since it can promote or suppress cell proliferation, cell death, acquisition of specific cell fates or differentiation programs (Kopan and Ilagan, 2009). This “ying-yang” behaviour of N signalling, besides uncovering a still not fully understood flexibility of the pathway that can account for the different outcomes triggered despite the apparent rigidity of the core pathway (see below), can also explain the controversial role of the signalling in multiple human disorders, including cancer. Indeed, different tumour cohorts can display aberrant gain or, at the opposite, loss of N signalling, so that the pathway exerts pro-oncogenic or tumour-suppressive functions depending on the tissue context (Ntziachristos *et al.*, 2014).

To date, it is well established that the core of this cell-cell signalling pathway in *Drosophila* is composed of a unique receptor, N, and 2 ligands, Dl and Ser; with regard to the nuclear downstream effectors, the transcription factor Su(H) (Suppressor of Hairless) and the coactivator Mam (Mastermind) mediate N activity to upregulate specific genes, while Hairless and Smrter are responsible for N targets downregulation.

The 300 kDa N receptor (Figure 12A), encoded by the haploinsufficient *N* locus on the X chromosome, is a type I single-pass integral protein. The extracellular domain is characterised by 36 EGF-like repeats. This region is crucial for ligand-receptor interaction: deletion of the 11-12 EGF-like repeats causes the receptor to be insensible to ligand stimulation (Rebay *et al.*, 1991). A single negative regulation region (NRR) follows EGF-like repeats, which prevents ligand-independent receptor activation and it also includes a heterodimerisation domain. At intracellular level, a long unstructured linker contains a nuclear localisation sequence (NLS) that connects the transmembrane portion to an ANK domain, that mediates the interaction between the receptor and other proteins. A PEST domain at the very C-terminal regulates protein stability and degradation (Kopan and Ilagan, 2009).

Both ligands Dl and Ser are also type I transmembrane proteins that own in their extracellular portion a DSL domain (this is typical of N ligands), specialised EGF-like repeats composing the DOS domain, and classical EGF-like repeats. Both the DSL and the DOS domains play a critical role in the interaction with the receptor molecule (Kopan and Ilagan, 2009).

N molecules undergo a complex series of post-translational modifications before and after its exposure on the cell surface and its interaction with the ligand (Figure 12B). N receptor is synthesised as a single protein; while it traffics in the ER, it gets cleaved in its lumenal domain at the so-called S1 site, very close to the transmembrane region, by the proteolytic activity of a furin-like convertase that generates a C-terminal and a N-terminal N fragments (CTF and NTF, respectively). In the Golgi apparatus, the two halves get jointed together again thanks to non-covalent interactions. While the receptor is cleaved, it also undergoes glycosylation events (Haines and Irvine, 2003). The glycosylation mediated by Fng has been particularly and intensively studied because of the role of this post-translational modification in the activation of N signalling in the wing disc (see paragraph 1.6.2). Generally, this secondary modification of the receptor alters its responsiveness to different ligand stimulation in specific context. Surface-exposed N receptor can be both a full-length or an heterodimeric protein; both molecules retain their ability to signal (Kidd and Lieber, 2002).

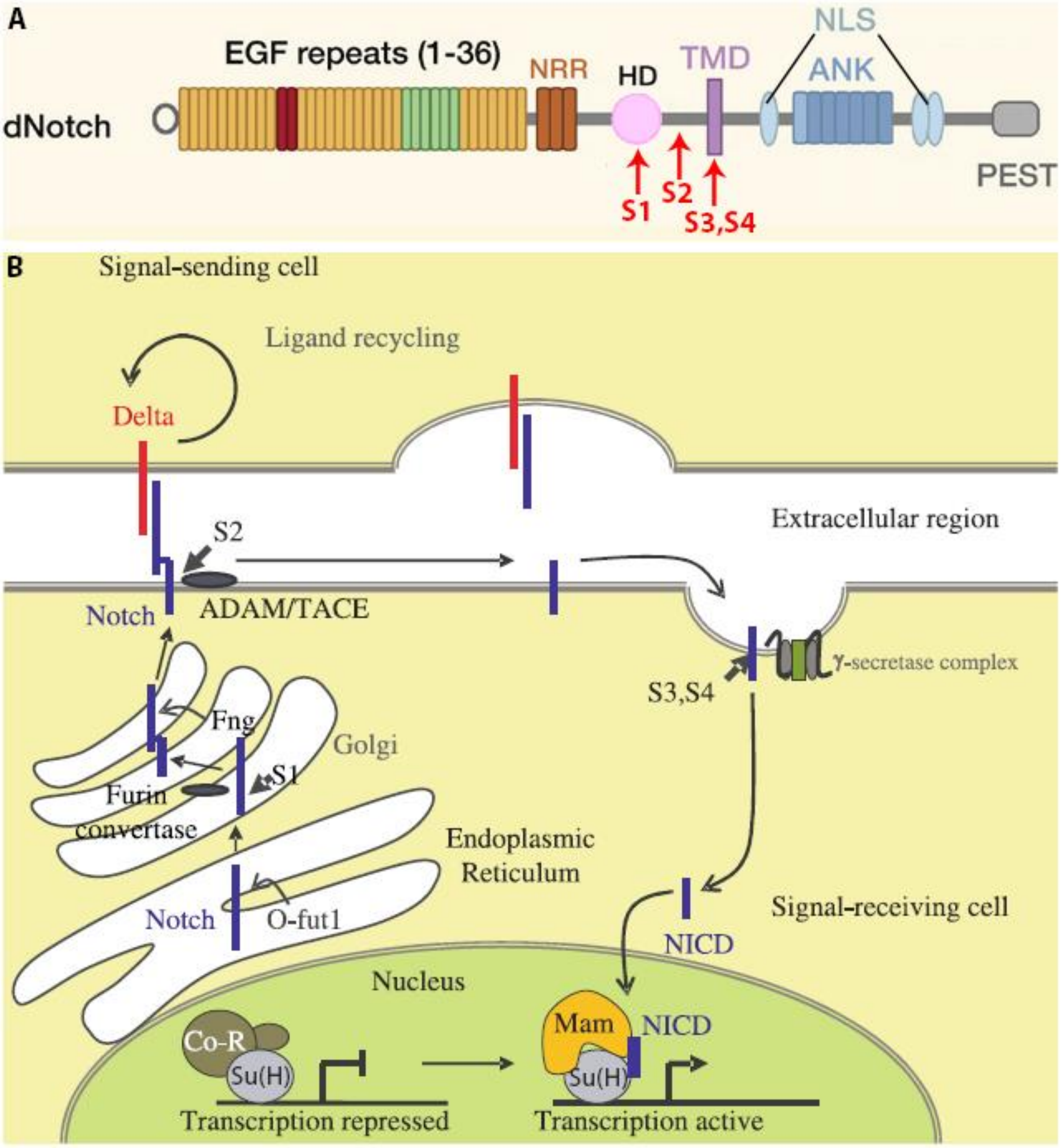
A
EGF repeats (1-36)
NRR
HD
TMD
NLS
ANK
dNotch
PEST
S1
S2
S3,S4
B
Signal-sending cell
Ligand recycling
Delta
Extracellular region
S2
ADAM/TACE
Notch
γ-secretase complex
S3,S4
Fng
Golgi
S1
Furin
convertase
Endoplasmic
Reticulum
Notch
O-fut1
Signal-receiving cell
NICD
Nucleus
Mam
NICD
Co-R
Su(H)
Su(H)
Transcription repressed
Transcription active

**Figure 12 N structure and post-translational modification events. (A)** Scheme of the *Drosophila* N receptor structure. The EGF repeats are in yellow, with the exception of those required for ligand-mediated activation and inhibition that are in red and green respectively. NRR region is in orange. In the heterodimerisation domain (HD in pink) the S1 cleavage occurs (indicated by the first red arrow). The HD is followed by the transmembrane domain (TMD in violet). The S2 cleavage (indicated by the second red arrow)occurs in the juxtamembrane region between the HD and TMD. In the TMD the S3 and S4 cleavages occur. Modified from Kopan and Ilagan, 2009. **(B)** N is translated in the endoplasmic reticulum, where it is glycosylated by the *O*-fucosyltransferase O-fut1. N then translocates into the Golgi apparatus, where it is cleaved by a Furin convertase at the S1 site and further modified by the *N*-acetylglucosaminyltransferase Fng. N then is translocated to the plasma membrane. Following ligand-mediated stimulation, a series of proteolytic cleavage events take place to produce the NICD fragment. For details, see text. Modified from Fiuza and Arias, 2007.

Interaction with a DSL ligand exposes the S2 site, otherwise masked by the NRR domain, that is the target of the proteases belonging to the ADAM/TACE/Kuz/Sup17 family. The S2 cleavage is necessary for further steps of receptor activation. Several different mechanisms have been proposed to explain how interaction with the ligands triggers N activation, ranging from mechanical force, allosteric effects or unmasking, without getting to any certain conclusion. Once the S2 cleavage has occurred, the NECD (Notch ExtraCellular Domain) fragment sheds; transcytosis into the signal-sending cell together with the ligand seems to have a central role in this detachment. The S2 cleavage also generates the NEXT (Notch EXtracellular Truncation) fragment, substrate of the γ-secretase proteolytic activity (Fortini, 2009). The γ-secretase is an aspartyl-protease consisting of 4 subunits: Presenilin, with catalytic activity (Struhl and Adachi, 2000), Nicastrin (essential to promote Presenilin cleavage, Lopez-Schier and St Johnston, 2002), Aph-1 (anterior pharynx defective 1) and Pen-2 (Presenilin enhancer, Fortini, 2002). The γ-secretase complex cleaves NEXT in the transmembrane domain at the S3 and S4 sites, releasing the NICD (Notch IntraCellular Domain) fragment and the Nβ peptide. The soluble NICD fragment presents an NLS, thus once generated, it can translocate to the nucleus where it gets in contact with its nuclear effectors, Su(H) and Mam, and mediates the transcriptional activation of different target genes; the best characterised ones are the *E(spl)* (*Enhancer of split*) gene family members. It is worth noting that each NICD molecule can signal just once and once, it has been generated, no other possibility to regulate its activity through ligand actions exists, that’s why consecutive proteolytic cleavages have been fine-tuned to guarantee the specific activation of the receptor.

Interestingly, recent studies pointed out the existence of a cis-inhibitory effect of the ligand on the receptor: indeed, ligands were found on the plasma membrane of cells together with receptors, and, in such cases, it turned out that ligands do inhibit, instead of activate, the receptor (Palmer *et al.*, 2014; Sprinzak *et al.*, 2010). Cis-inhibition requires 24-29 EGF-like repeats in the N receptor.

N signalling is commonly adopted by cells to undergo cell fate decisions. Particularly, 3 different types of developmental processes deploy N pathway (Bray, 1998): lateral inhibition, lineage decision and boundary formation (as in the DV boundary formation in the wing disc, see paragraph 1.7.2). Moreover, although N signalling generally dictates a binary cell-fate choice (all 3 biological processes above described essentially provide two possible opposing alternatives between which cells have to opt), there is at least an exception: in the germarium, multiple and different levels of N activation determine three distinct FCs types: polar, stalk and terminal FCs (see also paragraph 1.7.1 and Assa-Kunik *et al.*, 2007).

### 1.7.1 N signalling functions during *Drosophila* oogenesis

As previously mentioned (paragraph 1.4.1), N signalling plays fundamental and multiple roles during *Drosophila* oogenesis. The first sign of N requirement during oogenesis can be appreciated in the germarium. Ward and co-workers indeed showed that canonical N signal is a *sine-qua-non* condition for GSC niche maintenance, which in turn is necessary to retain GSC self-renewing abilities (Ward *et al.*, 2006). While overexpression of Dl in the GSCs is sufficient to induce niche cell number to increase (and, as a consequence, more GSCs are specified and supported), its reduction eventually leads to GSC loss. Authors propose a model in which a positive feedback loop between N and TGFβ pathway activation is necessary to maintain germarium homeostasis (Figure 13). Few months later, a paper from Xie lab reported that this requirement of N signalling in the niche is an early condition, since during larval gonad development misregulation of this pathway leads to alterations in the niche and GSC number and homeostasis (Song *et al.*, 2007).

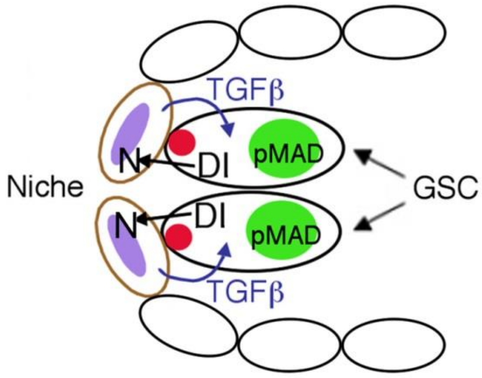

**Figure 13 N and TGFβ pathways act together in GSC maintenance.** Dl signal from the germline induces activation of N pathway in the cap cells. In turn, cap cells express TGFβ to maintain GSCs. Accumulation of pMAD identifies GSCs. Modified from Ward *et al.*, 2006.

Later, in regions 2a/2b of the germarium, N signalling is necessary to select and specify the polar and stalk cell fate (Vachias *et al.*, 2010). As mentioned in paragraph 1.4.1, Dl is present on the membrane of the germline cyst cells. Migration of precursor FCs to encapsulate cyst is accompanied by the upregulation of Fng that allows N receptor to become competent to respond to Dl signal from the germline (Grammont and Irvine, 2001). Precursor FCs that do not express Fng will become main body FCs and will express high levels of Kuzbanian-like (Kul) metalloprotease that attenuates in these cells N activation by proteolytic cleavage of Dl (Figure 14A, Assa-Kunik *et al.*, 2007). Activation of N signalling in 4-5 Fng-expressing cells will commit them to become polar cells (Althauser *et al.*, 2005). Subsequent Upd1 secretion by polar cells activates the JAK/STAT signalling pathway in the presumptive stalk cells (Figure 14B). Moderate N signal activation induced by polar cells in stalk cells is also necessary to specify their fate (Nystul and Spradling, 2010). The main body FCs closer to polar cells will be ultimately specified as terminal FCs by the end of stage 5. These cells also receive the Upd1 and Dl signals; since N signalling and JAK/STAT pathways antagonise each other, the specification of stalk cells versus terminal FCs rely on differences in modulation of the two pathways. The main body FCs, exhibit higher levels of N signal activation and therefore display N-dependent suppression of JAK/STAT activity. Stalk cells, instead, are able to transduce the JAK/STAT signal, implying that they experience a particularly low level of N activation (Assa-Kunik *et al.*, 2007).

Posterior polar cells are also specified in the region 2b of the germarium (Figure 14C). The anterior stalk cells of a cyst directly contact the younger cyst; grafted in the stalk cell cluster there are also the future posterior polar cells of the younger cyst. All these cells are exposed to Upd1 secreted by anterior polar cells of the older cyst; indeed, also in presumptive posterior polar cells JAK/STAT pathway is active and this probably is the reason why their specification is a little delayed. The switch to polar cell fate is determined by the N antagonising activity which out-competes the JAK/STAT pathway. Polar cell fate acquisition is linked to cell-cycle arrest achieved by N-mediated downregulation of String (Stg), the cdc25 mitosis-promoting phosphatase (Shyu *et al.*, 2009). The transient stalk-like fate of posterior polar cells causes them to upregulate E-Cadherin, and therefore preferentially targets the adhesive interactions of the oocyte to the future posterior polar cells, to generate a reproducible antero-posterior polarisation (Assa-Kunik *et al.*, 2007; Torres *et al.*, 2003). Thus, it could be claimed that N signalling contributes to the specification of polarity axes of the future embryo.

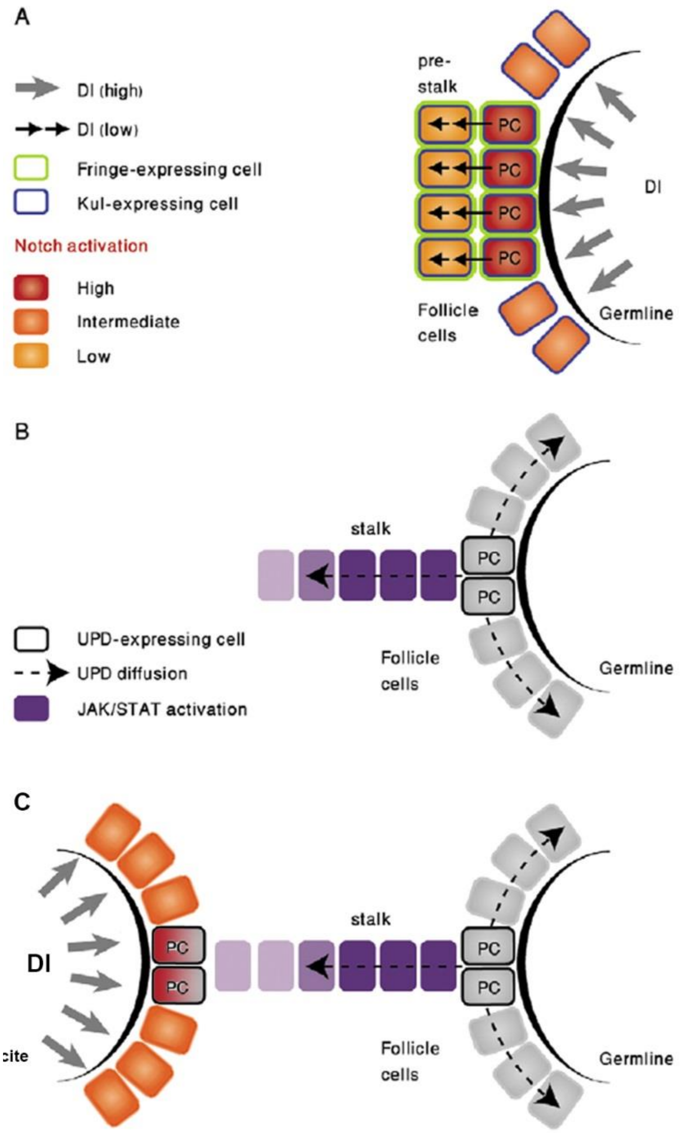
A
Dl (high)
Dl (low)
Fringe-expressing cell
Kul-expressing cell
Notch activation
High
Intermediate
Low
pre-stalk
PC
PC
PC
PC
Dl
Follicle cells
Germline
B
stalk
PC
PC
UPD-expressing cell
UPD diffusion
JAK/STAT activation
Follicle cells
Germline
C
Dl
cite
PC
PC
stalk
PC
PC
Follicle cells
Germline

**Figure 14 Determination of polar and stalk cell fate requires N and JAK/STAT pathways.** Both anterior and posterior polar cells are determined in the germarium. **(A)** High levels of Dl from the germline cyst induces in anterior polar and stalk cells activation of N signalling. The levels of pathway activity is modulated: while Fng enhances the signal in the presumptive polar cells, Kul metalloprotease slows down activation of N signal, allowing the determination of cuboidal follicle cells and stalk cells (that directly or not contact the germline, respectively). **(B)** In turn, polar cells start expressing Upd1 and then secrete it. Follicle cells which experience high or intermediate levels of N activation are refractory to JAK/STAT signalling and repress STAT nuclear localisation. By contrast, the pre-stalk cells, which are subject to low levels of N activation, undergo JAK/STAT activation. **(C)** Posterior polar cells of the younger cyst are embedded in the stalk cells induced by polar cells of the older cyst. As such, they have a transient nuclear localisation of STAT, allowing upregulation of DE-Cadherin. This allows the anterior polar cells to adhere to the oocyte and on the other hand forces posterior positioning of the oocyte. Direct exposure to the Dl signal from the germline (the oocyte) now antagonises JAK/STAT signalling and eventually induces the (anterior) polar cell fate. Modified from Assa-Kunik *et al.*, 2007.

N signalling activation during oogenesis also occurs during the transition from mitotic cycle to endocycle at stage 6-7 (Figure 15). This transition marks the acquisition of a mature state of FCs, making them competent for subsequent patterning and for polar axes formation. In a very pioneering work, Deng and colleagues demonstrated the requirement of N signalling in FCs to enter into the endocycle (Deng *et al.*, 2001). Dl ligand is upregulated in the germline by stage 6, to allow activation of N signalling in the somatic component of the ovary (Lopez-Schier and St Johnston, 2001). N-induced mitotic cycle-to-endocycle switch is mediated by Hindsight (Hnt, Sun and Deng, 2007). Hnt is a transcriptional repressor; among its targets there are *cut* (*ct*) and *stg*. Stg is the *Drosophila* homolog of Cdc25. Stg activity is necessary to activate Cdk1, the kinase that mediates G2/M transition. If Stg is absent, mitotic phase cannot occur. *ct* encodes a DNA-binding protein expressed in FCs from the 2b region of the germarium until stage 6 and from stage 10b until the end of oogenesis (Sun and Deng, 2005). Ct suppresses *fizzy-related* (*fzr*) expression. *fzr* encodes an adaptor for the APC/C E3 ligase necessary for the degradation of M phase cyclins. Hnt downregulates both *ct* and *stg* allowing the transition from mitotic cycle to endocycle. Among the other proteins required for the transition from mitotic cycle to endocycle there is the transcription factor Tramtrack (Ttk69). Ttk69 is not a N target gene but it works together with N to promote this transition. The two signalling pathways share common targets, as the Hh signalling. Recently, CoREST was identified as a positive modulator of N signalling, acting downstream the receptor proteolytic cleavage (Domanitskaya and Schupbach, 2012).

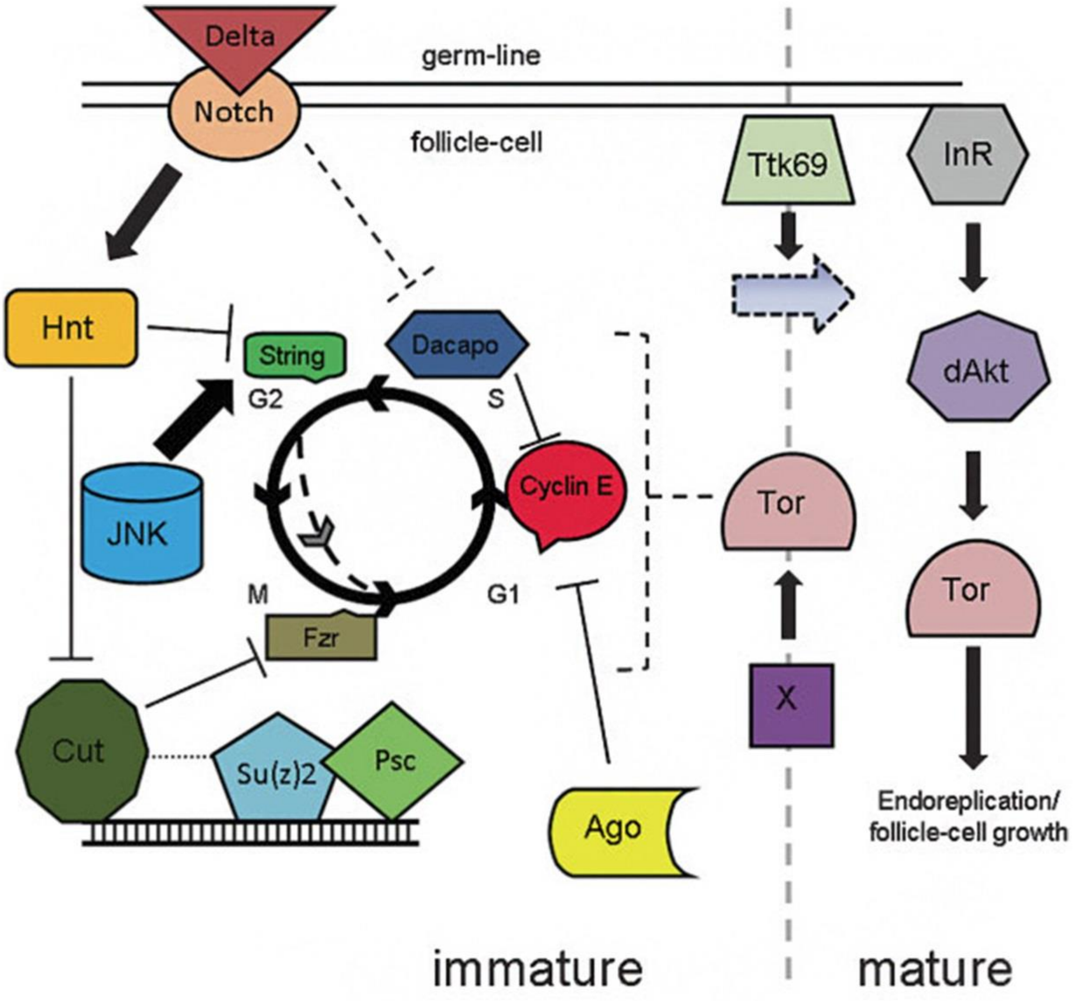

**Figure 15 Schematic illustration of the signalling pathway network involved in mitotic cycle-to-endocycle switch.** At stage 6-7, elevated germline Dl signal induces N activation in FCs. Activation of this demolishes multiple components required to the mitotic cell cycle by acting at multiple levels (transcription regulation, protein stability…) both directly and indirectly. First, activation of N causes upregulation of specific target genes, such as *hnt*. Hnt mediates the repression of *cut* (in the presence of Polycomb group members Psc and Su(z)2) and *stg*. In the absence of Cut, *fzr* is derepressed; Fzr degrades mitotic cyclins and promotes the endocycle. The N signalling pathway also inhibits expression of *p21*/*dacapo* (*dap*), which normally mediates the degradation of Cyclin E. Downregulation of *stg* and *dap* allows Cyclin E to oscillate: its levels indeed are critical to FC growth. JNK components are also downregulated while Ttk69 is required for the switch from immature to mature fate of FCs. Finally, progression of oogenic process requires coupling with nutrient availability. This is mediated by the InR/Akt/Tor signalling pathway. Modified from Klusza and Deng, 2011.

N signalling is also required for border cell migration. Wang and colleagues showed that specific activation of N together with elevation of Kul occurs in border cells at stage 9 and that alterations in N, Dl or Kul cause migration defects (Wang *et al.*, 2007).

### 1.7.2 N signalling functions during *Drosophila* wing disc development

N signalling plays also an important role in wing discs. As previously stated, N signalling activation occurs at the DV boundary, as a consequence of asymmetric distribution of Fng, Dl and Ser imposed by Ap-restriction in dorsal cells (see paragraph 1.6.2). N activation in a narrow stripe of cells induces *vestigial* (*vg*), *scalloped* (*sd*) and *wg* espression. Wg is expressed in an approximately five cell wide stripe of wide along the presumptive wing margin and then spreads across the wing epithelia regulating the expression of *Dl* and *Ser,* so maintaining N activity at the DV boundary in a feedback loop (de Celis and Bray, 1997), while it also contributes to wing patterning. It is worth noting that Wodarz and colleagues also demonstrated that Wg signalling modulates cadherin-mediated cell adhesion in wing discs (Wodarz *et al.,* 2006). Vg regulates wing growth and identity through the integration of positional signals from the two orthogonal axes (Kim *et al.,* 1996). It functions together with Sd to regulate gene expression. Finally, N, together with ecdysone signalling, upregulates *ct* expression at the DV boundary (Jia *et al.*, 2016). Ct is necessary to maintain Wg expression at the DV boundary (Micchelli *et al.*, 1997).

Besides its role in DV boundary establishment and maintenance, N signalling has also a primary role in the establishment of vein/intervein territories in the wing. Veins are cuticular structures that appear distributed according to a precise profile along the wing blade (Figure 9B). They absolve a structural role in the wing. Each vein is formed by a dorsal and a ventral components that are specified independently within the imaginal disc through an antagonist action with the EGFR signalling (De Celis, 2003).

Finally, N signalling has a fundamental role in the development of bristles, sensory organs covering the most part of the adult fly body, including wings. A sensory organ is formed by four cells: a socket cell, a bristle cell, a sheath cell and a neuron (Figure 16B, lower panel). These peculiar organs constitute part of the peripheral nervous system of the fly. During wing disc development, pro-neural clusters of cells emerge within the ectodermal cells of the epithelium. Sensory organ precursors (SOPs) get singled out in specific positions within the pro-neural clusters through a process named lateral inhibition involving N signalling. Indeed, N inhibition causes supernumerary SOPs to emerge. Once a SOP is determined, it inhibits surrounding cells to acquire the same fate (Figure 16A). The process is mediated by the existence of small differences in the amount of ligands and receptors exposed on the cell surface in each clusters at each given time. Through feedback loop these small differences get fixed and the cell with the highest levels of Dl will be sorted as the SOP and it will signal to the other cells, through activation of N signalling, not to acquire the neural fate (Figure 16A).

Lateral inhibition will participate also in each of the subsequent steps of SOP division to give rise to all the components of the bristle (Figure 16B, upper panel).

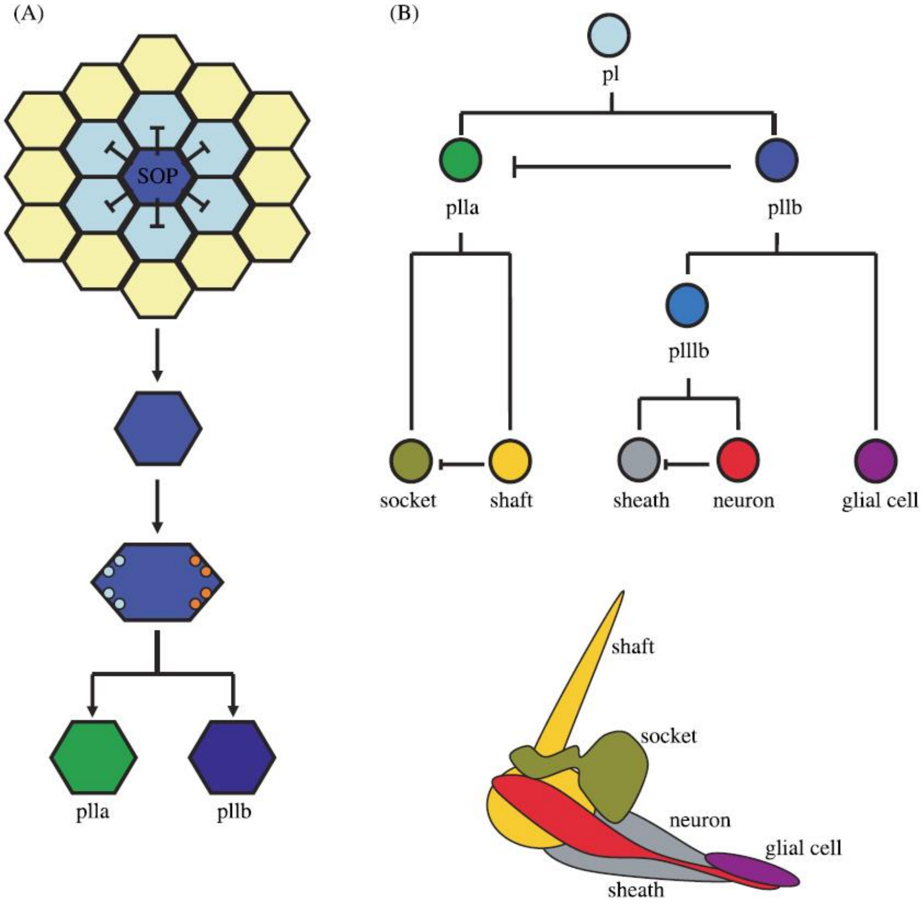

**Figure 16 Involvement of N signalling during *Drosophila* neurogenesis. (A)** Pro-neural cluster cells (light blue) express the neurogenic markers Achaete, Scute and Daughterless, that confer to epidermal cells the ability to become SOPs. The cells surrounding the pro-neural clusters (yellow) express high levels of Hairy, that suppresses the neurogenic genes. The selected SOP possesses a more ‘effective’ Dl that activates the N pathway in its neighbours and, through induction of *E(spl)*, blocks expression of *achaete* and *scute*, thereby shutting down their neurogenic programme. The first (asymmetric) division of the SOP, leading to the progenitor cells pIIa and pIIb, has been thoroughly investigated. During cell division, Neuralized, Numb and the AP-2 complex accumulate on one side of the SOP. The daughter cell possessing the higher content of these three proteins (pIIb, blue) loses its ability to receive N signals, but has an abundant capacity to transmit. Then, pIIb maintains the neural phenotype, while pIIa (green) does not. Indeed, pIIb will give rise to the neuron and glia cells, while pIIa to the socket and shaft. **(B)** The subsequent rounds of asymmetric cell divisions of pIIa and pIIb will drive binary switches in which N determines the outcome, determining cell lineage (shaft vs socket, sheath/neuron vs glia). Modified from Fiuza and Arias, 2007.

## 1.8 Cellular trafficking routes: endocytosis and exocytosis (secretion)

The possibility to sense the extracellular environment, to introduce nutrients and to secrete specific signals are all critical events for cell survival, both in Prokaryotes and Eukaryotes. Machineries mediating these processes most times are based on generation of small membrane-coated vesicles that allow internalisation of surface receptors or taking up of molecules from the surrounding medium. Moreover, in multicellular organisms, epithelial cells rely on intracellular protein trafficking to segregate proteins in specific subdomains (e.g., to restrict polarity proteins at the appropriate membrane compartment). Indeed, endocytosis has a critical role in shaping epithelia during morphogenesis and no surprise that mutations in genes involved in endocytosis have been implicated in tumour onset (Vaccari and Bilder, 2009). Most of the human proteins known to be involved in protein trafficking have homolog in *Drosophila* with a highly grade of similarity (Lloyd *et al.*, 2000), so it is possible to study their function in this powerful model system.

Endocytosis mediates the vesicular trafficking from the extracellular environment/plasma membrane to the intracellular compartments. Transport of cargoes to the specific subcellular compartments requires budding, movement and fusion of membrane-coated vesicles. Their trafficking must be finely regulated to ensure the specificity of the delivery. Endocytosis of plasma membrane receptors has been long considered essential for signal attenuation, because of addressing receptors to lysosome degradation. However, even if indeed endocytosis has a critical role in regulating the basal levels of plasma membrane proteins, more works pointed out that this process could also be essential to promote appropriate signal transduction (e.g., N signalling, see next paragraph, Le Borgne *et al.*, 2005).

Many different routes can be distinguished (Figure 17), in first place based on the requirement or not of the clathrin coat. Moreover, endocytosis can necessitate or not Dynamin function. In *Drosophila*, Dynamin is encoded by the *shibire* (*shi*) locus (Chen *et al.*, 1991; van der Bliek and Meyerowitz, 1991). Dynamin, a homo-hexameric protein, is a GTPase that acts in the very first phases of internalisation: it accounts for the pinching off of clathrin-coated vesicles from the plasma membrane (Sever *et al.*, 2000). Internalisation of different membrane receptors, as well as other plasma membrane components, must be finely regulated; to ensure accuracy of the endocytic process, specific adapter proteins interpose between clathrin coat and plasma membrane. They then recruit Dynamin. In this way, vesicles transporting different cargoes will be characterised by different adapter proteins, which confer specificity to this process. Then internalisation follows, with the recruitment of many other components that assist in membrane curvature.

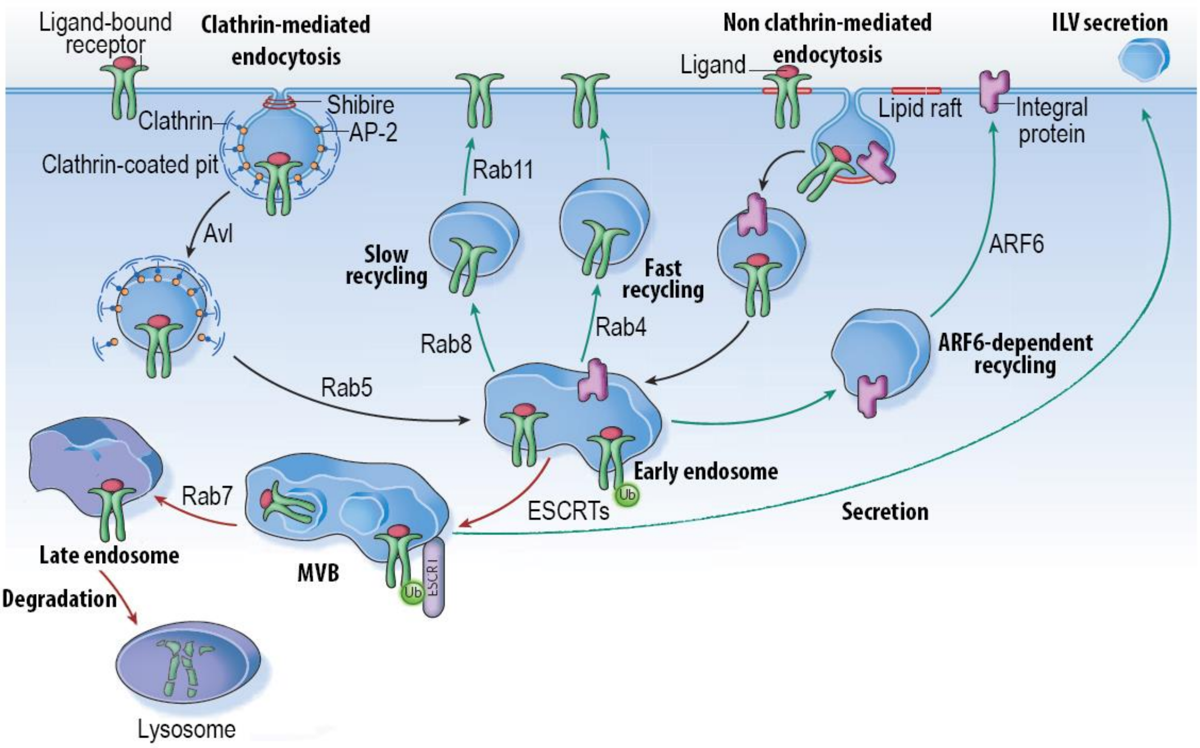
Ligand-bound receptor
Clathrin-mediated endocytosis
Non clathrin-mediated endocytosis
ILV secretion
Ligand
Shibire
AP-2
Clathrin
Clathrin-coated pit
Lipid raft
Integral protein
Rab11
Avl
Slow recycling
Fast recycling
ARF6
Rab8
Rab4
ARF6-dependent recycling
Rab5
Early endosome
Ub
Rab7
ESCRTs
Secretion
Late endosome
MVB
ESCRT I
Degradation
Lysosome

**Figure 17 Endocytic trafficking routes.** Transmembrane proteins (receptors and other integral proteins) can be internalised through Clathrin-dependent or independent mechanisms. Clathrin (present in Clathrin-coated pits) through adaptors, such as AP-2, is recruited to the membrane and then polymerizes. Invagination of the pit follows, which will eventually be released into the cytoplasm through the action of the GTPase Shibire. There are many forms of non Clathrin-mediated endocytosis, which, in some cases, depends on plasma membrane microdomains enriched in particular lipids (known as lipid rafts). After internalisation, by either Clathrin-mediated or non Clathrin-mediated endocytosis, pinched off vesicles are enriched in the Syntaxin Avl. Endocytic vesicles are then routed to early endosomes. Trafficking in the endosomal compartment is controlled by small GTP-binding proteins of the Rab and ARF (ADP-ribosylation factor) families, some of which are indicated. From the early endosome, cargo is either recycled to the plasma membrane (green arrows) or degraded (red arrows). Cargo can be recycled through a fast recycling route (which depends on Rab4) or a slow recycling route (which depends on the combined action of Rab8 and Rab11). In addition, proteins that have been internalised by non Clathrin-mediated endocytosis, can be recycled to the plasma membrane through ARF6-dependent pathways. Cargo can also be trafficked to multivesicular bodies (MVBs). A crucial signal in this route is ubiquitylation of the receptors. Ubiquitylated receptors are recognised by a series of ubiquitin-binding protein complexes: Hrs–STAM (also known as ESCRT-0), and endosomal sorting complex required for transport I (ESCRT-I), ESCRT-II and ESCRT-III. Finally, vesicles can be routed through a Rab7-dependent degradative pathway, to late endosomes, and then lysosomes. Modified from Scita and Di Fiore, 2010.

Most of the so-budded endocytic vesicles converge into the early/sorting endosomes, whose formation and maturation requires both the *Drosophila* homolog of Syntaxins 7/12 Avalanche (Avl, Lu and Bilder, 2005) and Rab5 (Bucci *et al.*, 1992). Early endosomes are also designed as sorting endosomes (or signalling endosomes, Miaczynska *et al.*, 2004; Vaccari and Bilder, 2009) because they act as relay stations. Indeed, cargoes that reach early endosomes could be destined for many different fates:

- vesicles could be addressed to the Golgi apparatus;
- recycling could occur, in at least two different routes, mediated by Rab4 (fast recycling) or Rab11 (slow recycling). This event mediates an exocytic route;
- endosomes could continue their maturation, becoming MVBs (multivesicular bodies).

In the latter hypothesis, at the vesicle surface, components belonging to the ESCRT (Endosomal Sorting Complex Required for Transport) complexes are recruited. 4 different ESCRT complexes have been characterised: 0 (also called Hrs-Stam complex, that recognises ubiquitylated proteins), I, II, III (Vaccari *et al.*, 2009). Formation of MVBs through the activity of ESCRTs generates, inside the endosome, intraluminal vesicles (ILVs, Henne *et al.*, 2011). ILVs could be subsequently secreted as a consequence of the fusion of MVBs with the plasma membrane (Cocucci *et al.*, 2009). Thus, it appears that MVBs constitute an extremely significant way to secretion. MVBs could also fuse with late endosomes, characterised by the presence of Rab7 on their membrane (Bucci *et al.*, 2000; Rink *et al.*, 2005), and be addressed to lysosomes for degradation. It is worth to point out that progressive maturation of endosomes along the endocytic route is accompanied by progressive acidification of lumenal compartments; disruption of the V-ATPase responsible for this acidification could alter ability to signal of those receptors that use the endosomal trafficking. Indeed, this is the case for N (Vaccari *et al.*, 2010; Yan *et al.*, 2009).

As mentioned, most of the endosomal compartments can be recognised because of the presence on the vesicle membrane of specific Rab proteins. Rabs belong to a huge family of Ras-like GTPase that act as membrane organisers inside cells (Zerial and McBride, 2001). Many effectors and regulatory proteins (such as GEFs and GAPs) have been identified that modulate Rab activities. Rabs are not only implicated in the endocytic route but also in the secretory pathway, as some previous considerations implied.

Exocytosis has been classically investigated in relation to neurotransmitters in nervous system. Exocytosis can be a basal constitutive process, in which vesicles, once produced, are secreted, or a regulated process, in which vesicles are stored in the cell until a signal triggers their secretion (as is the case for neurotransmitters). In both cases, the secretory pathway has its starting point into the ER, where folded proteins exit it in COPII (coat protein complex II)-coated vesicles to reach the Golgi apparatus. Proteins that display ER-retrieval signals are returned to the ER via COPI (coat protein complex I)vesicles (Baines and Zhang, 2007). Dynamin function is required in ER and Golgi apparatus to allow budding of vesicles that mediates communication among these two organelles (Gonzalez-Jamett *et al.*, 2013).

Once a vesicle has bud from Golgi, movement along the cytoskeleton finally address it to its definitive destination. Indeed vesicles could be addressed to the plasma membrane to be secreted, could be secured just beneath the membrane waiting for a signal able to trigger exocytosis or could be addressed to lysosomes (in this case, a clathrin-coat is present). Tethering to the target site is mediated, among others, by Rab proteins. Subsequent docking and fusion events require the activity of large protein complexes. In particular, during neurotransmitter release, SNARE (Soluble NSF Attachment protein REceptors) proteins have a primary role. The core of SNARE complex is composed of three proteins belonging to three different families: VAMP/Synaptobrevin, Syntaxin and SNAP-25. Rab proteins functionally link SNAREs to motor proteins. Typically vesicles own a so-called v-SNARE while target sites show a t-SNARE. Interaction between them ensures the accuracy of the recognition before proceeding with the fusion. Dynamin also intervenes in mediating vesicle fusion with the target site. Proteins lacking a secretion peptide can be secreted following different routes (Rabouille *et al.*, 2012).

Recently, secretion was linked to developmental processes mediated by morphogen spreading (Deitcher, 2002; Lakkaraju and Rodriguez-Boulan, 2008). In particular, Wg secretion has been deeply investigated and Korkut and colleagues, in an illuminating work, demonstrated that Wg secretion is mediated by the release of exosome-like vesicles containing Evenness Interrupted (Evi, Korkut *et al.*, 2009). It was suggested that Evi functions as a Wnt cargo receptor during trafficking from the Golgi to the plasma membrane and then it is recycled back to the Golgi (Franch-Marro *et al.*, 2008).

### 1.8.1 Role of endocytosis on N signalling pathway

A plenty of works have highlighted the role of endocytosis in the activation of N signalling. Endocytosis is critical both in signal-sending as well as in signal-receiving cells. One of the first evidence of the requirement of endocytic machinery to activate N signalling came from a work of Seugnet and colleagues: by using a temperature-sensible allele of *shi*, *shi*$^{ts}$, and performing clonal analyses, they demonstrated that the neurogenic phenotype of *shi* was not a simply phenocopy of the *N* one, but it strictly conceals the requirement of Dynamin to activate N signalling (Seugnet *et al.*, 1997). Further studies on the relationship between N signalling and endocytosis, both in cells and animal models, highlighted that correct N signalling requires endocytosis of the receptor in the signal-receiving cell. N entry and trafficking into the endosomal compartments are a *sine qua non* condition to activate the signal.

A milestone toward the comprehension of the role of receptor endocytosis in N signalling activation is the paper of (Vaccari *et al.*, 2008). In this work, the group of Bilder used clonal analysis approaches to generate cell clones in which the function of specific components of the endocytic pathway was disrupted. In these clones, in which N entry into the selected endosomal compartment was prevented, they systematically analyse localisation, receptor processing and signalling activation *in vivo*. They found that preventing N access to the early steps of endocytosis (e.g., sorting at the early endosomes) results in absence of signalling, accumulation of the receptor in endosome compartments preceding the one disrupted and reduced γ-secretase ability to process N. Indeed, most of the active γ-secretase has been shown to be associated with lipid rafts in endosome membranes (Vetrivel *et al.*, 2004). Moreover, in endosomes, pH is lower than in the cytosol and this is proposed to regulate the precision of γ-secretase protease activity, guaranteeing the generation of a stable NICD form (Tagami *et al.*, 2008). Indeed, it was shown that V-ATPase activity is required to N activation (Vaccari *et al.*, 2010). Vaccari and colleagues in the 2008 work also showed that blocking the N receptor entry into the last steps of endosomal pathway causes an ectopic activation of the signalling (Vaccari *et al.*, 2008). This evidence suggests that endosomal sorting is also critical for signal attenuation. Thus, their findings, overall, clearly indicates that endocytosis is a critical regulator of N signalling.

Seugnet and colleagues showed that endocytosis was also required in the signal-sending cell (Seugnet *et al.*, 1997). Beside the first-glance bizarre aspect of this requirement, many possible explanations have been proposed, ranging from the necessity of endocytosis to generate the force necessary to unmask the S2 cleavage site, to the existence of post-translational modifications of the ligand occurring in endosomal compartment and necessary to obtain an active ligand (Le Borgne *et al.*, 2005). It is important to point out that endocytosis of both ligands and receptor is a critical aspect in lateral inhibition processes, such as in SOP determination and asymmetric division.

.

## 1.9 The *Drosophila awd* gene

*awd* gene (CG2210) lies on the third chromosome, in the cytological region 100D2 and spans for less than 1 kb. To date, there are three strongly supported transcripts to which correspond three annotated proteins (2 of which are unique) of 17-18 kDa. Six Awd subunits organise themselves to form a homo-hexameric enzyme which possesses histidine-dependent protein kinase (Inoue *et al.*, 1996) and NDP kinase activities (Liotta and Steeg, 1990; Wallet *et al.*, 1990). Indeed, it has been shown that Awd accounts for more than 98% of the larval overall NDPK activity in *Drosophila* (Biggs *et al.*, 1990) and histidine 119 (H119) is the core residue for this biochemical activity.

By looking in Flybase (Attrill *et al.*, 2016), the biggest *Drosophila* database currently available, 3 other proteins encoding enzymes with NDPK activity are predicted (*nmdyn-D6*/CG5310, *nmdyn-D7*/CG8362 and CG15547), based on sequence, structural similarities or electronic annotation. However, no biochemical or genetic analyses have been performed on these gene products. Phylogenetic analyses assign *nmdyn-D6* closer to *Nme6* while *nmdyn-D7* and CG15547 are more closely related to *Nme10* (Bilitou *et al.*, 2009).

The first developmental and molecular characterisation of *awd* gene is due to Dearolf and co-workers (Dearolf *et al.*, 1988a; Dearolf *et al.*, 1988b). In Shearn lab they were interested in finding late larval/early pupal lethal mutations affecting the development of imaginal discs. They screened several mutants displaying defects in multiple larval and/or imaginal tissues. Wing disc defects in *awd*$^{b3}$ null mutant larvae were soon noted (this explains the reason behind gene name) and deeper analyses revealed that also leg and eye-antenna discs, lymph glands, larval brain and proventriculus were altered and/or poorly differentiated. It was then shown that Awd is 78% identical to Nme1 and Nme2 (Rosengard *et al.*, 1989) and it is curious and somehow incredible that the first works on Awd and Nme1 were both published in 1988. The finding of Nme1 and Awd homology, both with NDPK activity, fuelled the research in the field for the subsequent years: soon, the role of Awd was analysed *in vivo* in neoplastic tumours (Timmons *et al.*, 1993).

But the story was destined to become even more fascinating with an unattended dramatic turn of events. It was demonstrated, in the very same years, that a gene called *killer-of-prune* actually was an allele of *awd* (*awd*$^{Kpn}$, Biggs *et al.*, 1988). This scary-named allele of *awd* was isolated in 1956 by Sturtevant and it owes its name to the dominant lethal phenotype it confers to the otherwise viable *prune* (*pn*) loss-of-function background (Sturtevant, 1956). Individuals that cannot make a functional *prune* gene product are viable, but they have prune-coloured eyes rather than the red ones. The eye pigment is synthesised from drosopterin, the synthesis of which requires the enzyme GTP cyclohydrolase. In *prune* mutants, drosopterin levels are reduced. The neomorphic spontaneous mutation *Kpn*, viable in homozygosis, carries a substitution in a highly conserved proline residue in position 97 with a serine (P97S). This substitution does not affect the catalytic efficiency of the NDPK, as it was hypothesised in first instance (Ruggieri and McCormick, 1991; Teng *et al.*, 1991), but it makes the peptide chain in which this residue is inserted much more flexible (Lascu *et al.*, 1992). This suggests that the missense mutation could allow Awd to interact with other proteins beyond its physiological targets. It was then postulated that the mechanism of *prune/Killer of prune* lethality was dependent on an altered substrate specificity of Awd$^{\mathrm{Kpn}}$. In particular it was hypothesised that in *prune* mutant an unknown substance could accumulate and become a substrate for the altered NDPK activity of Awd$^{\mathrm{Kpn}}$. In this reaction, a toxic product is generated and individuals get killed (Timmons *et al.*, 1995).

*prune* gene product function was unknown; alignments of a deduced Pn protein sequence revealed homology with a bovine GAP responsible for Ras activity attenuation (Teng *et al.*, 1991). This revelation inflamed the stage because this could hide the link between the NDPK activity and metastasis suppression: intense screenings with different techniques were carried out in trying to find out revertants which could help in delineating a signalling pathway (Biggs *et al.*, 1988; Provost *et al.*, 2006; Timmons *et al.*, 1995), but with great efforts just a glutathione S-transferase (CG10065) was recovered (Provost *et al.*, 2006; Provost and Shearn, 2006). Further analysis revealed, however, that *prune* product is actually a phosphodiesterase.

Since the very earliest studies, the function of Awd during ovary development has been analysed. In *awd* null mutant larvae, ovaries do not develop properly. Through transplantation experiments, ovaries of mutant larvae were donated to surrogate ones: chimeric adult females were viable but sterile. This suggests a critical function of Awd in ovaries. By transplanting *awd* mutant polar cells (the precursors of germ cells) in surrogate embryos, ovaries differentiate properly (Xu *et al.*, 1996). Even if these findings suggest a critical requirement of Awd only in the somatic component of ovaries, care should be taken in stating this. Indeed, while the requirement of Awd in follicle cells development has been well established from accurate research works in the last 20 years, the role of Awd in the germ line did not receive the same grade of investigation.

The NDPK activity of Awd requires the presence of a histidine residue at position 119. By substituting it with an alanine residue, the NDPK function of Awd is abolished and the expression of Awd$^{H119A}$ under the control of the endogenous *awd* promoter can’t rescue the *awd* mutant lethal phenotype. This indicates that the NDPK activity of Awd is necessary for its biological function. Expression of Nme1 or alternatively of Nme2 under the control of the endogenous promoter of *awd* in an *awd* loss-of-function background rescues the lethal mutant phenotype, even if to a different extent. It appears that Nme2 is able to rescue lethality in a higher percentage of flies. However, it should be stated that the insertion points of the human Nme1 and Nme2 transgenes are not the same and indeed Nme proteins accumulated at different levels in the transgenic lines. Moreover, neither Nme1 nor Nme2 are able to give rise to fertile females. From these findings, one can conclude that Awd has more biological function than simply that of NDPK (Timmons and Shearn, 2000; Xu *et al.*, 1996). Indeed, several lines of evidence in literature suggest that *Drosophila* Awd behaves like a scaffolding protein, providing a stage in which different interacting proteins can act their different role in cells. So, it appears that in *Drosophila*, activities other than that of NDPK are physiologically relevant for Awd function.

The first interaction between NDPK and Dynamin was reported in *Drosophila* by Krishnan and co-workers (Krishnan *et al.*, 2001). Indeed, in a genetic screen designed to identify proteins involved in synaptic vesicle recycling, three *awd* alleles were recovered. To their purpose, Krishnan and colleagues used a temperature-sensitive mutant conditional allele of the GTPase Dynamin encoded by the *shibire* (*shi*) locus. The phenotype of *shi*$^{ts}$ mutants consists of a rapid paralysis upon exposure to the restrictive temperature, due to the failure of synaptic transmission caused by a block in the recycling of neurotransmitter vesicles at the neuromuscular junctions. This phenotype was enhanced when the *shi*$^{ts}$ mutation was combined with a null mutation of *awd*. However, attempts to identify a physical interaction between Awd and Shi failed. Thus, this study showed the existence of a functional and genetic interaction between Shi and Awd, suggesting an involvement of NDPK in clathrin-dependent endocytosis. This conclusion led the authors to suggest the hypothesis that Awd can act as a GEF for Dynamin. Even if this has not been proven in *Drosophila*, in human it was shown that Nme1 indeed physically interacts with Dynamin (Baillat *et al.*, 2002).

Subsequent studies gave other hints of the involvement of Awd in regulating intracellular trafficking routes. During *Drosophila* embryogenesis, an air-conducting system is built up, the tracheal system. Tracheas originate from groups of ectodermal cells that invaginate, forming tracheal plaques which build the entire system through coordinated cell migration. The chemotactic signal driving the migration of the tracheal tubules is mediated by Breathless (Btl), the *Drosophila* homolog of FGFR (Fibroblast Growth Factor Receptor). The FGF ligand Branchless (Bnl) is expressed from mesodermal cells surrounding the tracheal tubules. Bnl activates the receptor Btl in tracheal cells allowing tubules to migrate in the right direction. Dammai and collaborators have shown that Awd controls the migration of tracheal tubules by modulating the levels of FGFR on the cell surface, thus avoiding abnormal ectopic activation and migration (Dammai *et al.*, 2003).

As stated before, Awd role in the somatic component of the ovary has been deeply explored. In details, during oogenesis, Awd shows a dynamic subcellular localisation profile in FCs: in pre-stage 5 egg chambers, Awd is uniformly distributed in the cytoplasm of FCs. After stage 5, Awd gradually accumulates toward the basal side of the cell. The basal localisation becomes predominant in stage 6 and is firmly established after stage 8. At stage 10, Awd is associated exclusively with the basal cell domain (Figure 18, Woolworth *et al.*, 2009).

It was demonstrated that in FCs Awd regulates the distribution of the components of the adherent junctions, thus allowing the maintenance of the epithelium integrity. This function is performed through the regulation of internalisation processes of adherens junction components, such as DE-cadherin and β-catenin. This activity is mediated by the GTPase Rab5 (Woodman, 2000). In FCs, Awd positively regulates the expression levels of Rab5; through this indirect way it also plays a critical role in adherens juction component homeostasis. As a consequence, in *awd* null mutant FC clones, besides a downregulation of Rab5, which results barely detectable, phenotypes associated with alteration in FC adhesion can be observed, ranging from piling-up of cells, breaks in the epithelium to invasion of the germ cyst (Woolworth *et al.*, 2009).

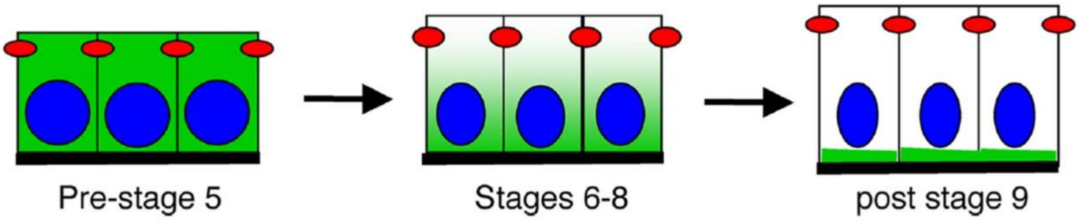

**Figure 18 Awd dynamics during FC differentiation.** In immature FCs, Awd spreads in all the cytoplasm. From stage 6, the protein starts to be more closely associated with the basal domain. By the end of stage 9, Awd is strictly confined at the basal domain. In red, position of adherens cell junctions are indicated; in blue, FC nuclei are highlighted; Awd is indicated in green. Modified from Woolworth *et al.*, 2009.

Moreover, it was shown that Awd is a negative regulator of border cell migration. Border cells are a subpopulation of FCs that is determined thanks to the release, by the anterior polar cells, of Upd1, the secreted ligand of Domeless (Dome) receptor. Ligand/receptor interaction in polar cell neighbours triggers a signalling pathway that culminates with activation of the Signal transducer and activator of transcription (STAT) factor. Once determined, these cells along with the polar cells at stage 9 of oogenesis start to migrate through the nurse cells to reach the oocyte. The precise movement of these cells is driven by the PDGF/VEGF signalling pathway, in which the Pvf ligand, produced by the oocyte, is received by the border cell complex through the Pvr receptor on the surface of these cells (Montell, 2003). Awd is strongly expressed in border cells before the migration begins; following delamination from the follicular epithelium, Awd protein is no longer detectable up to stage 10, when border cells reach the oocyte. This dynamic and specific expression profile allows to adjust the levels of Pvr at the cell surface: during the migration phase, Awd expression is suppressed allowing cells to accumulate enough Pvr on the plasma membrane to ensure a correct invasion of the germ cell cyst (Nallamothu *et al.*, 2008).

Finally, Awd presence was also reported in extracellular compartments. In particular, Koppen and colleagues isolated Awd from the culture medium of two *Drosophila* cell lines (Koppen *et al.*, 2011). Awd was incorporated into microvesicles, an umbrella term indicating extracellular vesicles of different origin (both directly budded from the plasma membrane or proper exosomes, present in the extracellular environment because of the fusion of MVBs with the plasma membrane and consequent release of their ILVs, Cocucci *et al.*, 2009). In parallel, proteomic studies showed that Awd is present into the haemolymph, the only *Drosophila* extracellular fluid (Guedes Sde *et al.*, 2003).

The high degree of similarities between Awd and Nme in human, combined with the powerful genetic techniques available in *Drosophila*, make this tiny creature amenable for investigating both the physiological functions of this intriguing NDPK family member and the mechanisms through which it moves through the many intracellular and extracellular environments, potentially shedding light on the role of its orthologues in the metastatic process.

# Chapter 2

## Aims of the thesis

Cancer metastasisation is the final outcome of malignant transformation. Several gene products have been identified manifesting a clear metastasis suppressor or, on the contrary, pro-metastatic activities. Moreover, many other proteins are currently under investigation for their potential involvement in metastasis onset, development or progression. The study of MSG and pro-metastatic gene functions could have important implication for cancer research since the identification of the signalling pathways in which such genes are involved could help clarify the metastasisation process.

*Nme1* is the first MSG discovered and members of *Nme* gene family are virtually present in all organisms. During my PhD, I used *Drosophila melanogaster* as a model system to analyse the function of Awd, the *Drosophila* ortholog of Nme1, during development. The aim of my study was to gain insights into the role of Nme proteins in cancer development and progression. To address this issue, I investigated *awd* gene function in multiple *Drosophila* tissues through molecular genetic approaches.

Several works uncovered a network of genetic and physic interactions linking Awd and small GTPases (such as Shi and Rab5) acting in vesicle trafficking (Dammai *et al.*, 2003; Krishnan *et al.*, 2001; Nallamothu *et al.*, 2008; Woolworth *et al.*, 2009). These works showed that *awd* function is required at different steps of the endocytic route. During my PhD, my study was also aimed at better understanding the functional significance of the interactions linking Awd, Shi and Rab5.

Most part of my PhD work was carried out in Gargiulo lab (University of Bologna). I also spent 6 months in Adryan lab (University of Cambridge) and, during this period, I focused my study on *dVHL* gene. The human *VHL* gene product is a TSG and several works on the

*Drosophila* homolog *dVHL* showed that it functionally interacts with Awd. I applied molecular biology and bioinformatics approaches in order to gain insights into the effects of *dVHL* gene lesion.

# Chapter 3

# Materials and methods

## 3.1 Stocks and genotypes

All flies were maintained on a standard corn meal medium at 25 °C, unless otherwise stated.

### 3.1.1 Fly food preparation

*Drosophila* strains were bred on a corn meal flour-culture medium supplemented with water, fresh yeast, glucose. The medium is also provided with methyl 4-hydroxybenzoate, an anti-fungine commonly known as nipagine, to prevent fungal and mould infection. A dose of the medium is prepared by adding 10 gr of agar and 50 gr of glucose to 1600 ml of water. When the solution raises the boiling point, 150 gr of corn meal flour are added and the medium is then cooked 20 minutes over medium heat. Then, 50 gr of fresh yeast are added and medium continues to be cooked for other 10 minutes. Finally, medium is supplemented with 4 gr of nipagine, previously dissolved in 16 ml of 95% ethyl alcohol. The medium at this point is poured into suitable containers and allowed to cool and dry.

### 3.1.2 Stocks used in this work

Most of the described strains were purchased from stocks centres as BDSC (Bloomington *Drosophila* Stock Center) or VDRC (Vienna *Drosophila* RNAi Center); in these cases, collection number is indicated.

- $y^1$, $w^{67c23}$; +/+; +/+: referred to as *yw* in the text and used as wild type stock;
- BDSC 7198: *w**; $Kr^{If-1}$/CyO; $D^1$/TM3, $Ser^1$;
- $w^-$; *If*/CyO; MKRS/TM6B;

- $y^{1}$, $w^{67c23}$; +/+; $FRT^{82B}$, $awd^{J2A4}$/TM3, $Sb^{1}$, $Ser^{1}$. This stock was obtained from Tien Hsu lab;
- $Gbe+Su(H)_{m8}lacZ$; +/+; TM2C, *Ubx*/TM6B, *Tb, Hu*. This stock was obtained from Sarah Bray lab (Furriols and Bray, 2001). In the promoter region of the $Gbe+Su(H)_{m8}lacZ$ reporter there are two binding sites for Su(H) derived from the *m8* gene which belongs to the *E(spl)* family. Upstream of these sequences there are three palindromic binding sites (named *Gbe*) for the transcription factor Grainyhead (Grh). The *Gbe* sites constitute a minimal promoter which confer ubiquitous expression at low levels. When N signalling is triggered, the transcription factor NICD translocates into the nucleus where it interacts with Su(H). Their complex acts as a transcriptional activator to promote the expression of *E(spl)* genes, including *m8*. Thus, if the construct *Gbe+Su(H)m8lacZ* is present in the genetic background of flies, in cells in which N signalling is active, NICD and Su(H) cooperate with Grh to mediate the expression at high levels of the *lacZ* gene;
- $y^{1}$, $w^{*}$, *hs-flp*; *act-Gal4, UAS-GFP*/CyO; $FRT^{82B}$, *act-Gal80*/TM6B, *Tb, Hu*. This stock was obtained from Bruno Lemaitre lab;
- BDSC 4779: $y^{1}$, $w^{*}$, P{*w[+mC]=GAL4-Act5C(FRT.CD2).P*}*D*; +/+; +/+ (Pignoni and Zipursky, 1997). In the text, the transgene will be referred as *act5c>CD2>Gal4*;
- BDSC 28832: P{*ry[+t7.2]=hsFLP*}*12*, $y^{1}$, $w^{*}$, P{*w[+mC]=UAS-mCD8::GFP.L*}*Ptp4E[LL4]*; $Pin^{1}$/CyO; +/+. In the text, the transgenes will be referred as *hs-flp, UAS-mcd8::GFP*;
- $w^{*}$; $UAS\text{-}NICD^{79\text{-}2}$/CyO; +/+. This stock was obtained from Sarah Bray lab. In the text, the transgene will be referred as *UAS-NICD*;
- $w^{*}$; *UAS-NEXT*/CyO; +/+. This stock was obtained from Mark Fortini lab;
- BDSC 2248: $shi^{2}$ (Grigliatti *et al.*, 1973). In the text, this mutation will be referred also as $shi^{ts}$. For the experiment described in Figure 35, freshly unclosed homozygous $shi^{ts}$ females were exposed at 29 °C (restrictive temperature) for 6 hours. At this restrictive temperature, Shi activity is arrested and Dynamin-dependent internalisation of molecules cannot occur. Females were then dissected in warmed PBS as described in paragraph 3.4;
- BDSC 30036: $y^{1}$, $w^{1118}$; $Pin^{1}$/CyO; P{$w^{+mC}$*=tubP-GAL4*}*LL7* P{$ry^{+t7.2}$*=neoFRT*}*82B*, P{$w^{+mC}$*=tubP-GAL80*}*LL3* (Lee and Luo, 1999). In the text, the transgenes will be indicated as *tub-Gal4*, $FRT^{82B}$, *tub-Gal80*;
- BDSC 9774: $y^{1}$, $w^{*}$; P{$w^{+mC}$*=UASp-YFP.Rab5.Q88L*}$l(2)k16918^{24}$; +/+ (Zhang *et al.*, 2007). In the text, the transgene will be referred as $UAS\text{-}YFP::Rab5^{Q88L}$ and the encoded protein as YFP::Rab5$^{CA}$;

- BDSC 7: P{$ry^{+t7.2}$*=hsFLP}1*, $y^{1}$, $w^{1118}$; +/+; $Dr^{Mio}$/TM3, $ry^{*}$, $Sb^{1}$ (Golic and Lindquist, 1989);
- BDSC 4775: $w^{1118}$; P{$w^{+mC}$*=UAS-GFP.nls}14*; +/+ (Robertson *et al.*, 2003). In the text the transgene will be referred as *UAS-nlsGFP*;
- BDSC 5822: w*; +/+; TM3, P{*w[+mC]=UAS-shi.K44A}3-10*/TM6B, $Tb^{1}$. In the text, the third chromosome carrying the transgene will be referred as *TM3,* $UAS\text{-}shi^{K44A}$, while the encoded protein will be indicated as $\mathrm{Shi}^{\mathrm{DN}}$;
- BDSC 26902: P{$ry^{+t7.2}$=*hs*FLP}1, $y^{1}$, $w^{1118}$; +/+; $Dr^{1}$/TM3, $Sb^{1}$ (Golic and Lindquist, 1989). In the text, the transgene will be referred as *hs-flp*;
- BDSC 3955: $w^{1118}$; P{*w[+mC]=UAS-lacZ.NZ}20b*; +/+. In the text, the transgene will be referred as *UAS-nlsLacZ*;
- $y^{1}$, $w^{67c23}$; P{$w^{+mC}$*=UAST-Lawd.eGFP}attP40*. This stock was generated in our lab. In the text, the transgene will be referred as *UAS-awd::eGFP* and the encoded protein as Awd::eGFP. The *UAS-awd::eGFP* transgene was produced by Biomatik. In a pUAST-attb vector (Bischof *et al.*, 2007), the sequence encoding the enhanced GFP variant fused to the N terminus of *awd* cDNA was cloned. The *Drosophila* stock carrying the *UAS-awd::eGFP* chimeric transgene has been produced by phiC31 integrase-mediated insertion into the *attP40* landing-site locus on the second chromosome by BestGene Inc.;
- *yw, hs-flp, tub-Gal4, UAS-nlsGFP*/FM7a, $B^{1}$; $FRT^{40A}$, *tub-Gal80*/CyO. This stock was obtained from Daniela Grifoni lab;
- BDSC 42702: P{*ry[+t7.2]=hsFLP}1*, $y^{1}$, $w^{*}$; $rab5^{2}$, P{*ry[+t7.2]=neoFRT}40A*/In(2LR)Gla, $wg^{Gla\text{-}1}$, $PPO1^{Bc}$. In the text, the transgene on X will be indicate as *yw, hs-flp*, while the second chromosome bearing the mutation in the *rab5* locus will be referred as $FRT^{40A}$, $rab5^{2}$.

## 3.2 Clonal analysis

### 3.2.1 MARCM mosaic analysis technique

Mosaic analysis involves the generation of homozygous mutant cells from heterozygous precursors via mitotic recombination. This analysis is particularly useful for amorphic, recessive lethal alleles since it allows to examine the phenotypes induced by the knock out of the specific gene function in a small group of cells in an otherwise phenotypically wild-type organism. In *Drosophila*, mosaic analyses employ the heterologous Flp/FRT binary system, a site-specific recombination system of *Saccharomyces cerevisiae* (Golic and Lindquist, 1989).

The recombinase Flp mediates site-specific recombination between FRT (Flp recombinase target site) sites.

The MARCM (Mosaic Analysis with a Repressible Cell Marker) technique (Lee and Luo, 1999) is a molecular genetic approach that enables to easily recognise cells homozygous for a mutation of interest since they will be positively marked through the expression of GFP. This technique couples the Flp/FRT system (to induce mitotic clones) with the yeast Gal4/UAS/Gal80 expression system. The Gal4 transcription factor is able to activate both in yeast and flies (Brand and Perrimon, 1993) the transcription of constructs subcloned into P element-derived vectors behind a tandem array of optimized Gal4 binding sites (hereafter referred to as the UAS, Upstream Activation Sequence; vector are then indicated as pUAS). The transcriptional repressor Gal80 antagonizes Gal4 activity, by binding to the activation domain of Gal4. Gal80-encoding transgene is placed in trans to the mutation of interest and both are in cis to a selected FRT site (Figure 19). Animals, then, are heterozygous for the selected null allele. The presence of the Gal80 protein impedes the Gal4-driven expression of *UAS* transgenes, such as the *UAS-GFP*. Expression of the transgene encoding the Flp recombinase (in this study expression was mediated through heat-shock treatment) in actively proliferating cells in the G2 phase induces the site-specific recombination at the level of the FRT sequences. In this way, the daughter cell that will lose the Gal80 protein will express the GFP and will be homozygous for the mutation of interest (Figure 19).

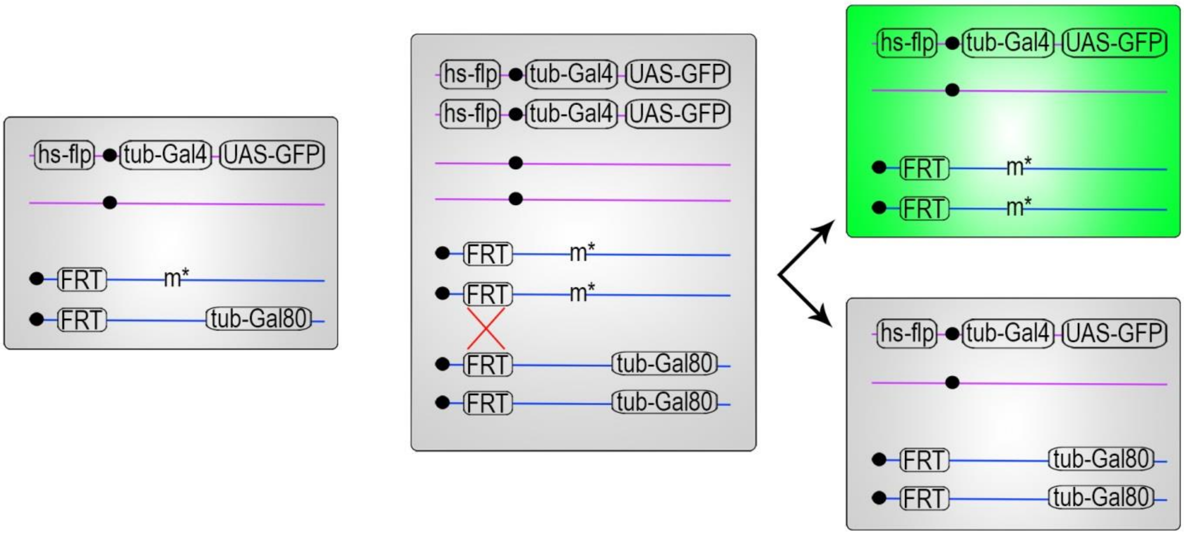

**Figure 19 The MARCM technique.** To induce site-specific recombination between two FRT sites, a transgene encoding the Flp recombinase must be present. In this study, the *flp* gene is under the control of a heat-shock promoter, whose induction is achieved by exposing flies at 37 °C. In the genetic background, transgenes encoding the transcription factor Gal4 and its repressor Gal80 are under the control of ubiquitous promoters, such as that of the *tubulin* (*tub*) or *actin* (*act*) genes. Transgenes encoding the GFP, Gal4 and Flp could be present on different chromosomes. The only restriction is that they must not be present on the same chromosome arm in which the FRT sites are. Instead, the mutation of interest (m*) and the transgene encoding the Gal80 must be located on homologue chromosomes and on the same arm, in a more telomeric position respect to the FRT sites. Somatic recombination event (red cross) in actively proliferating cells can generate a GFP-positive, m* homozygous cell. If such cell will proliferate, then a cell clone composed of mutant GFP-positive cells derived from the same recombination event will be recovered.

### 3.2.2 Induction of MARCM clones

To get *awd* MARCM clones, I used a *Drosophila* strain which bears on the third chromosome the *awd*$^{J2A4}$ mutation and an FRT insertion in position 82B (FRT$^{82B}$).

To induce *awd* MARCM clones in FCs, through appropriate crosses I obtained and selected females with the following genotype: *yw, hs-flp/Gbe+Su(H)m8lacZ; act-Gal4, UAS-GFP/+; FRT*$^{82B}$*, awd*$^{J2A4}$*/FRT*$^{82B}$*, act-Gal80*. This genetic background allows the induction, through heat shock treatment, of MARCM FC clones homozygous for the *awd*$^{J2A4}$ allele. In details, such females, over 24 hours, were subjected to three 1-hour heat shock treatments at 37 °C in order to induce the expression of the Flp protein that mediates the mitotic recombination at the FRT$^{82B}$ sites. In order to allow the formation of FC clones, mutant FCs must proliferate after the mitotic recombination has occurred. To allow this, females were kept at 25 °C for 4 days after the heat shock treatment and every day they were transferred to fresh yeasted food to stimulate oogenesis. Females were then dissected and ovaries collected and subjected to immunohistochemistry analyses.

To get *awd* MARCM clones overexpressing the NICD fragment in FCs, I obtained and selected females with the following genotype: *yw, hs-flp/Gbe+Su(H)m8lacZ; act-Gal4, UAS-GFP/UAS-NICD; FRT*$^{82B}$*, awd*$^{J2A4}$*/FRT*$^{82B}$*, act-Gal80*. Then I proceed with heat shock treatment as above described.

To get *awd* MARCM clones overexpressing the NEXT fragment in FCs, I obtained and selected females with the following genotype: *yw, hs-flp/Gbe+Su(H)m8lacZ; act-Gal4, UAS-GFP/UAS-NEXT; FRT*$^{82B}$*, awd*$^{J2A4}$*/FRT*$^{82B}$*, act-Gal80*. Then I proceed with heat shock treatment as above described.

To get *awd* MARCM clones overexpressing Rab5$^{CA}$ in FCs, I obtained and selected I obtained *yw, hs-flp/Gbe+Su(H)*$_{m8}$*lacZ; UAS-YFP:Rab5*$^{Q88L}$*/+; FRT*$^{82B}$*, awd*$^{J2A4}$*/tub-Gal4, FRT*$^{82B}$*, tub-Gal80* females. Then I proceed with heat shock treatment as above described.

To induce *awd* MARCM clones in wing discs, I set up appropriate crosses and let females laid egg for 24 hours. Progeny was then subjected to 1-hour heat shock treatment 48 hours after egg laying. When larvae reached the L3 stage, I selected those bearing the following genotype: *yw, hs-flp/Gbe+Su(H)m8lacZ; act-Gal4, UAS-GFP/+; FRT*$^{82B}$*, awd*$^{J2A4}$*/FRT*$^{82B}$*, act*-Gal80. These larvae were then subjected to immunohistochemistry experiments.

To induce *rab5*$^{2}$ MARCM clones in fat body, I used a *Drosophila* strain which bears on the second chromosome the rab52 mutation and an FRT insertion in position 40A (FRT$^{40A}$). Proliferation of adipocyte precursors occurs during embryonic development while, during larval life, they grow by increasing their polyploidy, as many other larval cells do. Since mitotic clones can be generated only in cells actively proliferating, this implicates that to generate MARCM clones in adipocytes *yw, hs-flp, tub-Gal4, UAS-nlsGFP/yw, hs-flp; FRT*$^{40A}$, *rab5*$^{2}$*/FRT*$^{40A}$*, tub-Gal80* animals must be subjected to heat shock treatment at the embryonic stage. During embryogenesis, active proliferation occurs in most tissues so, in order to avoid massive larval deaths due to generation of big *rab5* null MARCM clones throughout the animals, I set up a protocol in which 8 hours old embryos were heat-shocked 20 minutes at 37 °C and then let develop at 25 °C until they reached L3 stage. Larvae were then dissected and their tissues subjected to immunohistochemistry analyses.

### 3.2.3 The Flp-out/Gal4 technique

The Flp-out/Gal4 technique (Figure 20) allows to assess the effects of the overexpression of a gene of interest in small groups of cells (indicated as cell clones). The Flp-out transgene contains an ubiquitous promoter (e.g., from the *actin* gene) upstream of the so-called Flp-out cassette. The Flp-out cassette is composed of two direct FRT sites separated by a gene encoding a marker (in this study, the Flp-out cassette used contains the sequence encoding the CD2 protein as the marker) and a transcriptional terminator. Downstream of these sequences, there is the gene encoding the Gal4 protein. Such Flp-out transgene promotes the expression of the CD2 marker but not of the Gal4 protein because of the terminator sequence. Following expression of the Flp recombinase (in this study, the *flp* gene was under the control of an heat-shock promoter which gets activated at 37 °C), excision of the Flp-out cassette can occur. Cells in which such event takes place, will express the Gal4 protein while they will lose the *CD2* gene. Gal4 will then drive the expression of a responder transgene, in which the sequence encoding a gene of interest have been cloned downstream of UAS sites.

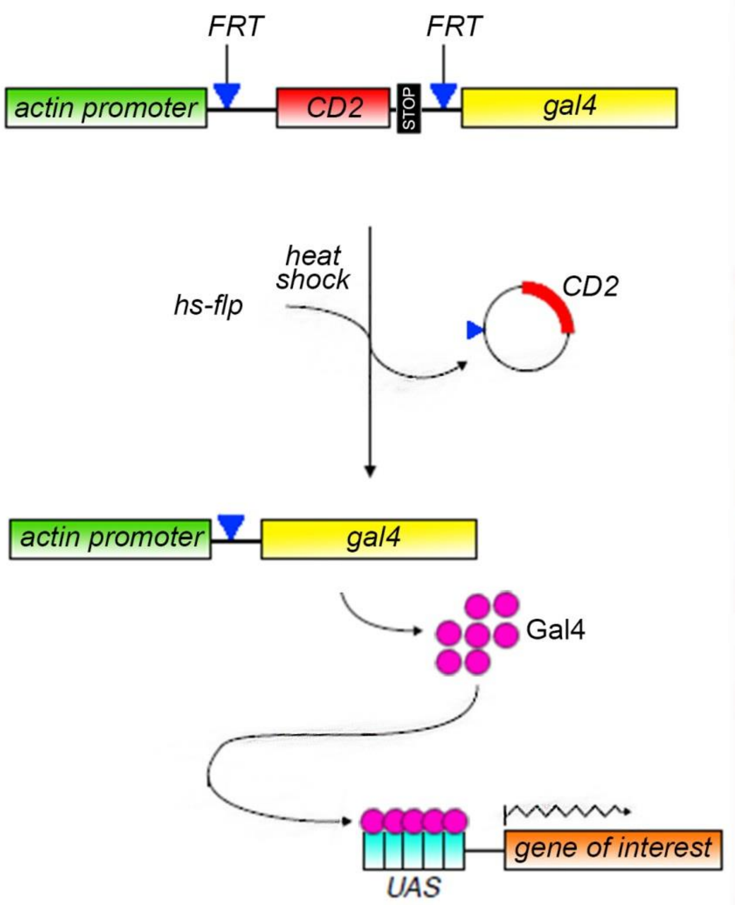

**Figure 20 Schematic representation of the Flp-out/Gal4 technique.** The Flp-out transgene used in this study contains the sequence encoding the rat CD2. CD2 is a T-cell surface antigen. The transcriptional terminator is indicated with a black rectangle accompanied by the STOP word**.** Modified from Pignoni and Zipursky, 1997.

### 3.2.4 Induction of Flp-out clones

To induce FC Flp-out clones overexpressing GFP and the NEXT fragment, through appropriate crosses I obtained and selected *yw, hs-flp, UAS-mCD8GFP/act>CD2>Gal4; UAS-NEXT/+* females that I heat-shocked twice at 37 °C for 1 hour. Then, females were incubated for 3 days at 25 °C before having their ovaries dissected.

To induce FC Flp-out clones overexpressing GFP and the NICD fragment, through appropriate crosses I obtained and selected *yw, hs-flp, UAS-mCD8GFP/act>CD2>Gal4; UAS-NICD/+* females that I heat-shocked twice at 37 °C for 1 hour. Then, females were incubated for 3 days at 25 °C before having their ovaries dissected.

In the epistasis test, I obtained and selected females of the following genotypes:

- *yw, hs-flp/act>CD2>Gal4; UAS-nlsGFP/+; TM3, UAS-shi*$^{K44A}$*/+;*
- *yw, hs-flp/act>CD2>Gal4; UAS-awd::eGFP/UAS-nlsLacZ*;
- *yw, hs-flp/act>CD2>Gal4; UAS-awd::eGFP/+; TM3, UAS-shi*$^{K44A}$*/+*.

To induce clone formation, such females were heat-shocked twice at 37 °C for 20 minutes and incubated for 4 days at 21 °C and for 14 hours at 29 °C before having their ovaries dissected.

To induce Flp-out clones in L3 larval fat body, the heat shock treatment must be performed during earlier phases of development. Induction during development of many clones overexpressing a dominant negative form of Shi could potentially be lethal (given the pleiotropic function of Dynamin). In order to avoid this problem, I did not perform a typical heat shock treatment but I forced the system to get spontaneous clones. To do this, 24-48 hours old larvae of genotype *yw, hs-flp/act>CD2>Gal4; UAS-nlsGFP/+; TM3, UAS-shi*$^{K44A}$/+ were shifted from 25 °C to 31 °C. The higher temperature enhances the sporadic spontaneous activation of the heat shock promoter leading to transcription of the *flp* gene. Larvae were let grown until L3 stage and then were dissected and their tissues subjected to immunohistochemistry analyses.

## 3.3 Antibodies

In this study, I used the following primary antibodies:

- protein-A purified polyclonal rabbit anti-Awd antibody was generated in Tien Hsu lab against a histidine-tagged whole Awd protein (Dammai *et al.*, 2003). It was used at 1:2000 dilution;
- monoclonal mouse anti-β-galactosidase antibody (40-1a, DSHB) recognizes the *E.coli* β-galactosidase sequence and was used at 1:25 dilution;
- mouse monoclonal anti-Hnt antibody (1G9, DSHB, Yip *et al.*, 1997) was generated against a GST-tagged *Drosophila* Hindsight protein (amino acids 824-1125) and was used at 1:30 dilution;
- monoclonal mouse anti-Cut antibody (2B10, DSHB, Blochlinger *et al.*, 1990) recognises a region of the *Drosophila* Cut protein (amino acids 1616-1836) and was used at 1:15 dilution;
- monoclonal mouse anti-Wg antibody (4D4, DSHB, Brook and Cohen, 1996) recognises a region of the *Drosophila* Wg protein (amino acids 3-468) and was used at 1:50 dilution;
- monoclonal mouse anti-NICD antibody (C17.9C6, DSHB, Fehon *et al.*, 1990) was generated against a recombinant fusion protein containing the amino acids 1791-2504 of the intracellular domain of N. It was used at 1:1000 dilution;

- monoclonal mouse anti-DE-cadherin antibody (DCAD2, DSHB, Oda *et al.*, 1994) is directed against a 41 amino acid-long region in the N-terminal domain of *Drosophila* DE-cadherin protein and was used at 1:25 dilution;
- polyclonal chicken anti-Avl antibody was generated in David Bilder lab (Lu and Bilder, 2005) and was used at 1:1000 dilution;
- polyclonal guinea pig anti-N-Hrs antibody was generated in Hugo Bellen lab (Lloyd *et al.*, 2002) against the N-Hrs fragment generated by thrombin cleavage of soluble GST-N-Hrs. The antibody was used at 1:1000 dilution;
- polyclonal rabbit anti-Rab7 antibody was generated in Akira Nakamura lab (Tanaka and Nakamura, 2008) against a synthetic peptide (amino acid residues 184-200) and was used at 1:2000 dilution;
- polyclonal rabbit anti-Rab11 antibody was generated in Akira Nakamura lab (Tanaka and Nakamura, 2008) against a synthetic peptide (amino acid residues 177-191) and was used at 1:8000 dilution;
- monoclonal mouse anti-CD2 antibody (MCA154G, SEROTEC, Whiteland *et al.*, 1995) recognizes the rat CD2 cell surface antigen, a 50-54 kDa glycoprotein expressed by thymocytes and mature T cells and was used at 1:250 dilution;
- mouse anti-Dynamin antibody (610245, BD Biosciences) was generated against the rat Dynamin I (amino acids 698-851). It was used at 1:400 dilution;
- polyclonal rabbit anti-Rab5 antibody was generated in Akira Nakamura lab (Tanaka and Nakamura, 2008) against a synthetic peptide (amino acid residues 11-28) and was used at 1:1000 dilution.

To detect primary antibodies raised in rabbit, I used the following fluorophore-conjugated secondary antibodies:

- BODIPY-conjugated goat anti-rabbit antibody (Sigma) at 1:2000 dilution;
- Cy3-conjugated goat anti-rabbit antibody (Invitrogen) 1:2000;
- Dylight 649-conjugated goat anti-rabbit antibody (Jackson) at 1:500 dilution.

To detect primary antibodies raised in mouse, I used the following fluorophore-conjugated secondary antibodies:

- Cy3-conjugated goat anti-mouse antibody (Jackson, with minimal reaction against antibodies raised in rat) at 1:1000 dilution;
- Dylight 647-conjugated goat anti-mouse antibody (Jackson) at 1:500 dilution;

To detect the anti-DE-cadherin primary antibody raised in rat, I used a Cy5-conjugated goat anti-rat antibody (Jackson) at 1:500 dilution, while to detect the anti-Hrs primary antibody raised in guinea pig I used a Cy5-conjugated sheep anti-guinea pig antibody (Jackson) at 1:500 dilution.

## 3.4 Immunofluorescent microscopy

Ovaries were dissected in PBS (10 mM sodium phosphate buffer, pH 7.5, 130 mM NaCl) at room temperature (with the exception of *shi*$^{ts}$ and *yw* flies that were dissected in warmed PBS) and then fixed for 20 minutes in a PBS solution containing 4% paraformaldehyde on a rotating wheel. Ovaries were then washed three times with PBT (1x PBS, pH 7.5 and 0.1% Triton-X- 100); after that, egg chambers separated by using insulin syringes and let permeabilise all night at 4 ° C in a PBS solution containing 1% Triton X-100. Then, after three 5 minutes-long washes with PBT, egg chambers were blocked for 15 minutes with PBT containing 3% BSA followed. Samples were then incubated at room temperature for 4 hours with primary antibodies at the correct dilution in a solution of PBT containing 3% BSA. Three 15 minutes-long washes with PBT followed before performing a 15 minute-long blockage with PBT containing 3% BSA. Samples were subsequently incubated at room temperature for two hours with fluorescent secondary antibodies. After three washes in PBT lasting 10 minutes each, egg chambers were mounted in Fluoromount G (Electron Microscopy Sciences), a mounting medium that reduces the quenching of fluorophores conjugated to secondary antibodies during fluorescence microscopy analysis. The sample observations were conducted both with conventional epifluorescence on a Nikon Eclipse 90i microscope and with TCS SL Leica confocal system. Images were then processed and assembled by using the Adobe Photoshop CS6 software.

For To-Pro-3 nuclear staining, after incubation with secondary antibodies, egg chambers were washed three times with 1x PBT and once with 1x PBS. Then, they were incubated for 2 hours in a PBS solution containing the To-Pro-3 dye (Molecular Probes) at the final concentration of 1 μM. Egg chambers were then washed three times with PBT and mounted in Fluoromount G.

For Lysotracker *ex vivo* staining, females were dissected in Schneider *Drosophila* medium (SDM) and ovaries were collected, finely separated and incubated for 5 minutes with SDM containing 5 μM Lysotracker dye (DND-99, Molecular Probes) in soft agitation at room temperature in the dark. Egg chambers were then then rapidly washed three times with SDM, mounted in Fluoromount G and immediately observed.

L3 larvae were dissected in 1x PBS at room temperature and fixed for 20 minutes in a PBS solution containing 4% formaldehyde. After three 5 minutes-long washes with 1x PBS, tissues were permeabilised for one hour in 0.3% PBT (1x PBS, pH 7.5 and 0.3% Triton-X-100). After three 5 minutes-long washes with 0.3% PBT, tissues were blocked for 15 minutes with a solution of PBT containing 2% BSA. Tissues were then incubated with primary antibodies at the correct dilution in a 0.3% PBT solution containing 2% BSA over night at 4 ° C. The next day, after 3 washes in 0.3% PBT lasting 10 minutes each, tissues were blocked for 10 minutes in a 0.3% PBT solution containing 2% BSA and then incubated with the secondary antibodies for 2 hours at room temperature. After three washes with 0.3% PBT, wing imaginal discs or fat body were collected and mounted in Fluoromount G. The sample observations were performed in a similar manner to those of egg chambers.

## 3.5 Co-localisation analyses and statistics

Colocalisation analyses of N with endosomal markers was performed in wild type as well as $awd^{J2A4}$ mutant FCs. Selected images in which the colocalisation was evaluated were first processed through Adobe Photoshop CS4 software to adjust the threshold level, in order to exclude the background staining. Then, processed images were analysed through the free CDA plugin for ImageJ software, which returns the Pearson’s coefficient. These values were finally statistically compared by applying the two tailed Student’s *t*-test and graphed by using GraphPad Prism 6 software.

# Chapter 4

## Results

The existence of a genetic interaction between Awd and Shi first suggested an involvement of the NDPK in the endocytic process (Krishnan *et al.*, 2001). In order to gain further insights into Awd function, works carried out in Tien Hsu lab unravelled a role for Awd in mediating endocytosis of the Btl and Pvr receptors, as well as of apical junction components (Dammai *et al.*, 2003; Nallamothu *et al.*, 2008; Woolworth *et al.*, 2009). It is important to point out here that endocytosis exercises different roles for these molecules: regarding the receptors, the endocytic process allows to adjust their levels in order to ensure an appropriate signalling. The case of Pvr is peculiar: it is the lack of endocytosis which allows accurate signalling in border cells. Indeed, during BC migration, the physiological deprivation of Awd and the consequent failure to trigger the endocytic process of the receptor allow to achieve extremely high levels of receptor proteins on the plasma membrane of BCs. These levels are critical for accurate invasion of germ cyst and attainment of the oocyte surface. Regarding the adherens junctions components, the endocytic process guarantees cellular homeostasis and tissue integrity. Despite these differences, all these endocytic processes require Awd. Moreover, the role of Awd as an endocytic mediator is required at different time points during development, from oogenesis to embryo development. In light of these considerations, it could be speculated that among the different functions Awd unrolls, its involvement in endocytosis is into the foreground.

As mentioned in paragraph 1.8.1, N signalling requires both receptor and ligand endocytosis. During my PhD, I explored the role of Awd in endocytosis of N receptor. This research vein led me also to analyse Awd trafficking itself. I conducted my analyses in different tissues and at diverse developmental time points with the aim to claim for a general requirement of Awd for accurate N signalling during development.

## 4.1 The loss of *awd* gene function arrests N signalling during the development of *Drosophila melanogaster*

In order to approach the study of the functional role played by the protein encoded by the *awd* gene, I used the null *awd*$^{J2A4}$ allele. It carries the insertion of a single P element in the 5' untranslated region of the gene, which results in the absence of protein product (Dammai *et al.*, 2003; Krishnan *et al.*, 2001). Loss of function mutations of *awd* gene are lethal by the end of larval/early pupal development (see paragraph 1.9, Dearolf *et al.*, 1988). I then took advantage of powerful molecular genetic techniques available in *Drosophila*. Indeed, it is possible to analyse the function of essential genes through clonal analysis approaches. These techniques allowed me to generate mutant cell clones homozygous for the *awd*$^{J2A4}$ allele surrounded by wild type cells. In specific, I mostly employed the MARCM (mosaic analysis with a repressible cell marker) technique (Lee and Luo, 1999) which combines the UAS/Gal4 binary system (Brand and Perrimon, 1993) with the Flp/FRT system (Golic and Lindquist, 1989; Xu and Rubin, 1993) and allows to identify mutant cells thanks to the expression of the GFP (see also paragraph 3.2.1).

Transcriptional reporter genes have been extensively employed in research to assess the function and regulation of transcription factors. Reporters contain DNA sequences that are designed to recruit their cognate transcription factors, followed by a minimal promoter and a gene, such as the *lacZ* gene, coding for the β-galactosidase protein, which is used as a functional readout. The transcription of *lacZ* occurs following the activation of the signalling pathway studied.

To analyse the correct activation of the signalling pathway mediated by the N receptor in cells homozygous for the *awd*$^{J2A4}$ allele, a stock bearing the transcriptional reporter *Gbe+Su(H)*$_{m8}$*lacZ* was used (hereafter referred as *Gbe*, Furriols and Bray, 2001).

### 4.1.1 *awd* function is required during oogenesis to activate N signalling in FCs

During stages 6-8, the signalling pathway mediated by the N receptor is activated in FCs to determine the switch in the proliferative program from mitotic cycle to endocycle. Dl in the germline and N in the FCs are required for this switch. In Figure 21, the scheme represents a sagittal section of a stage 8 egg chamber. Germline cells (in yellow) represent the signal sending cells, while somatic FCs (in grey) are the signal-receiving cells. Some FC clones are present and highlighted in green.

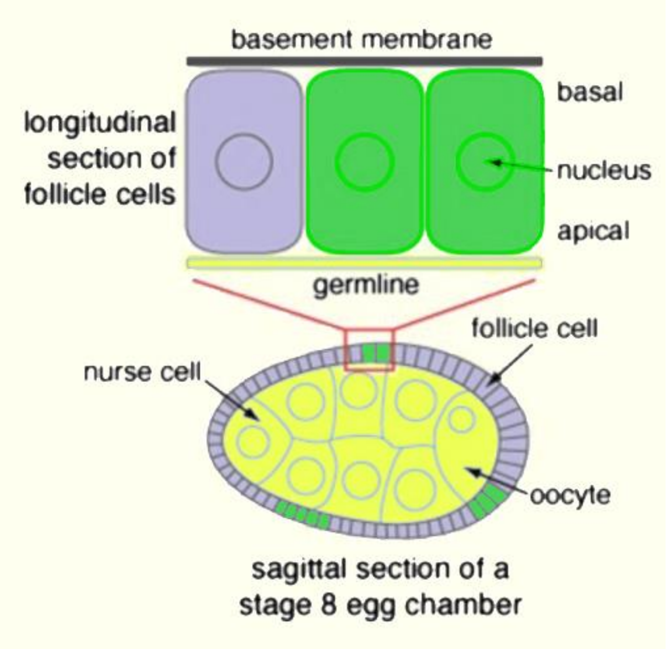
basement membrane
basal
longitudinal section of follicle cells
nucleus
apical
germline
follicle cell
nurse cell
oocyte
sagittal section of a stage 8 egg chamber

**Figure 21 Schematic drawing of a stage 8 egg chamber in which MARCM clones have been induced.** In a stage 8 egg chamber, follicular epithelium completely wraps a germline cyst. The oocyte is positioned at the posterior pole of the egg chamber. It has the smallest nucleus of the germ cyst since nurse cells are polyploid. The apical surface of FCs faces the germline, while the basal side is in front of the basement membrane. FCs gain their polyploid status after stage 6, by entry into the endocycle. Clones of FCs, like those generated through the MARCM methodical, are highlighted in green.

Preliminary results obtained in the lab suggested that the loss of *awd* function causes the extension of the normal proliferative program of FCs beyond stage 6. This is reminiscent of alterations in N signalling pathway. In order to probe Awd involvement in the correct activation of N signalling pathway during oogenesis, I decided to analyse *awd*$^{J2A4}$ mutant FC clones in stages 6-8 egg chambers.

To assess NICD activity in *awd*$^{J2A4}$ mutant FC clones, I took advantage of the *Gbe* reporter construct and I carried out an immunofluorescent staining using a rabbit polyclonal antibody directed against the Awd protein (Dammai *et al.*, 2003) and a mouse monoclonal antibody that recognises the β-galactosidase encoded by the *lacZ* reporter gene. *awd*$^{J2A4}$ FC MARCM clones devoid of Awd (Figure 22A,A') and expressing the GFP marker (Figure 22B,B') lack *Gbe* expression, as evidenced by the absence of the β-galactosidase protein (Figure 22C,C',D,D'). This result suggests that the signalling mediated by the N receptor is inhibited.

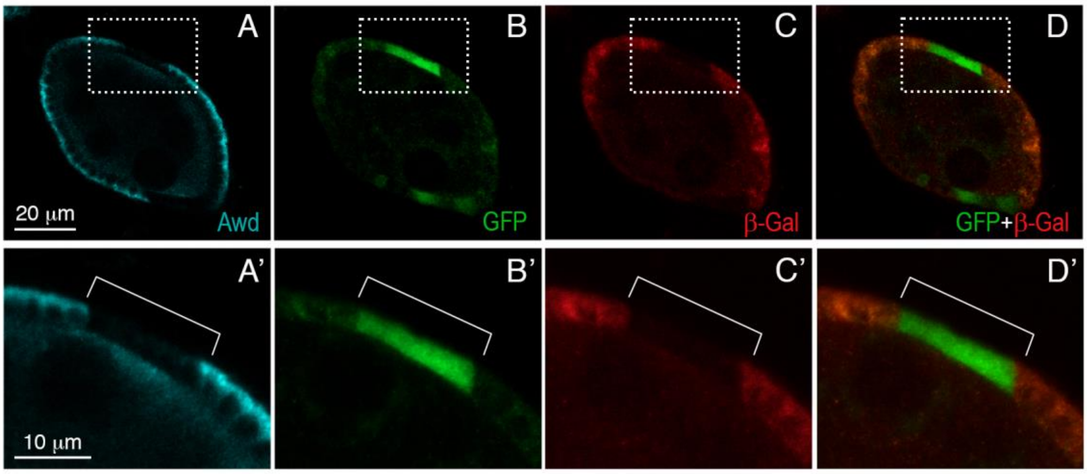

**Figure 22 In *awd*$^{J2A4}$ mutant FCs N signalling is arrested.** Panels A-D' show confocal images of a stage 7 egg chamber in sagittal section collected from *yw, hs-flp/Gbe+Su(H)*$_{m8}$*lacZ; act-Gal4, UAS-GFP/+; FRT*$^{82B}$*, awd*$^{J2A4}$*/FRT*$^{82B}$*, act-Gal80* female. **(A-D)** Awd protein staining (cyan, A) reveals homozygous *awd*$^{J2A4}$ FCs, also expressing GFP (green, B). The β-galactosidase protein (red, C) is encoded by the reporter gene *Gbe*. In D is showed the merge between the GFP signal and the β-galactosidase staining. **(A'-D')** Magnification of the areas included in the dotted boxes in A-D. The brackets in each panel signal the MARCM clone.

N-triggered endocycle entry depends on the expression of the N target gene *hnt*. As further evidence of an arrest of N signalling in *awd* loss of function FCs, egg chambers of the above mentioned genotype were subjected to an immunohistochemistry assay by using a monoclonal antibody against the transcriptional repressor Hnt (Yip *et al.*, 1997), whose expression is induced by N signalling at stage 6-7 (Sun and Deng, 2005, 2007). I found that, in stage 7 egg chambers (Figure 23A), in FCs homozygous for the *awd*$^{J2A4}$ mutation (Figure 23B) Hnt expression is lost (Figure 23C,D). FCs flanking the clone, instead, show high levels of Hnt protein.

Hnt is a transcriptional repressor that mediates the downregulation of *cut*. In *awd*$^{J2A}$ FCs (Figure2 3E,E', GFP$^{+}$ cells in Figure 23F,F') Cut expression persists after stage 5 (Figure 23G,G',H,H'). All these data are consistent with the inability of *awd*$^{J2A4}$ mutant FCs to enter endocycle. Cells lacking *awd* gene function continue to proliferate and do not perform the three rounds of endoreplication of their DNA content which allow the acquisition of polyploidy. The results obtained are in accordance with the reduced nuclear size of FCs homozygous for the *awd*$^{J2A4}$ mutation, as evidenced by nuclear staining with To-Pro-3 (asterisks in Figure 23A). Acquisition of polyploidy is also essential for FCs growth. Indeed, by the end of stage 10A, when endocycle terminates, wild type FCs have grown in dimensions. Instead, FCs homozygous for *awd*$^{J2A4}$ allele do not enter endocycle and, as a consequence, they will not grow (not shown). This leads to a thinning of the follicular epithelium where *awd*$^{J2A4}$ mutant FCs are present.

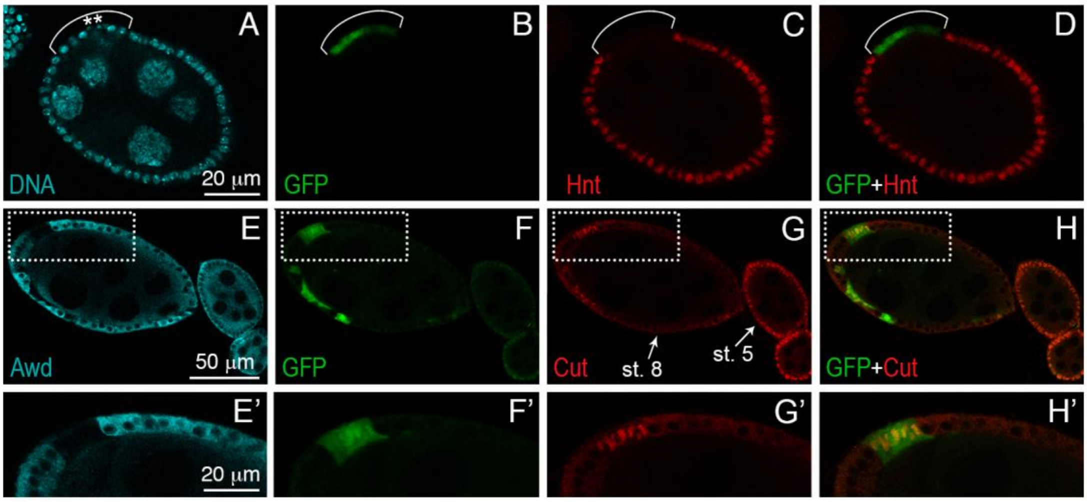

**Figure 23 N target are deregulated in *awd*$^{J2A4}$ FCs.** Panels A-H' show confocal images of stage 7-8 egg chambers in sagittal section collected from *yw, hs-flp/Gbe+Su(H)*$_{m8}$*lacZ; act-Gal4, UAS-GFP/+; FRT*$^{82B}$*, awd*$^{J2A4}$*/FRT*$^{82B}$*, act-Gal80* females. **(A-D)** In A, the staining with the far-red DNA dye To-Pro-3 highlight nuclei of FCs and nurse cells composing the egg chamber. GFP-positive FCs (green, B) are homozygous for the *awd*$^{J2A4}$ null allele. The brackets reported in each panel signal the position of the MARCM clone. At stage 7, the transcriptional repressor Hnt is strongly expressed, as showed by appropriate staining (red, C). However, *awd*$^{J2A4}$ mutant FCs are devoid of Hnt, as shown in the merge in panel D. Asterisks in E point to *awd*$^{J2A4}$ mutant FCs with very small nuclei. **(E-H')** Awd staining (cyan, E,E') is showed. GFP-positive cells (green, F,F') belong to MARCM clones. Positive revelation of Cut (red, G,G') is seen in FCs devoid of *awd* function (H,H') in a stage 8 egg chamber. The dotted boxes enclose the magnified areas showed in E'-F'.

### 4.1.2 *awd* function is required during wing disc development to activate N signalling at the DV boundary

N signalling unrolls an important function in the establishment and maintenance of the DV boundary in wing imaginal discs. In order to determine whether Awd involvement in N signalling is strictly context-dependent in FCs, or if Awd absolves to a more general requirement for the activation of this pathway, I generated and analysed *awd*$^{J2A4}$ mutant clones in wing discs. In details, I looked for clones that extended across the DV boundary where N signalling is active (Figure 24) and induces the expression of target genes such as *wg* (see paragraph 1.7.2, de Celis *et al.*, 1996).

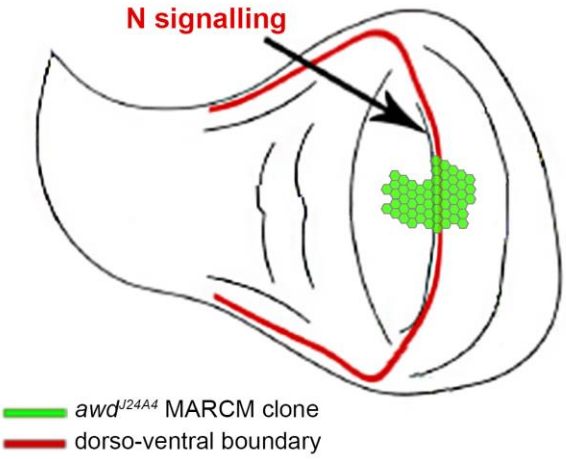

**Figure 24 Schematic drawing of a L3 wing imaginal disc.** At the dorso-ventral boundary (red) the N signalling is active and induces the expression of target genes. An *awd*$^{J2A4}$ clone that spans the dorso-ventral boundary region, showed in green in the Figure, allows to analyse the effects of *awd* loss of function on activation of N signalling in wing discs.

Immunodetection of the β-galactosidase protein reveals that in *awd*$^{J2A4}$ MARCM clones (Figure 25A,A’, GFP$^{+}$ cells in Figure 25B,B’), extending across the border between the dorsal and ventral compartments, the expression of the *Gbe* reporter gene is absent (Figure 25C,C’). The loss of *Gbe* expression is in precise correspondence with the mutant cell clone (Figure 25D,D’).

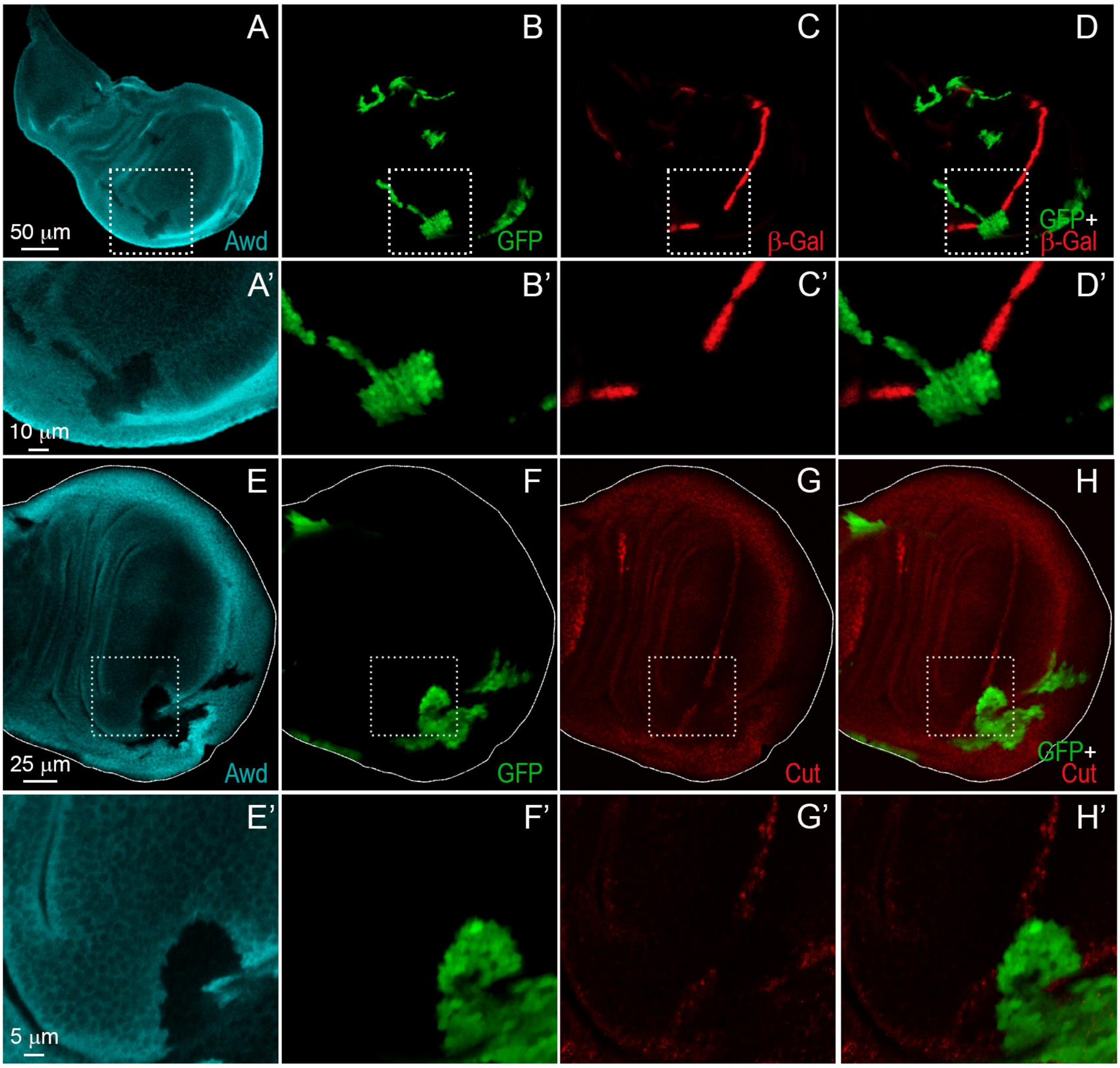

**Figure 25 The loss of *awd* gene function in wing disc cells disrupts N signalling at the DV boundary.** Confocal cross section of L3 wing discs dissected from *yw, hs-flp/Gbe+Su(H)*$_{m8}$*lacZ; act-Gal4, UAS-GFP/+; FRT*$^{82B}$*, awd*$^{J2A4}$*/FRT*$^{82B}$*, act-Gal80* larvae. **(A-D’)** Awd staining (cyan, A,A’) is showed. *awd*$^{J2A4}$ mutant cells are individuated by GFP expression (green, B,B’). β-galactosidase staining (red, C,C’) is absent in correspondence of the homozygous *awd*$^{J2A4}$ mitotic clone (D,D’). The dotted boxes in A-D indicate the region magnified in A’-D’. **(E-H’)** Awd staining (cyan, E,E’) is showed. *awd*$^{J2A4}$ mutant cells are individuated by GFP expression (green, F,F’). Cut staining (red, G,G’) is lost in homozygous *awd*$^{J2A4}$ mitotic clones (H,H’). The white lines in E-H individuate the wing disc, while the dotted boxes in E-H indicate the region magnified in E’-H’.

I also investigated *cut* expression that, in wing discs, is a positive N target at the DV boundary. At the DV boundary of wing discs, where cells devoid of Awd (Figure 25E,E’, GFP$^{+}$ cells in Figure 25F,F’) are present, Cut (Figure 25G,G’) is undetectable (Figure

25H,H'). Since loss of *awd* gene function arrests N signalling in different tissues, this indicates that Awd plays a fundamental role in activation of this signalling pathway.

Further confirmation of N arrest in *awd*$^{J2A4}$ mutant cells was obtained by analysing the expression of *wg* in wing imaginal discs. In wild type conditions, *wg* expression is induced at the DV boundary as a consequence of activation of the signalling pathway mediated by the N receptor (de Celis *et al.*, 1996). In homozygous *awd*$^{J2A4}$ wing disc cell clones (GFP$^{+}$ cells, Figure 26A,A') and located along the DV margin of the wing disc, the expression of Wg protein (Figure 26B,B') is lost (Figure 26C,C'). This result is in agreement with the previous ones, and supports once again the notion that *awd* function is necessary for the correct N signal transduction both in imaginal tissues and FCs.

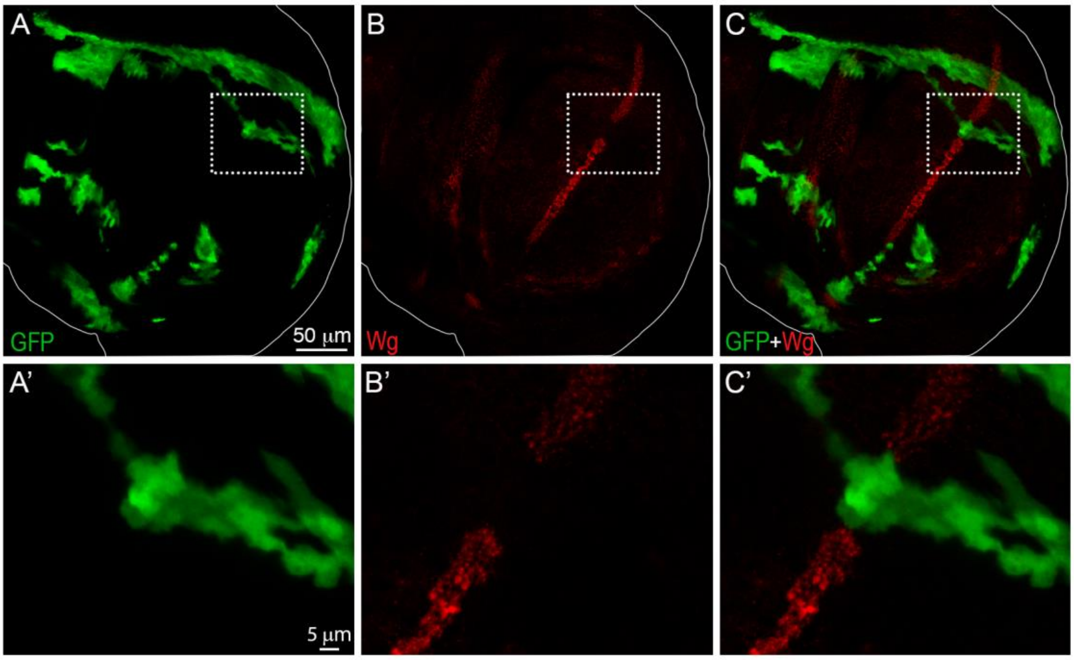

**Figure 26 Wg expression at the DV boundary of wing discs is inhibited in *awd*$^{J2A4}$ mutant cells. (A-C')** Confocal cross section of aL3 wing disc dissected from *yw, hs-flp/Gbe+Su(H)*$_{m8}$*lacZ; act-Gal4, UAS-GFP/+; FRT*$^{82B}$*, awd*$^{J2A4}$*/FRT*$^{82B}$*, act-Gal80* larvae. The GFP-positive cells (green, A,A') are homozygous for the *awd*$^{J2A4}$ null allele. Wg staining (red, B,B') is lost in correspondence of homozygous *awd*$^{J2A4}$ mitotic clones (C,C'). The white lines in A-C individuate the wing disc, while the dotted boxes in A-C indicate the region magnified in A'-C'.

## 4.2 The loss of *awd* gene function affects the intracellular distribution of N receptor

### 4.2.1 N receptor accumulates in endocytic vesicles in *awd*$^{J2A4}$ mutant FCs

In the past 25 years, accumulated evidence highlighted the requirement of Dynamin-dependent N receptor endocytosis to trigger activation of N signalling (Seugnet *et al.*, 1997). Mutations in regulators of the endocytic trafficking have been shown to alter intracellular distribution of N receptor and to cause aberrant activation as well as failure of the signalling, depending on the endosomal compartment that is affected (reviewed in Baron, 2012; Fortini and Bilder, 2009; Le Borgne, 2006). In wild type conditions, N is localised at the plasma membrane as well as in small intracellular vesicles. Particularly, it was shown that the receptor co-localises with several specific markers of early endosomes, including the GTPase Rab5 (Vaccari *et al.*, 2008). Moreover, the receptor was also detected in vesicles more mature than early endosomes, including the multivesicular bodies (MVBs). In light of the previously described results, of great interest to my research was the observation by Vaccari and collaborators that mutations altering N entry into early endosomes are associated with failure of transduction of N signalling pathway in FCs. I then analysed the intracellular distribution of the receptor in *awd*$^{J2A4}$ mutant FC clones through immunohistochemistry. In such FC clones (Figure 27A,A',E, GFP$^{+}$ cells in Figure 27B,B',F), I observed a strong accumulation of N receptor in small puncta (Figure 27C,C',G). This phenotype suggests that in homozygous *awd*$^{J2A4}$ FCs the receptor is stalled in subcellular vesicles (Figure 27D,D'H) as a consequence of a block in the endocytic route. The receptor appears strongly condensed into aggregates (Figure 27C',G) located just below the apical plasma membrane.

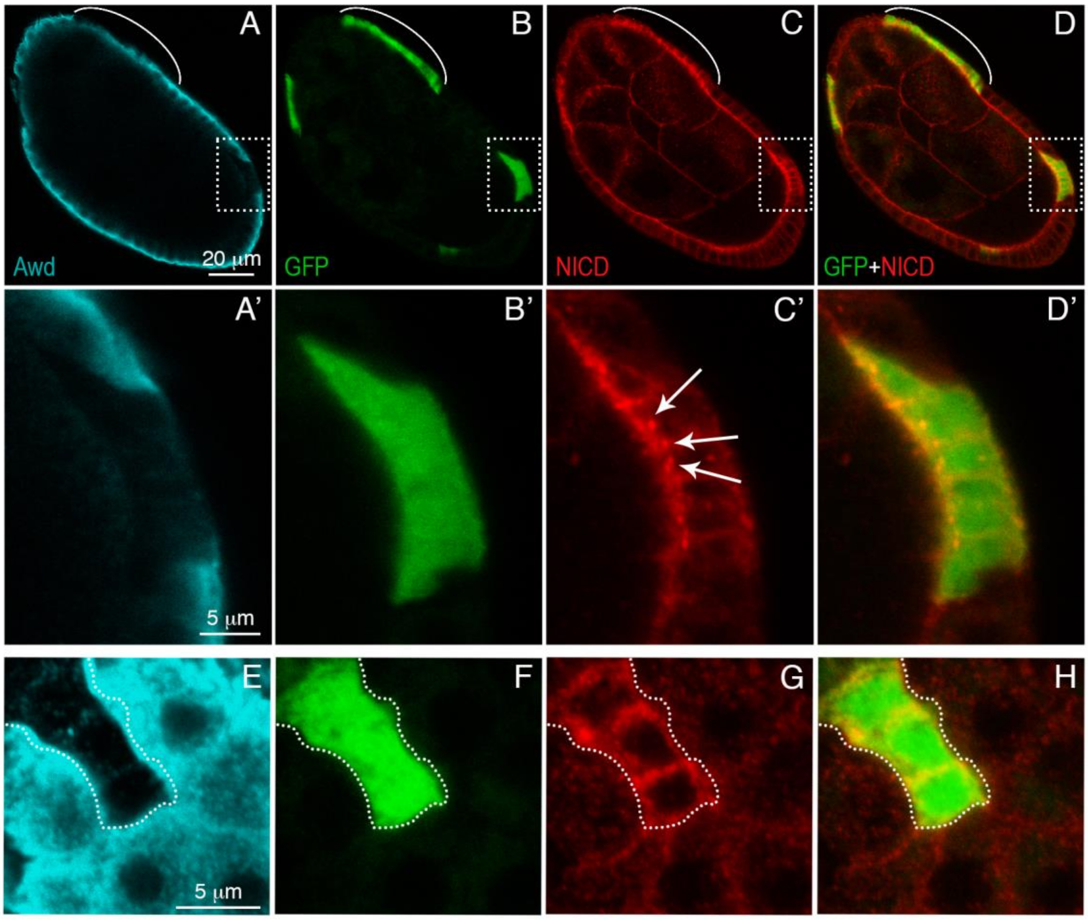

**Figure 27 N receptor is stalled and accumulates in *awd*$^{J2A4}$ mutant FCs.** Confocal cross section **(A-D')** and superficial section **(E-H)** of a stage 8 egg chamber dissected from *yw, hs-flp/Gbe+Su(H)*$_{m8}$*lacZ; act-Gal4, UAS-GFP/+; FRT*$^{82B}$, *awd*$^{J2A4}$*/FRT*$^{82B}$, *act-Gal80* female and stained for Awd (cyan A,A',E) and NICD (red, C,C',G). The dotted boxes in A-D include the region magnified in A'-D'. The brackets, instead, highlight an *awd*$^{J2A4}$ clone in which thinning of the follicular epithelium is already visible. In C' arrows point to intracellular vesicles containing NICD. These vesicles are bigger than those present in flanking GFP-negative cells, suggesting that the N receptor can't proceed along the endocytic route. In E-H the dotted lines hint the region in which *awd*$^{J2A4}$ mutant FCs are. In the superficial section showed in E-H, in wild type FCs flanking the clone, the N receptor displays a punctate distribution in which small vesicles are found both just under the plasma membrane and in inner regions of the cells. This suggests that the N distribution pattern results from a dynamic trafficking of the receptor within the cell. On the contrary, in *awd*$^{J2A4}$ mutant cells, the N pattern is completely different: first of all, the intensity of N signal is higher than that in wild type FCs. Moreover, N vesicles appear larger and their distribution is strongly restricted to the subcortical region of the cells.

### 4.2.2 The N signalling defect in homozygous *awd*$^{J2A4}$ cells is not correlated to the loss of cell polarity

Sasaki and co-workers in 2007 conducted an exquisitely elegant genetic analysis to explore N apical localisation in epithelial cells. They found that in epithelial cells N is specifically addressed to the subapical region, apically to adherens junctions (Figure 28) and that the knockdown of DE-cadherin (DE-cad), a component of the adherens junctions together with β-catenin, disrupts N localisation and signalling (Sasaki *et al.*, 2007).

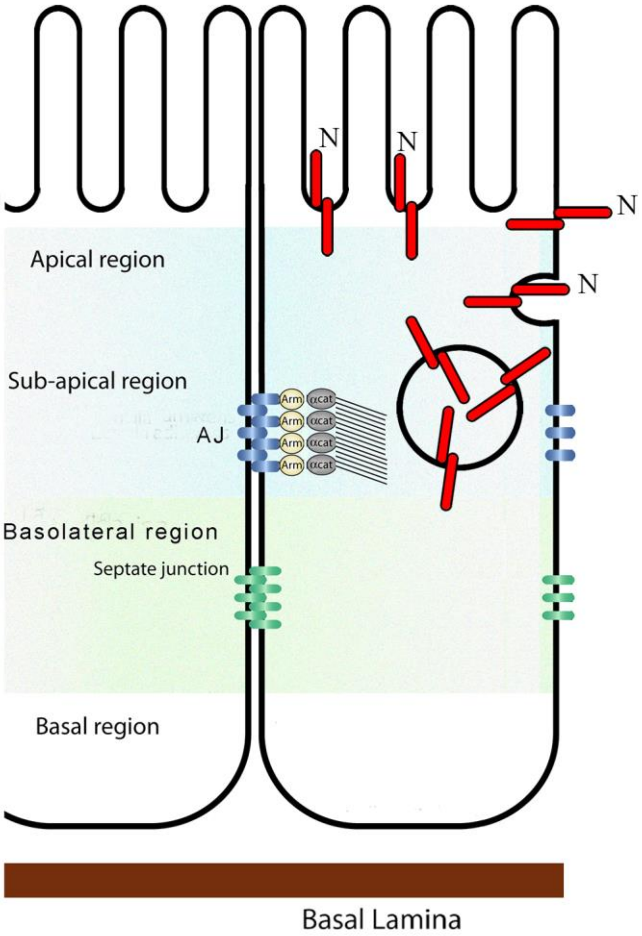

**Figure 28 Localisation of N receptor in epithelial cells.** N receptor (red) is localised at the subapical region of epithelial cells, where also aPKC resides. Adherens junctions (AJ), composed of DE-cad (blue) and Arm (yellow) separate the apical compartment from the basolateral region. Septate junctions (green) are also indicated.

Previous reports on *awd* function in FCs highlighted that it is required to maintain tissue integrity since in homozygous *awd*$^{J2A4}$ clones the adherens junctions components DE-cad and β-catenin fail to localise correctly (Woolworth *et al.*, 2009). In order to exclude that the observed arrest of N signalling in *awd*$^{J2A4}$ cells was an indirect effect of cell polarity alterations, I analysed N localisation and signalling in small monolayered FC clones through immunohistochemistry. I found that, in small *awd*$^{J2A4}$ FC clones (composed of less than 5 GFP$^{+}$ cells, Figure 29A), DE-cad is correctly localised and its pattern is indistinguishable from that of flanking FCs (Figure 29B). Indeed, alterations in its subcellular distribution are typically observed in clones of more than 10 cells. In small *awd*$^{J2A4}$ clones (*n=12*), NICD staining reveals that the N localisation defects still occur (Figure 29C,D). Moreover, in small *awd*$^{J2A4}$ FC clones (Figure 29E, GFP$^{+}$ cells in Figure 29F), failure of N signalling takes still place, since 93% of *awd*$^{J244}$ mutant FCs in stage 6-8 egg chambers can't upregulate Hnt (Figure 29G,H).

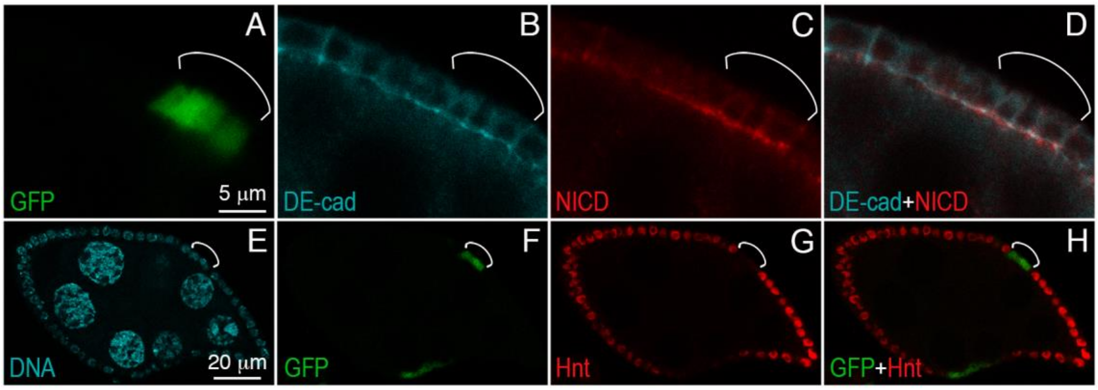

**Figure 29 N receptor accumulation and signaling defects occur in *awd*$^{J2A4}$ FC clones in absence of cell polarity alteration. (A-D)** Confocal cross section magnification of a stage 7-8 egg chamber dissected from *yw, hs-flp/Gbe+Su(H)*$_{m8}$*lacZ; act-Gal4, UAS-GFP/+; FRT*$^{82B}$*, awd*$^{J2A4}$*/FRT*$^{82B}$*, act-Gal80* female and stained for DE-cad (cyan, B) and NICD (red, C). DE-cad is localised in the subapical region and its signal helps in determining the cell number in each clone, composed of GFP-positive cells (green, A). The brackets hint clone position in each panel. In small homozygous *awd*$^{J2A4}$ clones, DE-cad is correctly localised in FCs and doesn't spread throughout the cell membrane as reported for bigger *awd* loss of function clones. However, N intracellular distribution appears altered (C and merge in D). **(E-H)** Confocal cross section of a stage 8 egg chamber dissected from *yw, hs-flp/Gbe+Su(H)*$_{m8}$*lacZ; act-Gal4, UAS-GFP/+; FRT*$^{82B}$*, awd*$^{J2A4}$*/FRT*$^{82B}$*, act-Gal80* female and stained for Hnt (red, G). The To-Pro-3 (cyan, E) stains the DNA, allowing to determine the cell number in each clone, composed of GFP-positive cells (green, F). The brackets hint clone position in each panel. In small homozygous *awd*$^{J2A4}$ clones, N signalling arrest is observed (merge in H).

I also investigated the relationship between N signalling defect and alteration in adherens junctions localisation in wing disc cells. To this purpose, I performed an immunofluorescent labelling of larval tissues by using the anti-Wg and anti-DE-cad antibodies. In wing discs carrying homozygous *awd*$^{J2A4}$ MARCM clones (Figure 30A), the mutant cells, positively marked by GFP (Figure 30B), show DE-cad correctly localised at the apical domain (Figure 30C,F,G). The clone showed in Figure 30 is quite large, suggesting that the previous reported alterations in cell polarity due to *awd* loss of function can't be extended at imaginal tissues but are restricted to FCs. Wg staining reveals that, despite cell polarity is not impaired, as assessed by normal DE-cad localisation, in *awd*$^{J2A4}$ mutant wing disc cells N signalling is prevented (Figure 30D,E).

Taken together, these results indicate that the altered N distribution in mutant *awd*$^{J2A4}$ cells can't be ascribed to defects in cell polarity but rather to specific alterations in intracellular trafficking of the receptor.

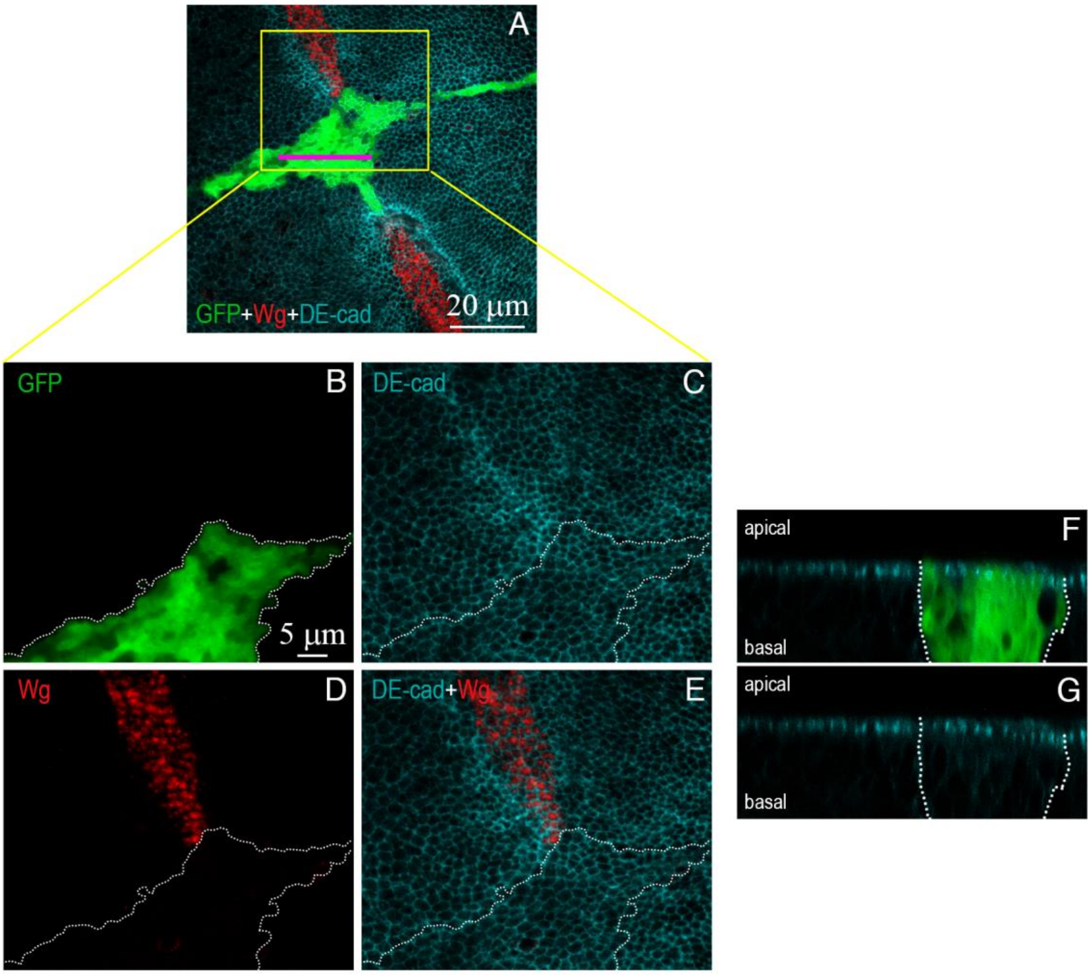

**Figure 30 *awd* loss of function does not impair DE-cad localisation in wing imaginal disc cells.** Confocal microscopy analysis of wing discs dissected from *yw, hs-flp/Gbe+Su(H)*$_{m8}$*lacZ; act-Gal4, UAS-GFP/+; FRT*$^{82B}$*, awd*$^{J2A4}$*/FRT*$^{82B}$*, act-Gal80* larvae stained for Wg (red in A,D,E) and DE-cad (cyan in A,C,E,F,G). **(A-E)** xy and **(F-G)** xz sections of an *awd*$^{J2A4}$ MARCM clone marked by GFP (green in A,B,F) at the DV boundary. The yellow box in A encloses the area magnified in B-E, while the pink line points to the position of the xz section shown in F-G. The dotted areas in B-E follow the boundary between homozygous *awd*$^{J2A4}$ (GFP-positive) and GFP-negative cells. At the DV boundary, mutant cells do not express Wg protein. DE-cad appears expressed at wild type levels (C,E) and correctly apically localised (F,G).

## 4.3 The loss of *awd* gene function arrests N proteolytic processing beyond the S2 metalloproteinase-mediated cleavage

N signalling transduction is mediated by interaction of the receptor with the Dl ligand exposed on the plasma membrane of the abutting germline cells (Figure 15). Members of the metalloprotease ADAM/TACE/Kuz/Sup17 family operate the S2 cleavage in the extracellular region of N receptor; this cleavage generates the NEXT fragment. NEXT is a ligand-independent γ-secretase-dependent constitutively active form of N. Through γ-secretase-mediated cleavage at the S3 and S4 sites NICD is produced. NICD is a constitutively active form of N, both ligand- and γ-secretase- independent. This means that, once produced, it can translocate to the nucleus and activate the transcription of specific target genes (Artavanis-Tsakonas *et al.*, 1995).

In the *Drosophila* community are available stocks bearing transgenes in which the NEXT or alternatively the NICD sequences have been cloned in a pUAST vector (Go *et al.*, 1998; Vaccari *et al.*, 2008), to which I will refer to as *UAS-NEXT* or *UAS-NICD* respectively. Effective overexpression of both constructs in FCs can be assessed by looking at N upregulated target genes, such as Hnt. To this aim, I employed the Flp-out/Gal4 technique (Pignoni and Zipursky, 1997) to randomly co-express the *UAS-NEXT* or *UAS-NICD* and the *UAS-mcd8GFP* (encoding for a fusion protein between the mouse lymphocyte marker CD8 and the GFP) transgenes in cell clones (see paragraph 3.2.3).

Figure 31A-C shows a stage 7-8 egg chamber stained with Hnt antibody (Figure 31B,C) containing one clone of GFP-positive FCs (Figure 31A) overexpressing the NEXT fragment. 92.5% (*n=40*) of these FCs exhibit enhanced Hnt staining.

Figure 31D-F shows a stage 7-8 egg chamber stained with Hnt antibody (Figure 31E,F) containing one clone of GFP-positive FCs (Figure 31D) overexpressing the NICD fragment. 51% (*n=100*) of these FCs exhibit enhanced Hnt staining. These results indicate that enhancement of N signalling can be induced through overexpression of both its constitutively active forms in FCs.

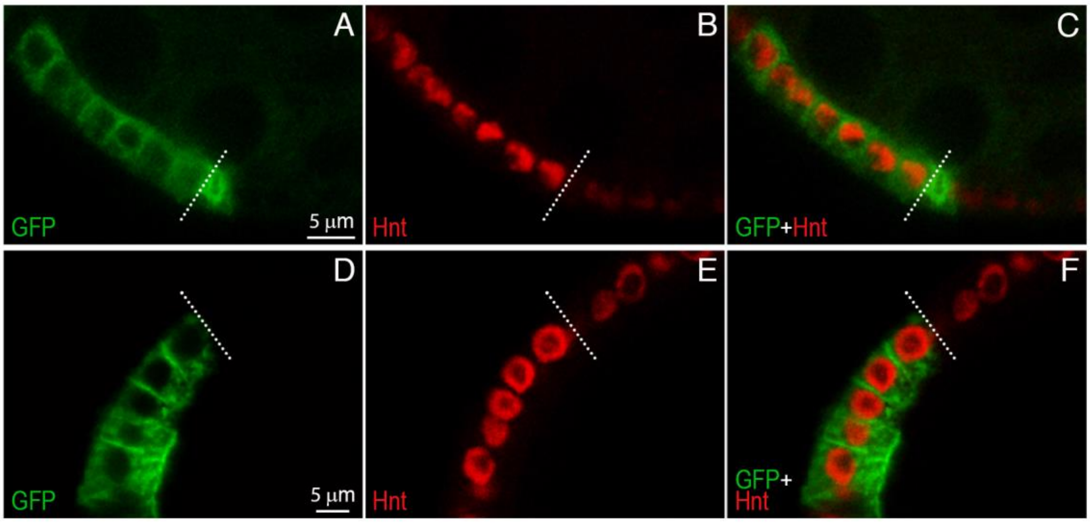

**Figure 31 N signalling in wild type FCs is upregulated by either NICD or NEXT overexpression.** Ovaries were dissected from **(A-C)** *hs-flp, UAS-mCD8GFP/act>CD2>Gal4; UAS-NEXT/+* or **(D-F)** *hs-flp, UAS-mCD8GFP/act>CD2>Gal4; UAS-NICD/+* females. Hnt signal (red, B,C,E,F) is visible. Clones are marked by a membrane-bound GFP (green A,D,C,F). Dotted lines mark the boundary between GFP-positive and GFP-negative cells.

It has been proposed that γ-secretase cleavage occurs during N trafficking into endosomal compartments and impairment of N entry into the early endosomes impedes signalling activation (Vaccari *et al.*, 2008). Moreover, data supporting the notion that the NEXT generation may not require entry into the endocytic pathway have also been collected (Struhl and Adachi, 2000). Indeed, S2 cleavage site is in a juxtamembrane domain at the plasma membrane (van Tetering *et al.*, 2009).

In order to gain insights into the *awd* gene function requirement in N signalling transduction, I generated *awd*$^{J2A4}$ MARCM clones in which the NEXT or alternatively the NICD fragments were overexpressed. The rationale of these experiments was to achieve the rescue of the N signalling defect in *awd*$^{J2A4}$ mutant cells. The rescue with one or both the two fragments could help identify the step of N proteolytic processing which requires *awd* function.

### 4.3.1 Overexpression of the NEXT fragment in homozygous *awd*$^{J2A4}$ FCs doesn't restore N signalling

In MARCM FC clones homozygous for *awd*$^{J2A4}$ mutation (Figure 32A, GFP$^+$ cells in Figure 32B) and overexpressing the NEXT fragment, there is no detection of the β-galactosidase signal (Figure 32C), indicating failure to activate transcription of the *Gbe* reporter gene in these cells (Figure 32D). The signalling mediated by the N receptor, therefore, is not restored by overexpression of the NEXT fragment in *awd*$^{J2A4}$ mutant FCs.

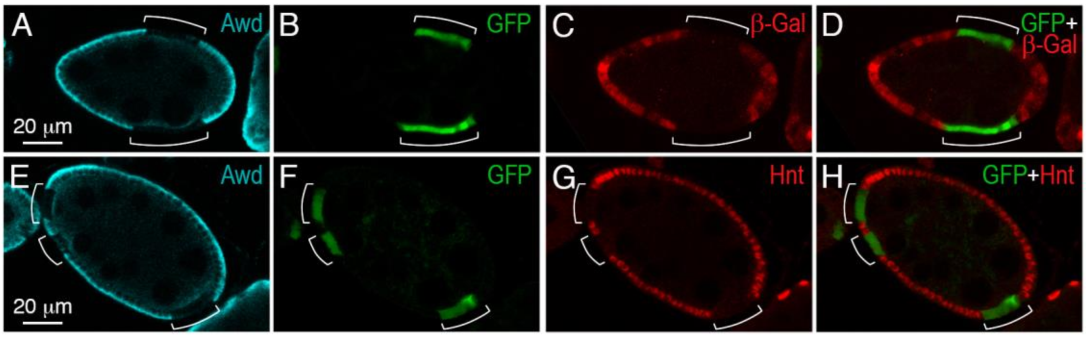

**Figure 32 NEXT overexpression in *awd*$^{J2A4}$ mutant FCs doesn't restore N signalling.** Sagittal sections of a stage 7 (A-D) and a stage 8 (E-H) egg chambers dissected from *yw, hs-flp/Gbe+*$Su(H)_{m8}$*lacZ; act-Gal4, UAS-GFP/UAS-NEXT;* $FRT^{82B}$*, awd*$^{J2A4}$*/*$FRT^{82B}$*, act-Gal80*. Images were taken by confocal microscopy. **(A-D)** Fluorescent signals related to the Awd protein (cyan, A) and GFP (green, B) which identify MARCM clones are visible. Clones are also indicated by brackets. In C, the immunodetection of the β-galactosidase protein encoded by the *Gbe* reporter gene is visible. In D, it is shown the merge of the signals in B and C: in both clones no β-galactosidase staining is detected. **(E-H)** Fluorescent signals related to the Awd protein (cyan, E) and GFP (green, F) which identify the MARCM clones are visible. Clones are also indicated by brackets. In G, the signal relative to the transcriptional repressor Hnt is visible. In H, it is shown the merge of the signals in F and G: no Hnt staining is detected in mutant FCs.

This is further remarked by the fact that in stage 8 egg chambers, *awd*$^{J2A4}$ MARCM clones (Figure 32E,F) overexpressing NEXT do not show Hnt expression (Figure 32G,H). These results indicate that *awd* gene function is required downstream of the S2 proteolytic cleavage mediated by the metalloproteinases.

Interestingly, in homozygous *awd*$^{J2A4}$ FCs (Figure 33A,A’,E,E’, GFP$^{+}$ cells in Figure 33B,B’,F,F’) overexpressing the NEXT fragment, NICD staining (Figure 33C,C’,G,G’) reveals a highly intense signal. This is probably due to the overexpressed NEXT fragment in these cells (Figure 33D,D’,H,H’) that still accumulates in intracellular vesicles (arrows in C’,G’), as the N receptor does in *awd*$^{J2A4}$ mutant FCs.

Previous works uncovered a requirement of *shi* function for N signalling activation. Indeed, in *shi* mutant embryos, N signalling is inhibited (Struhl and Adachi, 2000) and in FCs, as well as in wing disc cells in which a dominant-negative form of Shi is overexpressed, N transduction failure is recovered (Vaccari *et al.*, 2008). However, in both cases, overexpression of the NEXT fragment was shown to be able to restore signalling. Conversely, NEXT is unable to rescue N signalling in *awd*$^{J2A4}$ mutant FCs. This result strongly supports the notion that *awd* function is required downstream of Dynamin.

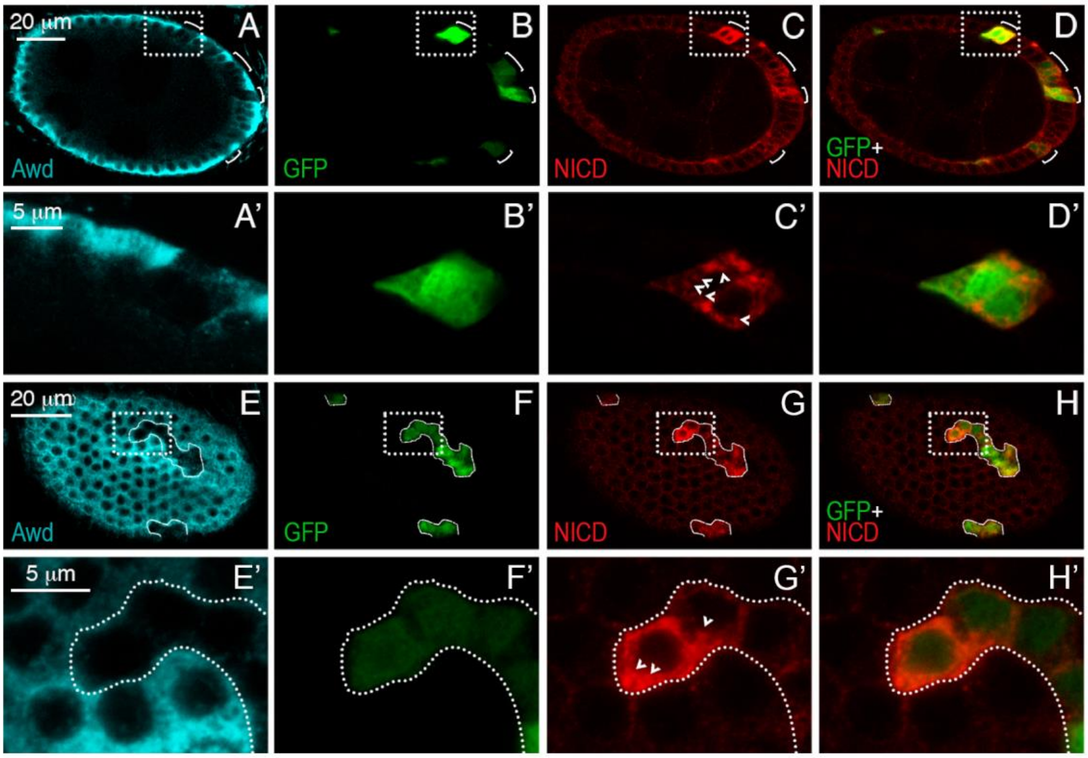

**Figure 33 NEXT overexpression in *awd*$^{J2A4}$ mutant FCs enhances accumulation of NICD-positive vesicles.** Confocal microscopy analysis of egg chambers dissected from *yw, hs-flp/Gbe+Su(H)*$_{m8}$*lacZ; act-Gal4, UAS-GFP/UAS-NEXT; FRT*$^{82B}$*, awd*$^{J2A4}$*/FRT*$^{82B}$*, act-Gal80*. Panels A-H’ show a cross section **(A-D’)** and a surface section **(E-H’)** of a stage 8 egg chamber containing homozygous *awd*$^{J2A4}$ MARCM clones, marked by GFP (green, B,B’,F,F’) and stained with an anti-Awd (cyan, A,A’,E,E’) and anti-NICD (red, C,C’,G,G’) antibodies. Brackets in A-D embrace the clonal FCs while the dotted boxes include the regions magnified in A’-D’. Arrowheads in C’ and G’ point to NICD-positive intracellular vesicles accumulated in mutant cells. In E-H, the white lines outline the clones while the dotted boxes enclose the regions magnified in E’-H’. In E’-H’ the white dotted lines help distinguishing FCs devoid of *awd* function from flanking cells.

### 4.3.2 Overexpression of the NICD fragment in homozygous *awd*$^{J2A4}$ FCs restores N signalling

I then also investigated the ability of NICD fragment to rescue the N signalling defect in *awd* mutant FCs. In MARCM clones of FCs homozygous for the *awd*$^{J2A4}$ null allele (Figure 34A, GFP$^{+}$ cells in Figure 34B) overexpressing the NICD fragment, I observed a partial recovery of the expression of the *Gbe* reporter (Figure 34C,D). This result is confirmed by staining egg chambers with the antibody against Hnt. In stage 6-8 egg chambers, in *awd*$^{J2A4}$ MARCM FC clones (Figures 34E,F) overexpressing NICD fragment, 60.49% of FCs (*n=329*) upregulate Hnt (Figures 34G,H). This percentage represents a significant rescue of the fully penetrant N signalling defect recovered in *awd*$^{J2A4}$ mutant FCs and indicates that the *awd* gene function is necessary in the endocytic processing steps leading to the release of the NICD fragment.

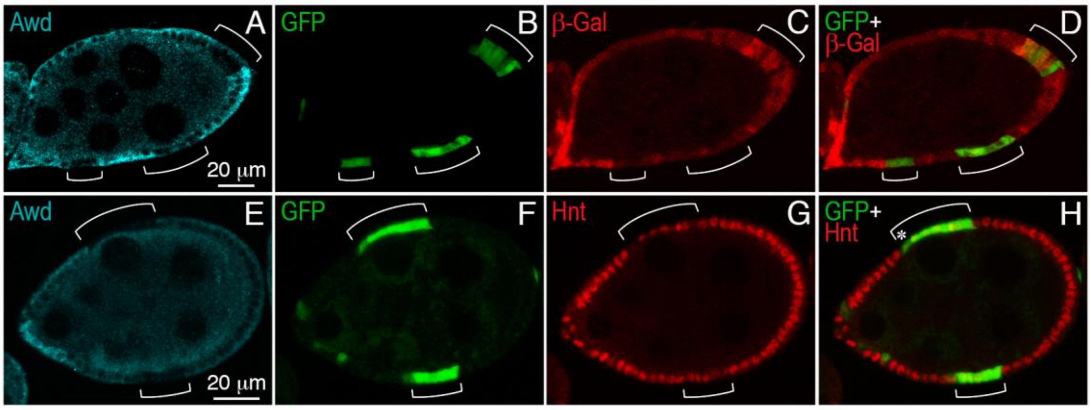

**Figure 34 NICD overexpression in *awd*$^{J2A4}$ mutant FCs restores N signalling.** Sagittal sections of stage 8 egg chambers dissected from *yw, hs-flp/Gbe+Su(H)$_{m8}$lacZ; act-Gal4, UAS-GFP/UAS-NICD; FRT$^{82B}$, awd$^{J2A4}$/FRT$^{82B}$, act-Gal80*. Images were taken by confocal microscopy. **(A-D)** Fluorescent signals related to the Awd protein (blue, A) and GFP (green, B) which identify the clones of FCs homozygous for the null allele. Clones are indicated by brackets. In C, the immunodetection of the β-galactosidase protein encoded by the *Gbe* reporter gene is visible. In D, it is shown the merge of the signals in B and C: in 2 out of 3 clones β-galactosidase staining is detected in some mutant FCs. **(E-H)** Fluorescent signals related to the Awd protein (blue, E) and GFP (green, F) which identify the clones of FCs homozygous for the null allele are visible. Clones are indicated by brackets. In G, the signal relative to the transcriptional repressor Hnt is visible. In H, it is shown the merge of the signals in F and G: Hnt staining is detected in some mutant FCs.

### 4.3.3 Comparison of N receptor intracellular distribution and signalling outcome in endocytic mutants suggests an endocytic defect in early steps beyond internalisation in *awd*$^{J2A4}$ mutant FCs

Previous works already supported an involvement of Awd in endocytosis (Dammai *et al.*, 2003; Krishnan *et al.*, 2001; Nallamothu *et al.*, 2008; Woolworth *et al.*, 2009). Trafficking of N receptor along the endocytic route is necessary to produce the NICD fragment, which is able to signal (Baron, 2012; Fortini and Bilder, 2009). Given that N processing and activation occur along the endocytic route, from my analysis it could be inferred that the observed inhibition of N signalling pathway in *awd*$^{J2A4}$ mutant cells is probably due to a failure in distributing N receptor to the appropriate endosomal compartment in which the receptor gets processed and NICD fragment release occurs. Hints supporting this derive from previous reported analyses of N localisation and signalling in FCs devoid of the function of key regulators of early endosomes, such as Avl and Rab5: in FC clones homozygous for the loss of function mutation *avl*$^{1}$ as well as *rab5*$^{2}$, N accumulates at the cell periphery, a phenotype reminiscent of that of homozygous *awd*$^{J2A4}$ FCs; moreover, in these *avl*$^{1}$ as well as *rab5*$^{2}$ mutant cells N fails to signal (Lu and Bilder, 2005). It was shown that Awd functionally interacts with Rab5 in FCs (Woolworth *et al.*, 2009), so no surprise that *awd* and *rab5* mutants phenocopy each other. On the other hand, it was shown that Awd also genetically interacts with Shi. It was demonstrated that the absence of Shi activity downregulates N signalling in FCs (Vaccari *et al.*, 2008). To gain insight into N subcellular distribution in FCs with no Shi activity I then took advantage of a temperature-sensitive allele of *shi*, *shi*$^{2}$ (hereafter referred as *shi*$^{ts}$). In egg chambers dissected from *shi*$^{ts}$ females kept at the restrictive temperature of 29°C, very large aggregates of N can be observed (Figure 35A-C) compared to control ovaries from *yw* females dissected and fixed under the same condition (Figure 35D-F). These aggregates are not restricted to the apical region of FCs but spread throughout the cell (Figure 35B). Such altered intracellular distribution is not caused by the culturing condition since in *yw* FCs N receptor signal is predominantly at the apical surface (Figure 35E).

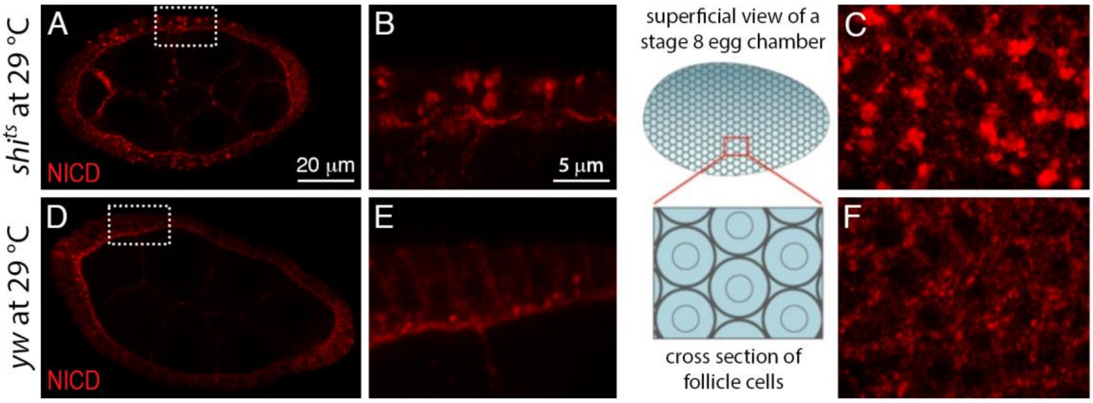
$shi^{ts}$ at 29 °C
yw at 29 °C
A
B
C
D
E
F
NICD
NICD
20 µm
5 µm
superficial view of a stage 8 egg chamber
cross section of follicle cells

**Figure 35 In absence of functional Shi activity, N accumulates in large vesicles in FCs. (A-C)** Confocal microscopy analysis of a stage 7 egg chamber dissected from *shi*$^{ts}$ female kept for 6 hours at 29 °C and stained with an anti-NICD antibody (red, all panels). The dotted box in A encloses the region magnified in B. Intense N signal is detected in FCs and large distinct puncta are visible both in cross (A,B) as well as superficial (C) sections. **(D-F)** Confocal microscopy analysis of a stage 8 egg chamber dissected from *yw* female kept for 6 hours at 29 °C and stained with an anti-NICD antibody (red, all panels). The dotted box in D encloses the region magnified in E. N-positive vesicles are detected in the apical region of FCs (D,E) and are definitively smaller than in *shi*$^{ts}$ FCs exposed at restrictive temperature (compare F with C). The scheme helps in the interpretation of images in C,F.

Trudi Schüpbach previously described this phenotype (Yan *et al.*, 2009) and she attributed the highly aberrant profile of N distribution observed in FCs devoid of *shi* function to the loss of receptor internalisation.

By comparing N localisation in homozygous *awd*$^{J2A4}$ and *shi*$^{ts}$ FCs, it appears that the pattern of the receptor distribution in the two mutant conditions significantly differs. Taken together these considerations, it could be stated that N receptor accumulates in intracellular vesicles in homozygous *awd*$^{J2A4}$ FCs and its pattern resembles that observed in *rab5*$^{2}$ or *avl*$^{1}$ mutant FCs but not that in *shi*$^{ts}$ FCs.

## 4.4 Analysis of N receptor localisation in *awd*$^{J2A4}$ mutant cells

The previously described results demonstrate that N signalling is defective in *awd*$^{J2A4}$ mutant FCs. In FCs devoid of *awd* gene function enhanced N staining is observed and overexpression of NICD fragment, but not of NEXT, rescues N activation. These results strongly suggest that the observed N signalling failure is imputable to a defect in N processing occurring along the endocytic route and linked to the inability of N receptor to entry in the appropriate endosomal compartment. I hypothesised that N is trapped in a subpopulation of vesicles in which, in wild type cells, the receptor transiently traffics in.

To gain further insights into N distribution in *awd*$^{J2A4}$ mutant FCs, I carried out a systematic analysis of N delivery to specific endosomal subpopulations, each of which is characterised by the presence of defined markers. Taking advantage of the freely available plugin CDA for the ImageJ software, the co-localisation extent of N receptor with each marker in several wild type as well as *awd*$^{J2A4}$ mutant FCs was evaluated. The CDA plugin returns the Pearson's coefficient, broadly used as a measure of the co-localisation grade between two signals. Pearson's coefficient ranges from +1 (complete correlation) to −1 (anti-correlation), with 0 meaning no correlation. Statistical comparison of mean Pearson's coefficient in wild type and *awd*$^{J2A4}$ mutant FCs using the two-tailed paired *t*-test was performed with GraphPad Prism 6 software. This analysis allowed me to evaluate N distribution in FCs and to determine in which endosomal compartment N is stalled in *awd*$^{J2A4}$ mutant FCs.

### 4.4.1 N receptor accumulates in immature early endosomes in *awd*$^{J2A4}$ mutant FCs

Since N processing in FCs has been shown to take place during transition from mature early endosomes to late endosomes (Vaccari *et al.*, 2008; Wilkin *et al.*, 2008), I first sought for *awd* defect in the steps before formation of late endosomes. N intracellular distribution was then evaluated respect to Avl in stage 6-8 egg chambers. The syntaxin Avl localises to early endosomes and is required for the transit of N from the plasma membrane into the early endosomes (Lu and Bilder, 2005). N accumulates in *avl* loss of function mutants and is unable to signal.

In wild type FCs (Figure 36A), Avl (Figure 36B) and N (Figure 36C) partly co-localise (Figure 36D), as previous reported. Surprisingly, in *awd*$^{J2A4}$ mutant FCs (Figure 36E), Avl-positive vesicles accumulate (Figure 36F) and N immunodetection (Figure 36G) reveals a strong overlap between the two signals (Figure 36H). To appropriately evaluate N and Avl co-localisation in *awd*$^{J2A4}$ mutant and flanking FCs, unbiased analysis was conducted using ImageJ software (Figure 36I). Statistical analysis of mean Pearson's coefficients reveals that N localisation in Avl-positive vesicles doubles in *awd*$^{J2A4}$ mutant FCs (Figure 36J). These results indicate that in *awd*$^{J2A4}$ mutant FCs most of N receptor accumulates in Avl-positive early endosomes.

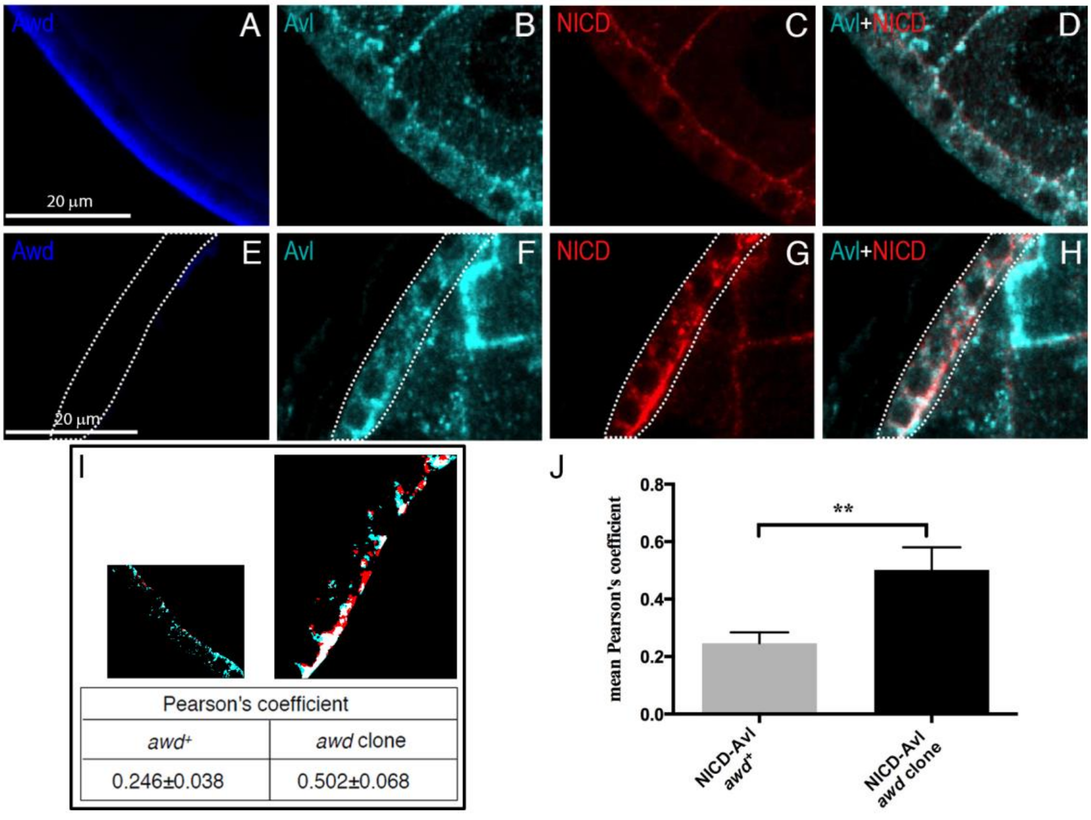

| Pearson's coefficient | |
|---|---|
| *awd*$^{+}$ | *awd* clone |
| 0.246±0.038 | 0.502±0.068 |

**Figure 36 Co-localisation analysis between N and Avl in FCs. (A-D)** Sagittal magnification of a stage 8 egg chamber dissected from a *yw* female (control). Images were taken by confocal microscopy. Awd (blue, A) is localised at the basal side of the egg chamber, as previously reported. Avl signal (cyan, B,D) partly co-localises with NICD-positive vesicles (red, C,D). **(E-H)** Sagittal magnification centred on an *awd*$^{J2A4}$ mutant clone. Images were taken by confocal microscopy. Awd staining (blue, E) is absent. Avl signal (cyan, F,H) strongly co-localises with NICD-positive vesicles (red, G,H) in mutant FCs. **(I)** Before using the CDA plugin, confocal snapshots have been treated with Adobe Photoshop to adjust thresholds. In I is reported the result of such procedure in wild type (*awd*$^{+}$) and *awd* mutant (*awd* clone) FCs for the NICD and Avl signals showed in D and H. Co-localisation of NICD and Avl was then evaluated in 4 *awd*$^{J2A4}$ mutant clones and wild type FCs. The resulting mean Pearson's coefficients are reported in the table. **(J)** Statistical analysis using the two-tailed paired *t*-test of mean Pearson's coefficients tabled in I. **, $p<0.01$.

Several proteins are known being recruited at the membrane of early endosomes while they become mature along the endocytic route. Among these proteins are Avl, Rab5 and Hrs. Avl co-localises with Rab5 to high extent (Lu and Bilder, 2005) in early endosomes

(Morrison *et al.*, 2008). In *hrs* mutants, cargoes accumulate in Rab5-positive endosomes (Jekely and Rorth, 2003) because they cannot proceed along the endocytic pathway. Rab5 itself shows co-localisation with Hrs, while Avl and Hrs have a lower co-localisation grade (Vaccari *et al.*, 2008). The MVB sorting protein Hrs preludes to the so-called MVB pathway (Komada and Kitamura, 2005).

In order to determine whether the Avl-positive endosomes in which N is trapped are immature early endosomes, I examined N distribution in relation to Hrs in *awd*$^{J2A4}$ mutant FCs. I found that in *awd* MARCM clones NICD and Hrs co-localisation is similar to that observed in wild type FCs, as revealed by mean Pearson's coefficient (Figure 37A). Both in *awd*$^{J2A4}$ mutant and flanking FCs low levels of N are found in mature early endosomes/MVBs and no statistically significant difference exists between them (Figure 37B).

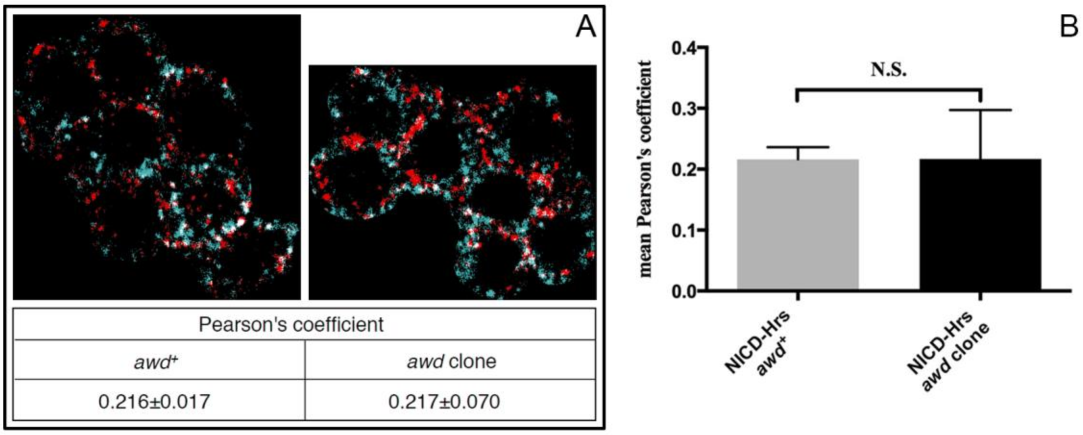

| Pearson's coefficient | |
|---|---|
| *awd*$^{+}$ | *awd* clone |
| 0.216±0.017 | 0.217±0.070 |

**Figure 37 Co-localisation analysis between N and Hrs in FCs. (A)** *yw, hs-flp/Gbe+Su(H)*$_{m8}$*lacZ; act-Gal4, UAS-GFP/+; FRT*$^{82B}$*, awd*$^{J2A4}$*/FRT*$^{82B}$*, act-Gal80* females were treated as previously described to induce MARCM clones and then dissected to collect their ovaries. Egg chambers were then subjected to an immunohistochemistry assay using an anti-NICD (red) and anti-Hrs (cyan) antibodies. Stage 7-8 egg chambers were then considered during confocal microscopy analysis sessions. Images in A are the result of Adobe Photoshop treatments to adjust thresholds before using the CDA plugin and have been generated from superficial magnification of *awd*$^{J2A4}$*/awd*$^{+}$ and homozygous *awd*$^{J2A4}$ FCs. Co-localisation of NICD and Hrs was then evaluated in 4 *awd*$^{J2A4}$ mutant clones and flanking FCs. The resulting mean Pearson's coefficients are reported in the table. **(B)** Statistical analysis using the two-tailed paired *t*-test of mean Pearson's coefficients tabled in A. N.S., not significant.

In *hrs* mutant FCs N signalling is not affected, suggesting that its function is dispensable for N activity (Vaccari *et al.*, 2008). However, even if at low grade, N receptor is found in Hrs-positive endosomes (Figure 37A, left panel). Moreover, the level of co-localisation of N and Hrs is very similar both in wild type and in *awd*$^{J2A4}$ mutant FCs (Figure 37A, table). In light of these considerations it could be speculated that this low level of N-Hrs co-localisation is due to the minor Rab5-independent routes which have been shown to exist for N trafficking (Vaccari *et al.*, 2008). Taken together, the presented results suggest that *awd* function is required for early endosome maturation since N receptor is trapped in Avl-positive endosomes.

### 4.4.2 N receptor does not accumulate in Rab7-positive late endosomes in *awd*$^{J2A4}$ mutant FCs

I then analysed in stage 6-8 egg chambers N distribution toward late endosomes by using anti-NICD and anti-Rab7 (Tanaka and Nakamura, 2008) antibodies. Rab7 belongs to the Rab family and it is well established that its function is critical for trafficking to late endosomes. Given that, Rab7 is broadly used as a marker of late endosomes. N entry into late endosomes preludes to its degradation and thus to modulation of the signal. Through my analysis I found that in *awd*$^{J2A4}$ mutant FCs expressing the GFP marker (Figure 38A) Rab7-positive vesicles are present (Figure 38B) and few N signal (Figure 38C) overlaps Rab7 (Figure 38D). To evaluate the co-localisation between N and Rab7, 6 clones were analysed through ImageJ software (Figure 38E) and the statistical analysis result is graphed in Figure 38F: no difference in the overlapping of the two signals exists between mutant and flanking FCs, as estimated by mean Pearson's coefficients.

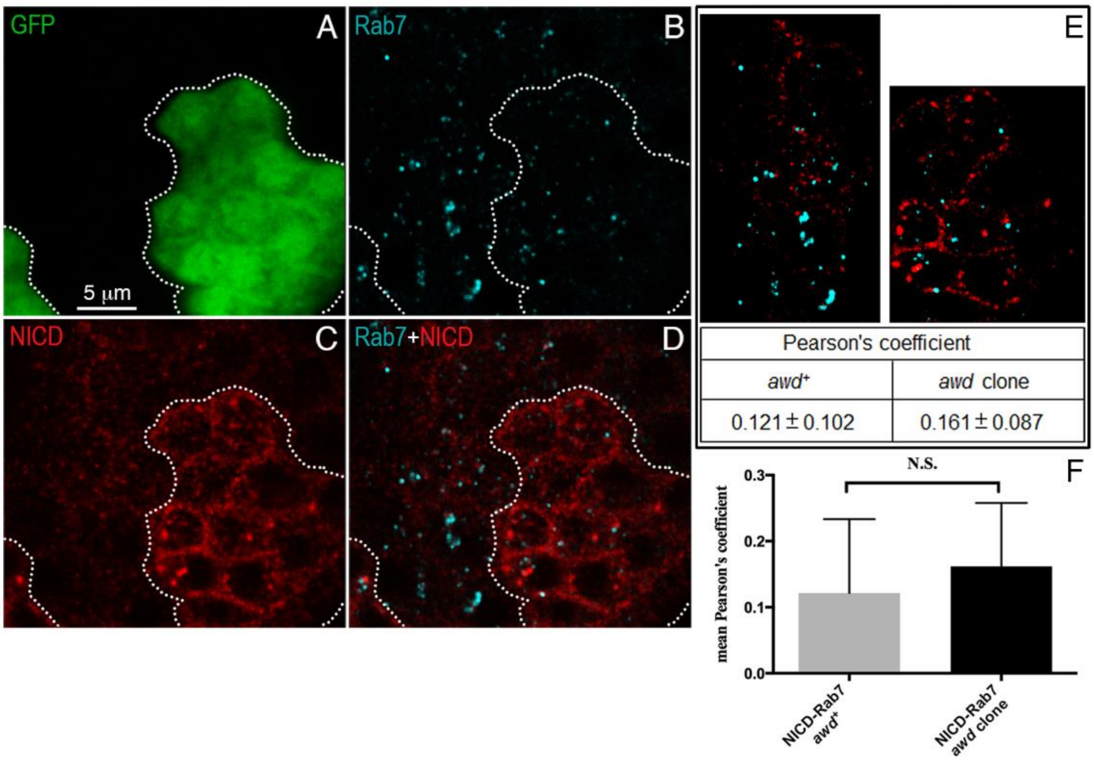

**Figure 38 Co-localisation analysis between N and Rab7 in FCs. (A-D)** Superficial magnification of a stage 7-8 egg chamber dissected from *yw, hs-flp/Gbe+Su(H)*$_{m8}$*lacZ; act-Gal4, UAS-GFP/+; FRT*$^{82B}$*, awd*$^{J2A4}$*/FRT*$^{82B}$*, act-Gal80* female. Images were taken by confocal microscopy. Fluorescent signal of GFP (green, A) identifies the *awd*$^{J2A4}$ MARCM clone, also highlighted by the dotted lines reported in each panel. Rab7 signal (cyan, B,D) partly co-localises with NICD-positive vesicles (red, C,D) both in wild type and mutant FCs. **(E)** Before using the CDA plugin, confocal snapshots have been treated with Adobe Photoshop to adjust thresholds. In E is reported the result of such procedure in wild type (*awd*$^{+}$) and *awd* mutant (*awd* clone) FCs for the NICD and Rab7 signals showed in D. Co-localisation of NICD and Rab7 was then evaluated in 6 *awd*$^{J2A4}$ mutant clones and flanking FCs. The resulting mean Pearson's coefficients are reported in the table. **(F)** Statistical analysis using the two-tailed paired *t*-test of mean Pearson's coefficients tabled in E. N.S., not significant.

The lack of significant co-localisation of N with Rab7 in *awd*$^{J2A4}$ mutant FCs is consistent with the notion that impeding N entry into late endosomes and MVBs causes ectopic activation of N signal, a phenotype opposite to that observed in homozygous *awd*$^{J2A4}$ cells.

### 4.4.3 Acidification of endosomal compartments is not affected in *awd*$^{J2A4}$ mutant FCs

It is well established that vesicle progression along the endocytic route is accompanied by lumen acidification mediated by V-ATPase activity. Two independent studies showed that perturbation of V-ATPase activity in FCs causes loss of acidified endosomal compartments, as deducted by the absence of Lysotracker-positive puncta. Moreover, impaired N signalling with accumulation of the receptor in endosomal vesicles is observed. It was also demonstrated that V-ATPase activity is required for N activation prior to the γ-secretase-mediated cleavage (Vaccari *et al.*, 2010; Yan *et al.*, 2009). Given these considerations, I also sought to determine if acidification of endosomal compartments occurs in FCs devoid of *awd* gene function. I then performed an *ex-vivo* staining with the Lysotracker dye. In homozygous *awd*$^{J2A4}$ FCs (GFP$^+$ cells in Figure 39A), Lysotracker puncta are present (Figure 39B) and are of comparable size and number to those found in flanking cells (Figure 39C).

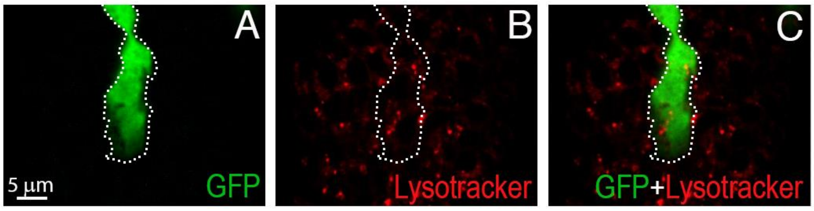

**Figure 39 Lysotracker staining pattern suggests that *awd* loss of function does not impair lumenal acidification of endosomes. (A-C)** Superficial magnification of a stage 7 egg chamber dissected from *yw, hs-flp/Gbe+Su(H)*$_{m8}$*lacZ; act-Gal4, UAS-GFP/+; FRT*$^{82B}$*, awd*$^{J2A4}$*/FRT*$^{82B}$*, act-Gal80* female. Images were taken by confocal microscopy. Fluorescent signal of GFP (green, A,C) identifies the *awd*$^{J2A4}$ MARCM clone, also highlighted by the dotted lines reported in each panel. Lysotracker signal (red, B,C) is similar in wild type and mutant FCs.

### 4.4.4 N receptor does not accumulate in Rab11-positive recycling endosomes in *awd*$^{J2A4}$ mutant FCs

I also analysed in stage 6-8 egg chambers N distribution in recycling endosomes by using anti-NICD and anti-Rab11 (Tanaka and Nakamura, 2008) antibodies. Rab11 is another member of the Rab family and it is broadly used as a marker of recycling endosomes (Dollar *et al.*, 2002). As their name suggests, recycling endosomes bring back to plasma membrane components which have been formerly endocyted in Rab5 endosomes. It has been recently shown that in *Drosophila* epithelial cells, excess of recycling through Rab11 activity upregulates N signalling (Johnson *et al.*, 2016). Since in *awd*$^{J2A4}$ mutant FCs N is blocked into immature early endosomes, it could be hypothesised that the lack of recycle of the receptor at the plasma membrane could account for the failure in N activity.

Through my analysis I found that in *awd*$^{J2A4}$ mutant FCs (GFP$^{+}$ cells in Figure 40A) Rab11-positive vesicles are present (Figure 40B) and very few N signal (Figure 40C) overlaps Rab11 (Figure 40D). To evaluate the co-localisation between N and Rab11, 4 clones were analysed through ImageJ software (Figure 40E) and the statistical result is graphed in Figure 40F: no difference in the overlapping of the two signals exists between mutant and flanking wild type FCs, as estimated by mean Pearson's coefficients.

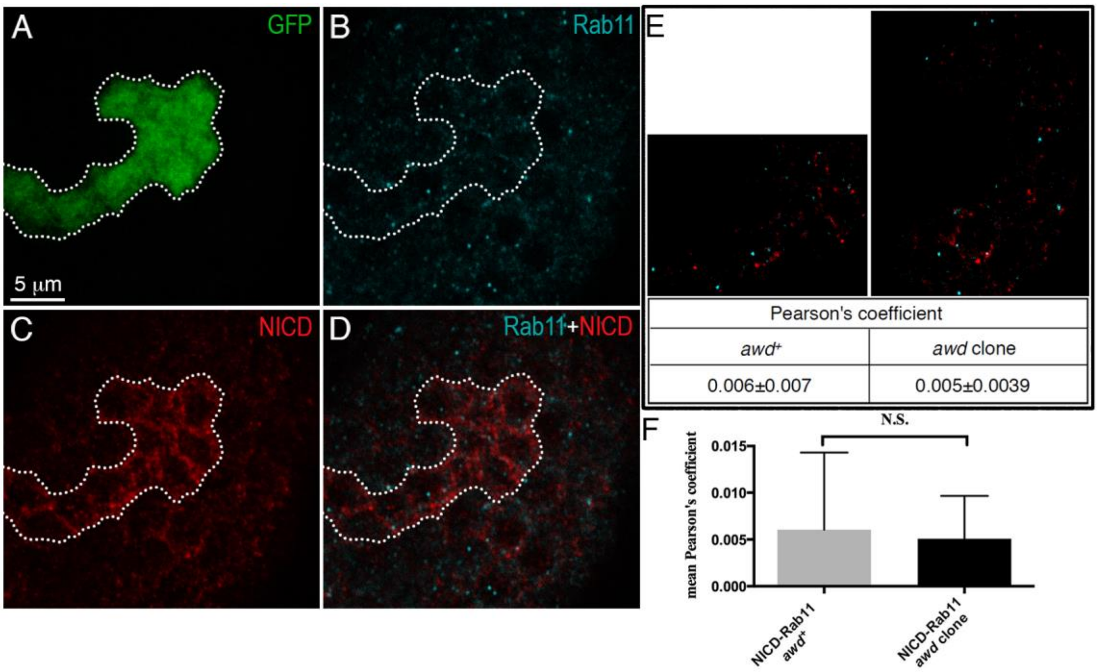

| Pearson's coefficient | |
|---|---|
| *awd*$^{+}$ | *awd* clone |
| 0.006±0.007 | 0.005±0.0039 |

**Figure 40 Co-localisation analysis between N and Rab11 in FCs. (A-D)** Superficial magnification of a stage 7-8 egg chamber dissected from *yw, hs-flp/Gbe+Su(H)*$_{m8}$*lacZ; act-Gal4, UAS-GFP/+; FRT*$^{82B}$*, awd*$^{J2A4}$*/FRT*$^{82B}$*, act-Gal80* female. Images were taken by confocal microscopy. Fluorescent signal of GFP (green, A) identifies the *awd*$^{J2A4}$ MARCM clone, also highlighted by the dotted lines reported in each panel. Rab11 signals (cyan, B,D) co-localise to a very low extent with NICD-positive vesicles (red, C,D) both in wild type and mutant FCs. **(E)** Before using the CDA plugin, confocal snapshots have been treated with Adobe Photoshop to adjust thresholds. In E is reported the result of such procedure in wild type (*awd*$^{+}$) and *awd* mutant (*awd* clone) FCs for the NICD and Rab11 signals showed in D. Co-localisation of NICD and Rab11 was then evaluated in 4 *awd*$^{J2A4}$ mutant clones and flanking FCs. The resulting mean Pearson's coefficients are reported in the table. **(F)** Statistical analysis using the two-tailed paired *t*-test of mean Pearson's coefficients tabled in E. N.S., not significant.

## 4.5 Genetic analysis of Awd and Rab5 interaction in N signalling activation

N aggregates in *awd*$^{J2A4}$ mutant FCs are Avl-positive early endosomes. A previous work from Tien Hsu lab showed that, in the follicular epithelium, Awd endocytic function is required to maintain appropriate levels of junction components at the plasma membrane of FCs. Authors showed that the most severe phenotypes caused by *awd* loss of function, such as stacking of FCs, can be rescued by the overexpression of a constitutively active form of the

GTPase Rab5 mediated by a *UAS-YFP::Rab5*$^{Q88L}$ transgene (Woolworth *et al.*, 2009). In the *UAS-YFP::Rab5*$^{Q88L}$ transgene (Zhang *et al.*, 2007), the cDNA encoding the Rab5 protein carries a mutation that causes the Q88L amino acid substitution in the translated protein: the glutamine in position 88 is replaced with a leucine. This substitution makes the Rab5 protein unable to hydrolyse GTP. In addition, Woolworth and colleagues also showed that in FC clones lacking *awd* function Rab5 is down-regulated.

Moreover, Vaccari and colleagues showed that N signalling is increased through overexpression of the Rab5$^{Q88L}$ mutant form. This was supposed to be due to a stimulation of endocytic vesicles to fuse with early endosomes, where N activation is presumed to occur (Vaccari *et al.*, 2008).

To further investigate *awd* endocytic function in the correct activation of N signalling pathway I took advantage of Rab5$^{Q88L}$ with the aim to determine if the overexpression of a constitutively active form of the GTPase Rab5 could rescue the N signalling defect recovered in *awd*$^{J2A4}$ mutant FCs.

### 4.5.1 N receptor accumulates in enlarged Rab5$^{CA}$-positive vesicles in *awd*$^{J2A4}$ mutant FCs

By applying an immunohistochemistry approach, I found that in mutant *awd*$^{J2A4}$ FCs (Figure 41A,A',E), overexpressing YFP::Rab5$^{CA}$ (Figure 41B,B'F), N receptor is highly condensed (Figure 41C,C',G) in enlarged puncta at the apical region of FCs (Figure 41D,D',H). The enlargement of the Rab5$^{CA}$-positive vesicles was previously observed by Zhang and co-workers when they tested their constructs; the most likely explanation for such phenomenon is that Rab5$^{CA}$ pushes endocytosis through early endosomes, thus causing more endocytic vesicles to fuse with them, generating enlarged early endosomes. It is worth noting that most, if not all, the N receptor is found in the lumen of the Rab5$^{CA}$-positive vesicles. The lumenal concentration of the receptor suggests that this N receptor population is unprocessed and destined to MVBs and late endosomes for degradation.

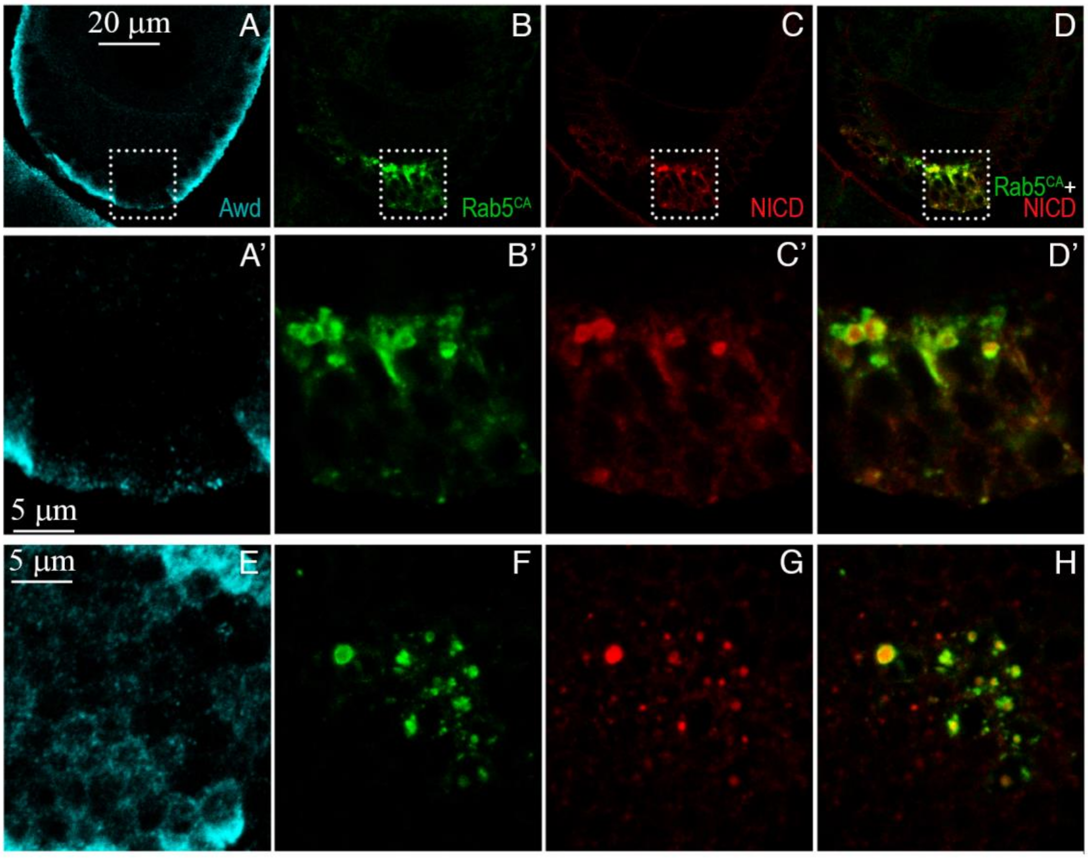

**Figure 41 Overexpression of Rab5$^{CA}$ in homozygous *awd*$^{J2A4}$ MARCM FC clones alters N receptor localisation.** Stage 8 egg chambers dissected from *yw, hs-flp/Gbe+Su(H)*$_{m8}$*lacZ; UAS-YFP:Rab5*$^{Q88L}$*/+; FRT*$^{82B}$*, awd*$^{J2A4}$*/tub-Gal4, FRT*$^{82B}$*, tub-Gal80* females. Images were taken by confocal microscopy. **(A-D)** Cross section in which the absence of Awd staining (cyan A) identifies FCs homozygous for the *awd*$^{J2A4}$ null allele. These cells also overexpress the YFP::Rab5$^{CA}$ protein (green, B). In C is the immunodetection with the anti-NICD antibody (red). In D is the merge between the NICD and Rab5$^{CA}$ signals. **(A'-D')** Magnification of the areas included in the dotted boxes in A-D. N receptor appears highly accumulated in the lumen of enlarged Rab5$^{CA}$-positive vesicles. **(E-F)** Superficial magnification of a stage 8 egg chamber in which a lot of enlarged Rab5$^{CA}$-positive vesicles is visible. In their lumen, accumulated N is strongly condensed.

### 4.5.2 Overexpression of Rab5$^{CA}$ in *awd*$^{J2A4}$ mutant FCs recruits Hrs to the membrane of N-containing vesicles

The high degree of N and Rab5$^{CA}$-positive vesicle co-localisation coupled with the peculiar N lumenal distribution prompted me to further investigate the ability of Rab5$^{CA}$ to stimulate endocytosis in *awd*$^{J2A4}$ mutant FCs. I then analysed the pattern of Hrs in *awd*$^{J2A4}$ MARCM clones overexpressing the constitutively active Rab5. I determined that in *awd*$^{J2A4}$ mutant FCs overexpressing YFP::Rab5$^{CA}$ (Figure 42A), 87.1% of N puncta (Figure 42B) co-localise with Rab5$^{CA}$ (Figure 42C) and 31.45% co-localise with Hrs (Figure 42D, *n=124*). To unbiasedly evaluate these co-localisations, 6 clones were analysed through ImageJ software to recover mean Pearson's coefficients (Figure 42E). Unpaired *t*-test statistical analysis through GraphPad Prism software revealed a significant enhancement ($p$=0.0041) of N and Hrs co-localisation with Rab5$^{CA}$ overexpression, as assessed by mean Pearson's coefficients (Figure 42F).

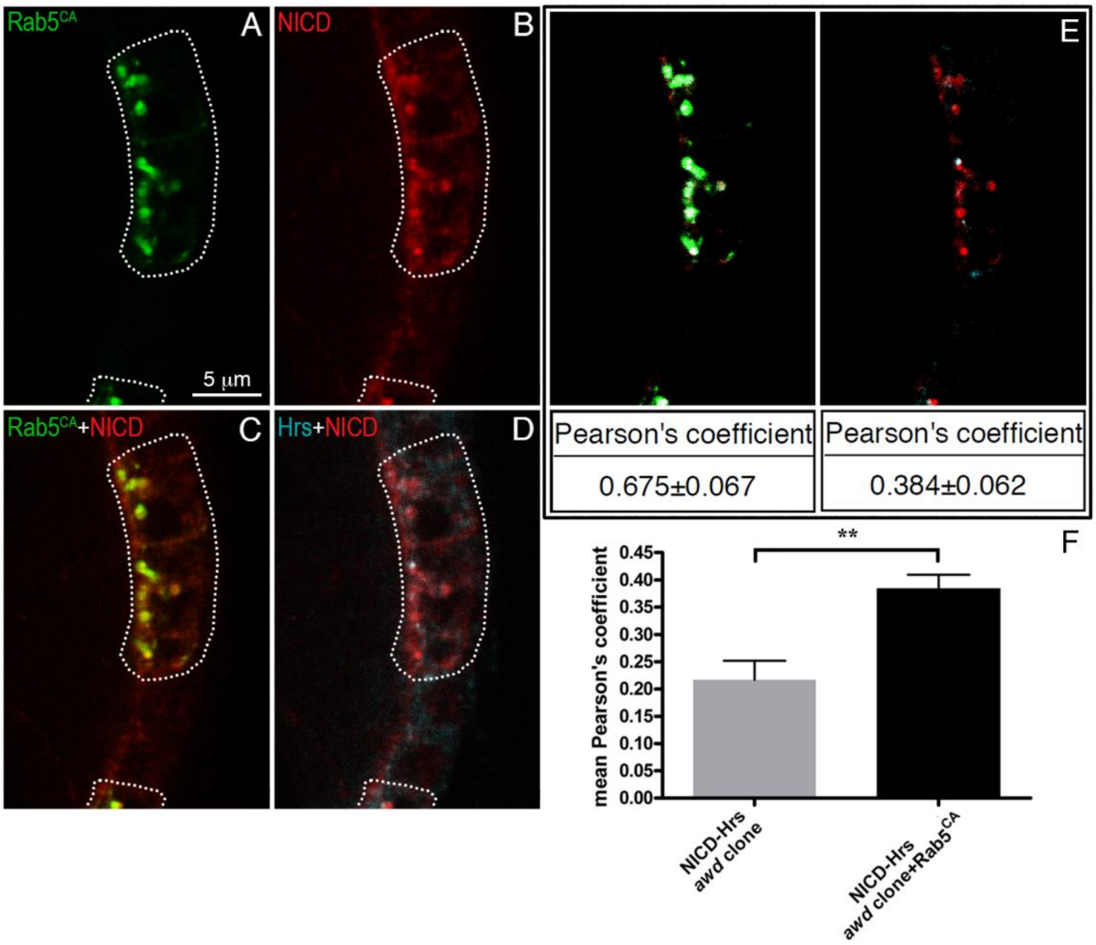

**Figure 42 Co-localisation analysis among N, Rab5$^{CA}$ and Hrs in *awd*$^{J2A4}$ FCs. (A-D)** Cross section magnification of a stage 8 egg chamber dissected from from *yw, hs-flp/Gbe+Su(H)$_{m8}$lacZ; UAS-YFP:Rab5$^{Q88L}$/+; FRT$^{82B}$, awd$^{J2A4}$/tub-Gal4, FRT$^{82B}$, tub-Gal80* female. Images were taken by confocal microscopy. Fluorescent signal of YFP::Rab5$^{CA}$ (green, A) identifies *awd*$^{J2A4}$ mutant FCs overexpressing the fusion protein. The MARCM clone is also highlighted by the dotted lines reported in each panel. NICD staining (red, B,C,D) shows that N co-localises to high extent with Rab5$^{CA}$-positive vesicles (C). Moreover, N also co-localises with Hrs (cyan, D). **(E)** Before using the CDA plugin, confocal snapshots have been treated with Adobe Photoshop to adjust thresholds. In E is reported the result of such procedure for snapshots showed in C (left panel) and D (right panel). Co-localisations of NICD with Rab5$^{CA}$ and of NICD with Hrs were then evaluated in 6 *awd*$^{J2A4}$ mutant clones overexpressing YFP::Rab5$^{CA}$. The resulting mean Pearson's coefficients are reported in the tables below each panel. **(F)** Statistical analysis using the two-tailed unpaired *t*-test of mean Pearson's coefficients tabled in E, right panel, and in Figure 37A, right panel. **, $p<0.01$.

These findings suggest that the constitutively active form of Rab5 is able to stimulate vesicle progression along the endocytic route; however *awd* function is necessary for Rab5-mediated early endosome maturation. This notion implies that the block in vesicle trafficking observed in *awd* loss of function cells is at the level or downstream of Rab5.

### 4.5.3 Overexpression of Rab5$^{CA}$ does not restore N signalling in *awd*$^{J2A4}$ mutant FCs

In order to determine whether the overexpression of Rab5$^{CA}$ is able to rescue N signalling defect in *awd*$^{J2A4}$ mutant FCs, I analysed the expression of the *Gbe* reporter gene. Immunodetection with the anti-β-galactosidase antibody reveals that FC MARCM clones lacking Awd protein (Figure 43A,A') and expressing YFP::Rab5$^{CA}$ (Figure 43B,B') display no *Gbe* expression, as shown by the absence of the β-galactosidase (Figure 43C,C',D,D'). This result suggests that the signalling mediated by the N receptor is still inhibited.

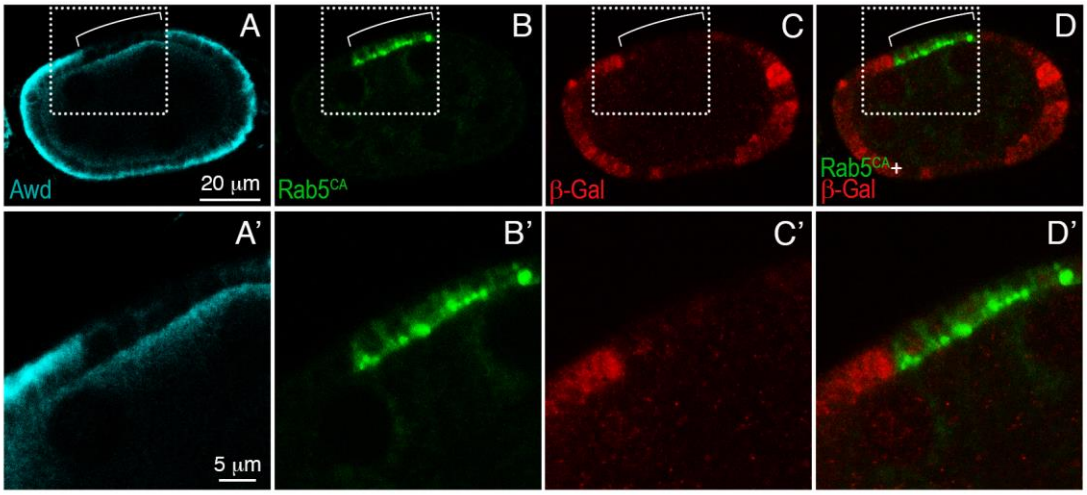

**Figure 43 Overexpression of Rab5$^{CA}$ in homozygous *awd$^{J2A4}$* MARCM FC clones does not restore *Gbe+Su(H)$_{m8}$lacZ* expression.** Stage 7 egg chamber dissected from *yw, hs-flp/Gbe+Su(H)$_{m8}$lacZ; UAS-YFP:Rab5$^{Q88L}$/+; FRT$^{82B}$, awd$^{J2A4}$/tub-Gal4, FRT$^{82B}$, tub-Gal80* female. Images were taken by confocal microscopy. **(A-D)** Cross section in which the absence of Awd staining (cyan A) identifies FCs homozygous for the *awd$^{J2A4}$* null allele. These cells also overexpress the YFP::Rab5$^{CA}$ protein (green, B). In C is the immunodetection with the anti-β-galactosidase antibody (red). In D is the merge between the β-galactosidase and Rab5$^{CA}$ signals. The brackets in A-D enclose the MARCM clone. **(A'-D')** Magnification of the areas included in the dotted boxes in A-D.

To further assess the N failure in *awd* loss of function FCs despite Rab5$^{CA}$ overexpression, I analysed Hnt expression and I found that in FC MARCM clones lacking Awd protein (Figure 44A,A') and expressing YFP::Rab5$^{CA}$ (Figure 44B,B') Hnt expression is still absent (Figure 44C,C'D,D'). FCs flanking the clone, instead, show high levels of Hnt protein.

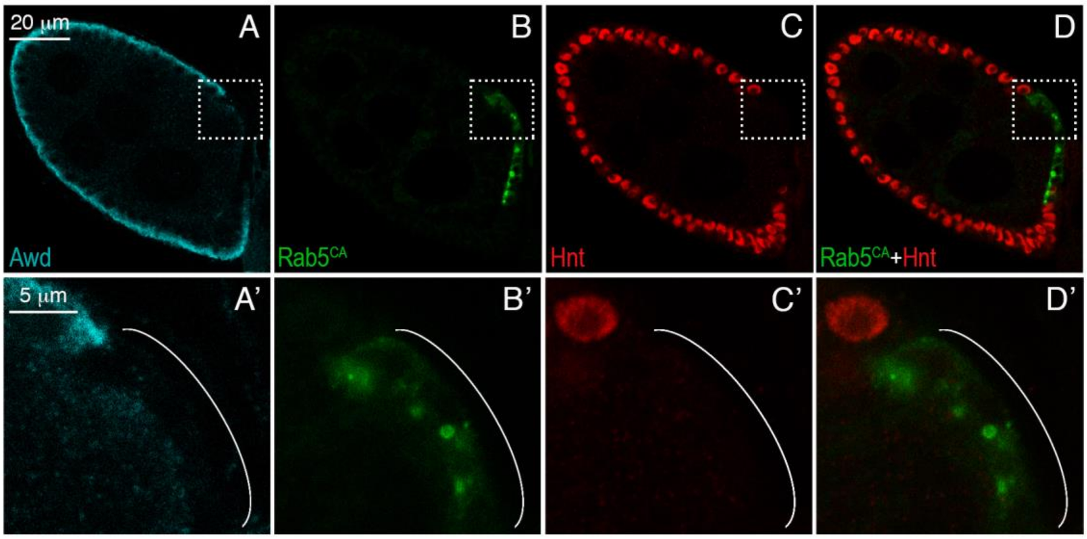

**Figure 44 Overexpression of Rab5$^{CA}$ in homozygous *awd$^{J2A4}$* MARCM FC clones does not restore Hnt expression.** Stage 7-8 egg chamber dissected from *yw, hs-flp/Gbe+Su(H)$_{m8}$lacZ; UAS-YFP:Rab5$^{Q88L}$/+; FRT$^{82B}$, awd$^{J2A4}$/tub-Gal4, FRT$^{82B}$, tub-Gal80* female. Images were taken by confocal microscopy. **(A-D)** Cross section in which the absence of Awd staining (cyan A) identifies FCs homozygous for the *awd$^{J2A4}$* null allele. These cells also overexpress the YFP::Rab5$^{CA}$ protein (green, B). In C is the immunodetection with the anti-Hnt antibody (red). In D is the merge between the Hnt and Rab5$^{CA}$ signals. **(A'-D')** Magnification of the areas included in the dotted boxes in A-D. The brackets in A'-D' enclose the MARCM clone.

Altogether, these results indicate that *awd* function is downstream of or is required for Rab5 function in promoting maturation of early endosomes and activation of N signalling.

All the results I described in paragraphs 4.1-4.5.3 have been published in BMC Biology (Ignesti *et al.*, 2014).

## 4.6 Genetic analysis of Awd and Shi interaction in N signalling activation

Involvement of the Dynamin Shi in correct N signalling activation has been long investigated by several authors in a multitude of *Drosophila* tissues. Plenty of works indeed demonstrated the requirement of Shi function for N endocytosis and signalling, also in the follicular epithelium (Vaccari *et al.*, 2008; Yan *et al.*, 2013).

A stringent relationship between Awd and Shi has been uncovered at the beginning of this millennium (Krishnan *et al.*, 2001) but since then, at least in *Drosophila*, the biochemical function performed by Awd and necessary for Shi activity has been only speculated, with most authors supposing a role for Awd as GEF-like for Shi. Despite this, the genetic interaction between these two proteins is fascinating. I then wondered if the N signalling arrest in FCs devoid of Shi activity, observed by previous authors, could be reverted by overexpression of Awd. Beside representing a classical epistasis test, this analysis also contributes to the understanding of the role of endocytosis in N pathway and, in particular, of the role of the NDPK Awd in N signal transduction.

### 4.6.1 Overexpression of a dominant negative form of Shi arrests N signalling

In order to gain insights into *shi* function in N signalling I took advantage of a *Drosophila* stock bearing a *UAS-shi*$^{K44A}$ transgene (Moline *et al.*, 1999). In this transgene, the cDNA of *shi* carries a mutation causing the amino acid substitution K44A: in the GTP-binding domain, the lysine in position 44 is substituted with an alanine. This mutant form of Shi fails to bind GTP, thus acting as a dominant negative.

By employing the Flp-out/Gal4 technique (Pignoni and Zipursky, 1997, see paragraph 3.2.3), I generated Flp-out FC clones in which the overexpression of Shi$^{DN}$ and of a GFP with a nuclear localisation signal (enabling the identification of clonal cells) was induced. Immunodetection with anti-NICD antibody confirms previously reported observations (Lu and Bilder, 2005; Vaccari *et al.*, 2008; Yan *et al.*, 2009): in Flp-out FC clones devoid of Shi activity and expressing the GFP protein (Figure 45A), the N receptor accumulates at the plasma membrane (Figure 45B,C). These N-positive aggregates are very similar to those found in *chc* (*clathrin heavy chain* gene) loss of function FCs (Yan *et al.*, 2009). Indeed, N endocytosis in FCs is both Dynamin- and clathrin-dependent (Le Borgne *et al.*, 2005).

Further, in FCs devoid of Shi activity (Figure 45E) N signalling is inhibited, as assessed by loss of Hnt staining (Figure 45F,G). The piling up of FCs overexpressing the Shi$^{DN}$ protein (Figure 45D,F) has also been previously noticed.

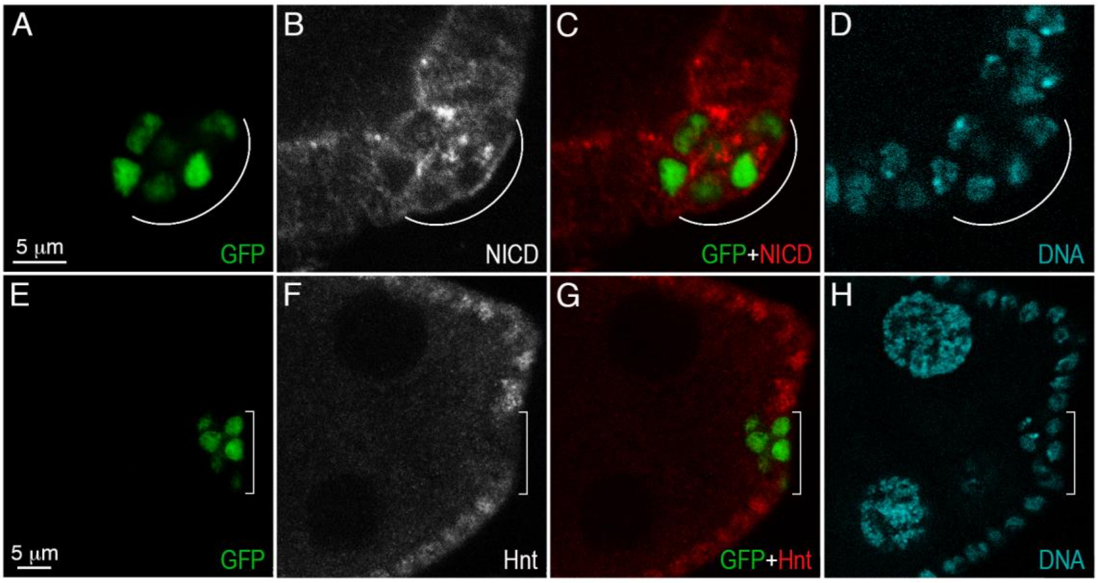

**Figure 45 Overexpression of Shi$^{DN}$ in Flp-out FC clones impairs N receptor localisation and signalling.** Ovaries were dissected from *yw, hs-flp/act>CD2>Gal4; UAS-nlsGFP/+; TM3, UAS-shi*$^{K44A}$/+ females. Images were taken by confocal microscopy. **(A-D)** Cross section magnification of a stage 7-8 egg chamber in which the nuclear GFP protein (green, A,C) marks FCs overexpressing the mutant form of Shi. The Flp-out clone is also highlighted by the brackets reported in each panel. NICD staining (grey in B, red in C) is visible. To-Pro-3 dye (cyan, D) stains cell nuclei. **(E-H)** Cross section magnification of a stage 8 egg chamber in which the nuclear GFP protein (green, E,G) marks FCs overexpressing the mutant form of Shi. The Flp-out clone is also highlighted by the brackets reported in each panel. Hnt staining (grey in F, red in G) is visible. To-Pro-3 dye (cyan, F) stains cell nuclei.

In the so-induced Flp-out clones the Gal4 protein drives the expression of two different *UAS* transgenes. Potentially, this could alleviate the phenotype induced by the loss of Shi activity because of a titration of the Gal4. Thus, this analysis, despite didn't produce any new finding, was important because it allowed me to be confident on the ability of the *UAS-Shi*$^{K44A}$ construct to block N signalling, even in the presence of a second transgene.

### 4.6.2 Overexpression of an enhanced GFP-tagged form of Awd does not perturb N signalling

In the lab, it was designed a transgene in which the enhanced GFP (eGFP) coding sequence is fused to cDNA of *awd* (see paragraph 3.1.2).

I then took advantage of this *Drosophila* stock to generate Flp-out FC clones in which the overexpression of Awd::eGFP was induced. A *UAS-nlsLacZ* transgene (encoding a β-galactosidase with a nuclear localisation signal) was also co-expressed with the *UAS-awd::eGFP* transgene so that two *UAS* constructs are present as was the case for the females analysed in previous paragraph. This allowed me to compare the results I obtained with *UAS-awd::eGFP* overexpression with those obtained with *UAS-shi*$^{K44A}$ overexpression.

First I looked at N distribution and I found that in FCs of stage 7-8 egg chambers (Figure 46A) overexpressing the Awd::eGFP protein (Figure 46B), the N receptor is present in distinct puncta (Figure 46C) whose pattern and dimensions are indistinguishable from that in flanking cells (Figure 46D). The, I assessed the activation of N signalling and I found that, in stage 6-8 egg chambers (Figure 46E) overexpression of the Awd::eGFP protein (Figure 46F) does not perturb N signalling, as assessed by the presence of Hnt signal (Figure 46G) in FC nuclei. The expression level of Hnt in Flp-out FC clones appears comparable to that observed in flanking cells (Figure 46H).

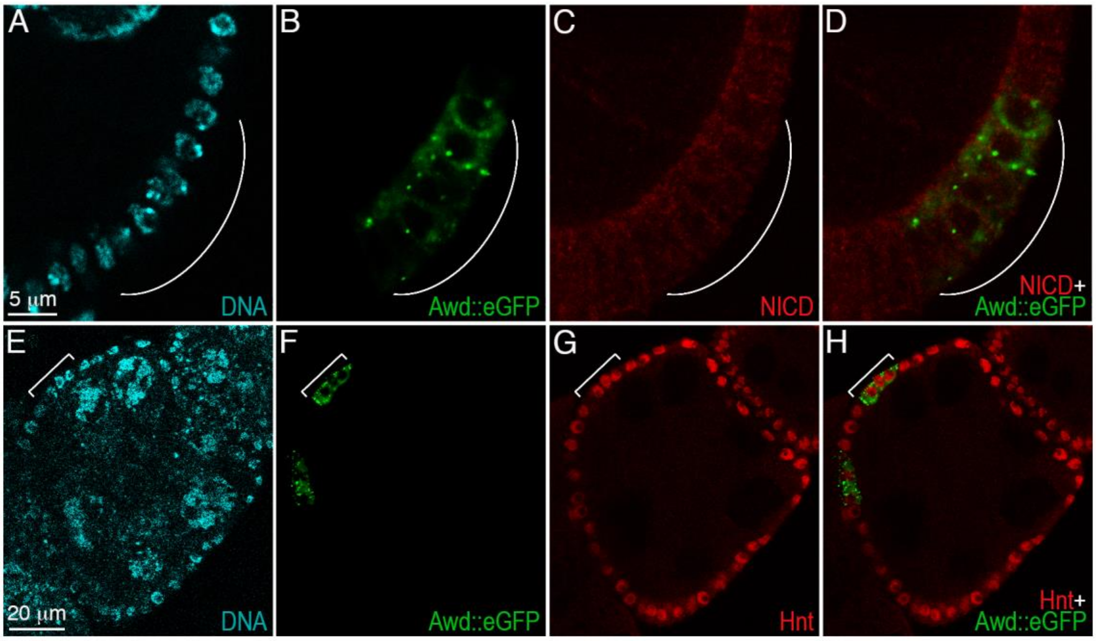

**Figure 46 Overexpression of Awd::eGFP in Flp-out FC clones does not impair N receptor localisation and signalling.** Ovaries were dissected from *yw, hs-flp/act>CD2>Gal4; UAS-awd::eGFP/UAS-nlsLacZ* females. Images were taken by confocal microscopy. **(A-D)** Cross section magnification of a stage 8 egg chamber stained with To-Pro-3 dye (cyan, A) to reveal cell nuclei. The green fluorescent signal of Awd::eGFP protein (green in B,D) individuates small intracellular puncta. The NICD signal is also visible (red, C,D). The brackets in A-D embrace the Flp-out clone in which the expression of Awd::eGFP was induced. **(E-H)** Cross section of a stage 7 egg chamber stained with To-Pro-3 dye (cyan, E) to reveal cell nuclei. The green fluorescent signal of Awd::eGFP protein (green in F,G) and the Hnt signal (red, G,H) are visible. The brackets in E-H embrace the Flp-out clone in which the expression of Awd::eGFP was induced.

Since *awd* gene loss of function arrests N signalling, I wondered if the overexpression of Awd protein could lead to precocious activation of the pathway. I then focused my attention on early oogenesis egg chambers and I used Hnt as a readout of signal activation. In stage 5 egg chambers (Figure 47A,A') FCs overexpressing Awd::eGFP (Figure 47B,B') do not show any Hnt staining (Figure 47C,C'), as flanking cells (Figure 47D,D').

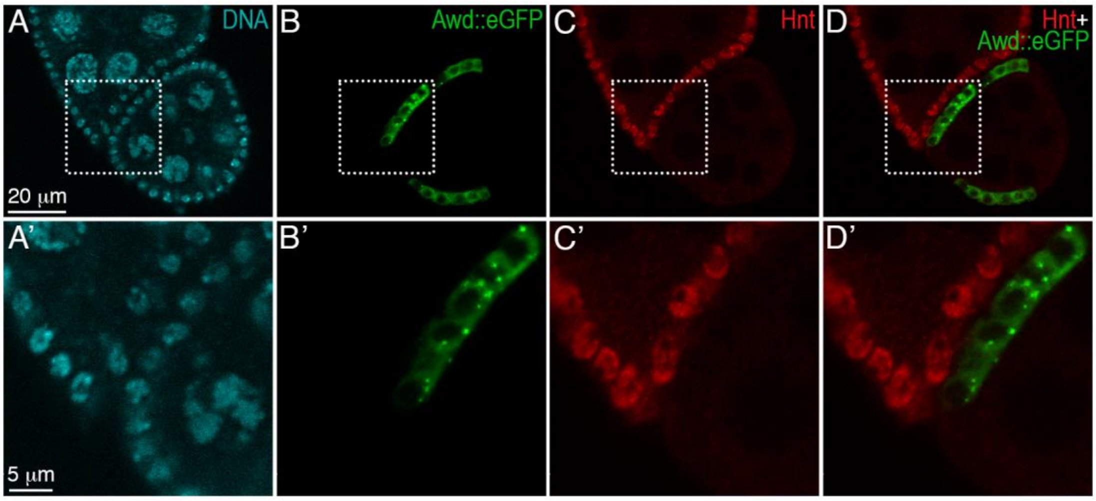

**Figure 47 Overexpression of Awd::eGFP in Flp-out FC clones does not precociously activate N signalling. (A-D)** Sagittal section of a stage 5 egg chamber dissected from *yw, hs-flp/act>CD2>Gal4; UAS-awd::eGFP/UAS-nlsLacZ* females. Images were taken by confocal microscopy. To-Pro-3 dye (cyan, A) reveals cell nuclei. The green fluorescent signal of Awd::eGFP protein (green in B,D) individuates the Flp-out clones. The Hnt signal is also visible (red, C,D). **(A'-D')** Magnification of the areas included in the dotted boxes in A-D.

### 4.6.3 Overexpression of Awd::eGFP in FCs devoid of Shi activity restores N signalling

Finally, I looked at N distribution and signalling in FCs overexpressing both a dominant negative form of Shi and the enhanced GFP-tagged Awd protein. The invasive properties due to overexpression of Shi$^{DN}$ (Figure 48A) are unchanged in FCs overexpressing also Awd::eGFP (Figure 48B). Moreover, intense NICD signal is still observed (Figure 48C,D). Despite this, in stage 8 egg chambers (Figure 48E) overexpression of Awd::eGFP (Figure 48F) in FCs devoid of Shi activity restores N signalling, as assed by detection of Hnt protein (Figure 48G,H) in such cell nuclei.

To better evaluate the significance of such rescue, in egg chambers of stages 6-8 I analysed several Flp-out clones in which the overexpression of either Awd::eGFP and LacZ, or Shi$^{DN}$ and GFP, or Shi$^{DN}$ and Awd::eGFP was induced. I then considered, in each background, the number of nuclei in each clone in which Hnt was present or absent. Finally, I graphed the results (Figure 49). In stage 6-8 egg chambers, 100% (*n=28*) of FCs overexpressing Awd::eGFP and LacZ showed correct N signalling activation (Hnt was expressed), while in 75.56% (*n=45*) of FCs expressing Shi$^{DN}$ and GFP no Hnt staining was visible. Finally, in 69.39% (*n=49*) of FCs overexpressing both Shi$^{DN}$ and Awd::eGFP showed Hnt staining at stage 6-8 of oogenesis.

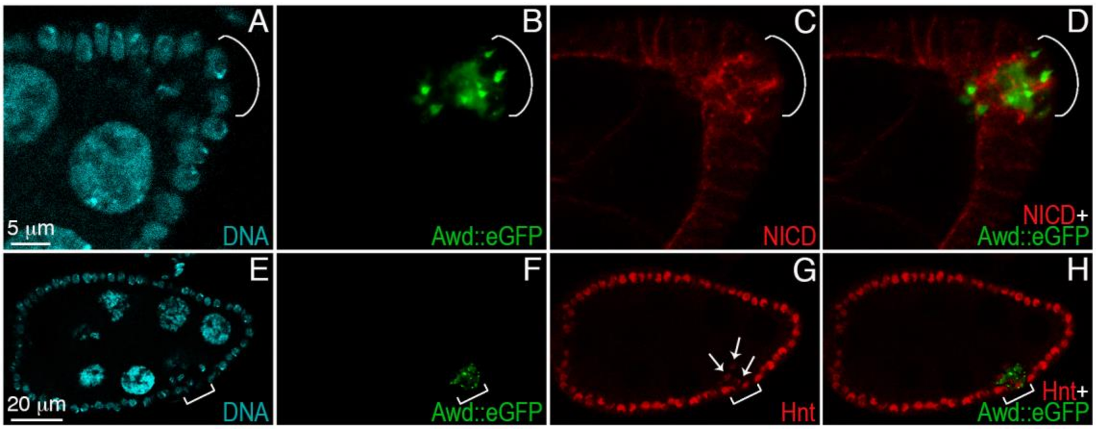

**Figure 48 Overexpression of Awd::eGFP restores N signalling in Flp-out FC clones devoid of Shi activity.** Ovaries were dissected from *yw, hs-flp/act>CD2>Gal4; UAS-awd::eGFP/+; TM3, UAS-shi*$^{K44A}$/+ females. Images were taken by confocal microscopy. **(A-D)** Cross section magnification of a stage 8 egg chamber stained with To-Pro-3 dye (cyan, A) to stain cell nuclei. The green fluorescent signal of Awd::eGFP protein (green in B,D) individuates small intracellular puncta. The NICD signal is also visible (red, C,D). The brackets in A-D embrace the Flp-out clone. **(E-H)** Cross section of a stage 8 egg chamber stained with To-Pro-3 dye (cyan, E) to reveal cell nuclei. The green fluorescent signal of Awd::eGFP protein (green in F,H) and the Hnt signal (red, G,H) are visible. The brackets in E-H embrace the Flp-out clone while the arrows in G point to clearly discernible Hnt-positive nuclei in the Flp-out clone.

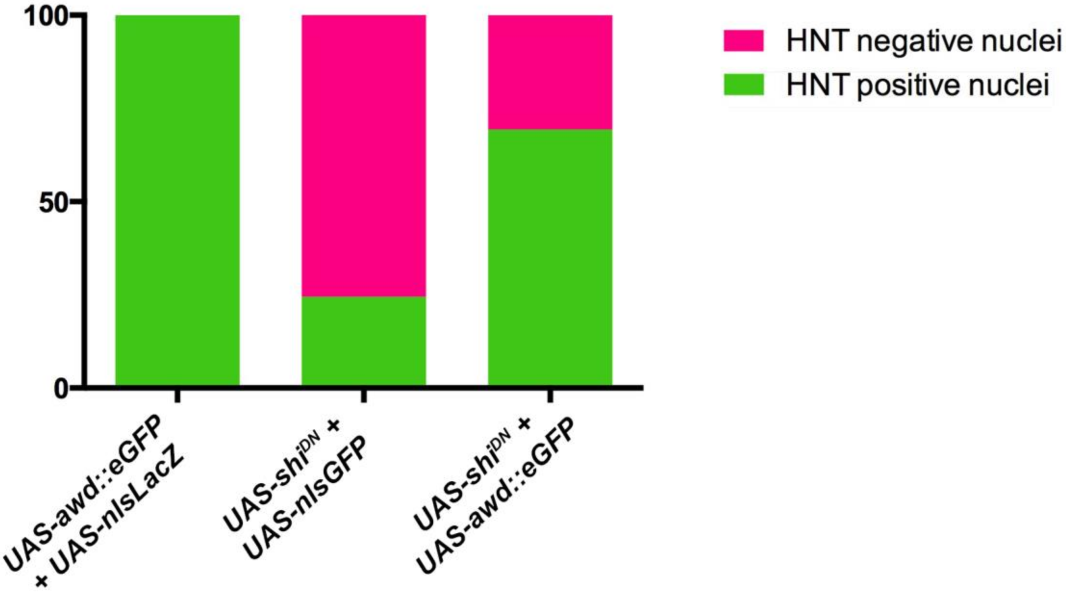

**Figure 49 Statistical evaluation of the effects of Awd::eGFP and Shi$^{DN}$ overexpression on N signalling activation.** Ovaries were dissected from *yw, hs-flp/act>CD2>Gal4; UAS-awd::eGFP/UAS-nlsLacZ* (first column), *yw, hs-flp/act>CD2>Gal4; UAS-nlsGFP/+; TM3, UAS-shi*$^{K44A}$/+ (second column) and *yw, hs-flp/act>CD2>Gal4; UAS-awd::eGFP/+; TM3, UAS-shi*$^{K44A}$/+ (third column) females and stained for Hnt. In each column, the total number of nuclei I analysed was normalised to 100%. The percentage of Hnt positive (green part of each column) and negative (red part of each column) nuclei is then quickly inferred.

These findings indicate that N signalling failure caused by mutations arresting Shi activity can be restored by overexpression of wild type Awd. This implicates that Awd activity is required beyond Shi function in N signalling activation. Moreover, this also further strengthens the genetic interaction between these two proteins.

## 4.7 Shi controls shuttling of Awd protein between the intracellular and extracellular milieux

The significant result of the previously described rescue experiment of N signalling defect due to loss of Shi activity by overexpressing a wild type copy of the Awd protein led me to further explore the relationship between Awd and Shi.

### 4.7.1 Awd level is strongly reduced in FCs overexpressing the dominant negative form of Shi

By analysing Flp-out clones overexpressing the dominant negative form of Shi ($CD2^-$ cells in Figure 50A,E), I found that in these FCs (Figure 50D) Awd is strongly downregulated (Figure 50B,F) in comparison to flanking cells (Figure 50 C,G).

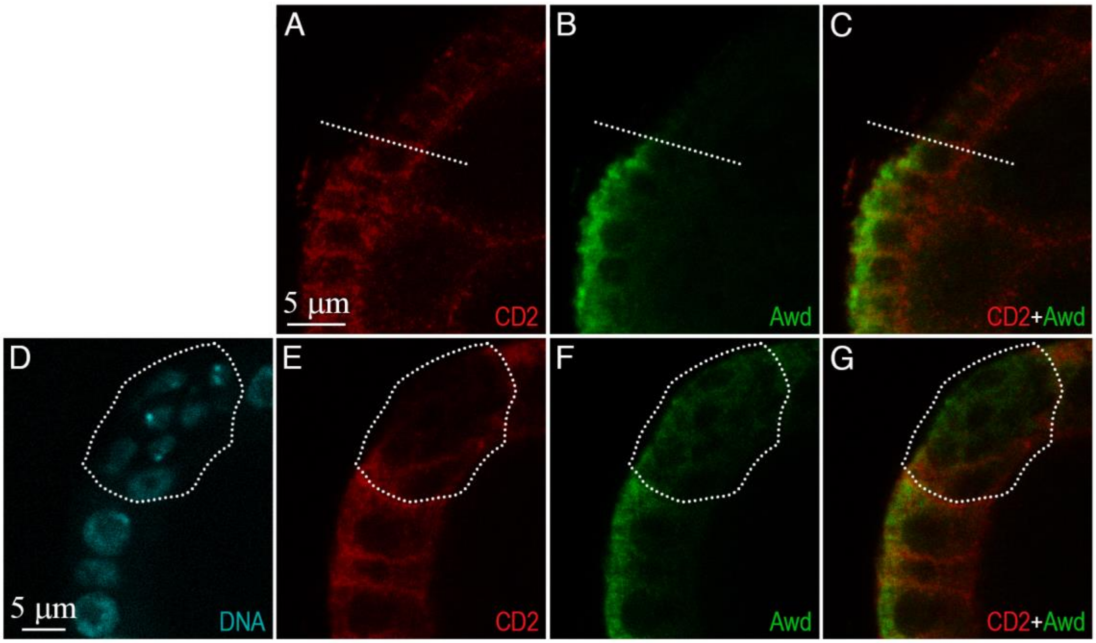

**Figure 50 Awd is barely detectable in FC Flp-out clones overexpressing $Shi^{DN}$.** Ovaries were dissected from *yw, hs-flp/act>CD2>Gal4; UAS-nlsGFP/+; TM3, UAS-shi*$^{K44A}$/+ females. Images were taken by confocal microscopy. **(A-C)** Cross section magnification of a stage 7 egg chamber in which the absence of the membrane-localised CD2 protein (red, A,C) is found in FCs overexpressing the mutant form of Shi. The dotted lines reported in each panel are at the boundary between CD2-positive and CD2-negative FCs. A FITC-conjugated anti-rabbit antibody was used to detect Awd protein (green B,C). In C, CD2 and Awd signals are merged. **(D-G)** Cross section magnification of a stage 9 egg chamber in which a CD2-negative Flp-out clone is present (CD2 is in red, E,G). These FCs overexpress the mutant form of Shi. The dotted lines reported in each panel encircle CD2-negative FCs. To-Pro-3 dye (cyan, D) reveals that the analysed clone is composed of multi-layered FCs. A FITC-conjugated anti-rabbit antibody was used to detect Awd protein (green F,G). In G, CD2 and Awd signals are merged.

### 4.7.2 Awd level is strongly reduced in adipocytes overexpressing the dominant negative form of Shi

In order to determine whether the reduction of Awd intracellular level in cells overexpressing $Shi^{DN}$ strictly occurs only in epithelial cells such as FCs, or if it is a more general effect of loss of Shi activity, I generated and analysed Flp-out clones overexpressing this mutant form of Shi in the fat body. This tissue shares with follicular epithelium the embryonic origin but while FCs acquire properties of epithelial cells, fat body are a more typical mesodermal derivative.

Surface (Figure 51A-D) and xz (Figure 51E) sections of fat cells overexpressing $\mathrm{Shi}^{DN}$ (Figure 51A) and marked by GFP (Figure 51B) clearly show a significant decrease of Awd staining (Figure 51C,D) compared to flanking wild type adipocytes in which Awd protein appears highly enriched in the peri-cellular region. Moreover, GFP-positive adipocytes with blocked Shi function (Figure 51F) display, in their subcortical region, a strong reduction of Awd staining (Figure 51G,H) especially in the periphery, at the secretory front. To statistically evaluate this phenomenon, I have analysed several adipocytes overexpressing $\mathrm{Shi}^{DN}$ and I found that 80.6% of them (*n=62*) showed a lowering of Awd intracellular level, without affected peri-cellular localisation.

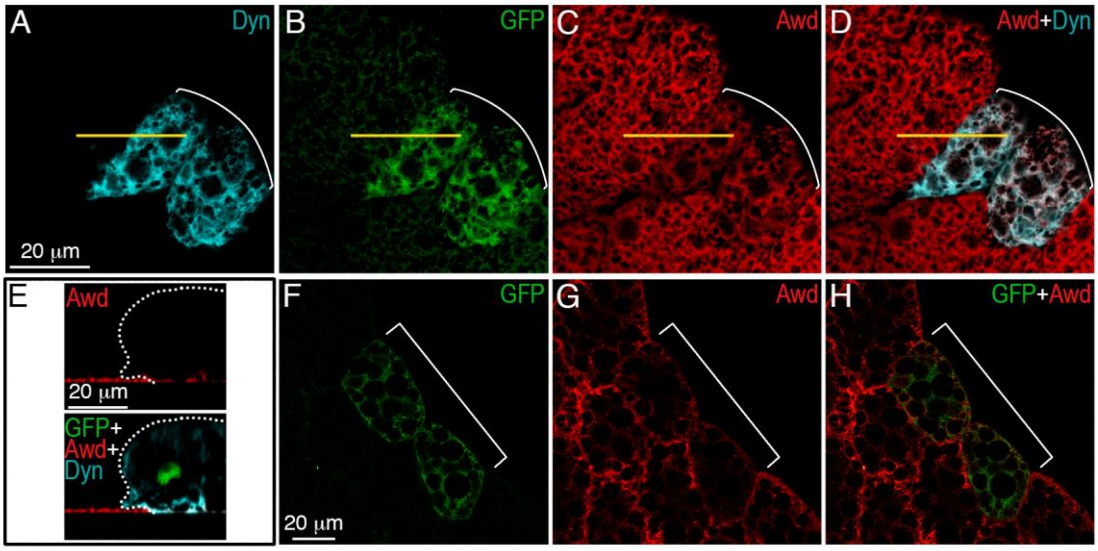

**Figure 51 Awd is diminished in adipocyte Flp-out clones overexpressing $\mathrm{Shi}^{DN}$.** Fat bodies were dissected from *yw, hs-flp/act>CD2>Gal4; UAS-nlsGFP/+; TM3, UAS-*$shi^{K44A}$*/+* larvae. Images were taken by confocal microscopy. **(A-D)** xy surface and **(E)** xz sections of adipocytes. Highly intense Dyn staining (cyan, A) is visible in Flp-out clones, marked by GFP (green, B). The immunodetection of Awd (red, C) is also showed. In D is the merge of the two antibody signals. The white brackets in each panel embrace the clonal region while the yellow lines indicate the position of the xz section showed in E. In E the dotted lines separates the $\mathrm{Shi}^{DN}$-overexpressing adipocyte from flanking cell. **(F-H)** xy cross section of fat body tissue in which a Flp-out clone, marked by the expression of the GFP (green, F) is present. Awd staining (red, G) is visible. In H the merge between GFP and Awd staining is showed. The white brackets in F-H facilitate the identification of the clonal region.

Since the relationship uncovered in FCs between impairment of Shi activity and lowering of Awd intracellular amount correlates also in adipocytes, these results suggest the existence of a regulatory mechanism mediated by Shi on Awd protein level. Such result could be interpreted in multiple ways. One can imagine an indirect control on *awd* gene expression as well as an enhancement of degradation or alteration in intracellular/extracellular equilibrium of Awd protein. Given the involvement of Shi in trafficking routes, hypotheses on alterations in such processes are preferred.

### 4.7.3 Adipocytes with impaired Shi activity accumulate Rab7-positive vesicles

The notion that impairment of Shi function could affect protein sorting toward degradation arises from the consideration that Dynamin has been proposed to be involved in the autophagosome degradation pathway (Ravikumar *et al.*, 2010a; Ravikumar *et al.*, 2010b). In order to assess if the lowering of intracellular Awd is due to enhanced protein degradation, I analysed late endosomal compartments in Shi$^{DN}$ adipocytes.

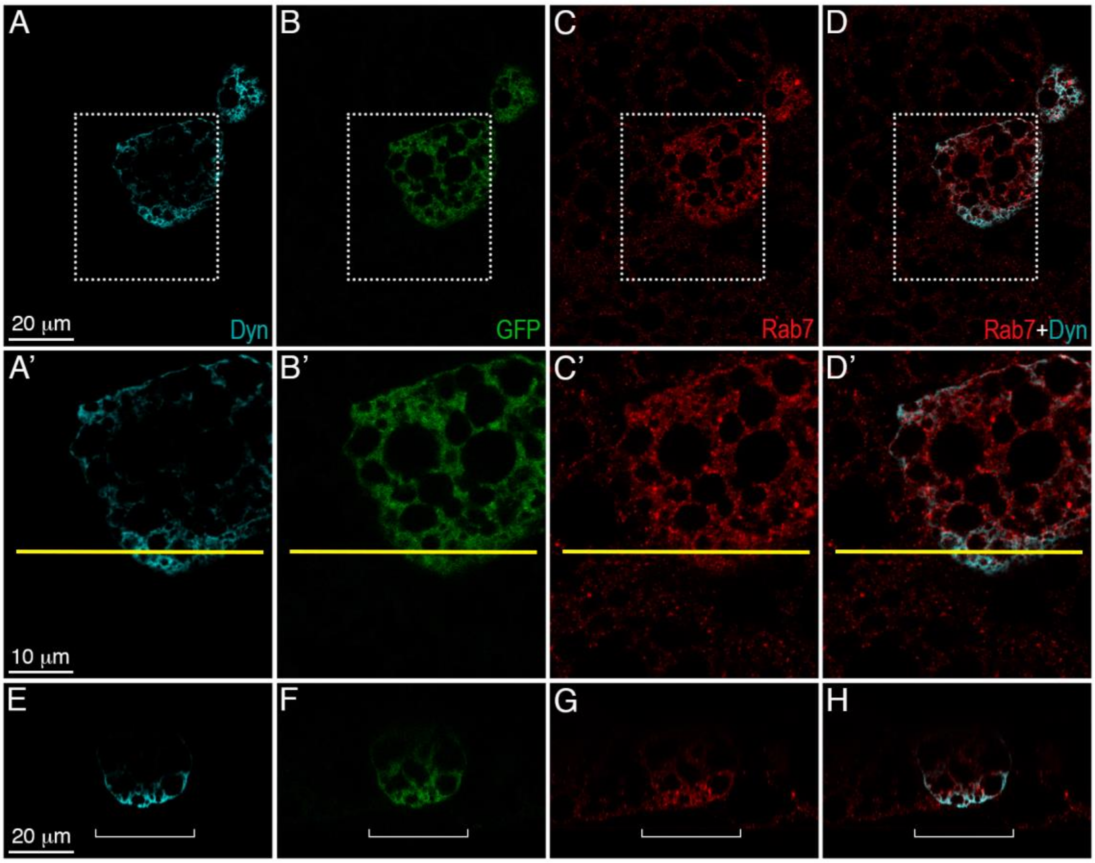

**Figure 52 Adipocyte Flp-out clones overexpressing Shi$^{DN}$ show enhanced Rab7-positive puncta.** Fat bodies were dissected from *yw, hs-flp/act>CD2>Gal4; UAS-nlsGFP/+; TM3, UAS-shi*$^{K44A}$/+ larvae. Images were taken by confocal microscopy. **(A-D')** xy surface and **(E-H)** xz sections of adipocytes. Highly intense Dyn staining (cyan, A,A',E) is visible in Flp-out clones, marked by GFP (green, B,B',F). The immunodetection of Rab7 (red, C,C',G) is also showed. In D,D',H are the merge of the two antibody signals showed in A-C; A'-C' and E-G respectively. **(A'-D')** Magnification of the areas included in the dotted boxes in A-D. The yellow lines indicate the position of the xz section showed in E-H. **(E-H)** The white brackets in each panel embrace the Shi$^{DN}$-overexpressing adipocyte showed in A'-D'.

I found that in adipocytes with blocked Shi function (Figure 52A,A',E, GFP$^{+}$ cells in Figure 52B,B',F), Rab7-positive vesicles accumulate (Figure 52C,C',G). Moreover, they appear enlarged compared to flanking wild type cells (Figure 52D,D'H). While I was performing such analysis, a paper from Tong group was published in which the authors demonstrated that in *Drosophila* adipocytes devoid of *shi* function lysosomal acidification defects and autophagy dysfunction occur, causing failure of lysosomal degradation (Fang *et al.*, 2016). In light of their findings, I could exclude that the accumulation of Rab7-positive vesicles could account for enhanced lysosomal degradation and lowering of intracellular Awd.

### 4.7.4 Shi controls extracellular Awd protein level

I then next explored the possibility that the lowering of the intracellular level of Awd was due to altered balance between intracellular and extracellular Awd in cells with impaired Shi function. Many considerations support this notion. First, it is worth to remind that proteomic approaches have already shown the presence of Awd into the larval haemolymph (Guedes Sde *et al.*, 2003). Moreover, in S2 cell line culture medium, Awd is recovered into microvesicles (Koppen *et al.*, 2011). These results indicate that the *Drosophila* NDPK can be secreted as the human orthologs Nme1 and Nme2 do and that it is wrapped within a membranous vesicle. Finally, a parallel data obtained in the lab showed that in the haemolymph collected from *shi*$^{ts}$ larvae exposed at the restrictive temperature of 31 °C for 8 hours, Awd protein level is higher than that recovered in the haemolymph collected from *yw* larvae treated in the same way (Romani *et al.*, 2016). This indicates that Shi activity is required to regulate extracellular Awd protein level.

Taking these findings and my results together, they suggest that Shi activity is required to modulate intracellular and extracellular Awd balance and that internalisation of extracellular Awd occurs through Shi-dependent endocytosis.

### 4.7.5 Role of Rab5 in regulating Awd intracellular level

To further characterise the mechanisms through which extracellular Awd is endocyted, I analysed the effects of *rab5* loss of function on Awd intracellular amount in adipocytes. To this aim, I used the *rab5*$^{2}$ null mutation. This mutant allele was generated through imprecise excision of a P element inserted in the *rab5* gene (Wucherpfennig *et al.*, 2003). *rab5*$^{2}$ carries a 4 kb deletion involving the promotor region, the 5' untranslated leader and the first exon of the open reading frame where a part of the GTPase domain is encoded. For these reasons *rab5*$^{2}$ is broadly accepted as a null allele. Since *rab5*$^{2}$ homozygotes die at early developmental stage, I analysed the function of *rab5* through the MARCM clonal analysis approach.

I first carried out an immunofluorescent staining using a rabbit polyclonal antibody directed against the Rab5 protein (Tanaka and Nakamura, 2008). Homozygous *rab5*$^{2}$ adipocytes, expressing the GFP marker (Figure 53A,D) are devoid of Rab5 protein (Figure 53B,C,E,F). Moreover, Rab5 shows a peri-cellular distribution in wild type adipocytes.

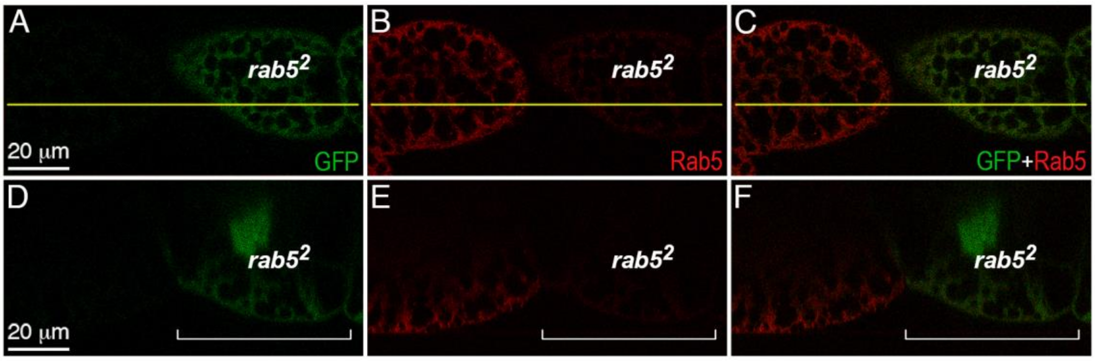

**Figure 53 *rab5*$^{2}$ is a null allele of *rab5*.** Fat bodies were dissected from *yw, hs-flp, tub-Gal4, UAS-nlsGFP/yw, hs-flp; FRT*$^{40A}$*, rab5*$^{2}$*/FRT*$^{40A}$*, tub-Gal80* larvae. Images were taken by confocal microscopy. **(A-C)** xy surface and **(D-F)** xz sections of adipocytes. Fluorescent signal of GFP (green, A,D) identifies the homozygous *rab5*$^{2}$ MARCM clone. The immunodetection of Rab5 (red, B,E) is also showed. In C,F are the merge of the GFP and Rab5 signals. The yellow lines in A-C indicate the position of the xz section showed in D-F, while the white brackets in D-F embrace the *rab5*$^{2}$ mutant adipocyte.

I then analysed the spatial distribution and amount of Awd in *rab5*$^{2}$ adipocyte MARCM clones. I found that in homozygous *rab5*$^{2}$ adipocytes (GFP$^{+}$ cells in Figure 54A), Awd protein amount (Figure 54B) is comparable to that in flanking cells (Figure 54C). Moreover, xz section shows that in wild type and mutant adipocytes (expressing GFP, Figure 54D) the subcellular distribution of Awd (Figure 54E) is identical (Figure 54F).

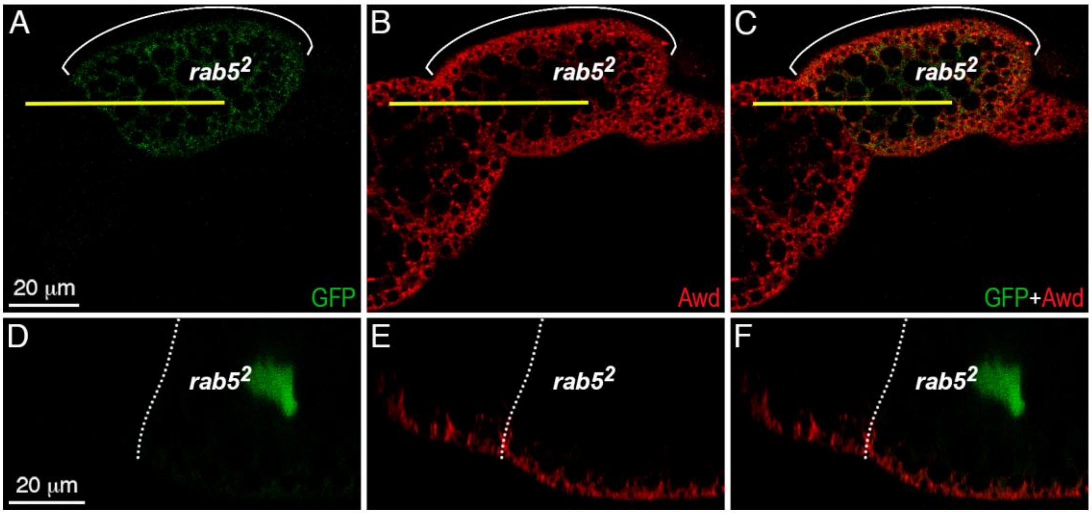

**Figure 54 *rab5* loss of function does not impair intracellular level and distribution of Awd in adipocytes.** Fat bodies were dissected from *yw, hs-flp, tub-Gal4, UAS-nlsGFP/yw, hs-flp; FRT*$^{40A}$*, rab5*$^{2}$*/FRT*$^{40A}$*, tub-Gal80* larvae. Images were taken by confocal microscopy. **(A-C)** xy subcortical and **(D-F)** xz sections of adipocytes. Fluorescent signal of GFP (green, A,C) identifies the homozygous *rab5*$^{2}$ MARCM clone. The immunodetection of Awd (red, B,E) is also showed. In C,F are the merge of the GFP and Awd signals. The white brackets in A-C embrace the *rab5*$^{2}$ mutant adipocyte while the yellow lines indicate the position of the xz section showed in D-F. The white dotted lines in D-F separate homozygous *rab5*$^{2}$ from flanking adipocytes.

# Chapter 5

## Discussion

N signalling pathway is a pleiotropic and highly evolutionarily conserved cell-cell communication pathway with a primary role in controlling and driving cell fate decisions occurring during animal development. Indeed, appropriate N signalling is crucial in many different homeostatic and developmental processes, such as lineage commitment, cell differentiation, morphogenesis, stem cell maintenance, regulation of proliferation and apoptotic events, and for the correct patterning of tissues and organs (Liu *et al.*, 2010; Wilson and Radtke, 2006). Exquisite mechanisms of signal transduction regulation and modulation are present. Among such N regulative processes, endocytosis of both ligands and receptors was shown to deeply influence signal outcomes (Bray, 2016).

Given the vast range of biological processes in which N signalling is implicated, there is no surprise in ascertaining that alterations in this pathway are often recovered in cancer patients. Moreover, emerging evidence highlight a strong context-dependence of N function as tumour-suppressor (Nowell and Radtke, 2017) or oncogene (Brzozowa-Zasada *et al.*, 2016). This peculiar feature of N signalling is clearly linked to its pleiotropy.

With these premises, it follows that uncovering modulators of this signalling could have important implications for cancer treatments.

In *Drosophila*, the N signalling pathway mediates cellular events that are critical for morphogenesis of epithelial tissues such as follicular epithelium and wing disc columnar layer. In particular, during oogenesis, at stage 6, activation of N pathway in FCs triggered by upregulation of the Dl ligand in germ cells, halts FC mitotic divisions and induces FC differentiation. In wing discs, at L2 stage, activation of the pathway at the DV boundary is critical for subsequent patterning and growth.

The data I presented in the previous chapter clearly demonstrate that the gene product of the *awd* locus is a key regulator of N signalling. Through my genetic analysis I showed that N signal transduction is inhibited in FCs, as well as in wing disc cells, lacking *awd* gene function. Indeed, upregulated N target genes, such as *hnt* in FCs and *wg* and *cut* in wing disc cells, are downregulated in *awd* mutant cells. In FCs, N signalling activation induces a cell differentiation event which is critical for follicular epithelium morphogenesis. In *awd* mutant FC clones, such differentiative event does not occur. Moreover, *awd* mutant cells do not express the N transcriptional reporter *Gbe*. The transcription factor NICD is released following N signalling activation and is necessary to induce *Gbe* expression. N signalling failure in producing NICD accounts for the absence of β-galactosidase in *awd* mutant clones. N signalling rescue experiment through overexpression of the NICD receptor fragment in *awd* mutant clones indicates that the defect occurs before or at the level of the S3 cleavage that indeed releases the NICD transcription factor. Thus, *awd* mutant cells cannot produce NICD. Since the overexpression of the NEXT fragment in *awd* mutant clones does not restore N signalling, this data strongly support the notion that *awd* function is required downstream of the S2 cleavage. How does this defect arise? NICD production occurs while the receptor traffics in endocytic compartments. The altered N receptor pattern profile recovered in cells devoid of *awd* suggests intracellular trafficking faults. Large vesicular aggregates are present at the apical side of homozygous $awd^{J2A4}$ FCs. Since previous reports uncovered a role for Awd as an endocytic mediator (Krishnan *et al.*, 2001; Nallamothu *et al.*, 2008; Woolworth *et al.*, 2009) and given the well-established role of endocytosis in modulating N signalling (Baron, 2012), an involvement of *awd* in the trafficking route of N receptor is highly realistic and further supported by my additional analyses. I indeed analysed N distribution in different endosome subpopulations and I found that in FCs lacking *awd* gene function the receptor strongly accumulates in immature early endosomes marked by Avl.

It was shown that in *awd* mutant FCs Rab5 level is greatly reduced and adherens junctions component accumulation is observed in these cells. The latter phenotype could be rescued through overexpression of a wild type as well as of a constitutively active form of Rab5 to similar extent (Woolworth *et al.*, 2009). Instead, the overexpression of the constitutively active form of Rab5 does not rescue N signalling defect occurring in *awd* mutants. This indicates that in the follicular epithelium *awd* function in guaranteeing tissue integrity by regulating FC cell junction homeostasis is genetically separable from its role in promoting tissue morphogenesis and cell differentiation by supporting N signalling activation. These results and considerations are in accordance with the observation that the N signalling defect still occurs in *awd* clones displaying wild type cell junctional complexes, in which it could be speculated that Rab5 level is not yet under the critical threshold below which disruption of such epithelial characteristics occur.

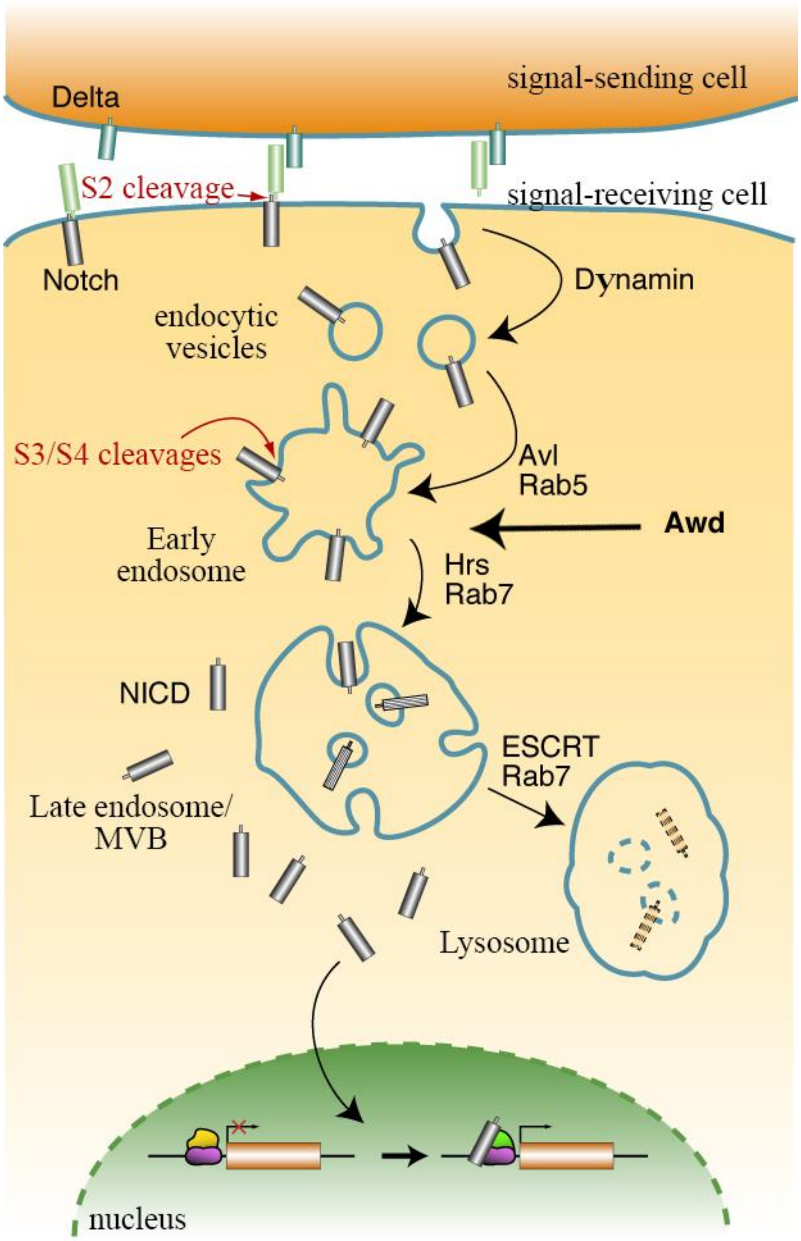
signal-sending cell
Delta
S2 cleavage
signal-receiving cell
Notch
Dynamin
endocytic vesicles
S3/S4 cleavages
Avl
Rab5
Awd
Early endosome
Hrs
Rab7
NICD
ESCRT
Rab7
Late endosome/ MVB
Lysosome
nucleus

**Figure 55 Schematic drawing of N endocytic trafficking route following ligand stimulation with indication of the endosomal compartments in which principal endocytic mediators act.** The bolded arrow points to the putative step of the endocytic trafficking route of N receptor at the level of which *awd* function is required to allow signal transduction. This *awd* requirement is inferred on the basis of the data presented in this PhD thesis.

The analyses I performed allowed me to gain insights into the endocytic step at level of which Awd function is absolutely necessary for N signalling. In Figure 55 the N trafficking route is schematised with indication of the receptor cleavages occurring during signal transduction. Awd function is required during N trafficking at the level of early endosomes. I could rule out, in relation to N signalling, a direct function of Awd on Shi since in *awd* mutant cells:

- N receptor accumulates in Avl positive vesicles, that forms after Dynamin-mediated pinching off of plasma membrane pits;

- N overall distribution highly differs from that observed in *shi* mutants;
- Presenilin expression level and punctate pattern are comparable to that of flanking cells (not shown, Ignesti *et al.*, 2014);
- a constitutively active form of Rab5 cannot rescue the N signalling defect, indicating that *awd* function is required at the level or downstream of Rab5, that acts downstream of Shi;
- NEXT overexpression does not restore N signalling, conversely to what observed in *shi* mutants.

Moreover, in FC devoid of Shi activity, overexpression of Awd is able to restore N signalling, indicating that in relation to this pathway, *awd* function is required downstream of *shi*.

For cancer research, the involvement of endocytosis in correct N signalling activation is highly and deeply significant since many of the known endocytic mediators have been shown to act as TSGs or proto-oncogenes and have been often found aberrant in cancer (Tzeng and Wang, 2016). The case of *awd* does not make an exception: *awd* is the homolog of *Nme1* and *Nme2*. These genes belong to the group I of *Nme* family and have been broadly implicated in cancer progression for their role as MSGs (Boissan and Lacombe, 2012; Thakur *et al.*, 2011). What, once again, emerges from a literature review on *Nme1* gene function as MSG is the stringent context-dependence of this capability. Indeed, in some tumour contexts, its downregulation correlates with poor prognosis but in some other cancer cohorts an inverse correlation has been verified. The parallelism between N signalling and Nme1 behaviours in different type of cancers is obvious. This opens up to the necessity of deeper analyses to correlate N signalling status and Nme1 level in cancer patients, keeping in mind the fundamental role exercised by the tissue context in which the tumour has developed.

What makes the function of Nme1 protein as metastasis suppressor intriguing is the notion that alteration of both its intracellular and extracellular levels were shown to have implication in cancer progression. To date, very little is known about the mechanisms regulating Nme1 presence in the extracellular environment, although this parameter is used in the clinic as a prognostic tool in AML (Niitsu *et al.*, 2000; Niitsu, 2001). Since Nme1 is found in the culture medium of cancerous cell lines (Anzinger *et al.*, 2001; Okabe-Kado *et al.*, 1992), a mechanism based on its secretion to justify its presence in the extracellular environment seems realistic, although some authors have also attributed the increased serum level of Nme1 to enhanced effete erythrocyte or tumour cell lysis (Okabe-Kado *et al.*, 2009; Willems *et al.*, 1998).

Proteomic data showed that Awd is present in the *Drosophila* haemolymph and that can be released from *Drosophila* S2 cells in the culture medium in microvesicles (Guedes Sde *et al.*, 2003; Koppen *et al.*, 2011). These findings make *Drosophila* attractive for studies designed to gain insights into the molecular mechanisms governing its shuttling between the intracellular and extracellular milieux. I found that depleting cells of Shi function dramatically decreases Awd intracellular level, tempting to speculate a defect in endocytosis of extracellular Awd in cells devoid of Shi. This is corroborated by the finding that in the haemolymph of *shi*$^{ts}$ larvae exposed at the restrictive temperature, the level of extracellular Awd is significantly higher than that in *yw* larval haemolymph, while the analysis of whole larvae protein extracts reveals that the overall Awd expression is the same in *yw* and *shi*$^{ts}$ larvae (Romani *et al.*, 2016). A parallel analysis from a group based at University of Bologna with which we collaborated demonstrated that the effect of *shi* depletion on extracellular Nme1 level is conserved in human cells (Romani *et al.*, 2016). A possible Awd trafficking model that takes into account these findings is reported in Figure 56.

The finding that the modulation of extracellular Awd/Nme1 levels is dependent on Shi/Dyn function has implication for cancer research since the uptake of extracellular Nme1 was shown *in vitro* to inhibit metastatic phenotypes in tumour cell lines and *in vivo* to block the establishment of metastases and to clear already-established metastases, significantly prolonging the survival of tumour-bearing animals (Lim *et al.*, 2011). In their work, Lim and colleagues engineered the Nme1 protein with a highly hydrophobic sequence to increase its cell permeability. From my analysis it could be inferred that enhanced Nme1 uptake could also be achieved by stimulating Dyn activity. Indeed, one of the future aims is to analyse the effects of overexpression of wild type or constitutively active Shi on Awd intracellular and extracellular levels.

I also found that *rab5* loss of function does not alter the intracellular level of Awd. This suggest that a Rab5-independent route is followed by Awd during its endocytosis. However, further analyses are certainly needed to confirm this and to deeper characterise the trafficking route followed by Awd in its internalisation. In parallel to this, also the investigation of Awd secretion is fascinating and in perspective future studies will be addressed to gain insights into this process with broad implication for cancer research. Indeed, the identification of the routes Nme1 follows during its shuttling between the intracellular and extracellular milieux could have deep impact on tumour and metastasis treatments, since regulative molecules involved in such trafficking pathways could be potential targets for drug development in order to modulate Nme1 levels.

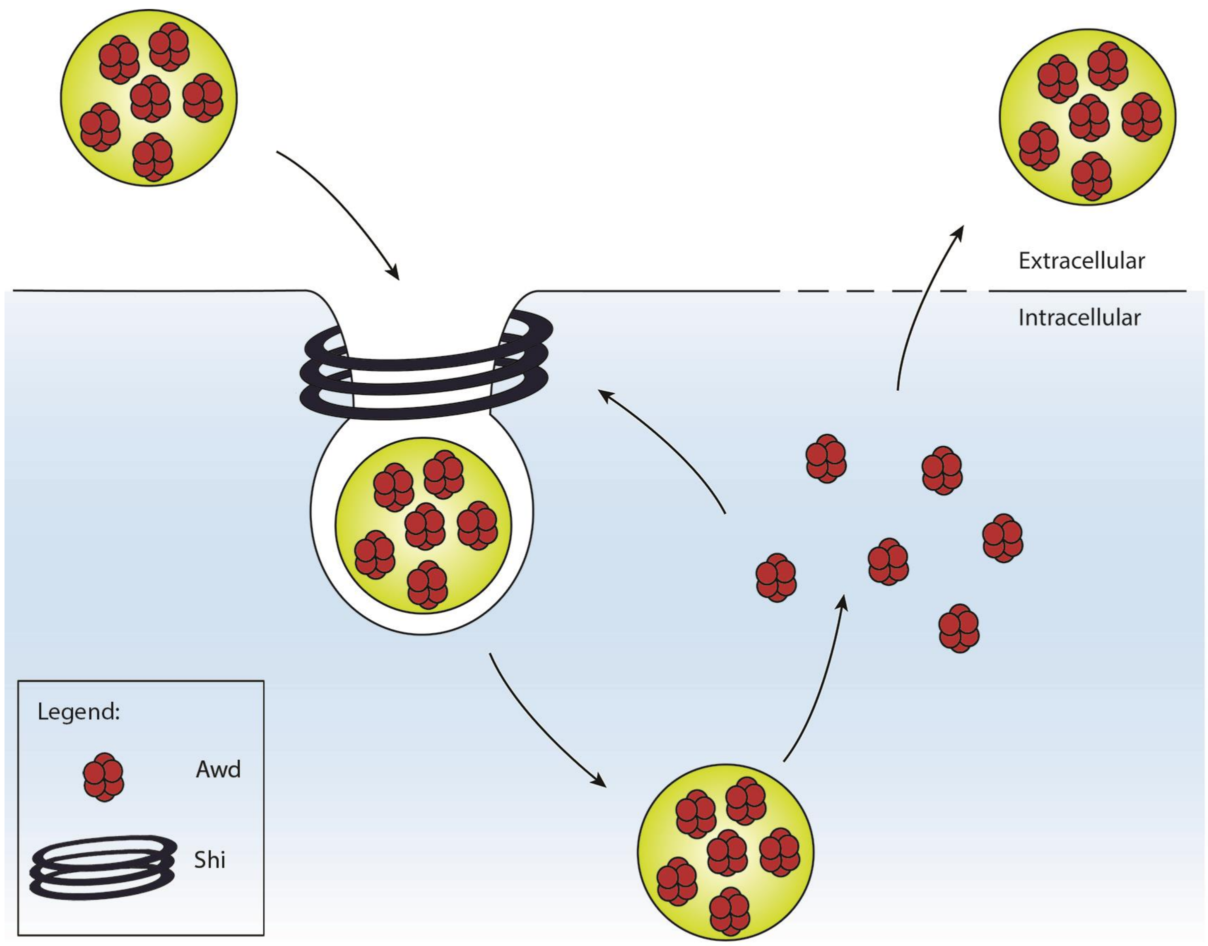

**Figure 56 Schematic drawing of the proposed Awd shuttling inside and outside cells.** On the basis of the data presented in this PhD thesis, it could be inferred that endocytosis of extracellular Awd requires *shi* function. At intracellular level, Awd is required for Shi-mediated endocytic events. Further investigations are needed to uncover the mechanism(s) regulating Awd secretion into the extracellular milieu.

# Chapter 6

# Appendix

## 6.1 Introduction

### 6.1.1 The human and the *Drosophila VHL* genes

The von-Hippel Lindau disease is a genetic disorder characterised by the onset during all lifelong of several highly vascularised benign and malignant tumours. Tumours generally arise in specific organs, typically the kidney (people with VHL disease commonly develop ccRCC, clear-cell renal cell carcinoma) and the central nervous system (development of hemangioblastoma). The VHL syndrome is an hereditary condition: affected people have usually inherited a germline mutation in the *VHL* gene from a parent; somatic inactivation of the other allele triggers the development of the pathology (Latif *et al.*, 1993). One allele is typically inactivated through mutation or promoter methylation, and the other is inactivated through a large deletion resulting in loss of heterozygosity (LOH, Gnarra *et al.*, 1994; Herman *et al.*, 1994). Thus, the *VHL* gene behaves as a typical TSG, in which mutations or epigenetic alterations resulting in its biallelic inactivation eventually predispose to cancer.

ccRCC is a terrible cancer type, untreatable with conventional chemotherapies, that generally leads to patient death. It is worth to note that in 70-90% of sporadic ccRCC inactivation of both *VHL* copies is recovered (Kaelin, 2007), highlighting the existence of tight correlation between *VHL* loss of function and tumour manifestation.

It is well-established that the protein encoded by the human *VHL* gene (pVHL) is the substrate-binding subunit of a SCF (Skp1-Cdc53/Cul-1-F-box protein) type E3 ubiquitin ligase also containing Cullin-2, Elongin B and C and Rbx-1 (Iwai *et al.*, 1999; Kamura *et al.*, 1999; Lonergan *et al.*, 1998). This E3 ubiquitin ligase has a critical role in oxygen sensing, together with prolyl-hydroxylase domain proteins (PHDs). HIF-1α is the master regulator gene that triggers the oxygen response when levels of this essential molecule become critical. Given its role, HIF-1α levels must be kept under stringent control. In particular, HIF-1α is the target of the prolyl-hydroxylase activity of PHDs, when oxygen levels are in a physiological range. The post-translational modification mediated by PHDs ensures VHL-mediated recognition of HIF-1α as a target of the SCF type E3 ubiquitin ligase (Maxwell *et al.*, 1999). Poly-ubiquitination of HIF-1α then addresses the protein to proteasomal degradation. Under hypoxic conditions, the prolyl-hydroxylases are inactive and HIF-1α is stabilised. Through dimerization with its partner, the constitutively expressed HIF-1β (also known as ARNT), it can function as a transcription factor upon translocation into the nucleus. HIF-1α/HIF-1 β best-known target genes encode proteins involved in glycolysis (e.g., phosphoglycerate kinase), glucose transport (Glut-1), angiogenesis (vascular endothelial growth factor, VEGF) and erythropoiesis (erythropoietin); that is, proteins that mediate the cellular response and adaptation to hypoxic conditions (Bader and Hsu, 2012). These functions support a critical role of VHL in regulating tumour progression, especially in hyper-vascularised tumours such as ccRCC. pVHL can undergo post-translational modification: indeed, it is the target of the phosphorylation activity of the CK2 (casein kinase 2) and it was demonstrated that this modification is essential for its tumour suppressor function (Lolkema *et al.*, 2005).

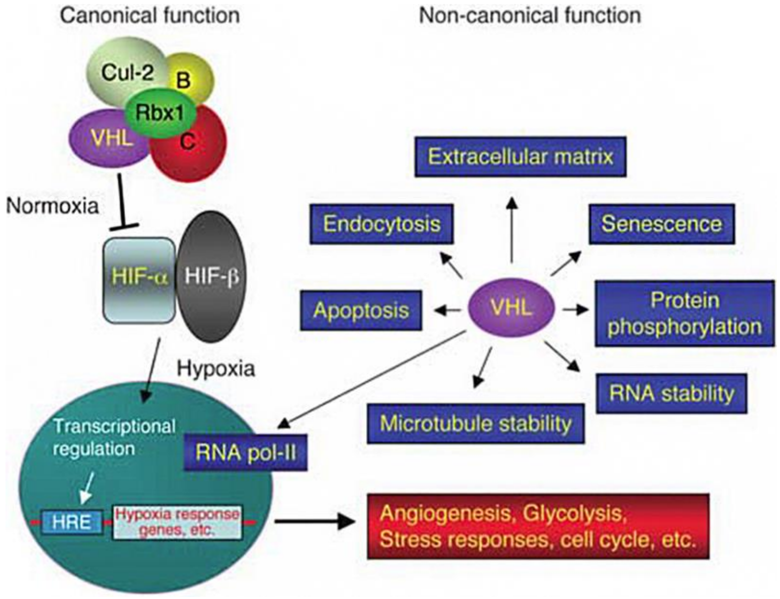
Canonical function
Non-canonical function
Cul-2
B
Rbx1
VHL
C
Normoxia
HIF-α
HIF-β
Hypoxia
Transcriptional regulation
RNA pol-II
HRE
Hypoxia response genes, etc.
Angiogenesis, Glycolysis, Stress responses, cell cycle, etc.
Extracellular matrix
Endocytosis
Senescence
Apoptosis
VHL
Protein phosphorylation
RNA stability
Microtubule stability

**Figure 57 Pleiotropic function of VHL.** The canonical functions refer to VHL-mediated regulation of HIF-1α stability. Normoxia stimulates HIF-1α degradation; in hypoxic condition, HIF-1α interacts with HIF-1β, so that transcriptional regulation of hypoxia-induced genes is triggered. Besides this canonical pathway, VHL seems to be involved in many other HIF-independent function, such as microtubule stability, endocytosis, regulation of extracellular matrix. For details, see text. Modified from Hsu, 2012.

While the above described function of VHL is referred to the canonical one, strictly related to HIF activity, a fascinating field of research is the investigation of potential HIF-independent VHL function (Figure 57). Many inputs in this direction came from animal models, like *C. elegans*, *D. rerio*, *M. musculus* and *D. melanogaster* (Hsu, 2012).

The first paper reporting the *Drosophila VHL* (*dVHL*) gene identification and function was published in 2000. Adryan and colleagues identified, through sequence homology, the *dVHL* gene on the second chromosome, right arm (Adryan *et al.*, 2000). Through RNA interference they demonstrated that *dVHL* is required during embryogenesis for the correct morphogenesis of the trachea, the *Drosophila* vascular system. Tracheal system is a complex network of vessels and tubules involved in the perception and transport of oxygen; the master regulator gene for trachea development is *trachealess* (*trh*, see also paragraph 1.9). This system of ducts, whose ramifications follow stereotyped profiles, is dramatically altered as a consequence of *dVHL* downregulation: disruptions in the major vessels accompanied by excessive looping of smaller branches are observed. Also an independent study identified the *dVHL* gene; authors demonstrated that dVHL can be co-immunoprecipitated with the *Drosophila* component of the SCF type E3 ubiquitin ligase and that this complex can target both HIF-1$\alpha$ and its *Drosophila* orthologue Sima (Aso *et al.*, 2000). While the development of *Drosophila* trachea partly requires the dVHL/Sima axis (Mortimer and Moberg, 2009), thus involving the canonical function of dVHL, this is not sufficient to explain all the observed phenotypes. Indeed, through generation of a specific loss-of-function mutation in the gene, $dVHL^{1.1}$, it was shown that $dVHL^{-/-}$ tracheal cells overactivate the FGFR pathway as a consequence of overaccumulation of the receptor at the cell surface (Hsouna *et al.*, 2010). The receptor appears stalled at the plasma membrane, a phenotype reminiscent of that in $shi^{ts}$ embryos exposed at the restrictive temperature: this revealed the involvement of dVHL in endocytosis. In particular, it was shown that dVHL endocytic role is mediated by its interaction with Awd. Their tracheal phenotypes, indeed, phenocopy each other. Moreover, *dVHL* appears to be an haploinsufficient gene, since tracheal phenotypes are already visible in heterozygous embryos.

In the attempt to further investigate the *dVHL* function in epithelia morphogenesis, in the lab in which I carried out my PhD were performed elegant genetic experiments in the follicular epithelium (Duchi *et al.*, 2010). They found that FCs devoid of *dVHL* gene function mislocalise aPKC, one of the component of the apical polarity complexes required for the establishment of the apico-basal polarity in epithelial cells. The mislocalisation appears to be a consequence of microtubule instability in $dVHL^{-/-}$ cells. Indeed, microtubules are essential to regulate trafficking of polarity markers in the appropriate cell membrane domains (see also paragraph 1.8). A more recent work suggested that VHL-mediated stabilisation of microtubules could also imply degradation of incorrect folded tubulin through the E3 ubiquitin ligase complex (Delgehyr *et al.*, 2012).

### 6.1.2 Development, structure and functions of *Drosophila* Malpighian tubules

Mammalian kidneys and insect Malpighian tubules are highly specialised renal organs that accomplish the essential functions of osmoregulation while removing potentially toxic compounds. The renal system of *Drosophila* is composed of two physically and functionally distinct organs (Denholm and Skaer, 2009): nephrocytes (of mesodermal origin) and Malpighian tubules (of ectodermal origin, Figure 58). In *Drosophila*, there are 2 types of nephrocytes: pericardial nephrocytes, which flank the heart, and garland nephrocytes, surrounding the oesophagus. In both cases, nephrocytes are organised as small clusters of cells. Malpighian tubules are haemocoel (the body cavity, which is filled up with the haemolymph) free-floating tubules connected to the upper part of the hindgut (the terminal region of the digestive tract involved in excretion). While nephrocytes are principally implicated in the removal of waste products from the haemolymph, Malpighian tubules perform functions more closely related to that of mammalian nephrons and collector ducts such as detoxification from pesticides and heavy metals and regulation of water balance and ion concentrations in the haemolymph thanks to active transporters and diffusion channels on the cell membranes. The tubules transport excess fluid and solutes and secrete them into the hindgut; the urine then will be excreted. For their specific roles, Malpighian tubules are considered the functional equivalent of mammalian kidneys.

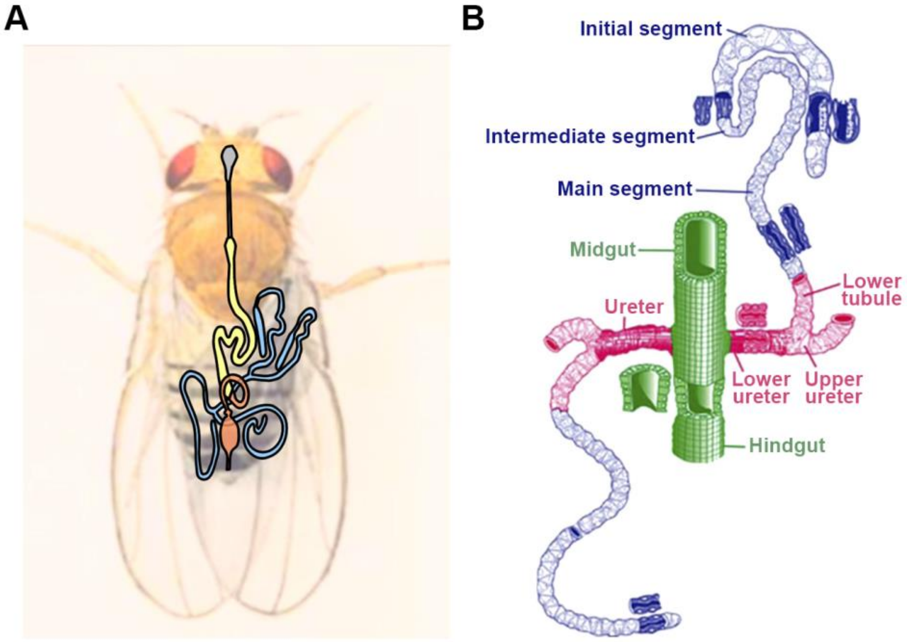

**Figure 58 *Drosophila* Malpighian tubules allocation and structure. (A)** Scheme of *Drosophila* digestive apparatus organisation. Modified from Dow and Romero, 2010. **(B)** Each tubule in a pair is jointed with the other at the boundary between the midgut and the hindgut thanks to a common ureter. Six different regions could be discerned and their names and positions are indicated in the panel. Modified from Singh *et al.*, 2007.

*Drosophila* has 2 pairs of Malpighian tubules, both connected with a common ureter that opens out into the alimentary canal (Figure 58A). The anterior pair is the longest one and it runs in parallel to the midgut; each anterior tubule contains 144±10 cells. The posterior pair is shorter and runs towards the hindgut; each posterior tubule is composed of 103±8 cells. On the basis of morphological features and molecular markers, in each tubules 4 different domains can be distinguished: initial, intermediate, main (secretory), and proximal (subdivided in upper and lower ureter and lower tubule) with reabsorptive function (Figure 58B). As for mammalian kidneys, activity of Malpighian tubules is strictly regulated through hormonal signals, secondary messages and neural peptides (Kean *et al.*, 2002; Talsma *et al.*, 2012).

Two different cell types reside in the initial, intermediate and main segments. They can be distinguished on the basis of nuclei dimension and expression of specific markers: type I, also known as principal cells have the biggest nuclei and express Cut; type II cells, also known as stellate cells express Teashirt (Tsh). To absolve their functions, apico-basal polarity of renal cells must be highly pronounced; moreover, tight junction must be present to avoid unregulated fluid movement. These features are in common with mammalian kidneys.

Malpighian tubules are monolayered epithelial tubes that form during embryogenesis: at stage 11, 4 ectodermal buds emerge from the hindgut anlage. These bud cells express Krüppel, which in turns upregulate the expression of *cut*. The buds start to elongate through cell proliferation. At middle embryogenesis, proliferation halts and tubules continue their elongation through cell rearrangements, such as cell intercalation and cell shape changes, including flattening. By the end of embryogenesis the monolayered epithelium is established and tubules are already able to perform their osmoregulatory functions (Pugacheva and Mamon, 2003). Stellate cells originate from the posterior mesoderm and then they undergo EMT to intercalate between principal cells (Denholm *et al.*, 2003). Stellate cells are characterised by the expression of Tsh. During larval life, organ growth is accomplished through cell growth mediated by polyploidy (principal cells reach 256C in DNA content, Lamb, 1982). In contrast with other larval tissues, Malpighian tubules during metamorphosis do not undergo histolysis; instead they are preserved to the adult stage, although some rearrangements occur during pupation.

In 2007, the group of Hou re-analysed the cell types of Malpighian tubules and found that in the proximal segment are located 3 different cell types: tiny cells with small nuclei that were thought to be involved in collecting the urine in the ureter (Sozen *et al.*, 1997); cells with large oval nuclei; cells with nuclei of intermediate dimension. They demonstrated that tiny cells indeed are multipotent renal stem cells (Singh *et al.*, 2007). This finding has important consequences for renal cancer research (Singh and Hou, 2008, 2009).

Multiple signalling pathways and genes have been implicated in the establishment of cell fate and morphogenesis of *Drosophila* Malpighian tubules (Wan *et al.*, 2000). Indeed, it was recently found that N signalling has a primary role in maintenance of renal stem cells: as in the ovary, stem cells express Dl and this is necessary to maintain their stemness (Li *et al.*, 2014). Interestingly, it was also found that mutations in *trh* gene alters Malpighian tubule elongations and ureter formation (Jack and Myette, 1999).

Great contributions toward the understanding of physiology and function of Malpighian tubules come from the Dow lab. Dow himself first adopted the Malpighian tubules as an amenable model for physiological studies (Dow *et al.*, 1994). 10 years later, in his lab, it was performed the first transcriptomic analysis of renal tubules, just 4 years later the completion of *Drosophila* genome sequence (Wang *et al.*, 2004). The functional analysis of the highly enriched genes in tubules allowed to get important insight into insect physiology (Dow and Davies, 2006). Since many of the genes implicated in human renal pathologies were found to be expressed in *Drosophila* Malpighian tubules, transcriptomic studies definitively elected Malpighian tubules as model system to study renal diseases (Dow and Romero, 2010; Miller *et al.*, 2013).

Beside their role in regulating fluid homeostasis, Malpighian tubules have also been implicated in the stress and innate immune response (Davies *et al.*, 2012). Particularly, in 2012 it was shown that starting from the 3rd instar and all lifelong, Malpighian tubules constitutively express specific antimicrobial peptides even in absence of an immune challenge. Authors propose that because tubules are free-floating in the haemolymph, they probably are the first epithelial tissue to sense a systemic invasion by intruders (Verma and Tapadia, 2012).

## 6.2 Objective of the research

To be affected by VHL disease is a terrible condition, since it implies you will never get rid of cancer. Patients carry, in their genetic background, a deletion in the *VHL* locus that makes them heterozygous for a loss of function mutation in the *VHL* gene. The complete loss of function of *VHL* tumour suppressor gene is recognised as the cellular molecular lesion that causes the onset of different types of cancers. The probability of developing ccRCC is extremely high and, because this cancer is untreatable with classical chemotherapy, it ultimately leads patients to death.

Although many studies in Mammals on VHL syndrome have been carried out, fine *in vivo* modelling of cancerous processes in mammalian systems is disseminated of difficulties.

Pagliarini and colleagues formerly remarked that genetic studies in *Drosophila*, a relatively simple but multicellular organism, can impact our understanding of how mutations in TSGs and oncogenes affect organs and tissues, and can also contribute to find new genes functioning in the processes related to cancer biology (Pagliarini *et al.*, 2003).

At first sight, mammalian kidneys and *Drosophila* Malpighian tubules are terribly distant: their different morphology (glomerular and aglomerular renal structures, respectively) is accompanied by consequent diverse mechanisms of function (e.g., urine formation is driven by ultrafiltrate reabsorption in Mammals while in insects it requires an active transport). Nevertheless, basic tasks performed by the two systems are fundamentally similar: transport, excretion, and osmoregulation. Moreover, Dow and Romero have stressed that both renal functions, and the underlying genes responsible, are rather well conserved. Indeed, the use of *Drosophila* to model human pathologies has reached the best performance for renal diseases, since many of the human renal disease loci have *Drosophila* cognates that are both very close in sequence similarity and with enriched expression in the *Drosophila* tubule (Dow and Romero, 2010). With these presuppositions, I performed, in 2014, in Dr. Adryan lab at University of Cambridge, a genome-wide gene expression profiling of Malpighian tubules heterozygous for a loss of function mutation of *dVHL*, the *Drosophila* homolog of human *VHL* gene. I then used a range of bioinformatics tools to glean information from this high-throughput dataset to try to further elucidate the renal genetic network that (*d*)*VHL* is involved in. *Drosophila* genetic amenability and usefulness in enabling comparative genomic studies with humans make it an excellent model for gene expression studies in genetic background mimicking that of *VHL* disease patients.

## 6.3 Materials and methods

The *Drosophila* stock $y^{1}$, $w^{67c23}$; $dVHL^{1.1}$/CyO was obtained from Tien Hsu lab and was cultured as described in paragraph 3.1.1.

### 6.3.1 *Drosophila* Malpighian tubule RNA extraction

Females of the appropriate genotype were transferred every day into vials with fresh yeasted food for 5 days. Malpighian tubules were then dissected and instantly frozen at -80 °C in 10 µl of PBS. When tubules from 50 females were collected, they were pulled together, PBS was removed and 400 µl of TRIzol were added to the sample; then tubules were homogenised using a disposable polypropylene pestle. Homogenisation was carefully performed keeping the sample on ice, in order to avoid overheating. 10 µg of linear polyacrylamide were added before centrifuging the sample at 16000g for 10 minutes. Supernatant was then transferred to a new tube, so that it was free of cell debris. 80 µl of chloroform were added and the sample was vortexed for 60 s and then centrifuged at 16000g for 15 minutes. The upper phase was transferred to a new RNase-free tube, while the interphase and the lower phase were discarded. 0.8 volumes of isopropanol were added to the tube that was then gently mixed by inversion. The RNA was then let precipitate for 1 hour at -20°C. In order to pellet the RNA, the sample was centrifuged at 16000g for 30 minutes. The pellet was then washed with 500 µl of 70% ethanol in DEPC (Diethyl pyrocarbonate) milliQ water and centrifuged at 16000g for 5 minutes. The ethanol was then carefully and completely removed, also by letting the sample air drying, before re-suspending it in 15 µl of DEPC water. Finally, RNA concentration and purity was assessed through Nanodrop spectrophotometer. Further details at the FlyChip website: http://www.flychip.org.uk/.

### 6.3.2 cDNA generation, amplification and labelling

Briefly, to amplify the RNA, I used the SMART (Atlas Switch Mechanism At the 5' end of Reverse Transcript) method using the SMARTer™ PCR cDNA synthesis kit from Clontech. Amplified cDNA was then labelled by using the Klenow labelling of double stranded DNA protocol.

In more details, for the retrotranscription reaction, to 500 ng of desiccated RNA were added: 1 µl of microarray spike RNA as a positive hybridisation control; 1 µl of 10 µM 3' SMART CDS Primer IIA (a modified oligo(dT) primer, sequence: 5'-AAGCAGTGGTATCAACGCAGAGTACTTTTTTTTTTTTTTTTTTTTTTTTTTTTTTVN-3', V=G+A+C; N=A+C+G+T); 1 µl of 10 µM SMART IIA chimeric oligonucleotide (necessary to synthesise a double-stranded cDNA, sequence: 5'-AAGCAGTGGTATCAACGCAGAGTACGC888-3', 8=riboG). The mix was then incubated at 70 °C for 5 min, and then snap cooled on ice. Finally 2 µl of 5x first strand buffer, 0.5 µl of 0.1M Dithiothreitol, 0.5 µl of 50x dNTPs (10 mM), 1 µl of 200U/µl of SuperScript III polymerase and 1 µl of DEPC water were added to the mix and sample was then incubated at 46 °C for 1.5 hours and at the end snap cooled on ice.

For cDNA amplification, in order to determine the optimal number of cycles required for generating products in exponential phase, I performed a PCR using the Advantage® II PCR kit from Clontech and following manufacture's protocol (5' PCR Primer II used: 5'-AAGCAGTGGTATCAACGCAGAGT-3'). 2 µl of the PCR products from a parallel run of each sample were loaded at every second cycle, from cycle 16 to 24, on 1% agarose gel. After that, cDNA amplification was performed stopping the reaction at the previous determined cycle number. DNA was then purified using the QIAquick PCR purification columns and then 900 ng of cDNA of each sample were labelled through incorporation of dCTP conjugated with Cy3 or Cy5 dyes using the BioPrime DNA Labelling System and following manufacture's protocol. In details, for each sample, 900 ng of cDNA were diluted in 25 µl of DEPC water and then 20 µl of 2.5x Random Primer reaction buffer were added. Samples were then incubated at 99 °C for 5 min, and then soon snap cooled on ice. To each sample, were then added a mix made of 1 µl of 10x Low C-dNTP, 2 µl of Cy3-conjugated or Cy5-conjugated dCTP and 1 µl of the Klenow fragment (40 U/ µl) and then they were incubated at 37 °C for 2 hours. The reaction was stopped by adding 5 µl of the stop buffer (0.5 M $Na_2EDTA$, pH 8.0). The Cy3 and Cy5 labelled sample and control pairs were combined in 1.5 ml tubes and the volume was reduced to 25-30 µl in a SpeedVac concentrator before proceeding with Sephadex G50 purification (two per sample) in order to eliminate unincorporated dyes. Sephadex G50 columns were assembled following manufacture's instruction, then samples were pipetted onto the centre of the column and centrifuged in a microfuge for 1 min at 2400g. To reduce sample volumes to 2-5 µl, a SpeedVac concentrator was used. Finally, 2 µl of 10 mg/ml sonicated salmon sperm DNA were added, together with 140 µl of hybridisation buffer. Samples were then boiled at 100 °C for 2 min, centrifuged at 16000g for 1 min and then hybridised on slides. Further Further details at the FlyChip website: http://www.flychip.org.uk/.

### 6.3.3 FL004 hybridisation

The FlyChip in-house printed FL004 gene expression arrays were used. Four biological were performed. Dye swaps were included. Samples were hybridised to arrays in an *ad ho*c hybridisation station. Slides were first blocked for 30 min using a solution containing 0.1% BSA, 0.2% SDS, 2x SSC (300 mM NaCl, 30 mM Na citrate, pH 7). Then, 135 µl of samples were loaded on arrays and left hybridise for 16 hours at 65 °C with agitation. After hybridisation, slides were carefully washed 3 times with abundant warmed 0.2x SSC in agitation in order to rinse the non-hybridised samples and avoiding light exposure of slides.

The slides were then rinsed with MilliQ water for 3 seconds at room temperature and then transferred into a slide box with tissue paper, dried in a centrifuge at 96 g for 5 min, and transferred into a dry slide box. Further Further details at the FlyChip website: http://www.flychip.org.uk/.

### 6.3.4 Data acquisition and processing

Slides were scanned using an Axon GenePix 4000B scanner. The standard FlyChip data analysis was used: manually spot-finding was operated through Dapple (Buhler *et al.*, 2000) in order to check for any spot-finding mistakes and areas with high background. Then, the variance stabilising normalisation (vsn) was applied (Huber *et al.*, 2002). The thresholds used to find the differentially expressed genes were: average M value <-0.5 or >0.5 (where the M-value is the $\log_2$ of the ratio of sample vs control intensities), and p-value <0.1.

### 6.3.5 qRT-PCR

Malpighian tubule total RNA was extracted in TRI Reagent (Sigma-Aldrich) and then treated with TURBO DNase (Ambion) to remove contaminating DNA from RNA preparations. RNA was then reverse transcribed using the high-capacity RNA-to-cDNA kit (Applied Biosystems) according to the manufacture's protocol. Quantitative real-time PCRs were performed in fast 48-well reaction plates (Applied Biosystems) and analysed by StepOnePlus real-time PCR system (Applied Biosystems) according to the manufacturer's suggested procedure. Expression of the housekeeping gene *rp49* served as an internal reference gene. The primers used were:

*dGrip75* forward: 5'-TTGGAGTTCTGCTCCCAAAT-3'
*dGrip75* reverse: 5'-TCATCTGTGATTCCCGTGAC-3'
*CG31955* forward: 5'-GTGAGCCCAGAAAACAGAGC-3'
*CG31955* reverse: 5'-GCGTTCTCACGTGTTCCTTT-3'
*rp49* forward: 5'-TCTGCATGAGCAGGACCTC -3'
*rp49* reverse: 5'-ATCGGTTACGGATCGAACAA-3'

Dissociation curve analysis was performed to determine target specificity and target mRNA levels were normalised to that of *rp49*. Fold changes in gene of interest expression levels were evaluated by using the ΔΔCt method. Three biological replicates were analysed, each of which composed of Malpighian tubules dissected from 30 females. The mean fold change and SD were calculated.

## 6.4 Results

During my PhD, I spent 6 months at the Cambridge System Biology Centre at the University of Cambridge, in Boris Adryan lab. There I was introduced to functional genomics.

### 6.4.1 Overview of the microarray technology

Starting from 2000, when *Drosophila* genome was completely sequenced (Adams *et al.*, 2000), omics approaches have become familiar to drosophilists.

In a genome-wide gene expression study, the transcriptome of two samples is compared. Samples subjected to comparison may differ at genetic level (e.g., in a sample a mutation in a specific gene is present while in the other, representing the control, wild type copies of that gene are present) or could have been treated in a different way (e.g., a drug treatment has been performed and comparison is between a sample treated with the drug and a sample not treated, representing the mock). Samples could range from whole organisms (typically whole embryos in *Drosophila*) to single isolated tissues (e.g., ovaries) and, of course, cultured cells.

As soon as this microarray technology diffused, researchers in the developmental biology field started to get closer to this new approach. Indeed, the advantage in undertaking an omics study is that no hypothesis-driven results can be “forced”. On the other hand, interpretation in terms of functionality requires a strong effort and bioinformatics support.

The Dow lab first adopted the genome-wide gene expression technology to gain insight into the developmental biology of *Drosophila* Malpighian tubules; his studies greatly contributed to the understanding of physiology and function these organs. Particularly, by comparing the transcriptomes of whole flies versus Malpighian tubules with microarray technology, Dow group showed that more than 200 genes are more than 10-fold enriched in these organs. Among that genes there are 30 transcription factors, not previously implicated in tubule development (Wang *et al.*, 2004). This work dictated a new radical view on tubule functions.

In a typical microarray experiment, RNA from samples is extracted, reverse-transcribed, amplified if necessary and then labelled. This is achieved by using deoxynucleotide triphosphates (dNTPs) that have a dye molecule directly coupled to the base. After that, RNA is hybridised to a microarray. Microarrays are slides in which specific oligonucleotides have been printed in given positions (spots). Besides many types of microarrays do exist depending on the purpose of the research, two types of microarray platforms are commonly adopted: Affimetrix GeneChip, based on a single-channel technology (Lockhart *et al.*, 1996) and dual-channel microarray, developed in Brown lab (Schena *et al.*, 1995). In a single-channel microarray experiment, the two samples are hybridised to different arrays and the intensity differences are compared *a posteriori*. In a dual-channel experiment, instead, the two samples are labelled with different fluorophores, then combined and hybridised on the same array.

In order to account for technical variability and natural occurring gene expression variability among samples, biological replicates are needed. This allows to apply the power of statistics to evaluate unbiased gene expression differences.

Both in single-channel and dual-channel experiments, once hybridisation and scanning of arrays have been performed, the ratio of the intensities of each spot is quantified, thus providing a relative measure of the abundance of each mRNA. If a dual-channel experiment is performed, then usually at least a dye swap between biological replicates is included to avoid differences in gene expression due to the different capability of Cy3- and Cy5- conjugated dNTPs to be incorporated during reverse transcription phase.

Normalisation of the raw data follows. This phase allows to eliminate some of the technic-intrinsic variability (such as background of used slides and overall brightness). Many different techniques to achieve normalisation can be employed, also depending on the overall quality of the experiment performed. After normalisation, statistical evaluation of gene expression ratios is possible through application of bioinformatics competences. This allows thresholding and determination of gene lists for further analysis (Russell *et al.*, 2009).

### 6.4.2 Differentially expressed genes in *dVHL*$^{1.1}$/+ Malpighian tubules

Individuals that develop VHL pathology are genotypically heterozygous for a loss of function mutation of *VHL*. This genetic condition predisposes to ccRCC, that manifests when somatic inactivation of the wild type allele occurs. In order to identify genes which are sensible to *dVHL* functional copy number and that could be responsible for the somatic inactivation of the *dVHL* wild type allele, thus having a primary role in cancer onset, I performed a tubule-specific microarray study using the FL003 chip. This array is composed of transcript-specific oligonucleotides and controls developed by the International *Drosophila* Array Consortium (INDAC). I performed a gene expression comparison between 5-days old adult female Malpighian tubules heterozygous for a null mutation of *dVHL, dVHL*$^{1.1}$ (Duchi *et al.*, 2010; Hsouna *et al.*, 2010) and 5-days old wild type adult female tubules. The dual-channel technology was employed. I performed the microarray analysis at the FlyChip, so I used all the reagents and instruments here present.

200 Malpighian tubules per sample were dissected. 4 biological replicates of each genotype were collected, as FlyChip common policy requires. RNA extraction, reverse transcription, amplification and labelling were performed (see paragraphs 6.3.1 and 6.3.2) and samples were hybridised on INDAC FL003 *Drosophila* gene expression arrays. Two dye swaps were included. Many quality check controls were performed to ensure microarray data quality.

Once array were scanned, I used Dapple software for spot finding (Buhler *et al.*, 2000). Dapple is a program for the quantification of spots from the images resulting from scanning microarrays. It allows to find the spots, assess their quality and quantify the total fluorescence intensity. I checked manually all the arrays, removing those spots with no clear signal. Spot intensities were then also quantified in Dapple.

With regard to normalisation, I used the Variance Stabilisation and Normalisation (vsn) package, the standard FlyChip normalisation method. The highly stringent Limma package was used to assess the statistical significance.

Selection of the differentially expressed genes was based on p-values and average M values. The M value represents the $\log_2$ of differential expression ratio for each spot and is calculated as follows:

$$M=\log_2(Cy5/Cy3)$$

where Cy5 and Cy3 represent the fluorescence intensity of a given spot in the 2 channels. Given that, if M value is +1 it means that Cy5 is 2-fold higher than Cy3; if M value is +2 it means that Cy5 is 4-fold higher than Cy3 etc. Numbers of equal value but opposite sign indicate equivalent fold change but in the opposite direction.

The thresholds to identify differentially expressed genes were set as follows: average M-value <-0.5 or >0.5 with a p-value <0.1. It is more common to set the p-value as <0.05. I decided to double it for two reasons: first, we used a highly stringent statistical package, which ensures high fidelity. Second, we are working in a sensitised background, that is a heterozygous condition for a partially haploinsufficient gene: it appears that a higher tolerance should be adopted. With these statistical parameters, I recovered a total of 331 hit genes whose expression levels are altered in *dVHL*$^{1.1}$/+ tubules; 118 appears to be upregulated, while 213 downregulated (Figure 59A). I then also decided to better refine my analysis using R. R is an open source software that allows to professionally program in R language. It is of particular usefulness for data science. By compiling a R script I highlighted those genes for which in 3 out of 4 slides the M values are in the allowed range (Figure 59B). This kind of selection outlines genes for which alteration in gene expression is reliable (based on the reproducibility of the alteration). By crossing data reported in Figure 59A with those in Figure 59B, I found a total of 187 genes that met both requirements: 106 are downregulated while 81 are downregulated (Figure 59C).

### 6.4.3 GO analysis

In the attempt to classify in broad categories the upregulated and downregulated genes, I took advantage of the FlyMine tool for gene ontology (GO) enrichment in biological processes (Lyne *et al.*, 2007). To perform this analysis I applied a p-value $\leq 0.05$. This p-value was generated using the hypergeometric test and was not corrected for multiple testing. In Table 1, top 10 GO enrichment terms for both the upregulated and downregulated genes are listed. By looking at these GO terms, it appears that most of the altered genes are involved in metabolic as well as transport processes, crucial activities for cell homeostasis.

As it was pointed out in paragraph 6.1.1 both HIF-dependent as well as HIF-independent function of VHL are required to induce the phenotypic alterations observed both in flies and mammals. Thus, beside the results obtained through FlyMine, I also decided to perform an "inverse analysis": I screened my candidate list with the genes belonging to the GO terms of the biological processes implying canonical and non-canonical function of VHL. The specific GO category lists are downloadable from FlyMine. To screen my candidate list with GO terms I used R. Among the genes I recovered, concerning the classical VHL HIF-dependent functions, I found alterations (in both senses) in the expression levels of genes involved in the regulation of cell cycle, in the cellular response to hypoxia, glycolysis and development of tubular structures (Table 2, upper part). Moreover, concerning the HIF-independent functions, I found alterations in the expression levels of genes involved in endocytosis, protein phosphorylation, and extracellular matrix build-up (Table 2, lower part).

**Figure 59 Scatter plots of differentially expressed genes in *dVHL*$^{1.1}$/+ Malpighian tubules.** In each panel, genes are represented as black spots. They are 14 444, which is the number of transcript-specific probes spotted in FL003 slides. In each graph on the X axis is reported the A value. A is a measure of the overall brightness of the spot. It is calculated as the $\log_2$ intensity of the spot. In details, $A=\log_2(Cy3*Cy5)/2$. On the Y axis, the M value is reported. **(A)** Genes that satisfy the p value cut-off ($p<0.1$) are highlighted in red (if also the average M is $>0.5$) or blue (if also average M is $<-0.5$). **(B)** This graph highlights in green those genes for which the alteration in gene expression ($M>0.5$ or $M<-0.5$) was recovered in 3 out of 4 slides. **(C)** This graph overlaps the cut-off conditions of (A) and (B). Those genes that satisfy both criteria are highlighted with a red triangle.

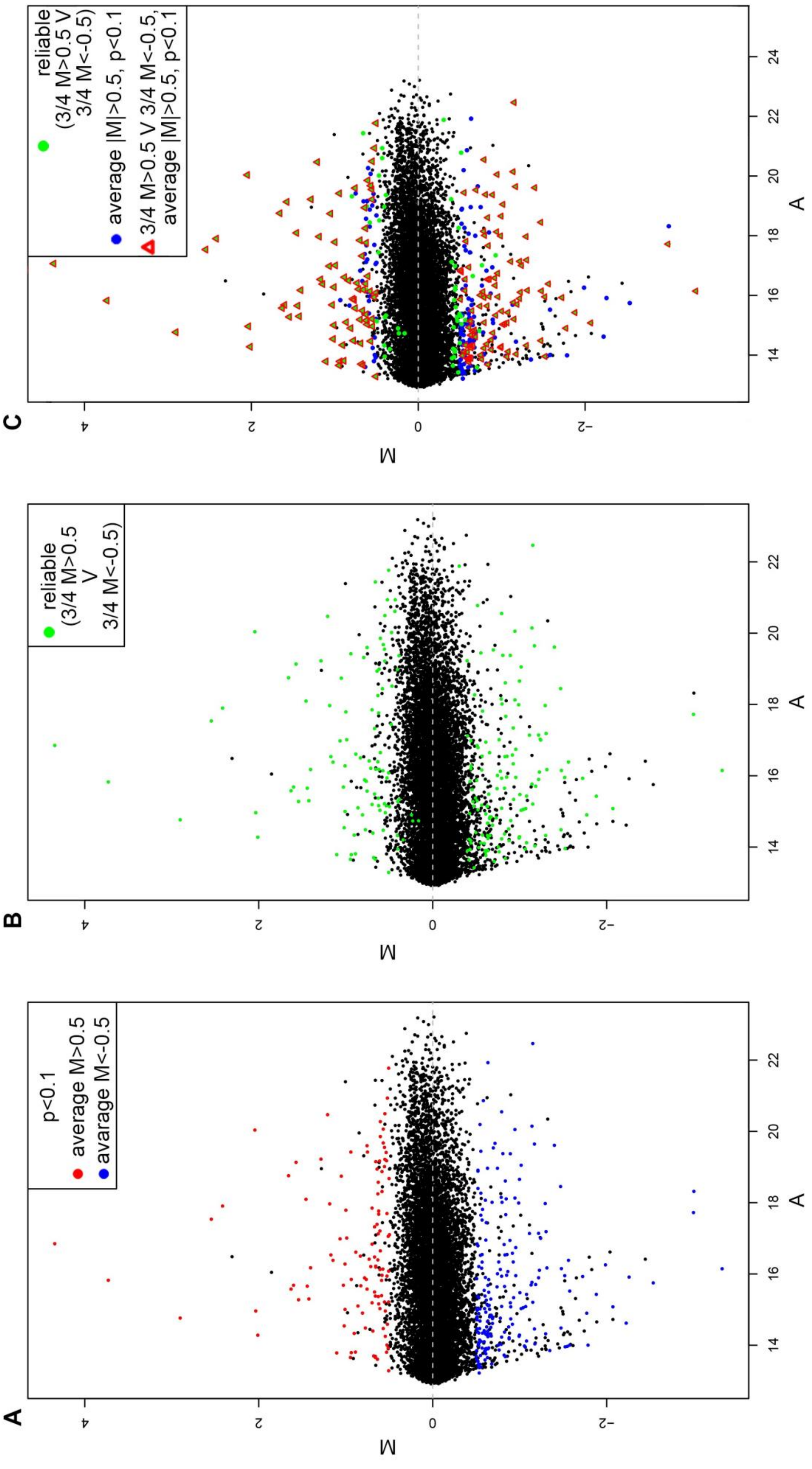
A
p<0.1
average M>0.5
avarage M<-0.5
M
4
2
0
-2
A
14
16
18
20
22
B
reliable
(3/4 M>0.5
V
3/4 M<-0.5)
M
4
2
0
-2
A
14
16
18
20
22
C
reliable
(3/4 M>0.5 V
3/4 M<-0.5)
average |M|>0.5, p<0.1
3/4 M>0.5 V 3/4 M<-0.5,
average |M|>0.5, p<0.1
M
4
2
0
-2
A
14
16
18
20
22
24

| **Gene Ontology(GO) term** | | **p-value** |
|---|---|---|
| | | |
| **Downregulated** | | |
| GO:0006325 | chromatin organization | 6.17E-07 |
| GO:0080163 | regulation of protein serine/threonine phosphatase activity | 2.08E-05 |
| GO:0043666 | regulation of phosphoprotein phosphatase activity | 1.50E-04 |
| GO:0009607 | response to biotic stimulus | 1.56E-04 |
| GO:0043207 | response to external biotic stimulus | 1.56E-04 |
| GO:0051707 | response to other organism | 1.56E-04 |
| GO:0043933 | macromolecular complex subunit organization | 2.62E-04 |
| GO:0010921 | regulation of phosphatase activity | 3.27E-04 |
| GO:0035304 | regulation of protein dephosphorylation | 3.88E-04 |
| GO:0035303 | regulation of dephosphorylation | 7.15E-04 |
| | | |
| **Upregulated** | | |
| GO:0006749 | glutathione metabolic process | 8.03E-08 |
| GO:0006575 | cellular modified amino acid metabolic process | 3.79E-07 |
| GO:0006790 | sulfur compound metabolic process | 3.15E-06 |
| GO:0015858 | nucleoside transport | 2.38E-05 |
| GO:1901642 | nucleoside transmembrane transport | 5.83E-05 |
| GO:1901264 | carbohydrate derivative transport | 2.75E-04 |
| GO:0044710 | single-organism metabolic process | 9.74E-04 |
| GO:0055114 | oxidation-reduction process | 0.001221 |
| GO:0015931 | nucleobase-containing compound transport | 0.002727 |
| GO:0006726 | eye pigment biosynthetic process | 0.003272 |

**Table 1 Top 10 GO terms significantly enriched.** This table was generated through FlyMine, $p<0.05$. In the upper part there is the top 10 GO terms enriched for the downregulated gene list, while in the lower part is the same for the upregulated gene list.

Among the recovered genes, some known interactors of VHL are present. As an example, in HEK-293 cell line, Cdc2c, the *Drosophila* homolog of CDK2 (Cyclin-dependent kinase 2), was shown to physically interact with VHL (Ewing *et al.*, 2007).

More recently it was shown that the checkpoint kinase-2 (encoded by the *lok* gene in *Drosophila*) binds to pVHL in case of DNA damage. This modification enhances pVHL-mediated transactivation of p53, by recruiting chromatin modification factors such as p300. It was also demonstrated that mutations of pVHL show a diminished ability to recruit coactivators, ultimately retarding p53-mediated growth arrest and apoptosis (Roe *et al.*, 2011).

I also screened my candidate list to find genes with DNA binding capability. Among them there are genes that encode transcription factors, such as *rno*. Rno is the *Drosophila* homolog of Jade1 and it was shown by a two-yeast hybrid screen to interact with VHL (Zhou *et al.*, 2002).

## HIF-dependent function of VHL

| FBgn | Gene Symbol | FlyAtlas Affy call | This array call |
|---|---|---|---|
| **Cell cycle** | | | |
| FBgn0002526 | LanA | down | down |
| FBgn0004107 | cdc2c | down | down |
| FBgn0019686 | lok | down | down |
| FBgn0011586 | e(r) | down | up |
| FBgn0050085 | Rif1 | down | down |
| FBgn0050291 | CG30291 | down | down |
| FBgn0051658 | Nnf1b | down | up |
| FBgn0011761 | dhd | down | down |
| FBgn0026431 | Grip75 | up | down |
| FBgn0026598 | Apc2 | down | up |
| FBgn0024227 | ial | down | down |
| FBgn0014189 | Hel25E | down | up |
| **Cellular response to hypoxia** | | | |
| FBgn0052296 | Mrtf | down | down |
| **Glycolisis** | | | |
| FBgn0038957 | CG7059 | up | down |
| **Open tracheal system development** | | | |
| FBgn0002526 | LanA | down | down |
| FBgn0016076 | vri | up | down |
| FBgn0052296 | Mrtf | down | down |
| FBgn0027363 | Stam | up | up |

## HIF-independent function of VHL

| FBgn | Gene Symbol | FlyAtlas Affy call | This array call |
|---|---|---|---|
| **Endocytosis** | | | |
| FBgn0027363 | Stam | Up | Up |
| **Protein phosphorylation** | | | |
| FBgn0004107 | cdc2c | down | down |
| FBgn0019686 | lok | down | down |
| FBgn0017581 | Lk6 | down | down |
| FBgn0020621 | Pkn | down | down |
| FBgn0050291 | CG30291 | down | down |
| FBgn0024227 | ial | down | down |
| FBgn0035089 | Phk-3 | none | up |
| **Extracellular matrix** | | | |
| FBgn0002526 | LanA | down | down |
| FBgn0036181 | Muc68Ca | up | down |
| FBgn0051901 | Mur29B | up | down |
| FBgn0001114 | Glt | down | down |

**Table 2 Genes with altered gene expression in *dVHL*$^{1.1}$/+ tubules segregated according to GO term.** The first column reports the Flybase ID, the second column the gene name or symbol accordingly to current usage. In the third column, up and down indicate that the gene is enriched or depleted in Malpighian tubules respect to the whole fly. None, instead, indicates that the gene expression is at the same level both in the whole fly and in the Malpighian tubules. These data are derived from FlyAtlas (Chintapalli *et al.*, 2007). In the fourth column up and down indicate that the gene is upregulated or downregulated, respectively, in *dVHL*$^{1.1}$/+ Malpighian tubules.

Cytoscape is an open source software platform for visualising complex networks and integrating these with any type of attribute data Shannon *et al.*, 2003. Boris Adryan, using Cytoscape, developed a map of connections between *Drosophila* genes, based on the physic and genetic interactions of gene products and also based on their so highly coincident expression patterns that allow to hypothesise a relationship between them (Adryan, unpublished). On this “interactomic map”, I was able to integrate data coming from my microarray experiment. The output network is reported in Figure 60. One half of the genes that are differently expressed in *dVHL*$^{1.1}$/+ Malpighian tubules are positively integrated in the interactomic map, suggesting that a relationship among these genes is subtended. For the other half of genes, no interaction with others was found (not reported in Figure 60).

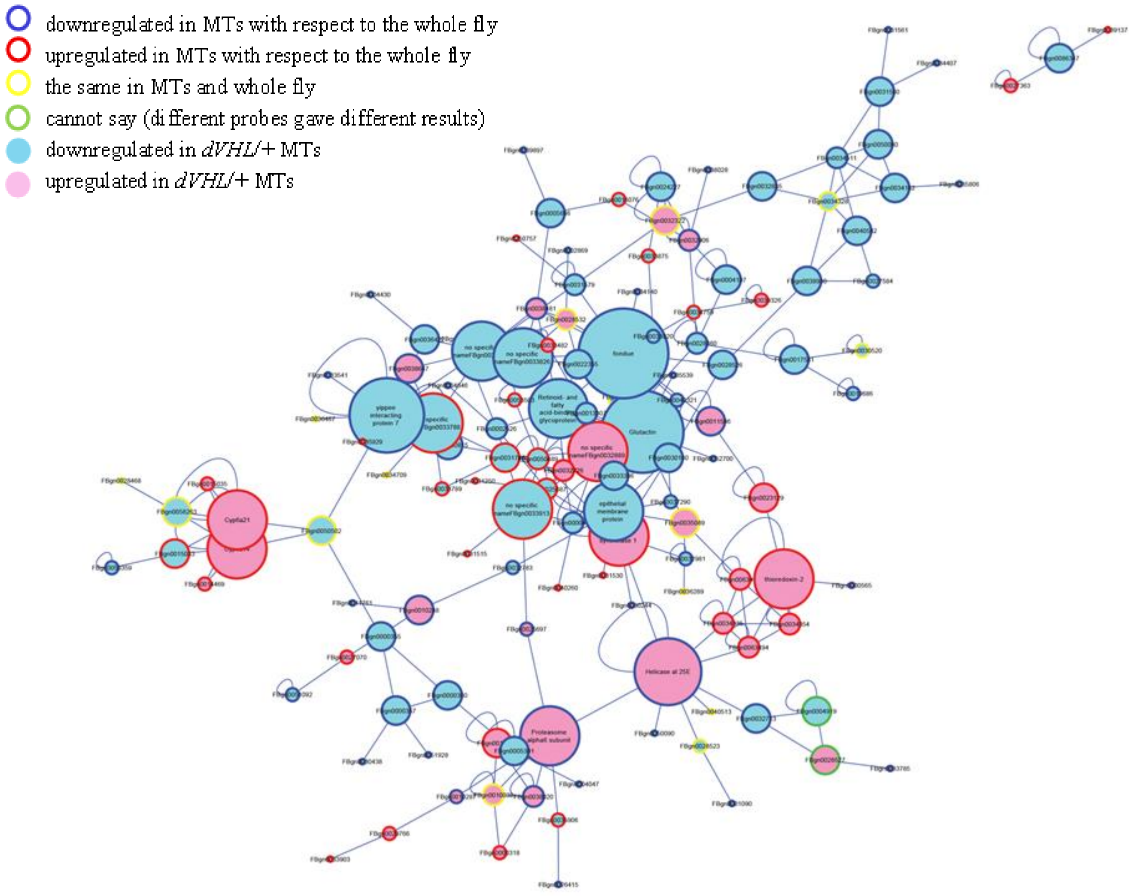
downregulated in MTs with respect to the whole fly
upregulated in MTs with respect to the whole fly
the same in MTs and whole fly
cannot say (different probes gave different results)
downregulated in dVHL/+ MTs
upregulated in dVHL/+ MTs
fondue
Glutactin
yippee interacting protein 7
Retinoid- and fatty acid-binding glycoprotein
epithelial membrane protein
Cyp6a21
thioredoxin-2
Helicase at 25E
Proteasome alpha6 subunit

**Figure 60 Interaction map of genes significantly altered in *dVHL*$^{1.1}$/+ Malpighian tubules.** The map highlights the existence of interactions among genes. Blue outlined genes and red outlined genes are downregulated and upregulated in Malpighian tubules respect to the whole fly, respectively. Yellow outlined genes have the same expression level in Malpighian tubules and in the whole fly, while green outlined genes have an uncertain expression in Malpighian tubules (data from FlyAtlas, Chintapalli *et al.*, 2007). Light blue colour filled genes and pink colour filled genes are downregulated and upregulated in *dVHL*$^{1.1}$/+ Malpighian tubules respectively. The bigger the circle the more connections the gene has.

### 6.4.4 Validation

The qRT-PCR is a technique that allows to measure the expression level of a selected gene respect to an internal reference gene (typically *rp49* or *Gapdh* are chosen as internal reference genes). It is also possible to compare the expression level of the selected gene between multiple samples respect to the same reference gene. This is a way to know the relative expression of the selected gene among samples. For this reason, usually the results obtained by a microarray experiment are validated by qRT-PCR. Generally a handful of genes are selected and their expression is evaluated by qRT-PCR. The RNA used in the qRT-PCR experiment should be from biological samples other than those used to perform the microarray analysis. Moreover, some biological replicates are also required to apply statistical significance to the qRT-PCR results. If these results are consistent with that from the microarray experiment, then the latter is validated.

In order to validate the results obtained from the microarray analysis, I therefore collected 40 Malpighian tubules from 5-days old *dVHL*$^{1.1}$/+ and wild type females. 3 biological replicates were included. Genes selected for validation are: *CG31955* and *dGrip75*. The internal reference gene used was *rp49*. Results are reported in Figure 61. Both *CG31955* and *dGrip75* are downregulated in *dVHL*$^{1.1}$/+ Malpighian tubules, as showed by both microarray and qRT-PCR analyses. These findings contribute to the validation of the microarray data.

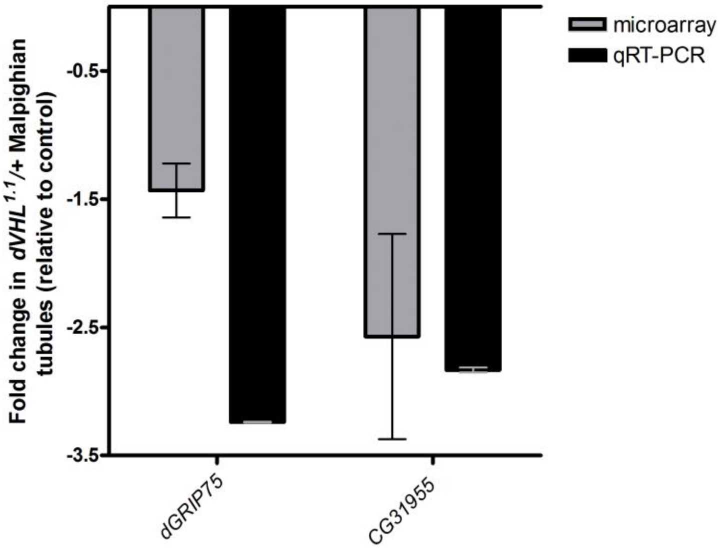

**Figure 61 Validation of microarray results by qRT-PCR.** Tubules from 5-days old *dVHL*$^{1.1}$/+ and wild type females were analysed. Gene specific primers were used in the qRT-PCR reaction to quantify mRNA transcripts. The qRT-PCR results (in black) derive from 3 independent biological replicates. The microarray data (in grey) derive from 4 biological replicates. qRT-PCR results are in accordance with microarray data.

## 6.5 Discussion

VHL disease is a syndrome with a well-recognised genetic base. Indeed, VHL patients are genetically heterozygous for a null mutation of the *VHL* gene. This genetic condition enhances the possibility that cells also loose the function of the other *VHL* copy, especially through somatic inactivation mediated by epigenetic alterations. The complete loss of function of the *VHL* locus determines the onset of cancerous phenotypes: indeed, VHL patients develop during their lives several types of tumours (Maher *et al.*, 2011). Most of such tumours arise in specific organs, especially the kidneys: the development of ccRCC represents a death sentence for the majority of VHL patients. Interestingly, loss of function mutations in the *VHL* gene are often also recovered in the sporadic cases of ccRCC, suggesting that *VHL* function is critical to maintain renal cell physiology and homeostasis (Kaelin, 2007). In this scenario, it appears that *VHL* is an haploinsufficient gene and that the complete loss of function of this gene ultimately leads to cancer onset.

It is undeniable that the identification of the gene functions that are more sensible to *VHL* gene dosage and thus that are more susceptible to be early altered in *VHL* heterozygotes could help in shedding light on the pathogenesis of the VHL syndrome and ultimately in identifying potential drug targets to impede cancer onset or progression. In this research vein could be inserted the genome-wide gene expression profiling I performed. It is worth noting that among the downregulated genes, the GO term with the highest score is chromatin organisation. Among the GO classes directly related to this GO term there are those referring to epigenetic modifications, such as chromatin remodelling, chromatin silencing, histone (de)acetylation and others. Establishment and maintenance of chromatin architecture is essential for cell identity and indeed it is broadly accepted that cancer is not simply a genetic disease but genetic and epigenetic alterations are both co-opted mechanisms driving tumorigenesis (Brower, 2011). The role of epigenetics in tumorigenesis was firmly demonstrated by Herman and colleagues in 1994, and chance would have that *VHL* was the target of their study. The authors indeed showed that in patients affected by sporadic ccRCC, the cancerous cells displayed silencing of both the *VHL* gene copies through promoter hypermethylation (Herman *et al.*, 1994). Since then, many other studies have followed investigating the role of epigenetic modifications in ccRCC and many affected genes have been found (Shenoy *et al.*, 2015; Shenoy and Pagliaro, 2016). It is also worth noting that in 2016 Peri and colleagues published a work in which they performed a genome-wide transcriptome analysis by using histologically normal renal cell lines from VHL patients (thus heterozygotes for a loss of function mutation of *VHL*) to monitor the earliest gene expression changes associated with a single-allele inactivation of this TSG. They found that, among the differentially expressed genes, many were associated with the GO term of histone acetylation (Peri *et al.*, 2016). It would be important to cross-check *Drosophila* and human cell data in order to identify strong hits whose gene expression alterations are recovered in both systems. *Drosophila* could then offer the possibility to genetically dissect the molecular pathways linking the *VHL* gene function and these hits.

Moreover, among the downregulated genes, I also recovered many GO terms associated with dephosphorylation activities. Awd displays an histidine-dependent protein kinase activity and phosphorylation mediated by many different types of kinases is a post-translational modification occurring during activation of several signalling pathways (e.g., those mediated by receptor tyrosine kinases, RTKs, Singh *et al.*, 2017). The dephosphorylation events are then essential for signal attenuation. Defective downregulation of RTKs can lead to cancer (Bache *et al.*, 2004). In light of these considerations, it would be important to understand which signalling pathways are impacted by alterations in the phosphorylation activities I recovered.

Among the upregulated genes I recovered in my analysis, the GO terms with the highest scores are associated with cell metabolism. Modification of cell metabolism in tumour cells and its adaptation to oxygen-depleted conditions are key events sustaining cancer growth and aggressiveness (Sajnani *et al.*, 2017). This is of particular interest for *VHL*, whose canonical function are linked to the regulation of HIF-1$\alpha$ stability. The VHL/HIF-1$\alpha$ axis is widely recognised as the major regulator of cell adaptive responsiveness to oxygen tension, which also include regulation of cell metabolism. Indeed, metabolic reprogramming/deregulated cellular energetics is a cancer hallmarks (Hanahan and Weinberg, 2011). One of the most-cited modification of cell metabolism occurring in tumour cells is the switch to glycolic energetics, even in presence of normal oxygen levels. This phenomenon of aerobic glycolysis is also known as Warburg effect (Warburg *et al.*, 1927) and the prototypical Warburg cancer is, indeed, ccRCC (Potter *et al.*, 2016). Given these considerations, alteration in metabolic processes where expected in *VHL* heterozygotes. Future studies will be addressed to further understand the role of the altered genes belonging to these GO terms in cancer progression.

The possibility to insert the upregulated and downregulated genes into a network of gene interactions and signalling pathway crosstalk could illuminate on the consequences of the *VHL* gene lesion. However, even if such kind of omics approaches are potent and allow a global view of the gene expression profile, functional studies are strictly required in order to genetically dissect gene functions and the molecular pathways in which they are involved.

This is a typical inverse genetic approach and, in this sense, candidate lists like those coming from microarray experiments can fuel the whole career of a researcher.

# Chapter 7

## Bibliography

Adams M.D., Celniker S.E., Holt R.A., Evans C.A., Gocayne J.D., Amanatides P.G., Scherer S.E., Li P.W., Hoskins R.A., Galle R.F. *et al.*, *The genome sequence of Drosophila melanogaster,* Science (2000), *287*, 2185-2195.

Adryan B., Decker H.J., Papas T.S. and Hsu T., *Tracheal development and the von Hippel-Lindau tumor suppressor homolog in Drosophila,* Oncogene (2000), *19*, 2803-2811.

Aldaz S. and Escudero L.M., *Imaginal discs,* Curr Biol (2010), *20*, R429-431.

Althauser C., Jordan K.C., Deng W.M. and Ruohola-Baker H., *Fringe-dependent notch activation and tramtrack function are required for specification of the polar cells in Drosophila oogenesis,* Dev Dyn (2005), *232*, 1013-1020.

Andersen D.S., Colombani J. and Leopold P., *Coordination of organ growth: principles and outstanding questions from the world of insects,* Trends Cell Biol (2013), *23*, 336-344.

Anzinger J., Malmquist N.A., Gould J. and Buxton I.L., *Secretion of a nucleoside diphosphate kinase (Nm23-H2) by cells from human breast, colon, pancreas and lung tumors,* Proc West Pharmacol Soc (2001), *44*, 61-63.

Arnaud-Dabernat S., Bourbon P.M., Dierich A., Le Meur M. and Daniel J.Y., *Knockout mice as model systems for studying nm23/NDP kinase gene functions. Application to the nm23-M1 gene,* J Bioenerg Biomembr (2003), *35*, 19-30.

Arquier N. and Leopold P., *Fly foie gras: modeling fatty liver in Drosophila,* Cell Metab (2007)*, 5*, 83-85.

Artavanis-Tsakonas S., Matsuno K. and Fortini M.E., *Notch signaling,* Science (1995), *268*, 225-232.

Artavanis-Tsakonas S. and Muskavitch M.A., *Notch: the past, the present, and the future,* Curr Top Dev Biol (2010), *92*, 1-29.

Aso T., Yamazaki K., Aigaki T. and Kitajima S., *Drosophila von Hippel-Lindau tumor suppressor complex possesses E3 ubiquitin ligase activity,* Biochem Biophys Res Commun (2000), *276*, 355-361.

Assa-Kunik E., Torres I.L., Schejter E.D., Johnston D.S. and Shilo B.Z., *Drosophila follicle cells are patterned by multiple levels of Notch signaling and antagonism between the Notch and JAK/STAT pathways,* Development (2007), *134*, 1161-1169.

Attrill H., Falls K., Goodman J.L., Millburn G.H., Antonazzo G., Rey A.J., Marygold S.J. and FlyBase C., *FlyBase: establishing a Gene Group resource for Drosophila melanogaster,* Nucleic Acids Res (2016), *44*, D786-792.

Attwood P.V. and Wieland T., *Nucleoside diphosphate kinase as protein histidine kinase,* Naunyn Schmiedebergs Arch Pharmacol (2015), *388*, 153-160.

Bacac M. and Stamenkovic I., *Metastatic cancer cell,* Annu Rev Pathol (2008), *3*, 221-247.

Bache K.G., Slagsvold T. and Stenmark H., *Defective downregulation of receptor tyrosine kinases in cancer,* EMBO J (2004)*, 23*, 2707-2712.

Bader H.L. and Hsu T., *Systemic VHL gene functions and the VHL disease,* FEBS Lett (2012), *586*, 1562-1569.

Baillat G., Gaillard S., Castets F. and Monneron A., *Interactions of phocein with nucleoside-diphosphate kinase, Eps15, and Dynamin I,* J Biol Chem (2002)*, 277*, 18961-18966.

Baines A.C. and Zhang B., *Receptor-mediated protein transport in the early secretory pathway,* Trends Biochem Sci (2007), *32*, 381-388.

Baonza A., Roch F. and Martin-Blanco E., *DER signaling restricts the boundaries of the wing field during Drosophila development,* Proc Natl Acad Sci U S A (2000), *97*, 7331-7335.

Baron M., *Endocytic routes to Notch activation,* Semin Cell Dev Biol (2012), *23*, 437-442.

Biggs J., Tripoulas N., Hersperger E., Dearolf C. and Shearn A., *Analysis of the lethal interaction between the prune and Killer of prune mutations of Drosophila,* Genes Dev (1988), *2*, 1333-1343.

Biggs J., Hersperger E., Steeg P.S., Liotta L.A. and Shearn A., *A Drosophila gene that is homologous to a mammalian gene associated with tumor metastasis codes for a nucleoside diphosphate kinase,* Cell (1990), *63*, 933-940.

Bilitou A., Watson J., Gartner A. and Ohnuma S., *The NM23 family in development,* Mol Cell Biochem (2009), *329*, 17-33.

Bischof J., Maeda R.K., Hediger M., Karch F. and Basler K., *An optimized transgenesis system for Drosophila using germ-line-specific phiC31 integrases,* Proc Natl Acad Sci U S A (2007), *104*, 3312-3317.

Bloch Qazi M.C., Heifetz Y. and Wolfner M.F., *The developments between gametogenesis and fertilization: ovulation and female sperm storage in Drosophila melanogaster,* Dev Biol (2003), *256*, 195-211.

Blochlinger K., Bodmer R., Jan L.Y. and Jan Y.N., *Patterns of expression of cut, a protein required for external sensory organ development in wild-type and cut mutant Drosophila embryos,* Genes Dev (1990), *4*, 1322-1331.

Boissan M., Dabernat S., Peuchant E., Schlattner U., Lascu I. and Lacombe M.L., *The mammalian Nm23/NDPK family: from metastasis control to cilia movement,* Mol Cell Biochem (2009), *329*, 51-62.

Boissan M., De Wever O., Lizarraga F., Wendum D., Poincloux R., Chignard N., Desbois-Mouthon C., Dufour S., Nawrocki-Raby B., Birembaut P. *et al., Implication of metastasis suppressor NM23-H1 in maintaining adherens junctions and limiting the invasive potential of human cancer cells,* Cancer Res (2010), *70*, 7710-7722.

Boissan M. and Lacombe M.L., *[NM23, an example of a metastasis suppressor gene],* Bull Cancer (2012), *99*, 431-440.

Boissan M., Montagnac G., Shen Q., Griparic L., Guitton J., Romao M., Sauvonnet N., Lagache T., Lascu I., Raposo G. *et al., Membrane trafficking. Nucleoside diphosphate kinases fuel dynamin superfamily proteins with GTP for membrane remodeling,* Science (2014), *344*, 1510-1515.

Bosnar M.H., Bago R. and Cetkovic H., *Subcellular localization of Nm23/NDPK A and B isoforms: a reflection of their biological function?,* Mol Cell Biochem (2009), *329*, 63-71.

Brand A.H. and Perrimon N., *Targeted gene expression as a means of altering cell fates and generating dominant phenotypes,* Development (1993), *118*, 401-415.

Bray S., *Notch signalling in Drosophila: three ways to use a pathway,* Semin Cell Dev Biol (1998), *9*, 591-597.

Bray S.J., *Notch signalling in context,* Nat Rev Mol Cell Biol (2016), *17*, 722-735.

Brogiolo W., Stocker H., Ikeya T., Rintelen F., Fernandez R. and Hafen E., *An evolutionarily conserved function of the Drosophila insulin receptor and insulin-like peptides in growth control,* Curr Biol (2001), *11*, 213-221.

Brook W.J. and Cohen S.M., *Antagonistic interactions between wingless and decapentaplegic responsible for dorsal-ventral pattern in the Drosophila Leg,* Science (1996), *273*, 1373-1377.

Brower V., *Epigenetics: Unravelling the cancer code,* Nature (2011), *471*, S12-13.

Bryant P.J. and Schmidt O., *The genetic control of cell proliferation in Drosophila imaginal discs,* J Cell Sci Suppl (1990), *13*, 169-189.

Brzozowa-Zasada M., Piecuch A., Dittfeld A., Mielanczyk L., Michalski M., Wyrobiec G., Harabin-Slowinska M., Kurek J. and Wojnicz R., *Notch signalling pathway as an oncogenic factor involved in cancer development,* Contemp Oncol (Pozn) (2016), *20*, 267-272.

Bucci C., Parton R.G., Mather I.H., Stunnenberg H., Simons K., Hoflack B. and Zerial M., *The small GTPase rab5 functions as a regulatory factor in the early endocytic pathway,* Cell (1992), *70*, 715-728.

Bucci C., Thomsen P., Nicoziani P., McCarthy J. and van Deurs B., *Rab7: a key to lysosome biogenesis,* Mol Biol Cell (2000), *11*, 467-480.

Buhler J., Ideker T. and Haynor D., *Dapple: Improved Techniques for Finding Spots on DNA Microarrays,* UW CSE Technical Report UWTR 2000-08-05 (2000).

Buszczak M. and Segraves W.A., *Insect metamorphosis: out with the old, in with the new,* Curr Biol (2000), *10*, R830-833.

Butterworth F.M., Bodenstein D. and King R.C., *Adipose Tissue of Drosophila Melanogaster. I. An Experimental Study of Larval Fat Body,* J Exp Zool (1965), *158*, 141-153.

Cadigan K.M., *Regulating morphogen gradients in the Drosophila wing,* Semin Cell Dev Biol (2002), *13*, 83-90.

Canavoso L.E., Jouni Z.E., Karnas K.J., Pennington J.E. and Wells M.A., *Fat metabolism in insects,* Annu Rev Nutr (2001), *21*, 23-46.

Cavaliere V., Taddei C. and Gargiulo G., *Apoptosis of nurse cells at the late stages of oogenesis of Drosophila melanogaster,* Dev Genes Evol (1998), *208*, 106-112.

Cavaliere V., Bernardi F., Romani P., Duchi S. and Gargiulo G., *Building up the Drosophila eggshell: first of all the eggshell genes must be transcribed,* Dev Dyn (2008), *237*, 2061-2072.

Cavodeassi F., Rodriguez I. and Modolell J., *Dpp signalling is a key effector of the wing-body wall subdivision of the Drosophila mesothorax,* Development (2002), *129*, 3815-3823.

Cetkovic H., Perina D., Harcet M., Mikoc A. and Herak Bosnar M., *Nme family of proteins--clues from simple animals,* Naunyn Schmiedebergs Arch Pharmacol (2015), *388*, 133-142.

Chaffer C.L. and Weinberg R.A., *A perspective on cancer cell metastasis,* Science (2011), *331*, 1559-1564.

Chambers A.F., Groom A.C. and MacDonald I.C., *Dissemination and growth of cancer cells in metastatic sites,* Nat Rev Cancer (2002), *2*, 563-572.

Chen M.S., Obar R.A., Schroeder C.C., Austin T.W., Poodry C.A., Wadsworth S.C. and Vallee R.B., *Multiple forms of dynamin are encoded by shibire, a Drosophila gene involved in endocytosis,* Nature (1991), *351*, 583-586.

Chintapalli V.R., Wang J. and Dow J.A., *Using FlyAtlas to identify better Drosophila melanogaster models of human disease,* Nat Genet (2007), *39*, 715-720.

Cocucci E., Racchetti G. and Meldolesi J., *Shedding microvesicles: artefacts no more,* Trends Cell Biol (2009), *19*, 43-51.

Cohen S.M., *Imaginal disc development*, Cold Spring Harbor Laboratory Press (1993, Plainview, N.Y.).

Colombani J., Raisin S., Pantalacci S., Radimerski T., Montagne J. and Leopold P., *A nutrient sensor mechanism controls Drosophila growth,* Cell (2003), *114*, 739-749.

Conery A.R., Sever S. and Harlow E., *Nucleoside diphosphate kinase Nm23-H1 regulates chromosomal stability by activating the GTPase dynamin during cytokinesis,* Proc Natl Acad Sci U S A (2010), *107*, 15461-15466.

Dammai V., Adryan B., Lavenburg K.R. and Hsu T., *Drosophila awd, the homolog of human nm23, regulates FGF receptor levels and functions synergistically with shi/dynamin during tracheal development,* Genes Dev (2003), *17*, 2812-2824.

Davies S.A., Overend G., Sebastian S., Cundall M., Cabrero P., Dow J.A. and Terhzaz S., *Immune and stress response 'cross-talk' in the Drosophila Malpighian tubule,* J Insect Physiol (2012), *58*, 488-497.

de Celis J.F., Garcia-Bellido A. and Bray S.J., *Activation and function of Notch at the dorsal-ventral boundary of the wing imaginal disc,* Development (1996), *122*, 359-369.

de Celis J.F. and Bray S., *Feed-back mechanisms affecting Notch activation at the dorsoventral boundary in the Drosophila wing,* Development (1997), *124*, 3241-3251.

De Celis J.F., *Pattern formation in the Drosophila wing: The development of the veins,* Bioessays (2003), *25*, 443-451.

de Cuevas M., Lilly M.A. and Spradling A.C., *Germline cyst formation in Drosophila,* Annu Rev Genet (1997), *31*, 405-428.

Dearolf C.R., Hersperger E. and Shearn A., *Developmental consequences of awdb3, a cell-autonomous lethal mutation of Drosophila induced by hybrid dysgenesis,* Dev Biol (1988a), *129*, 159-168.

Dearolf C.R., Tripoulas N., Biggs J. and Shearn A., *Molecular consequences of awdb3, a cell-autonomous lethal mutation of Drosophila induced by hybrid dysgenesis,* Dev Biol (1988b), *129,* 169-178.

Deitcher D., *Exocytosis, endocytosis, and development,* Semin Cell Dev Biol (2002), *13,* 71-76.

Delanoue R., Meschi E., Agrawal N., Mauri A., Tsatskis Y., McNeill H. and Leopold P., *Drosophila insulin release is triggered by adipose Stunted ligand to brain Methuselah receptor,* Science (2016), *353,* 1553-1556.

Delgehyr N., Wieland U., Rangone H., Pinson X., Mao G., Dzhindzhev N.S., McLean D., Riparbelli M.G., Llamazares S., Callaini G. *et al., Drosophila Mgr, a Prefoldin subunit cooperating with von Hippel Lindau to regulate tubulin stability,* Proc Natl Acad Sci U S A (2012), *109,* 5729-5734.

Deng W.M., Althauser C. and Ruohola-Baker H., *Notch-Delta signaling induces a transition from mitotic cell cycle to endocycle in Drosophila follicle cells,* Development (2001), *128,* 4737-4746.

Denholm B., Sudarsan V., Pasalodos-Sanchez S., Artero R., Lawrence P., Maddrell S., Baylies M. and Skaer H., *Dual origin of the renal tubules in Drosophila: mesodermal cells integrate and polarize to establish secretory function,* Curr Biol (2003), *13,* 1052-1057.

Denholm B. and Skaer H., *Bringing together components of the fly renal system,* Curr Opin Genet Dev (2009), *19,* 526-532.

DeSantis C.E., Lin C.C., Mariotto A.B., Siegel R.L., Stein K.D., Kramer J.L., Alteri R., Robbins A.S. and Jemal A., *Cancer treatment and survivorship statistics, 2014,* CA Cancer J Clin (2014), *64,* 252-271.

Desvignes T., Pontarotti P., Fauvel C. and Bobe J., *Nme protein family evolutionary history, a vertebrate perspective,* BMC Evol Biol (2009), *9,* 256.

Dollar G., Struckhoff E., Michaud J. and Cohen R.S., *Rab11 polarization of the Drosophila oocyte: a novel link between membrane trafficking, microtubule organization, and oskar mRNA localization and translation,* Development (2002), *129,* 517-526.

Domanitskaya E. and Schupbach T., *CoREST acts as a positive regulator of Notch signaling in the follicle cells of Drosophila melanogaster,* J Cell Sci (2012), *125*, 399-410.

Dong J.T., Suzuki H., Pin S.S., Bova G.S., Schalken J.A., Isaacs W.B., Barrett J.C. and Isaacs J.T., *Down-regulation of the KAI1 metastasis suppressor gene during the progression of human prostatic cancer infrequently involves gene mutation or allelic loss,* Cancer Res (1996), *56*, 4387-4390.

Dow J.A., Maddrell S.H., Gortz A., Skaer N.J., Brogan S. and Kaiser K., *The malpighian tubules of Drosophila melanogaster: a novel phenotype for studies of fluid secretion and its control,* J Exp Biol (1994), *197*, 421-428.

Dow J.A. and Davies S.A., *The Malpighian tubule: rapid insights from post-genomic biology,* J Insect Physiol (2006), *52*, 365-378.

Dow J.A. and Romero M.F., *Drosophila provides rapid modeling of renal development, function, and disease,* Am J Physiol Renal Physiol (2010), *299*, F1237-1244.

Duchi S., Fagnocchi L., Cavaliere V., Hsouna A., Gargiulo G. and Hsu T., *Drosophila VHL tumor-suppressor gene regulates epithelial morphogenesis by promoting microtubule and aPKC stability,* Development (2010), *137*, 1493-1503.

Ewing R.M., Chu P., Elisma F., Li H., Taylor P., Climie S., McBroom-Cerajewski L., Robinson M.D., O'Connor L., Li M. *et al., Large-scale mapping of human protein-protein interactions by mass spectrometry,* Mol Syst Biol (2007), *3*, 89.

Faguet G.B., *The war on cancer : an anatomy of failure, a blueprint for the future,* Springer (2005, Dordrecht).

Fan Z., Beresford P.J., Oh D.Y., Zhang D. and Lieberman J., *Tumor suppressor NM23-H1 is a granzyme A-activated DNase during CTL-mediated apoptosis, and the nucleosome assembly protein SET is its inhibitor,* Cell (2003), *112*, 659-672.

Fang X., Zhou J., Liu W., Duan X., Gala U., Sandoval H., Jaiswal M. and Tong C., *Dynamin Regulates Autophagy by Modulating Lysosomal Function,* J Genet Genomics (2016), *43*, 77-86.

Farrell J.A. and O'Farrell P.H., *From egg to gastrula: how the cell cycle is remodeled during the Drosophila mid-blastula transition,* Annu Rev Genet (2014), *48*, 269-294.

Fehon R.G., Kooh P.J., Rebay I., Regan C.L., Xu T., Muskavitch M.A. and Artavanis-Tsakonas S., *Molecular interactions between the protein products of the neurogenic loci Notch and Delta, two EGF-homologous genes in Drosophila,* Cell (1990), *61*, 523-534.

Fessler J.H. and Fessler L.I., *Drosophila extracellular matrix,* Annu Rev Cell Biol (1989), *5*, 309-339.

Fiuza U.M. and Arias A.M., *Cell and molecular biology of Notch,* J Endocrinol (2007), *194*, 459-474.

Foley K. and Cooley L., *Apoptosis in late stage Drosophila nurse cells does not require genes within the H99 deficiency,* Development (1998), *125*, 1075-1082.

Fortini M.E., *Gamma-secretase-mediated proteolysis in cell-surface-receptor signalling,* Nat Rev Mol Cell Biol (2002), *3*, 673-684.

Fortini M.E., *Notch signaling: the core pathway and its posttranslational regulation,* Dev Cell (2009), *16*, 633-647.

Fortini M.E. and Bilder D., *Endocytic regulation of Notch signaling,* Curr Opin Genet Dev (2009), *19*, 323-328.

Franch-Marro X., Wendler F., Guidato S., Griffith J., Baena-Lopez A., Itasaki N., Maurice M.M. and Vincent J.P., *Wingless secretion requires endosome-to-Golgi retrieval of Wntless/Evi/Sprinter by the retromer complex,* Nat Cell Biol (2008), *10*, 170-177.

Fristrom D. and Fristrom J.W., *The metamorphic development of the adult epidermis,* Cold Spring Harbor Laboratory Press (1993, Plainview, N.Y.).

Fujimoto Y., Ohtake T., Nishimori H., Ikuta K., Ohhira M., Ono M. and Kohgo Y., *Reduced expression and rare genomic alteration of nm23-H1 in human hepatocellular carcinoma and hepatoma cell lines,* J Gastroenterol (1998), *33*, 368-375.

Furriols M. and Bray S., *A model Notch response element detects Suppressor of Hairless-dependent molecular switch,* Curr Biol (2001), *11*, 60-64.

Garcia-Bellido A., Ripoll P. and Morata G., *Developmental compartmentalisation of the wing disk of Drosophila,* Nat New Biol (1973), *245,* 251-253.

Gnarra J.R., Tory K., Weng Y., Schmidt L., Wei M.H., Li H., Latif F., Liu S., Chen F., Duh F.M. *et al., Mutations of the VHL tumour suppressor gene in renal carcinoma,* Nat Genet (1994), *7,* 85-90.

Go M.J., Eastman D.S. and Artavanis-Tsakonas S., *Cell proliferation control by Notch signaling in Drosophila development*, Development (1998), *125*, 2031-2040.

Godt D. and Tepass U., *Drosophila oocyte localization is mediated by differential cadherin-based adhesion,* Nature (1998), *395,* 387-391.

Golic K.G. and Lindquist S., *The FLP recombinase of yeast catalyzes site-specific recombination in the Drosophila genome,* Cell (1989), *59*, 499-509.

Gomez-Skarmeta J.L., Campuzano S. and Modolell J., *Half a century of neural prepatterning: the story of a few bristles and many genes,* Nat Rev Neurosci (2003), *4,* 587-598.

Gonzalez-Jamett A.M., Momboisse F., Haro-Acuna V., Bevilacqua J.A., Caviedes P. and Cardenas A.M., *Dynamin-2 function and dysfunction along the secretory pathway,* Front Endocrinol (Lausanne) (2013), *4*, 126.

Grammont M. and Irvine K.D., *fringe and Notch specify polar cell fate during Drosophila oogenesis,* Development (2001), *128,* 2243-2253.

Grigliatti T.A., Hall L., Rosenbluth R. and Suzuki D.T., *Temperature-sensitive mutations in Drosophila melanogaster. XIV. A selection of immobile adults,* Mol Gen Genet (1973), *120*, 107-114.

Guedes Sde M., Vitorino R., Tomer K., Domingues M.R., Correia A.J., Amado F. and Domingues P., *Drosophila melanogaster larval hemolymph protein mapping,* Biochem Biophys Res Commun (2003), *312*, 545-554.

Haines N. and Irvine K.D., *Glycosylation regulates Notch signalling,* Nat Rev Mol Cell Biol (2003), *4*, 786-797.

Hanahan D. and Weinberg R.A., *Hallmarks of cancer: the next generation,* Cell (2011), *144*, 646-674.

Harbecke R., Meise M., Holz A., Klapper R., Naffin E., Nordhoff V. and Janning W., *Larval and imaginal pathways in early development of Drosophila,* Int J Dev Biol (1996), *40*, 197-204.

Hartl T.A. and Scott M.P., *Wing tips: The wing disc as a platform for studying Hedgehog signaling,* Methods (2014), *68*, 199-206.

Henne W.M., Buchkovich N.J. and Emr S.D., *The ESCRT pathway,* Dev Cell (2011), *21*, 77-91.

Herman J.G., Latif F., Weng Y., Lerman M.I., Zbar B., Liu S., Samid D., Duan D.S., Gnarra J.R., Linehan W.M. *et al.*, *Silencing of the VHL tumor-suppressor gene by DNA methylation in renal carcinoma,* Proc Natl Acad Sci U S A (1994), *91*, 9700-9704.

Herranz H. and Milan M., *Signalling molecules, growth regulators and cell cycle control in Drosophila,* Cell Cycle (2008), *7*, 3335-3337.

Horne-Badovinac S. and Bilder D., *Mass transit: epithelial morphogenesis in the Drosophila egg chamber,* Dev Dyn (2005), *232*, 559-574.

Hsouna A., Nallamothu G., Kose N., Guinea M., Dammai V. and Hsu T., *Drosophila von Hippel-Lindau tumor suppressor gene function in epithelial tubule morphogenesis,* Mol Cell Biol (2010), *30*, 3779-3794.

Hsu T., *Complex cellular functions of the von Hippel-Lindau tumor suppressor gene: insights from model organisms,* Oncogene (2012), *31*, 2247-2257.

Huber W., von Heydebreck A., Sultmann H., Poustka A. and Vingron M., *Variance stabilization applied to microarray data calibration and to the quantification of differential expression,* Bioinformatics (2002), *18 Suppl 1*, S96-104.

Ignesti M., Barraco M., Nallamothu G., Woolworth J.A., Duchi S., Gargiulo G., Cavaliere V. and Hsu T., *Notch signaling during development requires the function of awd, the Drosophila homolog of human metastasis suppressor gene Nm23,* BMC Biol (2014), *12*, 12.

Iiizumi M., Liu W., Pai S.K., Furuta E. and Watabe K., *Drug development against metastasis-related genes and their pathways: a rationale for cancer therapy,* Biochim Biophys Acta (2008), *1786*, 87-104.

Inoue H., Takahashi M., Oomori A., Sekiguchi M. and Yoshioka T., *A novel function for nucleoside diphosphate kinase in Drosophila,* Biochem Biophys Res Commun (1996), *218*, 887-892.

Iwai K., Yamanaka K., Kamura T., Minato N., Conaway R.C., Conaway J.W., Klausner R.D. and Pause A., *Identification of the von Hippel-lindau tumor-suppressor protein as part of an active E3 ubiquitin ligase complex,* Proc Natl Acad Sci U S A (1999), *96*, 12436-12441.

Jack J. and Myette G., *Mutations that alter the morphology of the malpighian tubules in Drosophila,* Dev Genes Evol (1999), *209*, 546-554.

Jekely G. and Rorth P., *Hrs mediates downregulation of multiple signalling receptors in Drosophila,* EMBO Rep (2003), *4*, 1163-1168.

Jia D., Bryant J., Jevitt A., Calvin G. and Deng W.M., *The Ecdysone and Notch Pathways Synergistically Regulate Cut at the Dorsal-Ventral Boundary in Drosophila Wing Discs,* J Genet Genomics (2016), *43*, 179-186.

Johnson S.A., Zitserman D. and Roegiers F., *Numb regulates the balance between Notch recycling and late-endosome targeting in Drosophila neural progenitor cells,* Mol Biol Cell (2016), *27*, 2857-2866.

Kaelin W.G., *Von Hippel-Lindau disease,* Annu Rev Pathol (2007), *2*, 145-173.

Kamura T., Koepp D.M., Conrad M.N., Skowyra D., Moreland R.J., Iliopoulos O., Lane W.S., Kaelin W.G., Jr., Elledge S.J., Conaway R.C. *et al.*, *Rbx1, a component of the VHL tumor suppressor complex and SCF ubiquitin ligase,* Science (1999), *284*, 657-661.

Kauffman E.C., Robinson V.L., Stadler W.M., Sokoloff M.H. and Rinker-Schaeffer C.W., *Metastasis suppression: the evolving role of metastasis suppressor genes for regulating cancer cell growth at the secondary site,* J Urol (2003), *169*, 1122-1133.

Kean L., Cazenave W., Costes L., Broderick K.E., Graham S., Pollock V.P., Davies S.A., Veenstra J.A. and Dow J.A., *Two nitridergic peptides are encoded by the gene capability in*

*Drosophila melanogaster,* Am J Physiol Regul Integr Comp Physiol (2002), *282,* R1297-1307.

Khammari A., Agnes F., Gandille P. and Pret A.M., *Physiological apoptosis of polar cells during Drosophila oogenesis is mediated by Hid-dependent regulation of Diap1,* Cell Death Differ (2011), *18*, 793-805.

Kidd S. and Lieber T., *Furin cleavage is not a requirement for Drosophila Notch function,* Mech Dev (2002), *115*, 41-51.

Kim H.L., Vander Griend D.J., Yang X., Benson D.A., Dubauskas Z., Yoshida B.A., Chekmareva M.A., Ichikawa Y., Sokoloff M.H., Zhan P. *et al., Mitogen-activated protein kinase kinase 4 metastasis suppressor gene expression is inversely related to histological pattern in advancing human prostatic cancers,* Cancer Res (2001), *61*, 2833-2837.

Kim J., Sebring A., Esch J.J., Kraus M.E., Vorwerk K., Magee J. and Carroll S.B., *Integration of positional signals and regulation of wing formation and identity by Drosophila vestigial gene,* Nature (1996), *382*, 133-138.

King R.C., *Ovarian development in Drosophila melanogaster,* Academic Press (1970, New York,).

Klein T., *Wing disc development in the fly: the early stages,* Curr Opin Genet Dev (2001), *11*, 470-475.

Klusza S. and Deng W.M., *At the crossroads of differentiation and proliferation: precise control of cell-cycle changes by multiple signaling pathways in Drosophila follicle cells,* Bioessays (2011), *33*, 124-134.

Komada M. and Kitamura N., *The Hrs/STAM complex in the downregulation of receptor tyrosine kinases,* J Biochem (2005), *137,* 1-8.

Kopan R. and Ilagan M.X., *The canonical Notch signaling pathway: unfolding the activation mechanism,* Cell (2009), *137,* 216-233.

Koppen T., Weckmann A., Muller S., Staubach S., Bloch W., Dohmen R.J. and Schwientek T., *Proteomics analyses of microvesicles released by Drosophila Kc167 and S2 cells,* Proteomics (2011), *11*, 4397-4410.

Korkut C., Ataman B., Ramachandran P., Ashley J., Barria R., Gherbesi N. and Budnik V., *Trans-synaptic transmission of vesicular Wnt signals through Evi/Wntless,* Cell (2009), *139*, 393-404.

Koyama T. and Mirth C.K., *Growth-Blocking Peptides As Nutrition-Sensitive Signals for Insulin Secretion and Body Size Regulation,* PLoS Biol (2016), *14*, e1002392.

Krishnan K.S., Rikhy R., Rao S., Shivalkar M., Mosko M., Narayanan R., Etter P., Estes P.S. and Ramaswami M., *Nucleoside diphosphate kinase, a source of GTP, is required for dynamin-dependent synaptic vesicle recycling,* Neuron (2001), *30*, 197-210.

Lakkaraju A. and Rodriguez-Boulan E., *Itinerant exosomes: emerging roles in cell and tissue polarity,* Trends Cell Biol (2008), *18*, 199-209.

Lamb M.J., *The DNA content of polytene nuclei in midgut and Malpighian tubule cells of adultDrosophila melanogaster,* Wilhelm Roux's Archives of Developmental Biology (1982), *191*, 381-384.

Lascu I., Chaffotte A., Limbourg-Bouchon B. and Veron M., *A Pro/Ser substitution in nucleoside diphosphate kinase of Drosophila melanogaster (mutation killer of prune) affects stability but not catalytic efficiency of the enzyme,* J Biol Chem (1992), *267*, 12775-12781.

Lascu I. and Gonin P., *The catalytic mechanism of nucleoside diphosphate kinases,* J Bioenerg Biomembr (2000), *32*, 237-246.

Latif F., Duh F.M., Gnarra J., Tory K., Kuzmin I., Yao M., Stackhouse T., Modi W., Geil L., Schmidt L. *et al., von Hippel-Lindau syndrome: cloning and identification of the plasma membrane Ca(++)-transporting ATPase isoform 2 gene that resides in the von Hippel-Lindau gene region,* Cancer Res (1993), *53*, 861-867.

Lawrence P.A. and Morata G., *Compartments in the wing of Drosophila: a study of the engrailed gene,* Dev Biol (1976), *50*, 321-337.

Lawrence P.A. and Struhl G., *Morphogens, compartments, and pattern: lessons from drosophila?,* Cell (1996), *85*, 951-961.

Le Borgne R., Bardin A. and Schweisguth F., *The roles of receptor and ligand endocytosis in regulating Notch signaling,* Development (2005), *132*, 1751-1762.

Le Borgne R., *Regulation of Notch signalling by endocytosis and endosomal sorting,* Curr Opin Cell Biol (2006), *18*, 213-222.

Lee T. and Luo L., *Mosaic analysis with a repressible cell marker for studies of gene function in neuronal morphogenesis,* Neuron (1999), *22*, 451-461.

Lemaitre B. and Hoffmann J., *The host defense of Drosophila melanogaster,* Annu Rev Immunol (2007), *25*, 697-743.

Li Z., Liu S. and Cai Y., *Differential Notch activity is required for homeostasis of malpighian tubules in adult Drosophila,* J Genet Genomics (2014), *41*, 649-652.

Lilly A.J., Khanim F.L. and Bunce C.M., *The case for extracellular Nm23-H1 as a driver of acute myeloid leukaemia (AML) progression,* Naunyn Schmiedebergs Arch Pharmacol (2015), *388*, 225-233.

Lim J., Jang G., Kang S., Lee G., Nga do T.T., Phuong do T.L., Kim H., El-Rifai W., Ruley H.E. and Jo D., *Cell-permeable NM23 blocks the maintenance and progression of established pulmonary metastasis,* Cancer Res (2011), *71*, 7216-7225.

Lin H. and Spradling A.C., *Germline stem cell division and egg chamber development in transplanted Drosophila germaria,* Dev Biol (1993), *159*, 140-152.

Liotta L.A. and Steeg P.S., *Clues to the function of Nm23 and Awd proteins in development, signal transduction, and tumor metastasis provided by studies of Dictyostelium discoideum,* J Natl Cancer Inst (1990), *82*, 1170-1172.

Liu J., Sato C., Cerletti M. and Wagers A., *Notch signaling in the regulation of stem cell self-renewal and differentiation,* Curr Top Dev Biol (2010), *92*, 367-409.

Lloyd T.E., Verstreken P., Ostrin E.J., Phillippi A., Lichtarge O. and Bellen H.J., *A genome-wide search for synaptic vesicle cycle proteins in Drosophila,* Neuron (2000), *26*, 45-50.

Lloyd T.E., Atkinson R., Wu M.N., Zhou Y., Pennetta G. and Bellen H.J., *Hrs regulates endosome membrane invagination and tyrosine kinase receptor signaling in Drosophila,* Cell (2002), *108*, 261-269.

Lockhart D.J., Dong H., Byrne M.C., Follettie M.T., Gallo M.V., Chee M.S., Mittmann M., Wang C., Kobayashi M., Horton H. *et al.*, *Expression monitoring by hybridization to high-density oligonucleotide arrays,* Nat Biotechnol (1996), *14,* 1675-1680.

Lolkema M.P., Gervais M.L., Snijckers C.M., Hill R.P., Giles R.H., Voest E.E. and Ohh M., *Tumor suppression by the von Hippel-Lindau protein requires phosphorylation of the acidic domain,* J Biol Chem (2005), *280,* 22205-22211.

Lonergan K.M., Iliopoulos O., Ohh M., Kamura T., Conaway R.C., Conaway J.W. and Kaelin W.G., Jr., *Regulation of hypoxia-inducible mRNAs by the von Hippel-Lindau tumor suppressor protein requires binding to complexes containing elongins B/C and Cul2,* Mol Cell Biol (1998), *18,* 732-741.

Lopez-Schier H. and St Johnston D., *Delta signaling from the germ line controls the proliferation and differentiation of the somatic follicle cells during Drosophila oogenesis,* Genes Dev (2001), *15,* 1393-1405.

Lopez-Schier H. and St Johnston D., *Drosophila nicastrin is essential for the intramembranous cleavage of notch,* Dev Cell (2002), *2,* 79-89.

Lu H. and Bilder D., *Endocytic control of epithelial polarity and proliferation in Drosophila,* Nat Cell Biol (2005), *7,* 1232-1239.

Lyne R., Smith R., Rutherford K., Wakeling M., Varley A., Guillier F., Janssens H., Ji W., McLaren P., North P. *et al.*, *FlyMine: an integrated database for Drosophila and Anopheles genomics,* Genome Biol (2007), *8,* R129.

Ma D., Xing Z., Liu B., Pedigo N.G., Zimmer S.G., Bai Z., Postel E.H. and Kaetzel D.M., *NM23-H1 and NM23-H2 repress transcriptional activities of nuclease-hypersensitive elements in the platelet-derived growth factor-A promoter,* J Biol Chem (2002), *277,* 1560-1567.

Ma D., McCorkle J.R. and Kaetzel D.M., *The metastasis suppressor NM23-H1 possesses 3'-5' exonuclease activity,* J Biol Chem (2004), *279,* 18073-18084.

Maher E.R., Neumann H.P. and Richard S., *von Hippel-Lindau disease: a clinical and scientific review,* Eur J Hum Genet (2011), *19,* 617-623.

Mann R.S. and Morata G., *The developmental and molecular biology of genes that subdivide the body of Drosophila,* Annu Rev Cell Dev Biol (2000), *16*, 243-271.

Martin-Castellanos C. and Edgar B.A., *A characterization of the effects of Dpp signaling on cell growth and proliferation in the Drosophila wing,* Development (2002), *129*, 1003-1013.

Maxwell P.H., Wiesener M.S., Chang G.W., Clifford S.C., Vaux E.C., Cockman M.E., Wykoff C.C., Pugh C.W., Maher E.R. and Ratcliffe P.J., *The tumour suppressor protein VHL targets hypoxia-inducible factors for oxygen-dependent proteolysis,* Nature (1999), *399*, 271-275.

Mazumdar A. and Mazumdar M., *How one becomes many: blastoderm cellularization in Drosophila melanogaster,* Bioessays (2002), *24*, 1012-1022.

Miaczynska M., Pelkmans L. and Zerial M., *Not just a sink: endosomes in control of signal transduction,* Curr Opin Cell Biol (2004), *16*, 400-406.

Micchelli C.A., Rulifson E.J. and Blair S.S., *The function and regulation of cut expression on the wing margin of Drosophila: Notch, Wingless and a dominant negative role for Delta and Serrate,* Development (1997), *124*, 1485-1495.

Miller J., Chi T., Kapahi P., Kahn A.J., Kim M.S., Hirata T., Romero M.F., Dow J.A. and Stoller M.L., *Drosophila melanogaster as an emerging translational model of human nephrolithiasis,* J Urol (2013), *190*, 1648-1656.

Mirth C.K. and Riddiford L.M., *Size assessment and growth control: how adult size is determined in insects,* Bioessays (2007), *29*, 344-355.

Moline M.M., Southern C. and Bejsovec A., *Directionality of wingless protein transport influences epidermal patterning in the Drosophila embryo,* Development (1999), *126*, 4375-4384.

Montell D.J., *Border-cell migration: the race is on,* Nat Rev Mol Cell Biol (2003), *4*, 13-24.

Morrison H.A., Dionne H., Rusten T.E., Brech A., Fisher W.W., Pfeiffer B.D., Celniker S.E., Stenmark H. and Bilder D., *Regulation of early endosomal entry by the Drosophila tumor suppressors Rabenosyn and Vps45,* Mol Biol Cell (2008), *19*, 4167-4176.

Mortimer N.T. and Moberg K.H., *Regulation of Drosophila embryonic tracheogenesis by dVHL and hypoxia,* Dev Biol (2009), *329*, 294-305.

Nallamothu G., Woolworth J.A., Dammai V. and Hsu T., *Awd, the homolog of metastasis suppressor gene Nm23, regulates Drosophila epithelial cell invasion,* Mol Cell Biol (2008), *28*, 1964-1973.

Nezis I.P., Stravopodis D.J., Papassideri I., Robert-Nicoud M. and Margaritis L.H., *Dynamics of apoptosis in the ovarian follicle cells during the late stages of Drosophila oogenesis,* Cell Tissue Res (2002), *307*, 401-409.

Niitsu N., Okabe-Kado J., Nakayama M., Wakimoto N., Sakashita A., Maseki N., Motoyoshi K., Umeda M. and Honma Y., *Plasma levels of the differentiation inhibitory factor nm23-H1 protein and their clinical implications in acute myelogenous leukemia,* Blood (2000), *96*, 1080-1086.

Niitsu N., *[Serum levels of mm23-H1 protein and their clinical implications in malignant lymphoma],* Rinsho Ketsueki (2001), *42*, 1155-1161.

Nowell C.S. and Radtke F., *Notch as a tumour suppressor,* Nat Rev Cancer (2017), *17*, 145-159.

Ntziachristos P., Lim J.S., Sage J. and Aifantis I., *From fly wings to targeted cancer therapies: a centennial for notch signaling,* Cancer Cell (2014), *25*, 318-334.

Nystul T. and Spradling A., *Regulation of epithelial stem cell replacement and follicle formation in the Drosophila ovary,* Genetics (2010), *184*, 503-515.

Oda H., Uemura T., Harada Y., Iwai Y. and Takeichi M., *A Drosophila homolog of cadherin associated with armadillo and essential for embryonic cell-cell adhesion,* Dev Biol (1994), *165*, 716-726.

Okabe-Kado J., Kasukabe T., Honma Y., Hayashi M., Henzel W.J. and Hozumi M., *Identity of a differentiation inhibiting factor for mouse myeloid leukemia cells with NM23/nucleoside diphosphate kinase,* Biochem Biophys Res Commun (1992), *182*, 987-994.

Okabe-Kado J., Kasukabe T., Honma Y., Kobayashi H., Maseki N. and Kaneko Y., *Extracellular NM23 protein promotes the growth and survival of primary cultured human acute myelogenous leukemia cells,* Cancer Sci (2009), *100,* 1885-1894.

Otsuki Y., Tanaka M., Yoshii S., Kawazoe N., Nakaya K. and Sugimura H., *Tumor metastasis suppressor nm23H1 regulates Rac1 GTPase by interaction with Tiam1,* Proc Natl Acad Sci U S A (2001), *98*, 4385-4390.

Pagliarini R.A., Quinones A.T. and Xu T., *Analyzing the function of tumor suppressor genes using a Drosophila model,* Methods Mol Biol (2003), *223*, 349-382.

Palacios F., Schweitzer J.K., Boshans R.L. and D'Souza-Schorey C., *ARF6-GTP recruits Nm23-H1 to facilitate dynamin-mediated endocytosis during adherens junctions disassembly,* Nat Cell Biol (2002), *4*, 929-936.

Palmer W.H., Jia D. and Deng W.M., *Cis-interactions between Notch and its ligands block ligand-independent Notch activity,* Elife (2014), *3*.

Palmieri D., Horak C.E., Lee J.H., Halverson D.O. and Steeg P.S., *Translational approaches using metastasis suppressor genes,* J Bioenerg Biomembr (2006), *38*, 151-161.

Peri S., Caretti E., Tricarico R., Devarajan K., Cheung M., Sementino E., Menges C.W., Nicolas E., Vanderveer L.A., Howard S. *et al., Haploinsufficiency in tumor predisposition syndromes: altered genomic transcription in morphologically normal cells heterozygous for VHL or TSC mutation,* Oncotarget (2016).

Pignoni F. and Zipursky S.L., *Induction of Drosophila eye development by decapentaplegic,* Development (1997), *124*, 271-278.

Postel E.H., Berberich S.J., Rooney J.W. and Kaetzel D.M., *Human NM23/nucleoside diphosphate kinase regulates gene expression through DNA binding to nuclease-hypersensitive transcriptional elements,* J Bioenerg Biomembr (2000), *32*, 277-284.

Postel E.H., *Multiple biochemical activities of NM23/NDP kinase in gene regulation,* J Bioenerg Biomembr (2003), *35*, 31-40.

Potter M., Newport E. and Morten K.J., *The Warburg effect: 80 years on,* Biochem Soc Trans (2016), *44*, 1499-1505.

Provost E., Hersperger G., Timmons L., Ho W.Q., Hersperger E., Alcazar R. and Shearn A., *Loss-of-function mutations in a glutathione S-transferase suppress the prune-Killer of prune lethal interaction,* Genetics (2006), *172*, 207-219.

Provost E. and Shearn A., *The Suppressor of Killer of prune, a unique glutathione S-transferase,* J Bioenerg Biomembr (2006), *38*, 189-195.

Pugacheva O.M. and Mamon L.A., *[Genetic control of development of the Malpighian vessels in Drosophila melanogaster],* Ontogenez (2003), *34*, 325-341.

Quinlan M.E., *Cytoplasmic Streaming in the Drosophila Oocyte,* Annu Rev Cell Dev Biol (2016), *32*, 173-195.

Rabouille C., Malhotra V. and Nickel W., *Diversity in unconventional protein secretion,* J Cell Sci (2012), *125*, 5251-5255.

Rajan A. and Perrimon N., *Drosophila cytokine unpaired 2 regulates physiological homeostasis by remotely controlling insulin secretion,* Cell (2012), *151*, 123-137.

Ravikumar B., Moreau K., Jahreiss L., Puri C. and Rubinsztein D.C., *Plasma membrane contributes to the formation of pre-autophagosomal structures,* Nat Cell Biol (2010a), *12*, 747-757.

Ravikumar B., Moreau K. and Rubinsztein D.C., *Plasma membrane helps autophagosomes grow,* Autophagy (2010b), *6*, 1184-1186.

Rebay I., Fleming R.J., Fehon R.G., Cherbas L., Cherbas P. and Artavanis-Tsakonas S., *Specific EGF repeats of Notch mediate interactions with Delta and Serrate: implications for Notch as a multifunctional receptor,* Cell (1991), *67*, 687-699.

Riechmann V. and Ephrussi A., *Axis formation during Drosophila oogenesis,* Curr Opin Genet Dev (2001), *11*, 374-383.

Rink J., Ghigo E., Kalaidzidis Y. and Zerial M., *Rab conversion as a mechanism of progression from early to late endosomes,* Cell (2005), *122*, 735-749.

Robertson K., Mergliano J. and Minden J.S., *Dissecting Drosophila embryonic brain development using photoactivated gene expression,* Dev Biol (2003), *260*, 124-137.

Roe J.S., Kim H.R., Hwang I.Y., Ha N.C., Kim S.T., Cho E.J. and Youn H.D., *Phosphorylation of von Hippel-Lindau protein by checkpoint kinase 2 regulates p53 transactivation,* Cell Cycle (2011), *10*, 3920-3928.

Romani P., Papi A., Ignesti M., Soccolini G., Hsu T., Gargiulo G., Spisni E. and Cavaliere V., *Dynamin controls extracellular level of Awd/Nme1 metastasis suppressor protein,* Naunyn Schmiedebergs Arch Pharmacol (2016), *389*, 1171-1182.

Rosengard A.M., Krutzsch H.C., Shearn A., Biggs J.R., Barker E., Margulies I.M., King C.R., Liotta L.A. and Steeg P.S., *Reduced Nm23/Awd protein in tumour metastasis and aberrant Drosophila development,* Nature (1989), *342*, 177-180.

Roth S., *Drosophila oogenesis: coordinating germ line and soma,* Curr Biol (2001), *11*, R779-781.

Ruggieri R. and McCormick F., *Ras and the awd couple,* Nature (1991), *353*, 390-391.

Russell S., Meadows L.A. and Russell R.R., *Microarray technology in practice,* Elsevier/Academic (2009, San Diego ; London).

Rusten T.E., Lindmo K., Juhasz G., Sass M., Seglen P.O., Brech A. and Stenmark H., *Programmed autophagy in the Drosophila fat body is induced by ecdysone through regulation of the PI3K pathway,* Dev Cell (2004), *7*, 179-192.

Sajnani K., Islam F., Smith R.A., Gopalan V. and Lam A.K., *Genetic alterations in Krebs cycle and its impact on cancer pathogenesis,* Biochimie (2017).

Sasaki N., Sasamura T., Ishikawa H.O., Kanai M., Ueda R., Saigo K. and Matsuno K., *Polarized exocytosis and transcytosis of Notch during its apical localization in Drosophila epithelial cells,* Genes Cells (2007), *12*, 89-103.

Schena M., Shalon D., Davis R.W. and Brown P.O., *Quantitative monitoring of gene expression patterns with a complementary DNA microarray,* Science (1995), *270*, 467-470.

Schupbach T., *Germ line and soma cooperate during oogenesis to establish the dorsoventral pattern of egg shell and embryo in Drosophila melanogaster,* Cell (1987), *49*, 699-707.

Scita G. and Di Fiore P.P., *The endocytic matrix,* Nature (2010), *463*, 464-473.

Seugnet L., Simpson P. and Haenlin M., *Requirement for dynamin during Notch signaling in Drosophila neurogenesis,* Dev Biol (1997), *192*, 585-598.

Sever S., Damke H. and Schmid S.L., *Dynamin:GTP controls the formation of constricted coated pits, the rate limiting step in clathrin-mediated endocytosis,* J Cell Biol (2000), *150*, 1137-1148.

Shannon P., Markiel A., Ozier O., Baliga N.S., Wang J.T., Ramage D., Amin N., Schwikowski B. and Ideker T., *Cytoscape: a software environment for integrated models of biomolecular interaction networks,* Genome Res (2003), *13*, 2498-2504.

Shenoy N., Vallumsetla N., Zou Y., Galeas J.N., Shrivastava M., Hu C., Susztak K. and Verma A., *Role of DNA methylation in renal cell carcinoma,* J Hematol Oncol (2015), *8*, 88.

Shenoy N. and Pagliaro L., *Sequential pathogenesis of metastatic VHL mutant clear cell renal cell carcinoma: putting it together with a translational perspective,* Ann Oncol (2016), *27*, 1685-1695.

Shevde L.A. and Welch D.R., *Metastasis suppressor pathways--an evolving paradigm,* Cancer Lett (2003), *198*, 1-20.

Shyu L.F., Sun J., Chung H.M., Huang Y.C. and Deng W.M., *Notch signaling and developmental cell-cycle arrest in Drosophila polar follicle cells,* Mol Biol Cell (2009), *20*, 5064-5073.

Silva D. and Jemc J.C., *Sorting Out Identities: An Educational Primer for Use with "Novel Tools for Genetic Manipulation of Follicle Stem Cells in the Drosophila Ovary Reveal an Integrin-Dependent Transition from Quiescence to Proliferation",* Genetics (2015), *201*, 13-22.

Singh S.R., Liu W. and Hou S.X., *The adult Drosophila malpighian tubules are maintained by multipotent stem cells,* Cell Stem Cell (2007), *1*, 191-203.

Singh S.R. and Hou S.X., *Lessons learned about adult kidney stem cells from the malpighian tubules of Drosophila,* J Am Soc Nephrol (2008), *19*, 660-666.

Singh S.R. and Hou S.X., *Multipotent stem cells in the Malpighian tubules of adult Drosophila melanogaster,* J Exp Biol (2009), *212*, 413-423.

Singh V., Ram M., Kumar R., Prasad R., Roy B.K. and Singh K.K., *Phosphorylation: Implications in Cancer,* Protein J (2017), *36,* 1-6.

Song X., Zhu C.H., Doan C. and Xie T., *Germline stem cells anchored by adherens junctions in the Drosophila ovary niches,* Science (2002), *296,* 1855-1857.

Song X., Call G.B., Kirilly D. and Xie T., *Notch signaling controls germline stem cell niche formation in the Drosophila ovary,* Development (2007), *134,* 1071-1080.

Sozen M.A., Armstrong J.D., Yang M., Kaiser K. and Dow J.A., *Functional domains are specified to single-cell resolution in a Drosophila epithelium,* Proc Natl Acad Sci U S A (1997), *94,* 5207-5212.

Spradling A.C., *Developmental genetics of oogenesis,* Cold Spring Harbor Laboratory Press (1993, Plainview, N.Y.).

Sprinzak D., Lakhanpal A., Lebon L., Santat L.A., Fontes M.E., Anderson G.A., Garcia-Ojalvo J. and Elowitz M.B., *Cis-interactions between Notch and Delta generate mutually exclusive signalling states,* Nature (2010), *465,* 86-90.

Srivastava S., Li Z., Ko K., Choudhury P., Albaqumi M., Johnson A.K., Yan Y., Backer J.M., Unutmaz D., Coetzee W.A. *et al., Histidine phosphorylation of the potassium channel KCa3.1 by nucleoside diphosphate kinase B is required for activation of KCa3.1 and CD4 T cells,* Mol Cell (2006), *24,* 665-675.

Stafford L.J., Vaidya K.S. and Welch D.R., *Metastasis suppressors genes in cancer,* Int J Biochem Cell Biol (2008), *40,* 874-891.

Steeg P.S., Bevilacqua G., Kopper L., Thorgeirsson U.P., Talmadge J.E., Liotta L.A. and Sobel M.E., *Evidence for a novel gene associated with low tumor metastatic potential,* J Natl Cancer Inst (1988), *80,* 200-204.

Steeg P.S., Ouatas T., Halverson D., Palmieri D. and Salerno M., *Metastasis suppressor genes: basic biology and potential clinical use,* Clin Breast Cancer (2003), *4,* 51-62.

Steeg P.S., Zollo M. and Wieland T., *A critical evaluation of biochemical activities reported for the nucleoside diphosphate kinase/Nm23/Awd family proteins: opportunities and missteps* *in understanding their biological functions,* Naunyn Schmiedebergs Arch Pharmacol (2011), *384*, 331-339.

Stewart B.W., Wild C. and International Agency for Research on Cancer W.H.O., *World cancer report 2014,* International Agency for Research on Cancer WHO Press (2014, Lyon, France - Geneva, Switzerland).

Struhl G. and Adachi A., *Requirements for presenilin-dependent cleavage of notch and other transmembrane proteins,* Mol Cell (2000), *6*, 625-636.

Sturtevant A.H., *A Highly Specific Complementary Lethal System in Drosophila Melanogaster,* Genetics (1956), *41*, 118-123.

Su G.H., Song J.J., Repasky E.A., Schutte M. and Kern S.E., *Mutation rate of MAP2K4/MKK4 in breast carcinoma,* Hum Mutat (2002), *19*, 81.

Sun J. and Deng W.M., *Notch-dependent downregulation of the homeodomain gene cut is required for the mitotic cycle/endocycle switch and cell differentiation in Drosophila follicle cells,* Development (2005), *132*, 4299-4308.

Sun J. and Deng W.M., *Hindsight mediates the role of notch in suppressing hedgehog signaling and cell proliferation,* Dev Cell (2007), *12*, 431-442.

Tagami S., Okochi M., Fukumori A., Jiang J., Yanagida K., Nakayama T., Morihara T., Tanaka T., Kudo T. and Takeda M., *Processes of beta-amyloid and intracellular cytoplasmic domain generation by presenilin/gamma-secretase,* Neurodegener Dis (2008), *5*, 160-162.

Takacs-Vellai K., Vellai T., Farkas Z. and Mehta A., *Nucleoside diphosphate kinases (NDPKs) in animal development,* Cell Mol Life Sci (2015), *72*, 1447-1462.

Talsma A.D., Christov C.P., Terriente-Felix A., Linneweber G.A., Perea D., Wayland M., Shafer O.T. and Miguel-Aliaga I., *Remote control of renal physiology by the intestinal neuropeptide pigment-dispersing factor in Drosophila,* Proc Natl Acad Sci U S A (2012), *109*, 12177-12182.

Tanaka T. and Nakamura A., *The endocytic pathway acts downstream of Oskar in Drosophila germ plasm assembly,* Development (2008), *135*, 1107-1117.

Tee Y.T., Chen G.D., Lin L.Y., Ko J.L. and Wang P.H., *Nm23-H1: a metastasis-associated gene,* Taiwan J Obstet Gynecol (2006), *45*, 107-113.

Teng D.H., Engele C.M. and Venkatesh T.R., *A product of the prune locus of Drosophila is similar to mammalian GTPase-activating protein,* Nature (1991), *353*, 437-440.

Thakur R.K., Yadav V.K., Kumar P. and Chowdhury S., *Mechanisms of non-metastatic 2 (NME2)-mediated control of metastasis across tumor types*, Naunyn Schmiedebergs Arch Pharmacol (2011), *384*, 397-406.

Timmons L., Hersperger E., Woodhouse E., Xu J., Liu L.Z. and Shearn A., *The expression of the Drosophila awd gene during normal development and in neoplastic brain tumors caused by lgl mutations,* Dev Biol (1993), *158*, 364-379.

Timmons L., Xu J., Hersperger G., Deng X.F. and Shearn A., *Point mutations in awdKpn which revert the prune/Killer of prune lethal interaction affect conserved residues that are involved in nucleoside diphosphate kinase substrate binding and catalysis,* J Biol Chem (1995), *270*, 23021-23030.

Timmons L. and Shearn A., *Role of AWD/nucleoside diphosphate kinase in Drosophila development,* J Bioenerg Biomembr (2000), *32*, 293-300.

Torres I.L., Lopez-Schier H. and St Johnston D., *A Notch/Delta-dependent relay mechanism establishes anterior-posterior polarity in Drosophila,* Dev Cell (2003), *5*, 547-558.

Tsuiki H., Nitta M., Furuya A., Hanai N., Fujiwara T., Inagaki M., Kochi M., Ushio Y., Saya H. and Nakamura H., *A novel human nucleoside diphosphate (NDP) kinase, Nm23-H6, localizes in mitochondria and affects cytokinesis,* J Cell Biochem (1999), *76*, 254-269.

Tzeng H.T. and Wang Y.C., *Rab-mediated vesicle trafficking in cancer,* J Biomed Sci (2016), *23*, 70.

Vaccari T., Lu H., Kanwar R., Fortini M.E. and Bilder D., *Endosomal entry regulates Notch receptor activation in Drosophila melanogaster,* J Cell Biol (2008), *180*, 755-762.

Vaccari T. and Bilder D., *At the crossroads of polarity, proliferation and apoptosis: the use of Drosophila to unravel the multifaceted role of endocytosis in tumor suppression,* Mol Oncol (2009), *3*, 354-365.

Vaccari T., Rusten T.E., Menut L., Nezis I.P., Brech A., Stenmark H. and Bilder D., *Comparative analysis of ESCRT-I, ESCRT-II and ESCRT-III function in Drosophila by efficient isolation of ESCRT mutants,* J Cell Sci (2009), *122*, 2413-2423.

Vaccari T., Duchi S., Cortese K., Tacchetti C. and Bilder D., *The vacuolar ATPase is required for physiological as well as pathological activation of the Notch receptor,* Development (2010), *137*, 1825-1832.

Vachias C., Couderc J.L. and Grammont M., *A two-step Notch-dependant mechanism controls the selection of the polar cell pair in Drosophila oogenesis,* Development (2010), *137*, 2703-2711.

van der Bliek A.M. and Meyerowitz E.M., *Dynamin-like protein encoded by the Drosophila shibire gene associated with vesicular traffic,* Nature (1991), *351*, 411-414.

van Tetering G., van Diest P., Verlaan I., van der Wall E., Kopan R. and Vooijs M., *Metalloprotease ADAM10 is required for Notch1 site 2 cleavage,* J Biol Chem (2009), *284*, 31018-31027.

Verma P. and Tapadia M.G., *Immune response and anti-microbial peptides expression in Malpighian tubules of Drosophila melanogaster is under developmental regulation,* PLoS One (2012), *7*, e40714.

Vetrivel K.S., Cheng H., Lin W., Sakurai T., Li T., Nukina N., Wong P.C., Xu H. and Thinakaran G., *Association of gamma-secretase with lipid rafts in post-Golgi and endosome membranes,* J Biol Chem (2004), *279*, 44945-44954.

Wagner P.D. and Vu N.D., *Phosphorylation of ATP-citrate lyase by nucleoside diphosphate kinase,* J Biol Chem (1995), *270*, 21758-21764.

Wagner P.D. and Vu N.D., *Histidine to aspartate phosphotransferase activity of nm23 proteins: phosphorylation of aldolase C on Asp-319,* Biochem J (2000), *346 Pt 3*, 623-630.

Wakimoto N., Yokoyama A., Okabe-Kado J., Nagata N., Motoyoshi K. and Honma Y., *Combined analysis of differentiation inhibitory factor nm23-H1 and nm23-H2 as prognostic factors in acute myeloid leukaemia,* Br J Cancer (1998), *77*, 2298-2303.

Wallet V., Mutzel R., Troll H., Barzu O., Wurster B., Veron M. and Lacombe M.L., *Dictyostelium nucleoside diphosphate kinase highly homologous to Nm23 and Awd proteins involved in mammalian tumor metastasis and Drosophila development,* J Natl Cancer Inst (1990), *82,* 1199-1202.

Wan S., Cato A.M. and Skaer H., *Multiple signalling pathways establish cell fate and cell number in Drosophila malpighian tubules,* Dev Biol (2000), *217,* 153-165.

Wang J., Kean L., Yang J., Allan A.K., Davies S.A., Herzyk P. and Dow J.A., *Function-informed transcriptome analysis of Drosophila renal tubule,* Genome Biol (2004), *5,* R69.

Wang S.H., Simcox A. and Campbell G., *Dual role for Drosophila epidermal growth factor receptor signaling in early wing disc development,* Genes Dev (2000), *14,* 2271-2276.

Wang X., Adam J.C. and Montell D., *Spatially localized Kuzbanian required for specific activation of Notch during border cell migration,* Dev Biol (2007), *301,* 532-540.

Warburg O., Wind F. and Negelein E., *The Metabolism of Tumors in the Body,* J Gen Physiol (1927), *8,* 519-530.

Ward E.J., Shcherbata H.R., Reynolds S.H., Fischer K.A., Hatfield S.D. and Ruohola-Baker H., *Stem cells signal to the niche through the Notch pathway in the Drosophila ovary,* Curr Biol (2006), *16*, 2352-2358.

Weinberg R.A., *The biology of cancer*, Garland Science (2007, New York, NY).

Weiss L., *Metastasis of cancer: a conceptual history from antiquity to the 1990s,* Cancer Metastasis Rev (2000), *19*, I-XI, 193-383.

Whiteland J.L., Nicholls S.M., Shimeld C., Easty D.L., Williams N.A. and Hill T.J., *Immunohistochemical detection of T-cell subsets and other leukocytes in paraffin-embedded rat and mouse tissues with monoclonal antibodies,* J Histochem Cytochem (1995), *43*, 313-320.

Wieschaus E. and Szabad J., *The development and function of the female germ line in Drosophila melanogaster: a cell lineage study,* Dev Biol (1979), *68*, 29-46.

Wilkin M., Tongngok P., Gensch N., Clemence S., Motoki M., Yamada K., Hori K., Taniguchi-Kanai M., Franklin E., Matsuno K. *et al.*, *Drosophila HOPS and AP-3 complex* *genes are required for a Deltex-regulated activation of notch in the endosomal trafficking pathway,* Dev Cell (2008), *15*, 762-772.

Willems R., Van Bockstaele D.R., Lardon F., Lenjou M., Nijs G., Snoeck H.W., Berneman Z.N. and Slegers H., *Decrease in nucleoside diphosphate kinase (NDPK/nm23) expression during hematopoietic maturation,* J Biol Chem (1998), *273*, 13663-13668.

Wilson A. and Radtke F., *Multiple functions of Notch signaling in self-renewing organs and cancer,* FEBS Lett (2006), *580*, 2860-2868.

Wodarz A., Stewart D.B., Nelson W.J. and Nusse R., *Wingless signaling modulates cadherin-mediated cell adhesion in Drosophila imaginal disc cells,* J Cell Sci (2006), *119*, 2425-2434.

Woodman P.G., *Biogenesis of the sorting endosome: the role of Rab5,* Traffic (2000), *1*, 695-701.

Woolworth J.A., Nallamothu G. and Hsu T., *The Drosophila metastasis suppressor gene Nm23 homolog, awd, regulates epithelial integrity during oogenesis,* Mol Cell Biol (2009), *29*, 4679-4690.

Wu X., Tanwar P.S. and Raftery L.A., *Drosophila follicle cells: morphogenesis in an eggshell,* Semin Cell Dev Biol (2008), *19*, 271-282.

Wucherpfennig T., Wilsch-Brauninger M. and Gonzalez-Gaitan M., *Role of Drosophila Rab5 during endosomal trafficking at the synapse and evoked neurotransmitter release,* J Cell Biol (2003), *161*, 609-624.

Xi R., McGregor J.R. and Harrison D.A., *A gradient of JAK pathway activity patterns the anterior-posterior axis of the follicular epithelium,* Dev Cell (2003), *4*, 167-177.

Xu J., Liu L.Z., Deng X.F., Timmons L., Hersperger E., Steeg P.S., Veron M. and Shearn A., *The enzymatic activity of Drosophila AWD/NDP kinase is necessary but not sufficient for its biological function,* Dev Biol (1996), *177*, 544-557.

Xu T. and Rubin G.M., *Analysis of genetic mosaics in developing and adult Drosophila tissues,* Development (1993), *117*, 1223-1237.

Yan J., Yang Q. and Huang Q., *Metastasis suppressor genes,* Histol Histopathol (2013), *28*, 285-292.

Yan Y., Denef N. and Schupbach T., *The vacuolar proton pump, V-ATPase, is required for notch signaling and endosomal trafficking in Drosophila,* Dev Cell (2009)*, 17*, 387-402.

Yip M.L., Lamka M.L. and Lipshitz H.D., *Control of germ-band retraction in Drosophila by the zinc-finger protein HINDSIGHT,* Development (1997)*, 124*, 2129-2141.

Zerial M. and McBride H., *Rab proteins as membrane organizers,* Nat Rev Mol Cell Biol (2001)*, 2*, 107-117.

Zhang H., Stallock J.P., Ng J.C., Reinhard C. and Neufeld T.P., *Regulation of cellular growth by the Drosophila target of rapamycin dTOR,* Genes Dev (2000)*, 14*, 2712-2724.

Zhang J., Schulze K.L., Hiesinger P.R., Suyama K., Wang S., Fish M., Acar M., Hoskins R.A., Bellen H.J. and Scott M.P., *Thirty-one flavors of Drosophila rab proteins,* Genetics (2007)*, 176*, 1307-1322.

Zhang Q., McCorkle J.R., Novak M., Yang M. and Kaetzel D.M., *Metastasis suppressor function of NM23-H1 requires its 3'-5' exonuclease activity,* Int J Cancer (2011)*, 128*, 40-50.

Zhijun X., Shulan Z. and Zhuo Z., *Expression and significance of the protein and mRNA of metastasis suppressor gene ME491/CD63 and integrin alpha5 in ovarian cancer tissues,* Eur J Gynaecol Oncol (2007)*, 28*, 179-183.

Zhou M.I., Wang H., Ross J.J., Kuzmin I., Xu C. and Cohen H.T., *The von Hippel-Lindau tumor suppressor stabilizes novel plant homeodomain protein Jade-1,* J Biol Chem (2002)*, 277*, 39887-39898.

Zhu J., Tseng Y.H., Kantor J.D., Rhodes C.J., Zetter B.R., Moyers J.S. and Kahn C.R., *Interaction of the Ras-related protein associated with diabetes rad and the putative tumor metastasis suppressor NM23 provides a novel mechanism of GTPase regulation,* Proc Natl Acad Sci U S A (1999)*, 96*, 14911-14918.